VOT 78382

THE POTENTIAL APPLICATION OF VIRTUAL REFERENCE STATION-REAL TIME KINEMATIC IN STRUCTURAL HEALTH MONITORING

ZUHAIDAH BINTI NORDIN

UNIVERSITI TEKNOLOGI MALAYSIA

UTM UNIVERSITI TEKNOLOGI MALAYSIA	**PUSAT PENGURUSAN PENYELIDIKAN (RMC)**	**UTM/RMC/F/0024 (1998)** **Pindaan: 0**

BORANG PENGESAHAN
LAPORAN AKHIR PENYELIDIKAN

TAJUK PROJEK :

THE POTENTIAL APPLICATION OF VIRTUAL REFERENCE STATION-REAL TIME KINEMATIC IN STRUCTURAL HEALTH MONITORING

Saya _____**ZUHAIDAH BINTI NORDIN**_____
(HURUF BESAR)

Mengaku membenarkan **Laporan Akhir Penyelidikan** ini disimpan di Perpustakaan Universiti Teknologi Malaysia dengan syarat-syarat kegunaan seperti berikut :

1. Laporan Akhir Penyelidikan ini adalah hakmilik Universiti Teknologi Malaysia.
2. Perpustakaan Universiti Teknologi Malaysia dibenarkan membuat salinan untuk tujuan rujukan sahaja.
3. Perpustakaan dibenarkan membuat penjualan salinan Laporan Akhir Penyelidikan ini bagi kategori TIDAK TERHAD.
4. * Sila tandakan (/)

[ ]	SULIT	(Mengandungi maklumat yang berdarjah keselamatan atau Kepentingan Malaysia seperti yang termaktub di dalam AKTA RAHSIA RASMI 1972).
[ ]	TERHAD	(Mengandungi maklumat TERHAD yang telah ditentukan oleh Organisasi/badan di mana penyelidikan dijalankan).
[√]	TIDAK TERHAD	

_____
TANDATANGAN KETUA PENYELIDIK

PROF. SR DR. WAN ABD AZIZ BIN WAN MOHD AKIB
Nama & Cop Ketua Penyelidik

CATATAN : * *Jika Laporan Akhir Penyelidikan ini SULIT atau TERHAD, sila lampirkan surat daripada pihak berkuasa/organisasi berkenaan dengan menyatakan sekali sebab dan tempoh laporan ini perlu dikelaskan sebagai SULIT dan TERHAD*

"~~I~~/We* hereby declare that ~~I~~/We* have read this thesis and in ~~my/~~our* opinion this thesis is sufficient in terms of scope and quality for the award of the degree of Master of Science (Geomatics Engineering)"

Signature : _____

Name of Supervisor I : PROF. SR DR. WAN ABDUL AZIZ BIN WAN MOHD AKIB

Date : _____

Signature : _____

Name of Supervisor II: MR. SR ZULKARNAINI MAT AMIN

Date : _____

** Delete as necessary*

THE POTENTIAL APPLICATION OF VIRTUAL REFERENCE STATION-REAL TIME KINEMATIC IN STRUCTURAL HEALTH MONITORING

ZUHAIDAH BINTI NORDIN

A thesis submitted in fulfillment of the
requirements for the award of the degree of
Master of Science (Geomatic Engineering)

Faculty of Geoinformation Science and Engineering
Universiti Teknologi Malaysia

DECEMBER 2009

"I hereby declare that this thesis entitled *"The Potential Application of the Virtual Reference Station- Real Time Kinematic in Structural Health Monitoring"* is my original work and the result of my own research except for quotations and summaries, each one of which 1 has clearly stated its source."

Signature :…….

Author : **ZUHAIDAH BINTI NORDIN**

Date :…….

Dedicated to:

My beloved mother and father- Norsiah bt Abdullah, and Nordin bin Jantan
&
My beloved husband- Mohd Hafiz bin Yahya

ACKNOWLEDGEMENT

Assalammualaikum wbt. First of all thanks to Allah S.W.T for giving me a beautiful live and give me a chance to finish this thesis. I would also like to take this opportunity to thank a number of individuals who have assisted me in accomplishing this project. First, I would like to express my gratitude to both my supervisors, Professor Sr Dr. Wan Abdul Aziz bin Wan Mohd Akib and Sr Zulkarnaini bin Mat Amin, for giving me the opportunity to pursue this project and providing invaluable advice, comment and patient guidance. I am also indebted to PM Sr Dr. Md Nor bin Kamarudin and PM Sr Khairul Anuar bin Abdullah and Dr. Baharin Ahmad for their guidance, advices and motivation. Without their continued support and interest, this thesis would not have been the same as presented here.

I would like to express my gratitude to my beloved parents. Norsiah Abdullah and Nordin Jantan for their unreserved support and concern for me to accomplish this thesis and also giving me full support and loves extend to my husband, Mohd Hafiz Yahya for his constant patience, inspiration, help and support in finishing my research. I would also like to thank my family, Mr Quek from Topcon Instrument Sdn. Bhd., all Geomatic lecturers, and others who have provided assistance at various occasions'.

Last, but not least, I would like acknowledge Public Service Department of Malaysia for study scholarship, Research Management Centre (RMC) UTM for supported this research under Vot. 78382 Initial Research Grant Scheme (IRGS) and the Geodesy Section, Department of Surveying and Mapping Malaysia (DSMM) for providing the MyRTKnet data used in this study.

ABSTRACT

Rapid growth in construction of large engineering structures such as dams, wide span bridges, highways, breakwater and high rise buildings are mainly essential for the development of a nation. Aging from these national structural inventories and the fact that many large engineering structures are carrying greater average loads than predicted during their designing stage, have significantly increased the need to monitor their health and stability performance. In order to ensure the safety and serviceability of these structures as well as to prevent disastrous consequences due to structural displacement, periodic monitoring and in-depth analysis of their structural behaviour based on a large set of variables contributing to the deformation are highly demanded. With advanced development of space-base positioning technique, GPS is one of the latest all-weather satellite-based sensors that can be used to detect first stage disaster and further mitigation. This study highlights the use of GPS network-based VRS-RTK technique for real-time structural health monitoring. Several tests have been conducted, including indoor observation at Topcon Building in Kuala Lumpur, breakwater monitoring in Kemaman, Terengganu and monitoring of the P23 Building, Faculty of Mechanical Engineering, Universiti Teknologi Malaysia. The study has proved that VRS-RTK have potential to be as accurate yet practical positioning tools used for Structural Health Monitoring. Provided that proper instrumentation setup applied during data acquisition, VRS-RTK is as well suitable in various monitoring environment either at outdoor or indoor area. On the basis of the structural health, no significant deformation detection have been observed for all these campaigns.

ABSTRAK

Pertumbuhan yang pesat dalam bidang pembangunan struktur besar seperti empangan, jambatan, tembok penahan ombak dan bangunan tinggi adalah penting bagi pembangunan negara. Mengikut senarai pembangunan nasional, kebanyakkan struktur besar ini memikul beban yang diramalkan semasa dari peringkat merekabentuk lagi dan akan meningkat dan memerlukan pengawasan kestabilan. Bagi memastikan keselamatan dan perkhidmatan struktur tersebut dan untuk menghalang daripada malapetaka yang dijangkakan seperti perubahan gerakan bangunan, pengawasan berkala dan analisis pergerakan struktur berasaskan perubahan-perubahan pergerakan adalah sangat diperlukan. Dengan perkembangan teknologi berasakan teknologi satelit, GPS merupakan satu daripada pengesan yang berasaskan satelit yang sesuai dengan semua keadaan cuaca dan boleh digunakan untuk pengesanan peringkat awal dan perubahan lanjutan. Kajian ini menekankan penggunaan berasaskan jaringan GPS menggunakan teknik VRS-RTK bagi pemantauan struktur masa hakiki. Beberapa ujian telah dilakukan termasuk pengawasan di dalam bangunan di bangunan Topcon, Kuala Lumpur, pengawasan tembok penahan ombak di Kemaman, Terengganu dan pengawasan bangunan P23, di Fakulti Kejuruteraan Mekanikal, Universiti Teknologi Malaysia. Kajian membuktikan bahawa teknik VRS-RTK mempunyai potensi untuk kerja pengawasan struktur dengan ketepatan yang tinggi. Dirisiap alat yang sempurna membolehkan teknik VRS-RTK ini sesuai digunakan untuk kerja pengawasan di dalam ataupun di luar bangunan. Daripada kajian yang dijalankan, kestabilan bangunan yang dikaji dalam keadaan yang baik.

TABLE OF CONTENTS

LIST OF TABLES

LIST OF FIGURES

LIST OF ABBREVIATIONS

SHM	Structural Health Monitoring
KLCC	Kuala Lumpur City Centre
WASHMS	Wind and Structural Health Monitoring System
GPS	Global Positioning System
VRS	Virtual Reference Station
RTK	Real Time Kinematic
DSMM	Department of Surveying & Mapping, Malaysia
MyRTKnet	Malaysia real-time kinematic network
EDM	Electronic Distances Measurement
CRP	Close Range Photogrammetry
CCD	Charge Couple Device
INCA	Intelligent Camera
GSI	Geodetic Service Inc
LSA	Least square adjustment
DoD	Department of Defense
FOC	Full operational capability
MCS	Master Control Station
MS	Monitoring station
GA	ground antennas
OCS	Operational Control Segment
Hz	Hertz
MHz	Megahertz

C/A	Course Acquisition
UERE	User Equivalent Range Error
DOP	Dilution of Precision
PDOP	Positioning dilution of precision
HDOP	Horizontal dilution of precision
VDOP	Vertical dilution of precision
TDOP	Time dilution of precision
GDOP	Geometric dilution of precision
ppm	Part per million
DGPS	Real-time differential GPS
RTCM	Radio Technical Commission for Maritime Service
OTF	on-the-fly
CORS	continuously operating reference station
LAN	local area network
GSM	Global System for Mobile communications
GPRS	General Packet Radio Service
3G	Third Generation
TS	Terminal Server
CSV	comma separated value
v	Observation residuals
RMS	Residuals Root Mean Square
R	Central earth radius
ρ	Curvature distance on meridian
v	Curvature distance on ecliptic plane
mm	millimetre
cm	centimeter
m	meter
TGO	Trimble Geomatic Office
TTFF	time to first fix
PGB	PETRONAS Gas Berhad
WGS84	World Geodetic System 1984

RSO	Rectified Skew Orthomorphic
LJT	*Lembaga Jurukur Tanah*

LIST OF APPENDICES

CHAPTER 1

INTRODUCTION

1.1 Background

High-rise building is defined as a multi-storey building mainly designed for accommodations, economical and commercial purposes. Among other important factors in designing high-rise building include the need to withstand the lateral forces imposed by winds effect and ground movements. Furthermore, the foundation of the building must support extremely heavy gravity loads. Aging of our national structural inventory and the fact that many large civil structures are carrying greater average loads than predicted during their design, have significantly increased the need over the past few years to monitor their stability performance.

Structural health monitoring (SHM) refers to the act of observing changes of a deformable body undergo in its shapes, dimension and position. The need for SHM on large engineering structure such as dams, wide span bridges, highways and high rise buildings are often arises from awareness and concerns among construction industry

players such as contractors, professionals, consultants and even public associated with structural integrity, durability and reliability.

Large engineering structures such as bridges, dams and high-rise buildings are subject to deformation due to factors, for example changes of ground water level, tidal phenomena, tectonic phenomena, etc. To date, there are a large number of structural engineering especially in the aspect of high-rise buildings in Malaysia than in the past. These include Petronas Twin Towers (---m), Kuala Lumpur City Centre (KLCC) (452m), KOMTAR Tower (232m), Am Finance Building (210m), and Menara Alor Setar (165.5m) (Figure 1.1).

Kuala Lumpur City Centre (KLCC)

Am Finance Building

KOMTAR Tower

Menara Alor Setar

Figure 1.1: High-rise buildings in Malaysia.

The SHM is an active area of research and practice in recent years. The key point of the SHM is damage diagnosis, which include damage detection, damage localization and damage severity estimation. Over the past few decades, the subject of the SHM has been receiving a growing amount of interest from researchers in diverse fields of engineering who are interested in a wide spectrum of application ranging from monitoring the health of aerospace structures to detecting the damage in civil infrastructure systems, and methods making detecting and localization of damages have been the subject of many researchers. The SHM is becoming an attractive and challenging area for intelligent infrastructure, in which high technologies such as smart sensor, wireless sensor networks, signal acquisition and processing, real-time data transferring and management are integrated. The SHM aims to give at every moment during the life of a structure, a diagnosis of the 'state' of the constituent materials, of the different parts, and the full assembly of this part constituting the structure as a whole. Being a new and improved way to make a Non-Destructive Evaluation. (Balageas, 2006, Balageas, 2001, and Chang, 1999). The SHM involves the integration of sensors, possibly smart materials, data transmission, computation power and processing ability inside the structure. Figure 1.2 presents the principle and the organization of the SHM system.

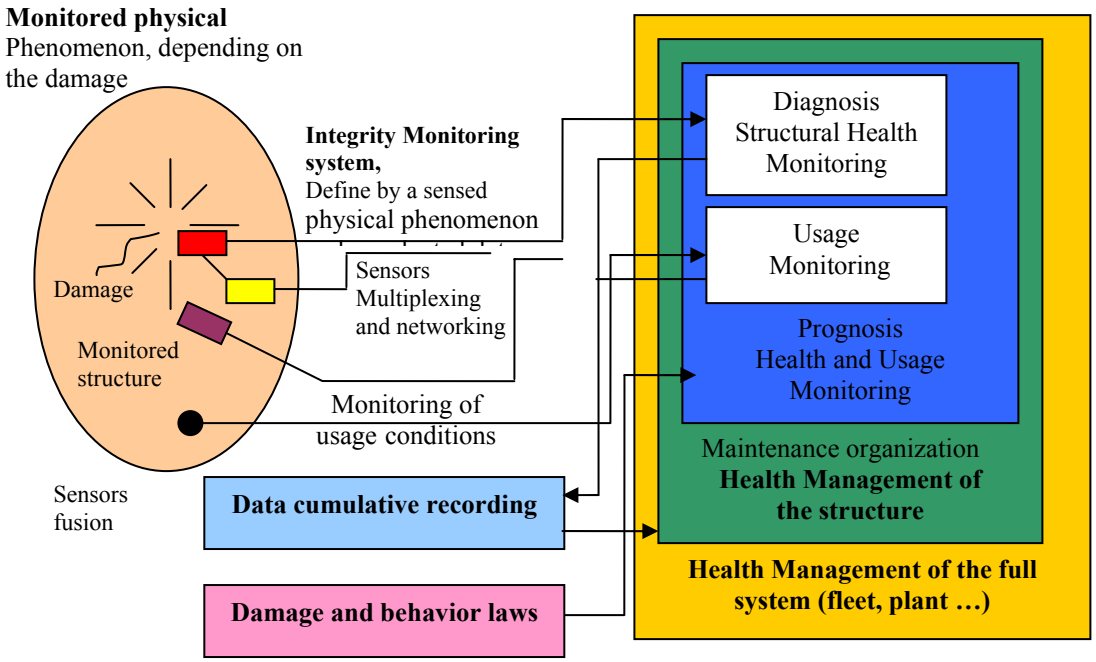

Figure 1.2: Principle and organization of SHM

Most countries worldwide spent a large amount for SHM to ensure the health or stability of their building. For example, Hong Kong Highways Department for example has spent about US$1.3 million to develope Wind and Structural Health Monitoring System (WASHMS) for bridge monitoring (e.g. Tsing Ma Bridge, Ting Kau Bridge and Kap Shui Mun Bridge) operating 24 hours, seven days a week. This system consists of hundred sensors for data recording as an early system to monitor the health condition of the bridge.

In most cases, the displacements of large engineering structures are generated by the lateral forces imposed by the strong winds, the extreme temperature variation, the load changes and the earthquakes excitation. Several important procedures such as the data snooping, the variance ratio test, the stability conformation and the deformation allocation test are needed to detect certain deformation. To ensure the sustainability of these structures so as to prevent disastrous consequences due to structural displacement,

periodic monitoring and in-depth analysis of their structural behavior based on a large set of variables contributing to the deformation are highly demanded.

To date, there are lots of tragedies associated with the structural displacement and lack of understanding on SHM. Amongst them is the collapse of Penang Ferry Terminal Bridge at Jeti Pengkalan Sultan Abdul Halim on 31 July 1988, which caused the deaths of 32 people and injured 1674 people (see Figure 1.3). The tragic episode followed by the collapse of Highland towers condominium in Hulu Kelang Selangor. Occurred on 11 December 1993, this tragedy caused the deaths of 48 people (see Figure 1.4). These tragedies have awakened the public awareness and concern of the structural health.

Figure 1.3: Penang Ferry Terminal Bridge Tragedy[1].

[1] Source-http://en.wikipedia.org/wiki/Sultan_Abdul_Halim_ferry_terminal_bridge_collapse

Figure 1.4: Highland Towers Tragedy. [2].

Malaysia is situated near two borderlines where active seismic plates meet: to the west is the borderline where Indo-Australian Plate and Eurasian meet while to the east is the borderline where Eurasian Plate and Philippines Sea Plate meet. Based on this natural even, Peninsular Malaysia is one of the countries that receive the most vibration effects from the earthquake activities. The vibration of large magnitude earthquakes, which often take place along the borderline, can be detected in Malaysia. Figure 1.5 shows the location of Malaysia around Inter-plate Boundaries and Epicentres of Earthquake.

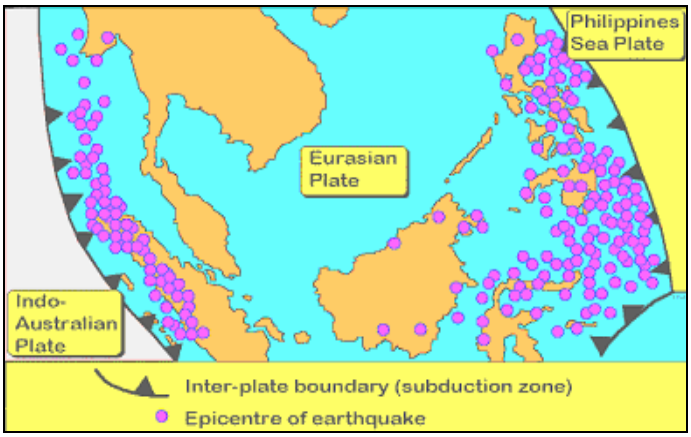

Figure 1.5: Inter- plate Boundaries and Epicenters of Earthquake

[2] Source-http://en.wikipedia.org/wiki/Highland_Towera_collapse

One of the natural events, tsunami induced by the Indian Ocean earthquake occurred on 24 December 2004. This rector scale achieve to 9.6 which caused the deaths numbers of about 200 000 people and cause the full damage of the area of Banda Acheh, Sumatra, Indonesia. The aftershocks cause by the earthquake still continues in this region. The public feel the shake of this natural even, base on this even they concern weather our building can withstand properly or not.

According to Teskey and Poster (1988), the SHM techniques can be divided into geotechnical, survey and geodetic methods. The geodetic method (surveying sensor) can be carried out in two different ways i.e. terrestrial positioning system and global positioning system (Mat Amin et. al. 2007). Geodetic methods includes Global Positioning System (GPS), close range photogrammetry, total station, very long baseline interferometer and satellite laser ranging. The survey methods can be further subdivided into the survey network method and direct measurement methods. Sensor systems which monitor the geometry and deformations of large civil structures are not new. For many years, the geotechnical method is used to monitor the dynamic behaviors of structure. The instruments that can be used are accelerometer, anemometer, strain gauge, extensometer, inclinometer, pressure cells, till meters, crack meter and temperature sensor.

Being one of the latest positioning tools in surveying technologies, GPS can also be used for detecting first stage disaster and further mitigation. GPS technology is a satellite based navigation system that permits users to obtain their 3D position (X, Y, Z or latitude, longitude and height), velocity information and time in common reference system 24-hour a day. GPS combines high accuracy of the results with the possibility of surveying continuously in all weather conditions and the ease of the equipment installation. As it capable of obtaining results in real-time, GPS holds promise as an essential way for a continuous and automated structural health monitoring, especially when swift results could save lives and property.

With the advance of GPS technology and the development of the full satellite constellation, continuous and automated monitoring becomes increasingly practical and cost-effective. According to Ogaja C., et. al. (2001), GPS technology can be used to measure directly the positioning coordinates and relative displacements at rates of 10Hz and higher. Capable of monitoring up to sub-centimeter displacement, GPS provides a great opportunity to be used as an alternative to other commonly used sensors for deformation monitoring.

In reference to conventional RTK-GPS technique, the effects of the atmospheric refraction restrict the distance between the rover and the base station up to only 15-20 km. These systematic errors result in reduced accuracy and increased initialization time as the distance increases. Virtual Reference Station (VRS) is one of the latest innovations in RTK-GPS measurements in which capable to overcome the aforementioned issue. Recently provided by Department of Surveying & Mapping, Malaysia (DSMM) through the establishment of Malaysia real-time kinematic network (MyRTKnet), this research tends to highlight the serviceability of MyRTKnet for SHM application.

For the purpose of the study, the SHM using "modern" RTK (VRS-RTK technique) were conducted through simulation test and real observation on selected buildings within in dense area which in the UTM campus area and Kuala Lumpur and less dense area which is in Terengganu. It is suggested that the outcome of this research is merely significant to provide clear understanding on the periodic monitoring and in-depth analysis of the future structured engineering using network-RTK. In this study, the new approach of monitoring technique for SHM will be proposed by using the new sophisticated technique of GPS which is network-RTK or MyRTKnet.

1.2 Problem Statements

For the past decades, Malaysia is witnessing rapid growth in the construction of large engineering structures such as long-span bridges, high-rise building and massive hydroelectric dams to meet the requirement for the nation's economic growth, societal activities and the aspirations of its population. These engineering structures are however, subject to deformation undergoes in its shapes, dimension and position caused by heavy loading, geotechnical movement and severe weather conditions. Similarly, according to Jauhari Taib (2006), Director of the Works Ministry's Maintenance Regulatory Division, "the concern now lies in the fact that most high-rise buildings in Malaysia have not been built to be earthquake-proof"[3]. In order to ensure the safeties and serviceability of engineering structures, continuous monitoring, data recording and comprehensive analysis of the structural fatigue history are thus important towards increasing the durability and the life-time of the structures.

Arises from awareness and concerns among construction industry players such as contractors, professionals, consultants and even public associated with structural integrity, durability and reliability, much attempt has gone into the designing and testing of various structural health monitoring techniques so as to prevent disastrous consequences due to the structural displacement. In addition to the accelerometer, close range photogrammetry, laser interferometer, EDM (Electronic Distances Measurement) and Total Station, amongst others include the fully-operational space-based positioning approach known as GPS.

GPS technology permits users to obtain their 3D position (X, Y, Z or latitude, longitude and height), velocity information and time in common reference system 24-hour a day. Compared to the accelerometer and close range photogrammetry, GPS combines high accuracy of the results with the possibility of surveying continuously in

[3] Source-New Straight Times (26 April 2006).

all weather conditions and the ease of the equipment installation. Moreover, unlike the laser interferometer, EDM and Total Station, GPS does not require a clear line of sight during data acquisitions. Conventionally, there are two ways of using GPS for structural health monitoring. The first is using Static observation technique while the other is using single-based Real Time Kinematic (RTK) technique. The principle of Static GPS observation technique is having at least two receivers where one being placed at known location whiles the other at the interest point for a certain period of time. Apart from at least two GPS receivers, single-based RTK technique on the other hand requires additional radio-communication device and a handheld survey data collector/computer.

GPS Static observation has been widely used in high accuracy geodetic applications. Nevertheless, apart from its distinct capability to capture 3D coordinates at high-level of accuracy, GPS Static observation has certain limitation in displaying the observed data for prompt and on-site analysis. In addition, single-based RTK technique is as well suffers from similar latency for rapid data analysis (despite of its capability in "capturing" 3D coordinates in real-time). Moreover, the maximum distance between the reference and the rover receivers using this approach must not exceed 10 kilometers to rapidly and reliably resolve the carrier phase ambiguities.

The progressive degradation of results over distance due to systematic errors (distance-dependent biases) experienced by the GPS Static observation and single-based RTK has given way to concept of Network RTK. Though not wholly dependent on cellular communications, the move from single-based RTK and radio has been coincident with the move towards network RTK and cellular packet data for transmission and data corrections. This technique called Network-RTK is used in DSMM projects, known as MyRTKnet. In MyRTKnet, the virtual reference stations (VRS) further simplifies the usage for rapid data acquisition and analysis in the field. MyRTKnet infrastructure offers the flexibility of enabling both RTK and DGPS operations during data acquisition. MyRTKnet provides high performance solution for real-time data collection needs of Malaysian users. The network, which includes the

provision of redundancy at the data collection, transmission and processing layers, has a high degree of service reliability. This research focus on structural health monitoring using space-based monitoring tools known as VRS-RTK. The survey have been conducted in various condition including indoor observation at Topcon Building in Kuala Lumpur, breakwater structure in Kemaman, Terengganu and monitoring of the P23 Building, Faculty of Mechanical Engineering, Universiti Teknologi Malaysia

1.3 Research Objectives

The objectives of this study include:

a. To study the concept of conventional RTK and VRS-RTK technique in structural monitoring
b. To conduct VRS-RTK technique for structural monitoring under various measurement condition
c. To analyze the performance thus identifying the best approach of SHM using VRS-RTK technique

1.4 Research Scopes

The scopes of this study include:

a. To study the concept of conventional RTK and VRS-RTK technique in structural monitoring
    i Reviews on the issue of accuracy, feasibility and effectiveness of conventional RTK and VRS-RTK technique
    ii Reviews on the current implementation of conventional RTK and VRS-RTK technique in structural health monitoring

b. To conduct VRS-RTK technique for structural monitoring under various measurement condition
    i Conducts structural monitoring using TOPCON Hyper GA which include the process of calibration prior observation project
    ii Conducts structural monitoring under various measurement condition such as:
        (a) within dense network (Johore and Kuala Lumpur) and less dense network (Kemaman,Terengganu)
        (b) in real-time (VRS-RTK) and in post-processing mode with different data approach (CORS data and virtual RINEX)
    iii Case study includes high-rise building and breakwater structure
    iv Trimble Geomatic Office for data processing (post processing mode)

c. To analyze the performance thus identifying the best approach of structural monitoring using VRS-RTK technique
    i Statistical approaches for data analysis
    ii Provide suggestions on the best approach of structural monitoring using VRS-RTK technique

1.5 Research Contributions

i The proposed method/technique is significant as deformation sensor for structural monitoring.

ii This study clarifies the roles of VRS technique in SHM and this technique can be emerging as a stand-alone technique.

iii The study will be a guide for publishing a standards or guidelines of using VRS-RTK technique for SHM besides helping future research.

iv As a platform for future work, using VRS-RTK with network-RTK for structural health monitoring or deformation detection.

v Contribute to the knowledge itself especially in related studies such as a structural and landslide monitoring.

vi Beneficial to government agencies such as JKR and property management such as KLCC, Telecom Tower and, Penang Bridge for their structural monitoring.

1.6 Research Methodology

The research methodology is basically a series of research activities executed to get to the final output. Figure 1.6 shows the research flow in graphics representation.

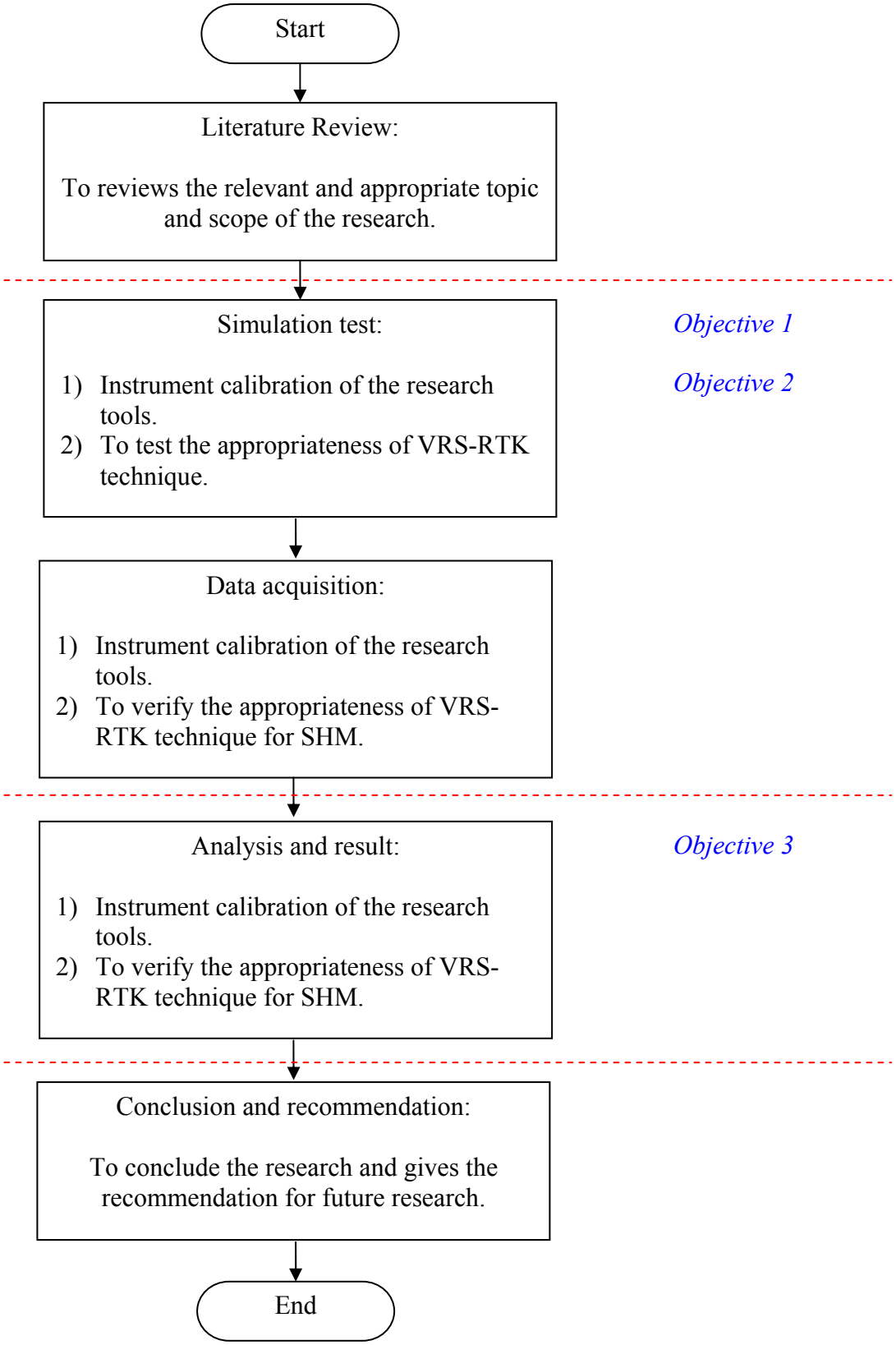

Figure 1.6: Research Methodology

1.7 Outline of the Thesis

This thesis consists of six chapters and five appendixes.

Chapter 1 gives the introduction to the research by delivering the background, problem statements, research objective, research scope, research contribution, and outline of the thesis.

Chapter 2 reviews the structural health monitoring tools which include conventional method and modern method, overview of Global Positioning System (GPS), the GPS technique and application of GPS in structural health monitoring.

Chapter 3 reviews the structure and the advantage of Real-Time kinematic network. Moreover the details of Malaysian Real-Time kinematic network (MyRTKnet) are discussed which included of MyRTKnet component and its accuracy.

Chapter 4 describes about the calibration tests of the instrument and simulation test of VRS-RTK performing.

Chapter 5 focuses on all study cases which are include breakwater monitoring and building monitoring using VRS-RTK technique and network-RTK. The result is statistical analyses and discusses.

Chapter 6 gives the conclusion remark of the research and the recommendation for the future works.

Appendix A attaches the specification of Topcon HiPer GA Receiver

Appendix B presents the results of simulation test of VRS-RTK.

Appendix C presents the results of assisted-GPS indoor GPS.

Appendix D presents the results of GPS-based building monitoring

Appendix E presents the results of GPS-based breakwater monitoring.

CHAPTER 2

REVIEW ON METHODS IN STRUCTURAL HEALTH MONITORING

2.1 Introduction

This chapter describes the current and future trends on structural health monitoring scheme. Deformation refers to changes of a deformable body (natural or man-made objects) undergoes in its shapes, dimension and position. According to Chrzanowski et al. (1986) there are two types of geodetic method known as reference (absolute) and relative network. Theoretically, there are three important procedures in deformation detection. These include data snooping and variance ratio test, S-Transformation and stability conformation and deformation allocation. Deformation or structural displacement can be monitored using several techniques; each with its own advantages and limitations. In general, the method can be divided in to two main methods: conventional method and modern method (Global Positioning System (GPS)). Each method will be explained in detail the following subtopics.

2.2 Conventional Monitoring Method

Throughout the decade, there were numerous monitoring tools and techniques used in monitoring survey. They include geotechnical, geodetic and surveying technique with their own advantages and limitations. In general, accelerometer, close range photogrammetry, laser interferometer and total station are amongst numerous tools used for conventional structural monitoring method. Details of these monitoring tools are as follows.

2.2.1 Accelerometer

Accelerometer is a common instrument used by the structural engineer (see Figure 2.1). It detects structural displacement using frequency shift methods that infer damage by analyzing the frequency response of a structure. One of the limitation to this instrument is it requires a direct contact with the structure. In order to link the accelerometers to a central recording unit, it also requires a very tedious wiring work in which contributes to a great possibility of damage, installation error and a high cost in maintenance. Calibration of these instruments with respect to temperature is necessary for accurate results, especially when the temperature varies throughout their network. Despite of its capability to accurately detect vibration frequencies up to several hundred Hertz or even higher, accelerometer is facing a major problem to accurately detect ‘very low’ vibrations (i.e. structural movements that happen slowly) in which are evident for long span structures (Xiolin, M., et. all 2004).

Figure 2.1: Example of accelerometer

2.2.2 Close Range Photogrammetry

Photogrammetry allows the use of photographs to determine displacements over long period of time. This technology can be used to measure, document, or monitor almost anything that is visible within a photograph. In addition to the distance of the camera from the subject, the use of photogrammetry method depends on the scale of the object being measured. Close Range Photogrammetry (CRP) is one of the photogrammetry approaches that have an object-to-camera distance of less than 300 m. As far as CRP is concern, the most important equipment required for this method is the digital sensor which comprise of the digital camera of various forms, costs, resolutions and formats, the Charge Couple Device (CCD) camera, and the video camera.

In addition to the Intelligent Camera (INCA) developed by the Geodetic Service Inc (GSI), compact camera can also be used for CRP. The precision attainable with compact digital cameras however, are only 1: 20 000 which is in the order of two-third (2/3) of that achievable with SLR digital camera. Though CRP can be applied especially when a fast and not necessarily too accurate analysis is required, it is suggested that CRP is not an effective approach when the accuracy of the measurements need to be at the highest level. Due to complex and difficult conditions surrounding, it is also not always possible to use CRP alone in structural health monitoring as CRP needs to be integrated

with other auxiliary instruments. Example of close-range photogrametry instrument shows in Figure 2.2.

Figure 2.2: Example of close-range photogrammetry instrument

2.5.3 Laser Interferometer

Laser interferometer measures the variation in distance between the interest point and the reference point. To obtain distance to the interest point, a prism or reflective film need to be mounted on the structure. Variation in distance can be measured and be further analyzed to determine dominant frequencies and corresponding amplitudes throughout the observation. This method has the advantages of high accuracy, but it is difficult to fix the interest point when vibration of the structure is too big. Moreover, laser interferometer is also quite expensive. Apart from its limitation to detect 3D displacement, automation is also a major problem whenever this method is being used. Real time measurement to the interest point need to be made manually by at least two personnel since it cannot be automated. Another major drawback of this method is laser interferometer is climate dependent. As it is difficult to conduct a measurement during rainy condition due to interference on the line of sight, it is suggested that in most cases, laser interferometer is not rather suitable for continuous monitoring of manmade structures in Malaysia

2.5.4 Total Station

Total Station is a combination of digital theodolite and EDM instrument. This instrument is capable of providing easting, northing coordinates, height differences and horizontal distances. Nowadays, some total stations have a memory card and Bluetooth connection capabilities to record data directly to the data recorder or notebook for further processing. Robotic or motorised, reflectorless and target recognition total station is yet another recent advance in total station technologies. Even though it is currently being used for periodical (repeated) structural health monitoring scheme, the most common limitation is the pointing error and inter-visibility requirement between stations. It also requires redundancy in measurement to detect the possibility of human error. As it is also weather dependent instrument, the use of total station is not quite suitable as regards to the weather condition in Malaysia. It is also requiring a clear line of sight between the reference stations and the structures of interests. Given clear line of sight is achievable, the estimated accuracy of total station method is 5 mm horizontally and 10 mm vertically.

The total station technique has been used by Salleh C. Z. (2007) to monitor a breakwater structure located at Pangkalan Laut 1, Tanjung Gelang, nearby Kuantan Port, Kuantan. In this campaign Leica^{TM} TPS 400 total station were used. The port which is a deep sea commercial port is situated at midway along the East Coast of Peninsular Malaysia. It is an inner breakwater belongs to Kuantan Port but now it is used by TLDM for domestic purpose. Figure 2.3 depicts the overview of the breakwater structure.

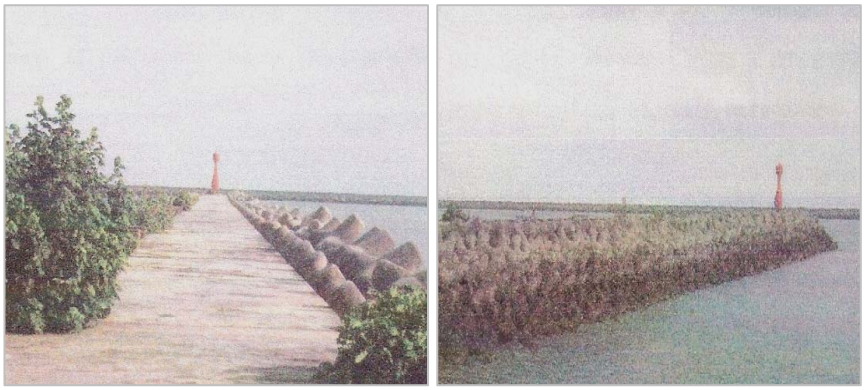

Figure 2.3: Breakwater Structure

Principally, the number of control stations is dependable on the size of the structure. Since total station is only capable of measuring points from approximately 1 to 4 km, three concrete monuments were established 20 m away from the breakwater structure. A total of two epoch with an interval of four weeks time (26 December 2006 and 28 February 2007), were carried out during the observation. After applying least square adjustment (LSA), Table 2.1 shows the output of the computation.

Table 2.1: Single Test Point Result (Saleh C. Z.,2007)

Station	ΔX	ΔY	Disp. Vector	Fcom	Ftab	Status
1	-0.0013	-0.0005	0.0014	0.01	5.85	Stable
2	0.0016	0.0007	0.0017	0.01	5.85	Stable
3	-0.0003	-0.0002	0.0004	0.00	5.85	Stable
4	0.0031	0.0257	0.0259	0.02	5.85	Stable
5	0.0028	0.0147	0.0149	0.02	5.85	Stable
6	-0.0012	0.0113	0.0114	0.03	5.85	Stable
7	0.0015	0.0084	0.0086	0.02	5.85	Stable
8	0.0010	0.0004	0.0011	0.01	5.85	Stable
9	-0.0002	0.0012	0.0012	0.01	5.85	Stable
10	-0.0005	0.0008	0.0010	0.01	5.85	Stable
11	0.1990	0.1064	0.2257	0.02	5.85	Stable
12	-0.3145	-0.1648	0.3551	0.08	5.85	Stable

Displacement vector can be defined as length of the displacement in error ellipse. Fcom is the Fisher value computation obtained from LSA whereas Ftab is the Fisher value taken from the degree of freedom and confidence level. Providing that value of Fcom is less than Ftab, conclusion can be made that the breakwater structure was in stable condition.

2.6 **Global Positioning System (GPS)**

Global Positioning System (GPS) is a modern method for SHM. GPS is a space-based navigation system develops and operates by the US Department of Defense (DoD). The satellites generation include of five phases. The first series known as Block I satellites include of 11 satellites was launched on 22 February 1978. This launching is for experimental purposes but all the last Block I satellite was taken out of service on 18 November 1995. The second series known as Block II and third series known as Block IIA. The Block IIA is an advanced version of Block II. Block II/IIA include of 28 satellite were launched between February 1989 to November 1997. Two other phases (new generation) is Block IIR and IIF. Block IIR consist of 21 satellite and capable of operating 180 days without ground correction. Block IIF consists of 33 satellites. Block IIF satellite is under GPS modernization program that improved the positioning accuracy. (Hofmann-Wellenhof and Licthenegger 1997; Seeber, G. 2003 Kaplan and Hergarty 2006).

GPS is comprises of three segments: the space segments, the control segment and the user segment (see Figure 2.4). Generally, it is implemented in navigation and surveying. It has been used for the geodetic solution since about 1983.

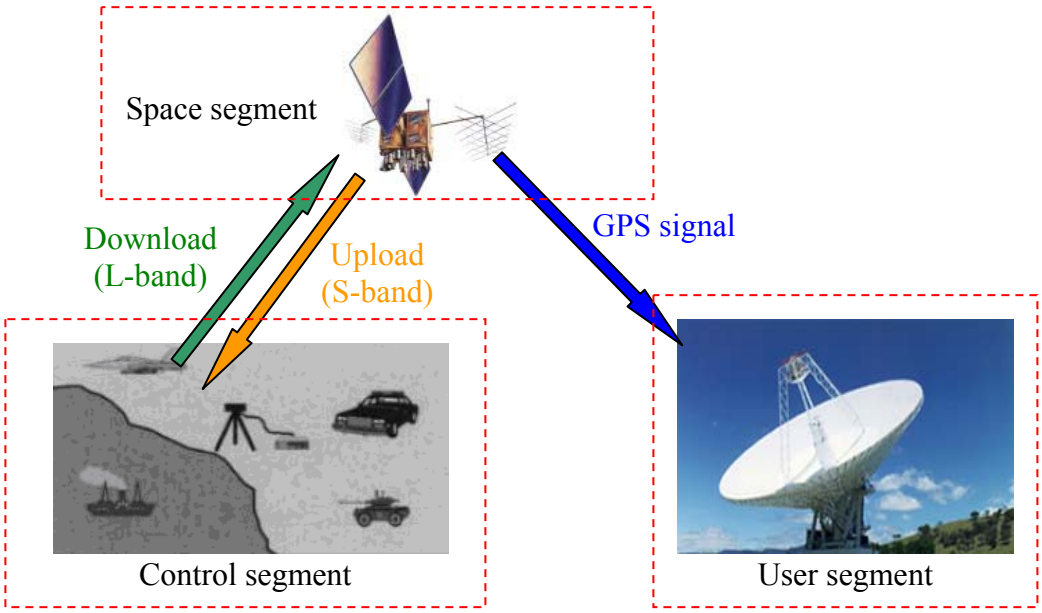

Figure 2.4: GPS Segment

GPS Space Segment consists of satellite constellation. The system normally consists of 32 satellites placed in orbits of about 20 200 km altitude above the earth's surface (Seeber, G. 2003). Each plane is inclined by 55° relative to the equatorial. The semi major axis of a GPS orbit is about 26, 560 km. since the GPS system achieved full operational capability (FOC) on 17 July 1995, the availability of at least 24 operational. Beside that, number of GPS satellite has always been increased. The satellite constellations provide the ranging signal and data message to user equipment. Figure 2.5 presents the GPS constellation.

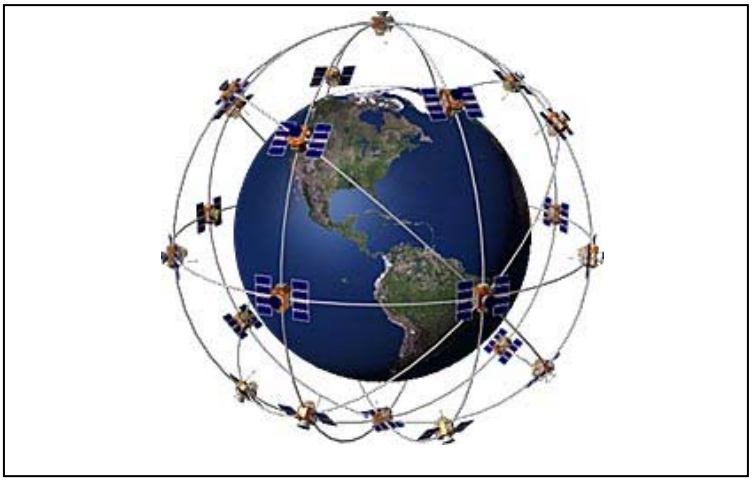

Figure 2.5: GPS constellation[4]

GPS Control Segment on the other hand consists of a network of tracking stations and ground antenna, that include the Master Control Station (MCS), several unmanned monitoring stations (MS) located around the world, and ground antennas (GA). The Operational Control Segment (OCS) for GPS consist of the MCS near Colorado Springs, four monitor stations and co-located ground antennas in Ascension Island, Cape Canaveral, Kwajalein and Diego Garcia and two more monitor stations in Colorado Spring and Hawaii (Seeber, G. 2003).

The User Segment consists of the GPS receivers, users and GPS instrumentation. With a GPS receiver connected to a GPS antenna, a user can received a GPS signal to obtain the position anywhere in the world.

With the advance of GPS technology, and the development of the full satellite constellation, continuous and automated monitoring using GPS becomes increasingly practical and cost-effective. The main goal of GPS is to provide worldwide, all weather, continuous radio navigation support to users in determining one position, velocity and time throughout the world (Hofmann-Wellenhof et. al., 1994). GPS have several

[4] Source-http://mytreo.net/archives/2005/09/the_great_treo_gps_roundup.php

advantages. GPS is used for the accuracy acquisition from decameter up to millimeter level. GPS can measure directly positioning coordinates and even can detect the drift or displacement of object in high precision rate of 0.1s or higher using real-time mode. The sampling frequency of GPS receiver can receive about 0.05Hz, and the location precision can approach 5~10mm. This provides a great opportunity for GPS to be used as a sensor for deformation monitoring. One of the demonstrations of the potential for GPS to be used as sensors was done by Leach and Hyzak (1994)

2.3.1 GPS Signal Structures

GPS observation is distance measurement to satellites that have geometrical position. All satellites transmit ranging signals on two L-band frequencies, designated as L1 and L2. The L1 carrier frequency is 1575.42 MHz and has a wavelength of approximately 19 cm. The L2 carrier frequency is 1227.60 MHz and has a wavelength of approximately 24 cm. GPS is a one-way ranging system capable of both pulsed-type measurements (pseudo-range measurements using one of the codes) and continuous wave-type measurements (carrier beat phase measurements). Both codes can be used to determine the range between the user and a satellite. There are two types of GPS observation, pseudo range observation and carrier phase observation.

These carrier phases are modulated into two types of codes, namely Course Acquisition – C/A code and Precise – P code. L1 carrier phase is modulated with P-code together with C/A-code, while L2 carrier phase is modulated with P-code only. Frequency of C/A-code is 1.023 Mhz (f_0 / 10) and its wavelength is 300 meter. On the other hand, frequency of P-code is 10.23 Mhz (f_0) and its wavelength is 30 meter (Wells et. al., 1999).

Pseudo range observation is the observation based on how much time it takes for the transmitted satellite signal to arrive at user's receiver. In other word, pseudo-range is the time delay between the satellite clock and the receiver clock, as determined from C/A- or P-code pulses. Distance between satellite and receiver equals to time (from satellite to receiver) times velocity. Equation of pseudo-range observation is shown in equation 2.1. Figure 2.6 represent the concept of pseudo-range measurement.

$$P = p + c(dT - dt) + d_{ion} + d_{trop} + d_p + \varepsilon_p \tag{2.1}$$

in which,

P	=	pseudo-range observation,
ρ	=	geometric distance from receiver to satellite,
C	=	light velocity, dt is satellite clock drift,
dT	=	receiver clock drift,
d_{ion}	=	ionospheric error (positive if there is latency),
d_{trop}	=	tropospheric error,
d_p	=	orbital error,
ε_p	=	pseudo-range observation noise.

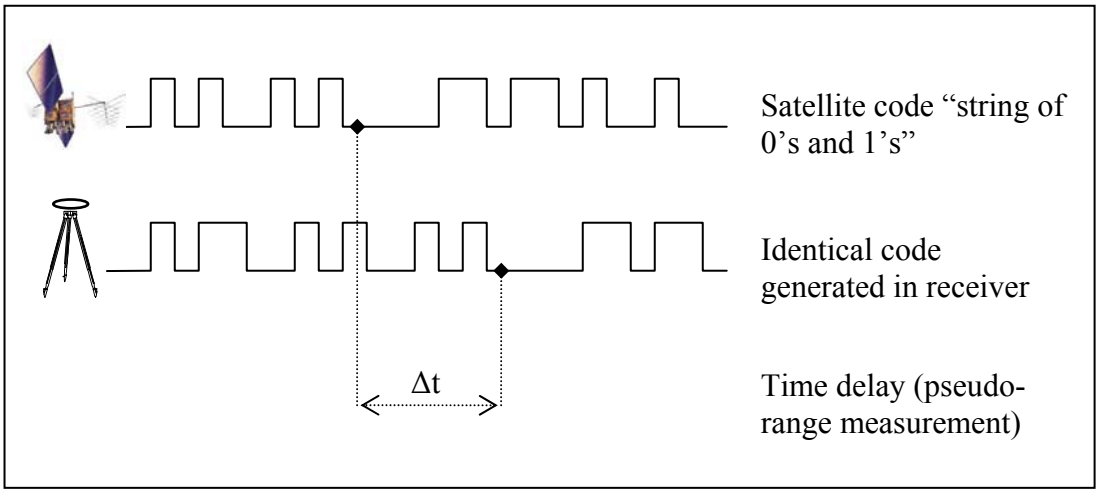

Figure 2.6: Pseudo-range measurement.

Carrier phase is the observable at the centre of high accuracy surveying application of GPS. Carrier phase observation is based on length of wavelength where it is converted from cycles to length unit. In order to obtain the distance from satellite to receiver from the carrier phase observation, it must take into account the ambiguity term to get unknown number of cycle integer between satellite and receiver at certain epoch t_o. The range determined with the carrier is most accurate than the pseudorange. Therefore carrier phase observation equation is as the followings equation 2.2. Figure 2.7 shows the concept of carrier phase measurement.

$$\Phi = \rho + c(dT - dt) + \lambda N - d_{ion} + d_{trop} + d_{\rho} + \varepsilon_{\Phi} \qquad (2.2)$$

in which,

Φ = carrier phase observation in length,

N = cycle integer ambiguity,

λ = carrier phase wavelength,

ε_{Φ} = receiver noise function,

d_{ion} = ionospheric error (negative because of premature phase),

d_{trop} = tropospheric error.

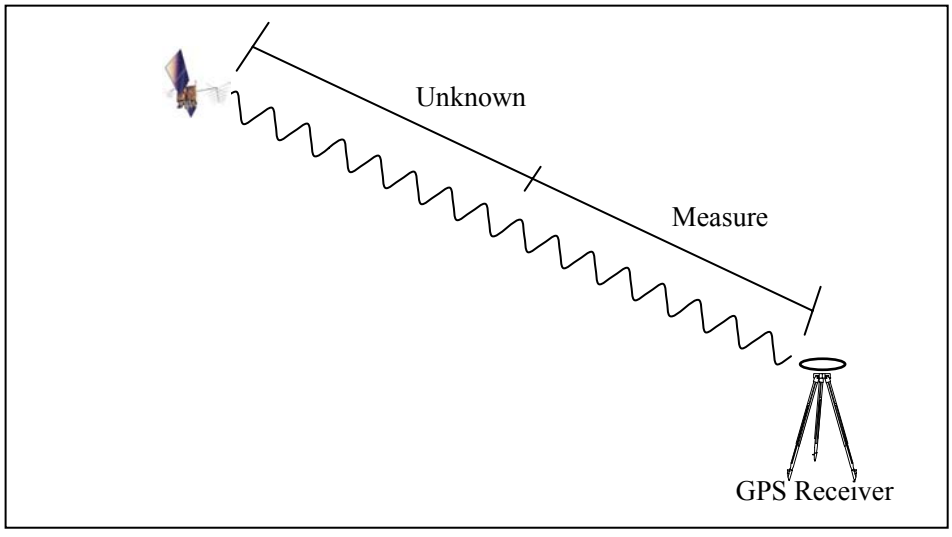

Figure 2.7: Carrier-phase measurement.

Each GPS satellite transmits data on two L-bands modulate frequencies namely L1 and L2 used to determine distance between satellite and the receiver by measuring the radio travel time of the signals. L1 frequency (1575.42MHz) has a wavelength of about 19cm whereas L2 frequency (1227.60MHz) has a wavelength of about 24cm. The L1 signal is modulated with a Coarse/Acquisition Code (C/A-code) and a Precision Code (P-code). The L2 on the other hand signal is modulated with only the P-code. All satellites transmit these two frequencies which are different for each satellite. The frequencies are modulated with two types of code and navigation message. The codes are the civilian C/A-code and the military P(Y)-codes.

One of the advantage of GPS is GPS can determine one position in three-dimensional coordinates (lat, long,height) even without intervisibility between stations. The GPS technology directly measures the position coordinate in high precision range from centimetres up to millimetres level. The GPS accuracies depend on the satellite geometry, observation technique, precise data and processing technique. The GPS system is usually designed to provide the user with the information of determining 3D-user's position, expressed in geodetic coordinate system latitude, longitude and altitude (ϕ, λ, h) and/or in Cartesian coordinate system (X, Y, Z).

2.3.2 GPS Accuracy and Error Source

GPS accuracy is dependent on two main factor, the accuracy of single pseudorange measurement that expressed by User Equivalent Range Error (UERE) and the geometry configuration of satellite used (Seeber, G., 2003).

Dilution of Precision (DOP) is the geometric effect of the satellites relative to the user. There are many varieties of DOP:

PDOP = Positioning dilution of precision

HDOP = Horizontal dilution of precision

VDOP = Vertical dilution of precision

TDOP = Time dilution of precision

GDOP = Geometric dilution of precision

PDOP represent the contribution of satellite geometry of 3D (latitude, longitude, height) positioning. PDOP affects the horizontal component (HDOP) and vertical component (VDOP). Normally, the VDOP is larger than HDOP, this is because GPS user can track the satellite above the horizontal. To ensure the high accuracy, it is recommended that a PDOP is five or less. Figure 2.8 show the satellite geometry and PDOP.

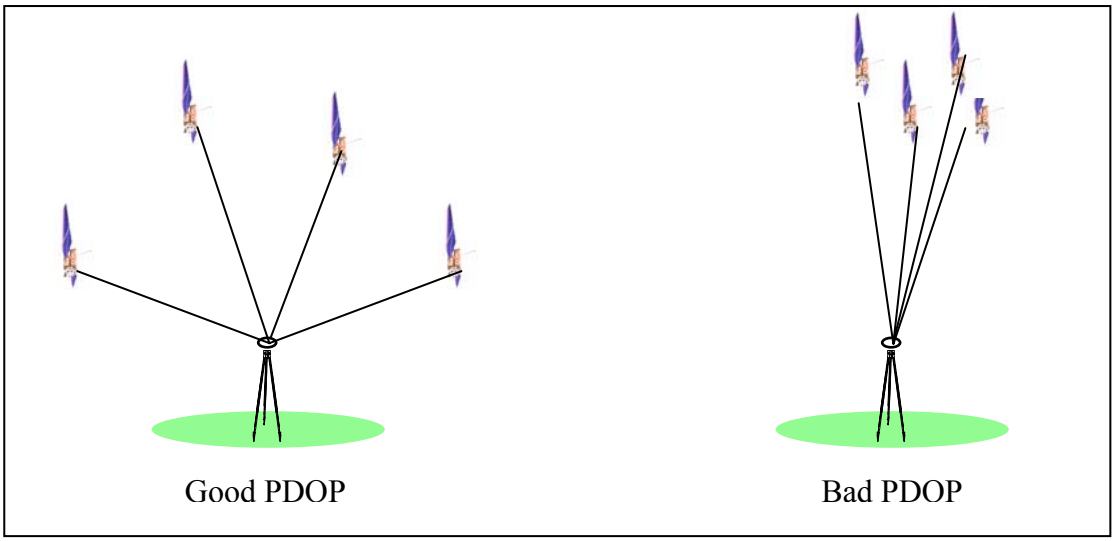

Figure 2.8: Show the satellite geometry and PDOP.

Beside that, GDOP is representing the combination of positioning dilution of position (PDOP) and the time dilutuion of precision (TDOP).

$$\text{GDOP} = \sqrt{(PDOP)^2} + (\text{TDOP})^2 \qquad (2.3)$$

UERE represents the combined effect of satellite biases, signal propagation dependent biases and station biases. The satellite biases include orbit biases and satellite clock error. The Main GPS error and biases contribution is summaries as shown in Table 2.2. (Seeber, G. 2003, Wells et al., 1999).

Table 2.2: Main GPS error contribution

Error Source	RMS Range Error
Satellite dependent	
- Orbit biases	1 – 2 m
- Satellite clock model biases	1 – 2 m
Signal Propagation	
- ionosphere (2 frequencies)	cm – dm
- ionosphere (model, best)	1 – 2 m
- ionosphere (model, average)	5 – 10 m
- ionosphere (model, worst)	10 – 50 m
- troposphere (model)	dm
- multipath	1 – 2 m
Station dependent	
- observation noise	0.2 – 1 m
- hardware delays	dm – m
- antenna phase center	mm – cm

Multipath occurs when one or more reflect signal and direct signal reaches the antenna. Multipath in general affect both code and carrier phase measurement and its can be reflect off horizontal, vertical and inclined surface, however its size is much largest in code or pseudorange measurement. There are several recommendations to reduce and minimize the multipath effect. This includes by making sure the observation

site has no reflecting object in the vicinity to the receiver and careful attention on antenna setting. Figure 2.9 illustrates the multipath effect.

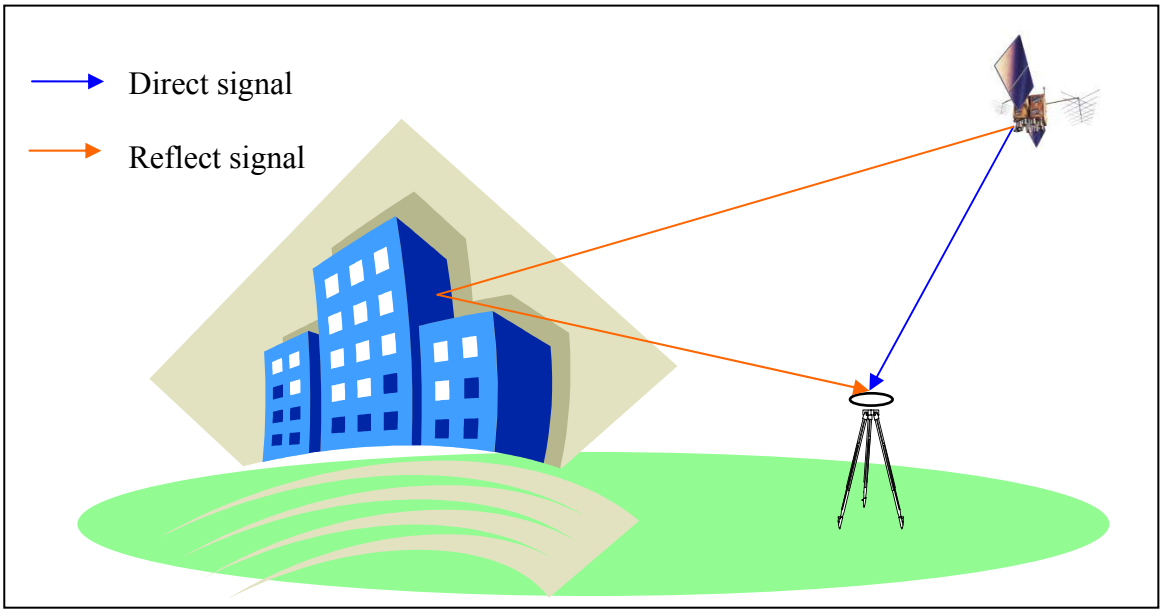

Figure 2.9: Multipath effect.

2.3.3 GPS Positioning Concept

GPS positioning concept can be divided into two, namely point positioning and relative positioning. This discussion will give a brief overview on matters related to GPS positioning which include the point positioning and relative positioning. For more detailed discussions on GPS theory, readers are referred to GPS textbooks (for examples Kaplan and Hegarty, (2006), Parkinson and Spilker, (1996), Leick, (1995), Hofmann-Wellenhof and Lichtenegger, (1997) and Rizos, C. (1999).

2.3.3.1 Point Positioning

GPS point positioning is one of the basic techniques of GPS positioning. Known as standalone or autonomous positioning, this technique sometimes can be referred as absolute[5] positioning. Point positioning employs one GPS receiver which measures code ranges to determine one position. The receiver simultaneously tracks normally four or more satellites to determine coordinates of a single point with respect to the centre of the Earth. Using either C/A-code or P(Y)-code the obtained receiver coordinates will be in reference to WGS 84 system. Figure 2.10 depicts the concept of point positioning. The concept is quite simple. Apparently, point positioning is frequently used in low accuracy applications.

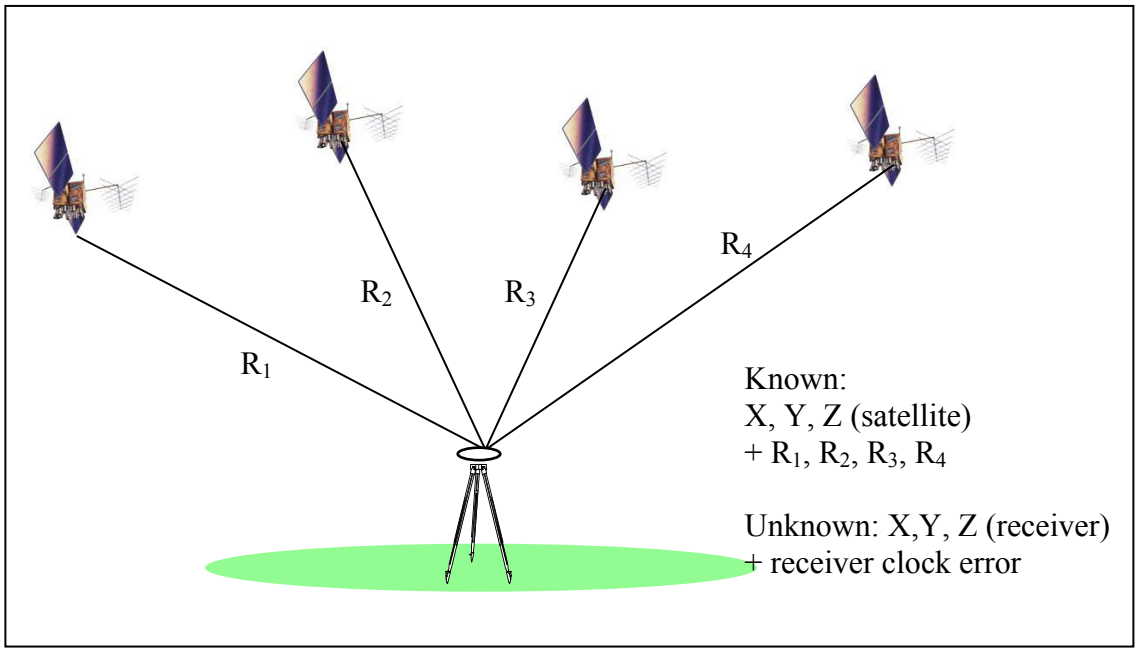

Figure 2.10: The concept of point positioning

[5] The term absolute reflects the opposite of relative.

2.3.3.2 Relative Positioning

Relative positioning is a technique where by two receivers are used to track satellites simultaneously to determine one position. Also known as differential positioning, the accuracy is better than point positioning if both receivers manage to track at least four common satellites.

Relative positioning useds carrier-phase and/or pseudorange measurement. The term “relative” is used in the case of carrier-phase while the term “differential” is used in the case of code range observation. Relative positioning can be made either in real-time or post-processing. This technique is mainly used for high-accuracy application such as surveying, mapping, and navigation. Figure 2.11 illustrates the concept of relative positioning. Basically, coordinates of one receiver are known as the position of the other receiver is to be determined relatively to the known coordinates. Known receiver (base station) remains stationary during observation while the other receiver (rover) with unknown coordinates may or not may be stationary.

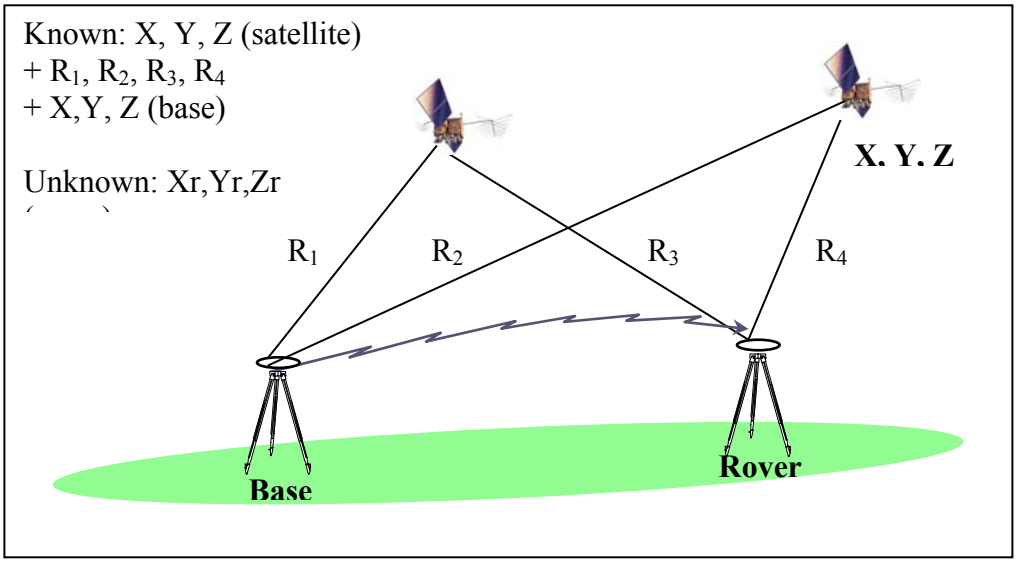

X. Y. Z **Xr. Yr. Zr**

Figure 2.11: The concept of relative positioning

2.3.4 GPS Techniques

There are many techniques in GPS, the techniques include with static GPS, kinematic GPS, real-time kinematic GPS (DGPS), and classical real-time kinematic technique, and the latest technique is network-RTK technique. Further subchapter will explain every technique, however the network-RTK technique will explain in detail in chapter 3.

2.3.4.1 Static Survey GPS

Static survey is a relative positioning method using carrier-phase measurements. Static GPS employs two or more stationary receivers to track the same satellite. In survey works, the used of static surveying includes the control survey, boundary survey and deformation survey. The concept of static survey is based on tracking the simultaneous measurements at both base and rover receivers respectively. Figure 2.12 shows the concept of static GPS.

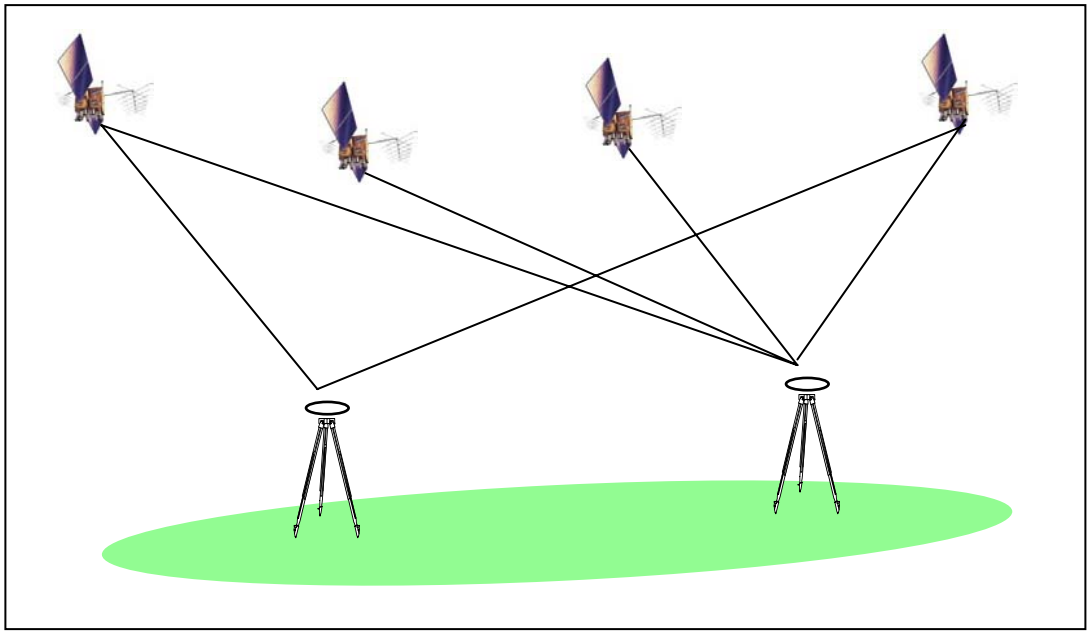

Base **Rover (Unknown)**

Figure 2.12: The concept of static GPS

One receiver is set up as base receiver at known point such as GPS monument (with precise coordinates), while the other receiver is set up as rover at any point (unknown point). Base receiver supports any number of rover receivers as long as both receivers track a minimum of four common satellites.

The observation time for this technique is about 20 minutes to a few hours. Normally static survey requires 60 minutes to 120 minutes observation periods. Static technique ensures high precision positioning, 1 ppm to 0.1 ppm accuracies in which equivalent to millimeter accuracy for baseline up to some kilometers. (Hoffmann-Wellenhof et al, 1994). Static technique with carrier-phase is the most accurate positioning technique. The expectation of accuracy level for 20 km baseline is typically 5mm + 1 ppm (ppm for parts per million and rms for root-mean-square) and for 10 km baseline is 1.5 cm. The measurement recording interval is 15 or 20 seconds. Both single and dual frequency receivers can be use for static positioning.

2.3.4.2 Kinematic GPS

Kinematic technique refers to applications in which the trajectory of a moving object is determined instead of coordinating stationary points and disregarding the trajectory of the rover receiver moves from point to point, the intention of kinematic is to determine the position of the antenna while it is in motion.

Kinematic relative positioning involves at least one stationary receiver as a reference plus one receiver for rover. Similar to static GPS technique, kinematic relative positioning requires all receivers to maintain its lock to at least four or more satellites. To achieve maximum efficiency with this technique, users however need to consider a minimum of five satellites during observation. In general, kinematic technique is suitable for open area that is free of any obstructions. As this technique initialize before the survey by resolving the phase ambiguity to avoid delay, the kinematic GPS technique is suitable for high accuracy work including the gravity field survey, photogrammetry, marine, and producing the topographic map.

2.3.4.3 Real-Time Differential GPS (DGPS)

Real-time differential GPS (DGPS) is more often to be referred as code-based relative positioning. DGPS technique employs two or more receivers to track common satellites simultaneously. One receiver is set up as reference station or base and the other is set up as rover receiver. This method is based on the fact that the GPS errors in the measured pseudoranges at both base and rover receivers within a few hundred kilometers of baseline length are essentially the same.

In principle, this technique requires all receivers to collect pseuodoranges from the same satellites, so the errors corrected by the base receiver are common to a rover receiver. The base receiver remains stationary over the known point. The built-in software in base receiver calculates the differential corrections to obtain the pseudorange errors or DGPS correction. These corrections are transmitted in a format known as Radio Technical Commission for Maritime Service (RTCM) to rover receiver through a communication link. These corrections are used to compute the rover coordinate. Figure 2.13 shows the concept of Real-time differential GPS technique.

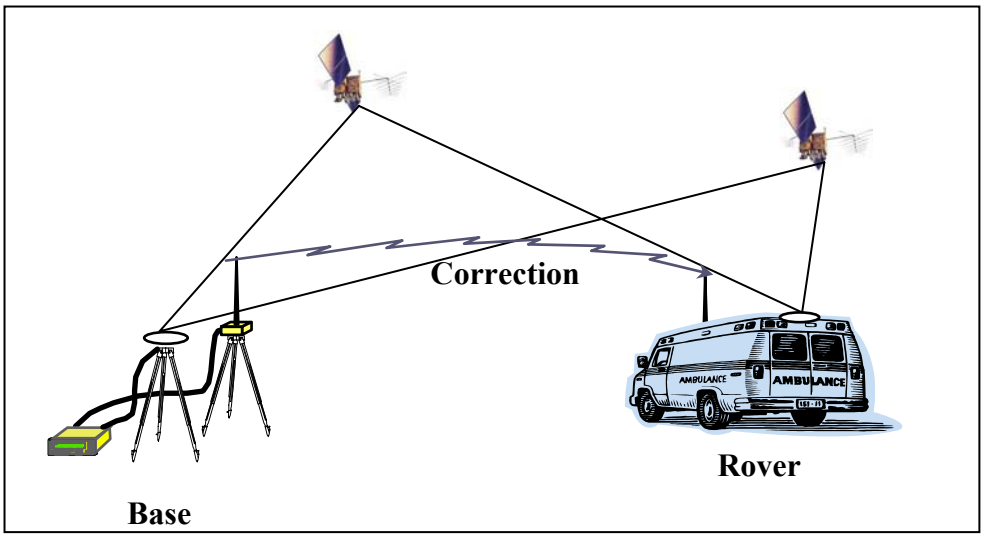

Figure 2.13: The concept of real-time differential GPS technique

According to Hofmann-Wellenhof et al. (1994), this method is capable of obtaining accuracy ranging from submeter to 5m. The accuracy depends on baseline length, the performance of C/A-code receiver and the transmission rate of correction. This is the method that improves the pseudorange accuracy.

2.3.4.4 Real Time Kinematic (RTK-GPS)

In late 1980's, the "modern GPS"[6] positioning begin in earnest. Kinematic technique uses carrier phase and resolved the ambiguity "on-the-fly". This technique is also known as stop-and-go kinematic survey Real-Time Kinematic GPS (RTK) is another name for carrier-phase differential GPS. RTK technology makes GPS a universal surveying tool, replacing traditional surveying technique. RTK technology is based on the first, transmition of pseodurange and carrier phase data from a reference station (base station) to the user station (rover) in real-time, second is resolution of ambiguities at the rover station "on the way" or "on the fly" (OTF) and third, reliable determination of the baseline vector in real-time of near real-time (Seeber, G. 2003).

[6] The year when the first production satellite, Block II was launched.

Nowadays, RTK technique has become widely used for accurate engineering and construction surveys, such as topographic site mapping, construction stake out, construction equipment location, machine control, mineral exploring hydrographic and cadastral surveying. Moreover, this technique is not time consuming. In the early used of GPS, survey result were only available after the survey work had been complete after post process. RTK-GPS technique was introduced to overcome the limitation on conventional technique in GPS. RTK gives the position of a point only at one minute to four minute of time. In RTK-GPS, its real time solutions had help users to know there is any deformation in the structure at real time. The utilization of Real Time Kinematic GPS (RTK-GPS) technique capable of providing 3D coordinates.

The GPS system is usually designed to provide the user with the information of determining 3D-user's position, expressed in geodetic coordinate system latitude, longitude and altitude (ϕ, λ, h) and/or in Cartesian coordinate system (X, Y, Z). With recent advance in GPS technology, cm-level accuracy can be obtained by using a differential GPS carrier-phase approach or RTK-GPS. According to (Ogaja C., et. al., 2000), the advantage of GPS is that the tool can detect the movement if the structure has moved a few cm relative to some reference or baseline while the accelerometers cannot detect directly the absolute or relative displacements of the structure.

RTK-GPS which is as good as static carrier phase positioning in term of accuracy works in real-time. The precision of RTK-GPS is 10 mm ± 1 to 2 ppm (horizontally) and 15-20 mm ± 2 ppm (vertically) component. The sampling frequencies of 10 Hz or even 20 Hz are now available from several GPS receiver. All of these improvements provide a great opportunity to monitor dynamic characteristics of large structure in real-time or near real-time.

In principle, RTK-GPS hardware configuration consists of two or more GPS receivers, three or more radio-modems and a handheld survey data collector/computer survey requires two or more receivers. RTK-GPS can take less than 10 seconds where the receivers are tracking a large constellation of satellites, small PDOP, using dual frequency receiver, no multipath, and low receiver noise. A communication link between the reference and rover receivers is required. Furthermore, RTK-GPS is best used when the distance between the base and rover receiver is approximately 10 km.

In RTK-GPS, one receiver is located over a known point (base receiver or base) and the other receivers called rovers (roving receivers) is located over the observed point (see Figure 2.14). Real-time survey uses radio system to transmit measurements from base receiver. Capable of determining coordinates in real time, the rover receiver will display the rover coordinates in the field.

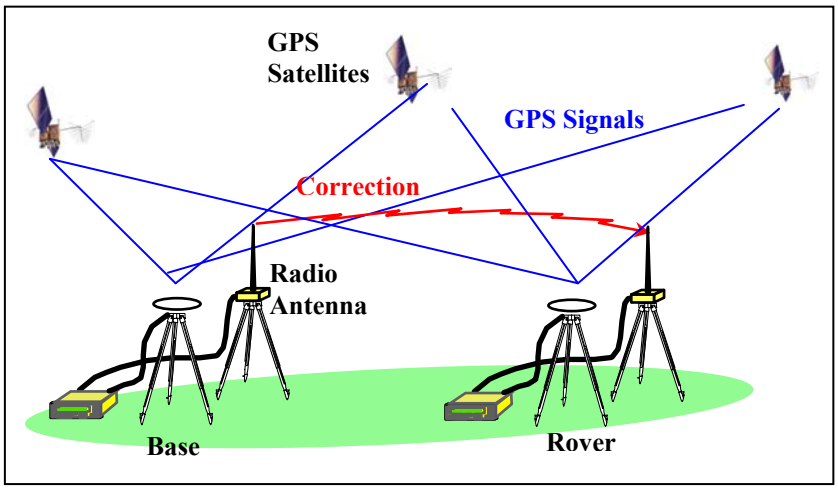

Figure 2.14: RTK Overview

The accuracy and the reliability of the RTK solution decreases with increasing distance from the reference or base station. In practice this means that a temporary RTK base station must be established close to the work area with maximum distance between reference and rover receiver must not exceed 10 to 20 kilometers.

This limitation of classical RTK is caused by distance-dependent biases such as orbit error, and ionosphere and troposphere signal refraction. (Wanninger, L., 2004). According to Al Marzooqi, Y., et al. (2005) the limitation of classical RTK is not only a systematic errors, also range of available radio telemetry solutions. the base station must be established around 5km at work area to ensure accuracy. The classical RTK also need a good coverage of control network. Beside that, productivity of the surveyor is decreased each time the base station has be set up at difference station. Moreover, the other limitation is each surveyor need two sets of GPS receiver to perform the RTK-GPS survey.

Another continuous RTK-GPS observation campaign were conducted to monitor structural behavior and the stability of a wide span bridge namely Penang Bridge (Wan and Ghazali 2003). The total length of the bridge is 13.5 km in span. It is currently the longest bridge in Asia and third longest in the world. Figure 2.15 depicts the overview of the bridge.

Figure 2.15: Penang Bridge, Penang

The result shows that one of the points (PP5) cannot perform properly because the distance between PP5 and reference station is 10.210km. The average of data quality

is 0.340m. Figure 2.16 illustrates the distribution of the interest points on the bridge during the observation.

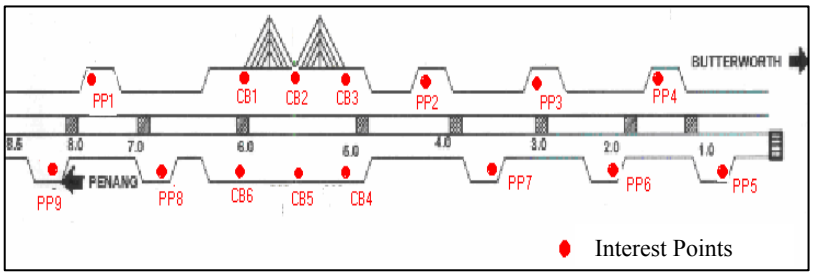

Figure 2.16: The Distribution of 15 Interest Points on Penang Bridge (Wan and Ghazali, 2003)

However, the morden RTK technique of RTK-GPS positioning called Network-RTK with the concept of Virtual Reference Station (VRS) can resolve such limitations. This gives a lot of benefits compared to classical RTK surveys.

2.4 Application of GPS in Structural Health Monitoring

Nowadays, GPS has evolved as an important tool for estimating structural deformation in large engineering structures for examples bridges, dams and high-rise buildings. Continuous GPS measurement can be employed in order to ensure that the engineering structures is exhibiting safe deformation behaviour for the purpose of safety assessment as well as preventing any disaster in the future.

In principle, the RTK-GPS hardware configuration consists of two or more GPS receivers, three or more radio-modems and a handheld survey data collector/computer. In RTK-GPS, one receiver occupies a known reference station and broadcasts a

correction message to one or more roving receivers. The roving receivers process the information to solve the WGS-84 vectors by solving the integers in real-time within the receiver to produce an accurate position relative to the reference station. Precision of RTK-GPS is +/-2 cm + 2 ppm. Furthermore, the sampling frequencies of 10 Hz or even 20 Hz are now available from several GPS receiver. All these improvements provide a great opportunity to monitor dynamic characteristics of large structure in real-time or near real-time.

As engineered structures such as tall buildings are designed and built, an increase in the efficiency of detecting deflections or drift of each building under loading for example wind loading becomes necessary. The equipment such as GPS, which can directly, derives displacement that recently has focused on structures monitoring. The GPS also provides opportunity for a rapid assessment of the state of structures after extreme events for example typhoon or related wind effects. The use of GPS for monitoring tall buildings has evolved rapidly since the onset of processing and instrumentation improvement of the technology. For the health monitoring of structures, sensors, which are reliable and robust, portable, non-destructive and automated such GPS, are well suited. GPS also offer an opportunity for real time or near real-time monitoring that may be able to detect structural failures.

One of the demonstrations of the potential for GPS to be used as sensors was done by Leach and Hyzak (1994). They showed that GPS could be as motion sensor to detect transient and long-term motions of a large cable-stayed bridge. GPS has been utilized for many years in monitoring applications, mainly for crustal and earth deformation. Only recently it has been investigate in the context of continuous monitoring for engineering structures. The capabilities of GPS to provide data on demand and detect any short term variation such as measurement due to wind or traffic loadings has recently been investigated by Lovse et al., (1995); Guo and Ge, (1997), Ashkenazi et al., (1998), Nakamura, (2000), , Tamura et al., (2002), Mat Amin et al., (2002), Mat Amin and Wan, (2003), Breuer et al., (2002), Guo et al., (2005) and

Kijewski-Correa et al., (2006). The aim of these researches is to prove the potential of GPS in deformation survey.

According to Celebi, (2000), relative displacements, which are key to assessing drift and stress conditions of structures, are difficult to be measured directly. Measuring acceleration response requires a double integration process to arrive at displacements and this process can lead to errors in calculation of velocities and displacements. This problem is more acute for permanent displacements. Moreover, accelerometer measurement cannot be used to cover the permanent displacement at centimetre level. Therefore, GPS technology recording at 10 samples per second allows reliable monitoring of long structures such as suspension or cable-stayed bridges and tall buildings.

RTK is a latest GPS positioning technique which offers up to centimetre-level accuracies. In conclusion, RTK techniques are fast, stable, accurate and well suited to deformation monitoring. Kinematic positioning can be very useful in assessing the damage to a building (Celebi et al., 1998, Mat Amin, Z, 2003a & b, 2007, Wan et al, 2005). In addition, the displacement measurement can be made directly in real-time. RTK as the data collection technique can be used to monitor structures, landslides, volcanoes and many others where there is compelling need for continuous and real-time solution.

Duff and Hyzak, (1997) asserts that GPS surveying has several advantages as a monitoring tool for engineering structures. With rapid advancement in the GPS receiver technology and data-processing software, it seems that in the near future, GPS technology will be a much more convenient, fast, accurate and cost-effective method for monitoring the large structural deformation behavior, especially in areas where quick results could save lives and property. Nevertheless, a study that leads to the development

of an efficient real-time health monitoring system for engineering structures is highlighted in this paper.

Numerous researches were done by a number of researchers using GPS for deformation monitoring. Leach and Hyzak (1994) demonstrated the potential of GPS to be used as a sensor. The result showed that GPS could be as motion sensor to detect transient and long-term motions of a large cable-stayed bridge. In Malaysia, the researchers have demonstration the potential of GPS to be used as sensors for monitoring applications. A case study was conducted on the KOMTAR Plaza, Penang, one of the tallest building in Penang with 65 stories and 245 m height. To study the stability of Penang Bridge, Wan Akib. W. A. et al., (2001), conducted two different epochs in November 2003 and February 2001. The continuous RTK-GPS application has been successfully applied as a monitoring tool for a high rise building. The research was performed at Sarawak Business Tower which is located at Johor Bahru. This building's structure is consisted of 30 stories tower. (Wan et al., 2005). Figure 2.17 depicts the overview of the building.

Figure 2.17: Sarawak Business Tower

Both studies showed the stability of the structure through static test. The demonstration of RTK-GPS for continuous monitoring was conducted during these studies. The results have show that the continuous RTK can provide the highest accuracy in deformation monitoring. The RTK technique represents a technological solution to the problem of obtaining high productivity.

2.5 Summary

This chapter gives many info about monitoring tools include the conventional and modern technique. Each tool has advantages and disadvantages. however, this chapter focuses on the brilliant GPS technique and the used of GPS in SHM.

CHAPTER 3

VIRTUAL REFERENCE STATION AND MALAYSIAN RTK NETWORK

3.1 Introduction

This chapter overviews the concept, system architecture and example of the sophisticated network-RTK used in solving the limitation of classical RTK-GPS technique. Further discussions include the overviews on the Malaysian network-RTK namely MyRTKnet and its novel contributions and advantages in supporting services rendered by GPS for local navigation, engineering and mapping purposes.

3.2 RTK Network

Nowadays, series of GPS continuously operating reference station (CORS) network or RTK network has been established in many parts of the world. The architecture of the network can be divided into single reference station and multiple reference stations. In general, the concept of single reference station relies on a GPS receiver, data communication link to user or radio link, the reference station and interface for communication link. As single reference station is limited to limited number of station at one time, the multiple reference station on the other hand connects to a central control station that connects multiple reference stations using ingenious data communication link. Example of the data communication link used in this concept includes wireless radio link and cable connection via local area network (LAN).

Compared to the single reference station, multiple reference station includes modem for data transfer and data modification of the station software. The RTK network in general models the orbital and atmospheric errors over the network area, which decreases the number of necessary reference stations similarly. The network RTK enables positioning the accuracy up to a few centimeters in both horizontal and vertical component of operating over distances up to tens of kilometers. As the reference station must be developed in a dense enough pattern to model distance-dependence error, Figure 3.1 shows the area coverage of single reference station and RTK network.

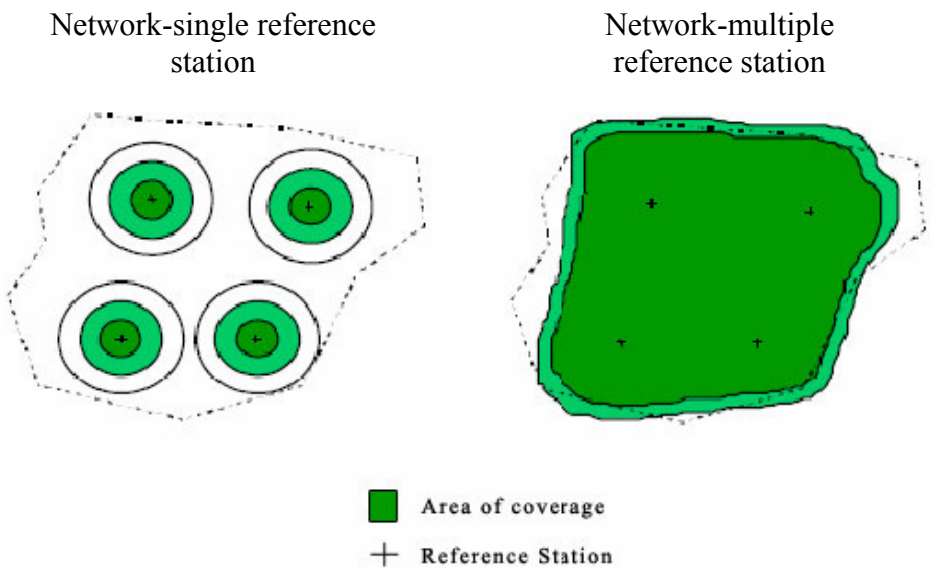

Figure 3.1: Area coverage of single reference stations versus RTK Network (Wahlund, S. 2002)

The use of a network of reference stations instead of a single reference station allows to model systematic errors in the region and thus provides the possibility of an error reduction. Apparently, in addition to the German SAPOS system currently, there are six major state have decide to use the Trimble solution (Landau, et. al., 2002). These include the RTK network infrastructure in Denmark and Switzerland, for example it also using a Trimble solution with Trimble references station receivers and Trimble network server software GPSNet. The virtual reference station network concept was firstly introduced in a part of German reference station network SAPOS (Trimble, 2001). Figure 3.2 shows the system architecture of VRS concept.

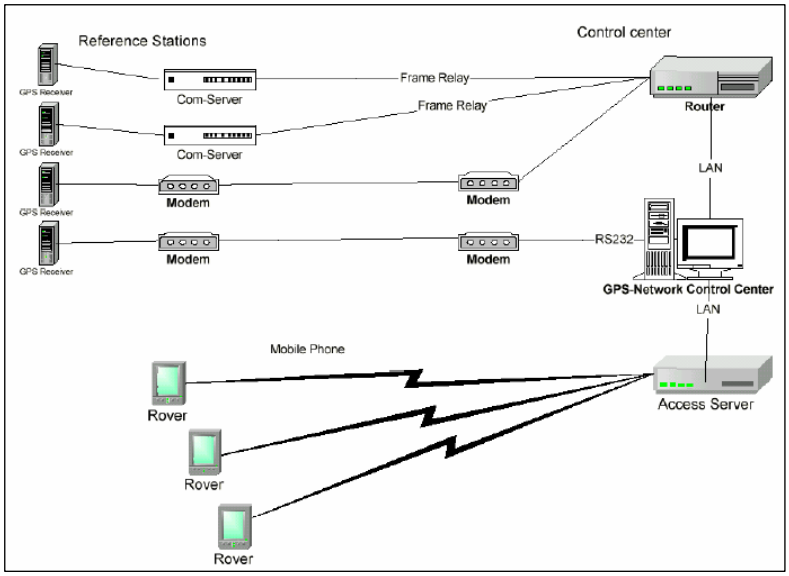

Figure 3.2: System architecture of the VRS concept (Trimble, 2001)

The presented concepts are implemented in a number of reference station networks. Amongst others well-known networks included Germany (see Figure 3.3), Denmark (see Figure 3.4), Japan (see Figure 3.5), Switzerland (see Figure 3.6) Australia (see Figure 3.7), and Singapore (see Figure 3.8).

The number of reference stations developed within these networks varies accordingly. In German for example, there are 14 stations available in total. As far as the Denmark VRS network is concerned, there are 27 stations, followed by 7 stations in Sydney, Australia, and 5 stations in Singapore.

Figure 3.3: VRS Network in Germany (Landau, et. al., 2002)

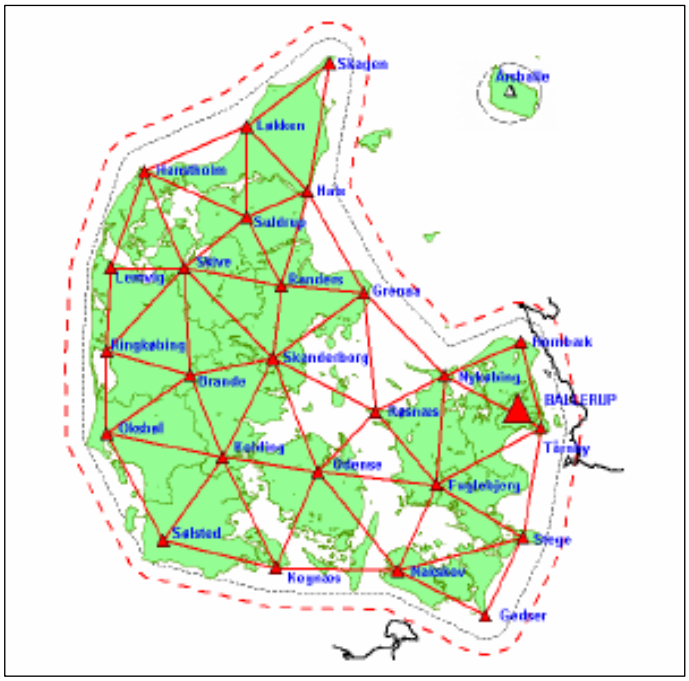

Figure 3.4: VRS Network in Denmark (Landau, et. al., 2002)

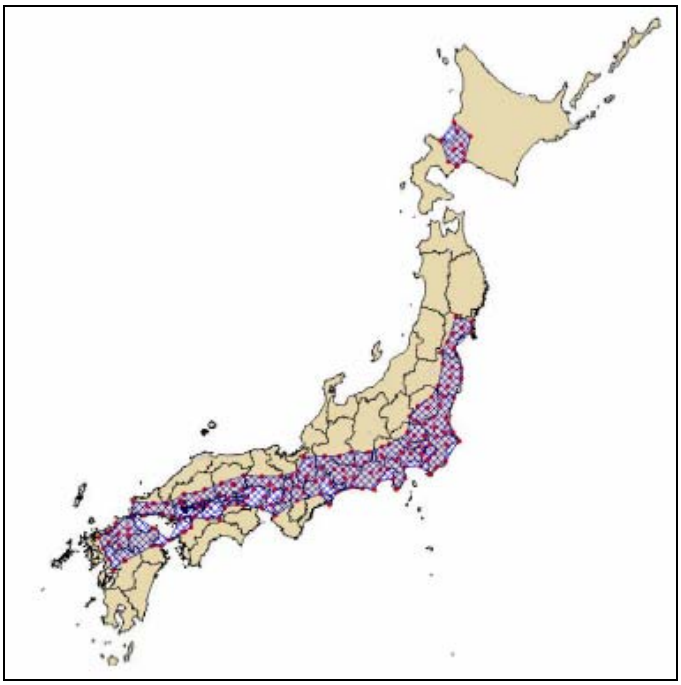

Figure 3.5: VRS Network in Japan (Landau, et. al., 2002)

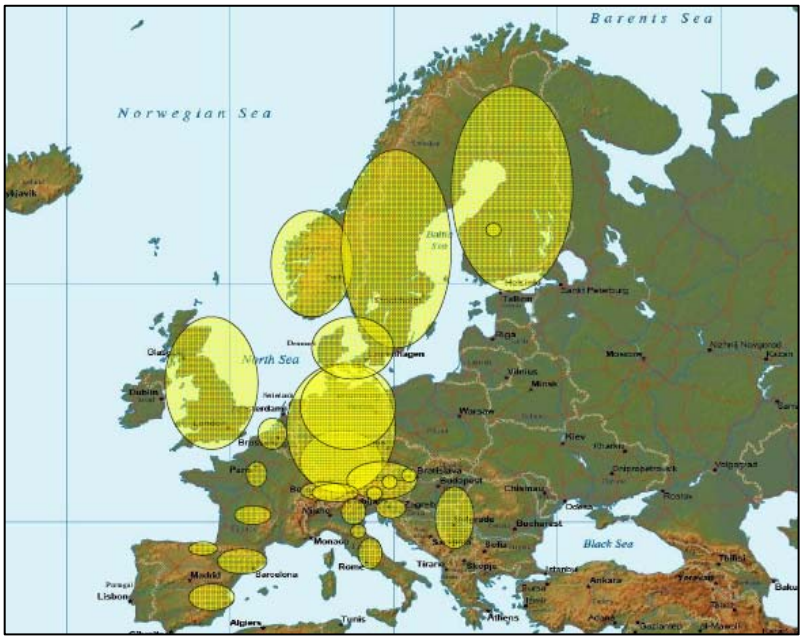

Figure 3.6: VRS Network in Switzerland European (Landau, et. al., 2002)

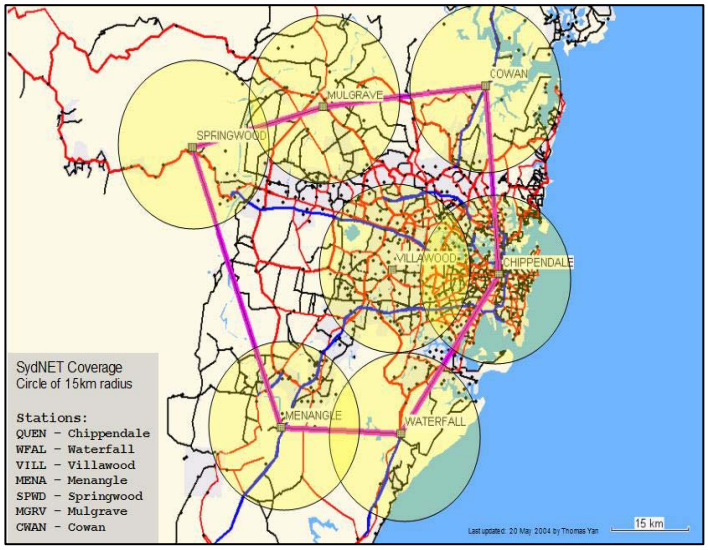

Figure 3.7: VRS Network in Sydney Australia[7]

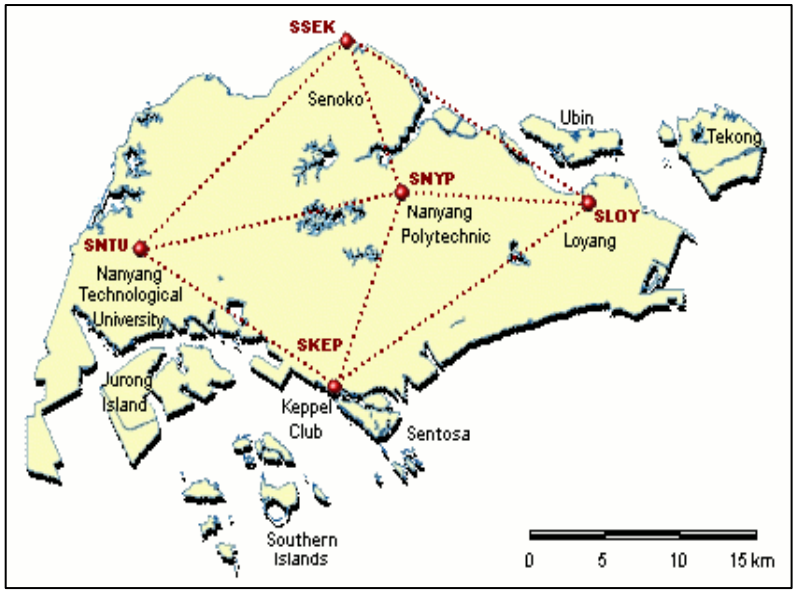

Figure 3.8: VRS Network in Singapore[8]

[7] Source-http://sydnet.lands.nsw.gov.au/sydnet
[8] Source-http://www.sirent.inlis.gov.sg/body/docs/SiReNT_papers

Landau, et. al., (2002) performed a study to evaluate the performance of RTK in single-baseline and network modes. Based on around Munich, Germany of BLVA network in Bavaria, four concurrent tests were conducted over a 40-hour period. In general, the results of network corrected data provide noticeable benefits especially in term of the time-to-initialize statistics. The majority of initializations process based on network corrected data.

Santala, and Totterstrom, (2002) has demonstrated that VRS is the solution for reduce or eliminate the RTK relative positioning error depending on the distance of rover from base station. Beside that, VRS improve significantly both productivity and measurement quality. A few permanent reference stations are linked together to form RTK network. Moreover, the VRS-RTK Network software monitor continuously in real time the whole RTK Network system and all data send to users are high quality checked.

RTK network is a way of increasing the range of the RTK corrections. Since the atmospheric errors are distance dependent, the single station RTK corrections may not work on distances above 10 km or less (Vollath et al. 2000). This means that there will be a great number of reference stations if one intends to cover a larger area. Network-RTK models the orbital and atmospheric errors over the network area, which decreases the number of necessary reference stations. This technique of creating raw reference station data for a new, invisible, unoccupied station is what gives the concept its name, “The Virtual Reference Station Concept” (see Figure 3.9).

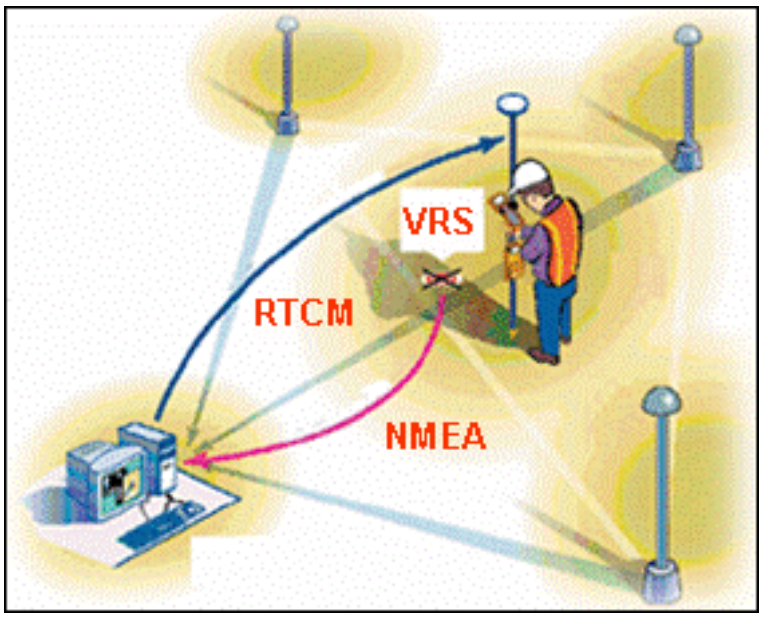

Figure 3.9: The concept of Virtual Reference Station (DSMM 2005)

A working system for RTK network consists of several important and complicated steps; generate the error corrections by modeling atmospheric errors, parameterization of these corrections in a way understandable to the rover receiver, transfer of the corrections to the user and fix ambiguity resolution in real time. Each of these steps must work in a satisfactory way, independently and together, to form a working system.

In conclusion, the RTK network are easy, quick, hands-off, accurate, homogenous, repeatable, cost efficient, labour saving, all these term describe the RTK network which bring private sector surveyors in large number to use this network to great benefit and becoming increasingly for many precise application which included surveying, construction and many other (Henning, W., 2006). This can be drew that network-RTK have been well resolved the error and biases for good accuracy and this network-RTK is competent for SHM, the following subchapter will discuss on Malaysian network-RTK in detail.

3.3 Malaysia Real-Time Kinematic Network (MyRTKnet)

MyRTKnet is a new nation-wide GPS network and system infrastructure developed for GPS users to provide RTK and DGPS services with unmatched accuracy and coverage for positioning applications across the country. As a wide area satellite based service, the broadcast MyRTKnet corrections can be obtained anywhere in Malaysia. The positioning data from MyRTKnet reference stations is optimized for Malaysia, resulting in superior centimeter-level accuracy with most GPS receivers.

Initially comprised of 25 RTK reference stations by 2007 the DSMM have made an effort to enhance the MyRTKnet servicebality by building more MyRTKnet stations in Malaysia. Currently, there are 73 RTK reference stations forming the MyRTKnet network, covering the whole of Peninsular Malaysia and two major cities in Sabah and Sarawak. The stations track GPS signals and send them via dedicated data lines to a central network server at DSMM Geodesy Section, which manages and distributes GPS correction data to subscribers in real time. Subscribers will be receiving data on their own devices via wireless technology using internet-based infrastructure. MyRTKnet broadcasts a 1 Hz dual-frequency data sampling rate using standards Radio Technical Commission for Maritime services (RTCM) data format continuously, 24 hours a day.

In general, there are dense network and less dense network. The present coverage of MyRTKnet includes three dense networks that provide centimeter accuracy around Lembah Klang, Pulau Pinang and Johor Bahru, and a sparse network covering the whole nation. Other areas in the vicinity of 30 km radius from the permanent reference stations will also provide centimeter accuracy. Figure 3.10 shows the RTKnet stations in Malaysia

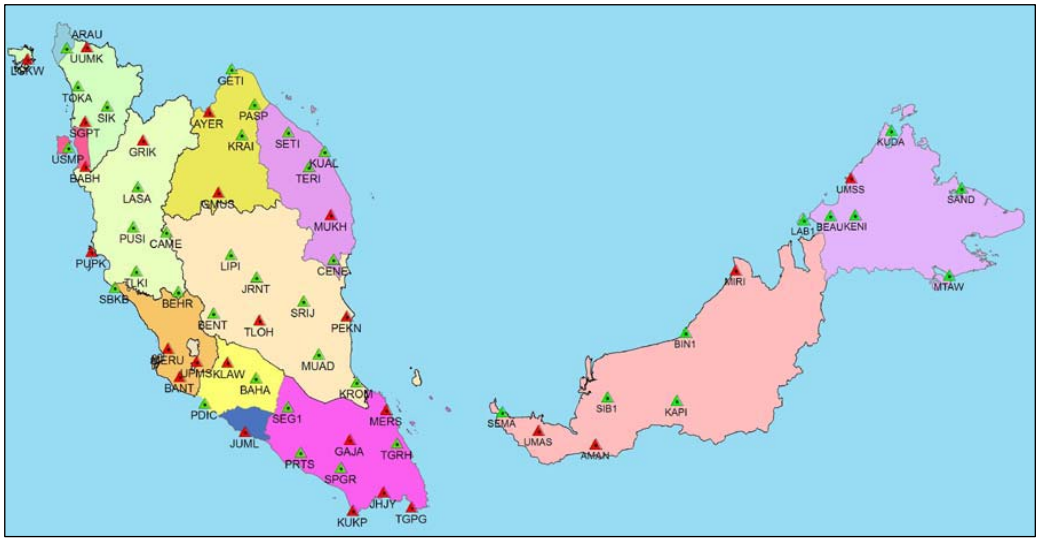

Figure 3.10: RTKnet stations in Malaysia (DSMM, 2008)

The MyRTKnet offers the flexibility of enabling both RTK and DGPS operations. While RTK operations are limited to 30 km from MyRTKnet reference site, the DGPS operations can extend further, advisably to 150 km. MyRTKnet provides high performance solution for real-time data collection needs for Malaysian users. The network, which includes the provision of redundancy at the data collection, transmission and processing layers, has a high degree of service reliability. Figure 3.11 illustrates the MyRTKnet system.

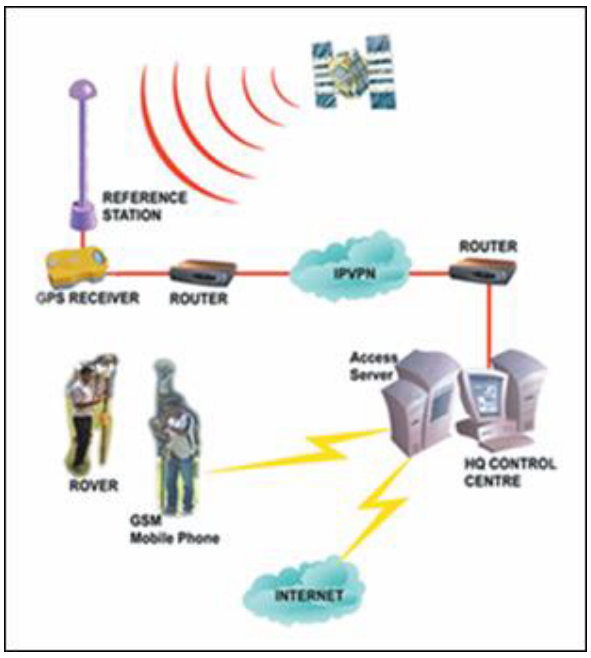

Figure 3.11: MyRTKnet system (DSMM, 2008)

The network-RTK is able to serve multiple concurrent VRS users, and provide these users with correction data for their surveys MyRTKnet provides various levels of GPS correction and data. Their use will depend on the technique and application to be employed by the users. Virtual Reference System (VRS) data, Single Base data and Network Base DGPS data are meant for real time applications whereas Virtual RINEX and RINEX data are for post-processed applications.

The rover receiver sends the approximate position to the control center that is running GPSNet using a mobile phone data link, such as GSM (Global System for Mobile communications), 3G (Third Generation: developed by the global GSM community as its chosen path for 3G evolution) and GPRS (General Packet Radio Service), to send a standard NMEA (National Marine Electronics Association) position string called GGA (GPS fix information). The control center will accept the position, and responds by sending RTCM correction data to the rover. As soon as it is received, the rover will compute a high quality DGPS solution, and update its position. The rover then sends its new position to the control center. The network server will calculate the

new RTCM corrections so that they appear to be coming from a station right beside the rover. It sends them back out on the mobile phone data link. This VRS technique provides integrity monitoring with all users sharing the same common established coordinate frame.

In this country, there are many companies providing the mobile phone data link services such as Celcom, Maxis and Digi. Figure 3.12 and 3.13 depict the distribution of network coverage of Maxis and Celcom.

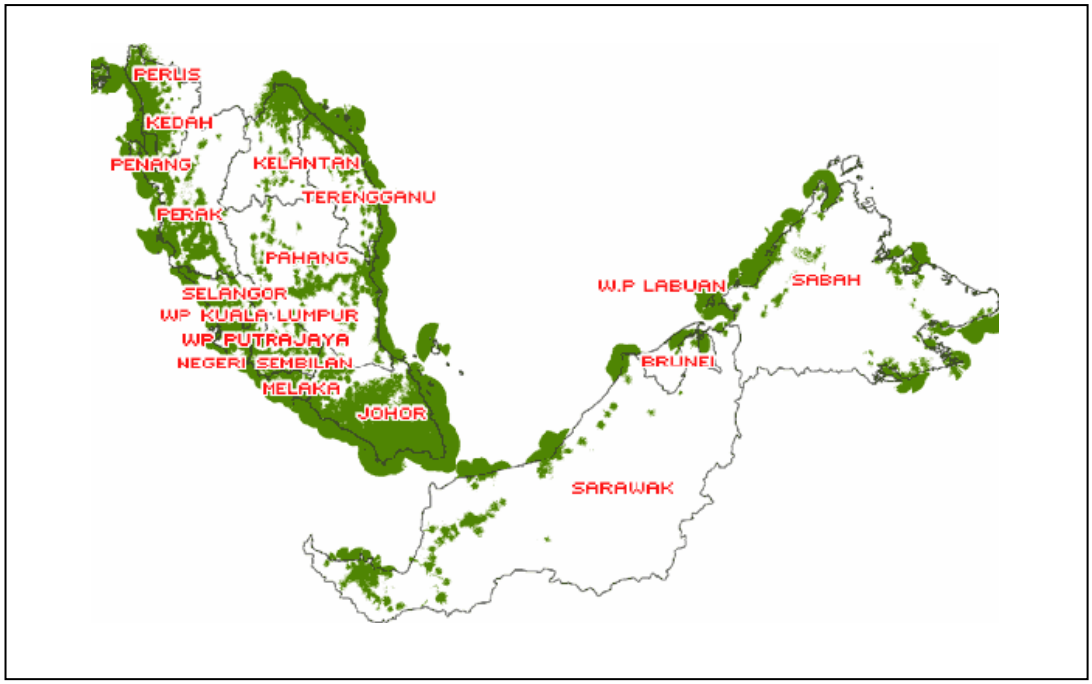

Figure 3.12: Maxis Coverage in Malaysia [9]

[9] Source-http://www.maxis.com.my/3G/coverage_local.asp

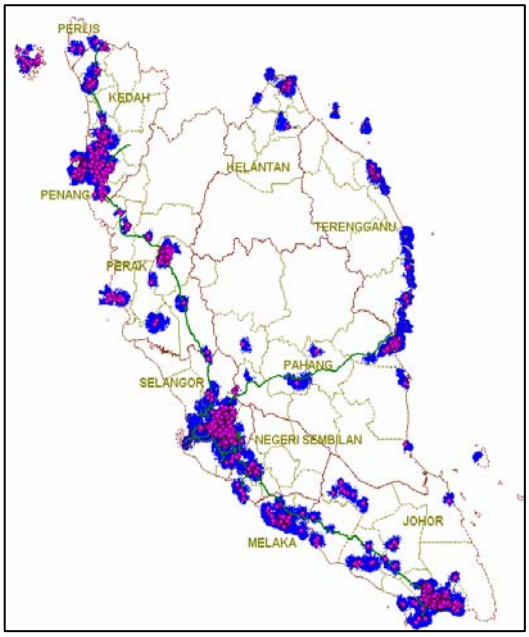

Figure 3.13: 3G Celcom Coverage with HSDPA sites in Penisular Malaysia in 2007[10]

3.3.1 MyRTKnet Reference Station Configuration

The configuration of the MyRTKnet is included with configuration of RTK reference station and configuration of MyRTKnet control centre. According to Ali, H. et. al. (2005) and Abu, S. (2006) each RTK reference station consists of seven components as follows:

1. Cisco 1721 router
2. Dlink 5 port 100/10M switch
3. Trimble 5700 CORS with Zephyr antenna
4. Moxa 5410 terminal server
5. Advantech Adam 6017 A/D module
6. Micromate UPS for minimum 3 days backup power
7. Associated lightning protection

[10] Source-http://www.gsmworld.com/cgi-bin/ni_map.

Configuration of RTK reference station is as illustrated in Figure 3.14. The example of reference station monument pillars on the other hand is as shown in Figure 3.15. Figure 3.16 illustrates the example of the reference station cabin and equipment

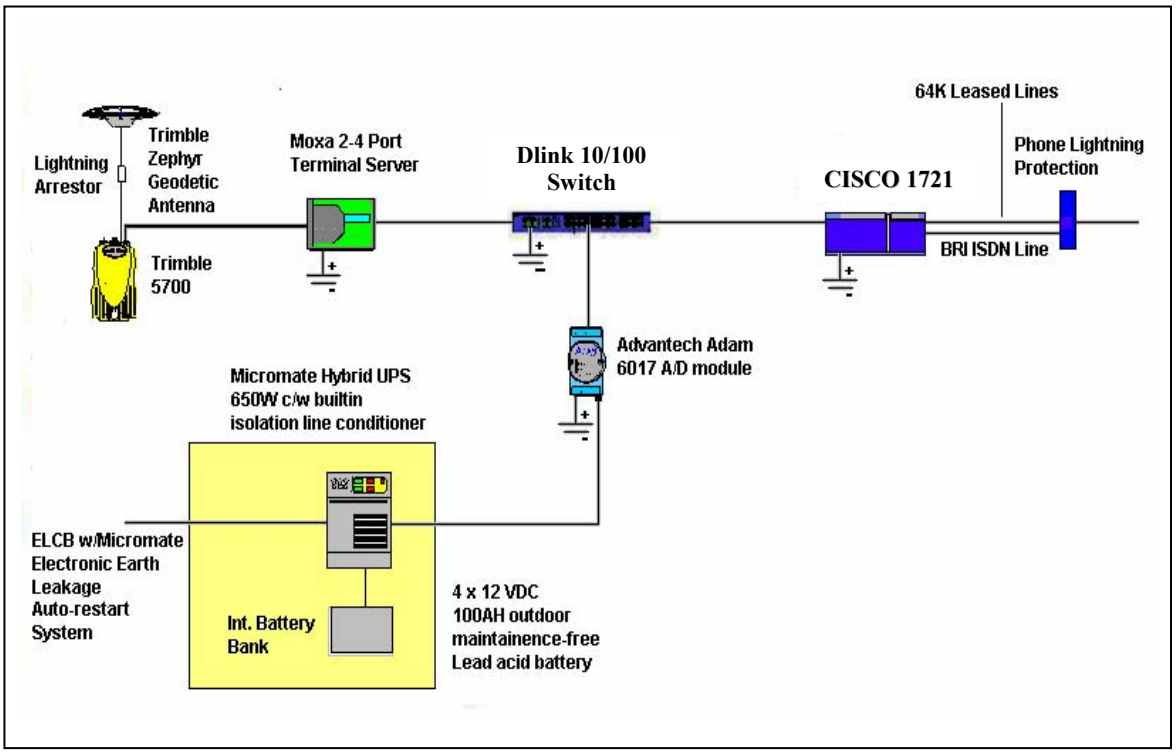

Figure 3.14: Configuration of RTK reference station (DSMM, 2005)

Figure 3.15: Reference Station Monument Pillars

Figure 3.16: Example of Reference Station Cabin and Equipment

Directly connected to the MOXA 5410 Terminal Server (TS) serial, Trimble 5700 is a 24 channel dual frequency RTK GPS receiver that have been used in every reference stations of MyRTKnet. With tough, lightweight and fully sealed magnesium alloy casing, this receiver is well-equipped with Trimble Zephyr Geodetic Antenna to provide low multipath and elevation tracking with sub-millimeter phase center accuracy.

In each RTK reference station, GPS receiver records observables such Coarse Acquisition (C/A) code, P/Y code and L1/L2 carrier phases simultaneously 24 hour a day. These data will be then transmitted from RTK reference stations to the Control Center through leased line with ISDN backup in IPVPN communication network.

In general, RTK reference stations have been established after some considerations on site conditions such satellite availability and station access. Sky visibility, on-site power sources, nearby electrical installations and possible multipath causing surfaces such metallic fences, structures and water surfaces have also been taken into account.

3.3.2 MyRTKnet Control Centre

Control Center which is situated at Geodesy Section in DSMM Headquarter consists of twelve components as follows (Ali, H., et. al. 2005 and Abu, S. (2006)):

1. Trimble GPSnet (DGPSnet & RTKnet) Software
2. GPSNet1 & GPSNet2 server
3. Maintenance server for system monitoring and data archiving
4. CISCO 3745 router for access to the Internet and GITN cloud
5. HP Printer
6. UPS to hold the system for 3 days backup
7. Monitor for GPSNet Servers
8. Monitor for GPStream Server
9. KVM Keyboard for GPSNet Servers
10. GPStream server for web server and data distribution
11. Monitor for Maintenance Server
12. 3 COM 24 ports 10/100/1000 switch

Received by CISCO 3745 router in the Control Center, collected data from the reference stations will be then transmitted to servers in the system rack via 3 COM 24 ports connector. Technically, these data will be managed and distributed by GPStream server to GPSNet1 server before being logged and delivered to subscribers in real time. If an error occurred to GPSNet1 server, GPSNet2 which is also online through Ethernet link and works as secondary server will automatically replace and pursue its function

instantaneously. This provides a good performance in term of data availability using MyRTKnet.

Apart from storing RINEX and alarming data to CD for post processed application, another server called Maintenance and Archiving Server is also capable of monitoring the physical status of RTK reference stations within 5 minutes interval in order to ensure MyRTKnet data are free from errors and omissions. Furthermore, this server is also capable of monitoring logged subscribers for every second. Figure 3.17 depicts the Control Center configuration followed by an overview of its networking scheme in Figure 3.18. Figure 3.19 illustrates the overview of MyRTKnet Control Centre at DSMM, Kuala Lumpur.

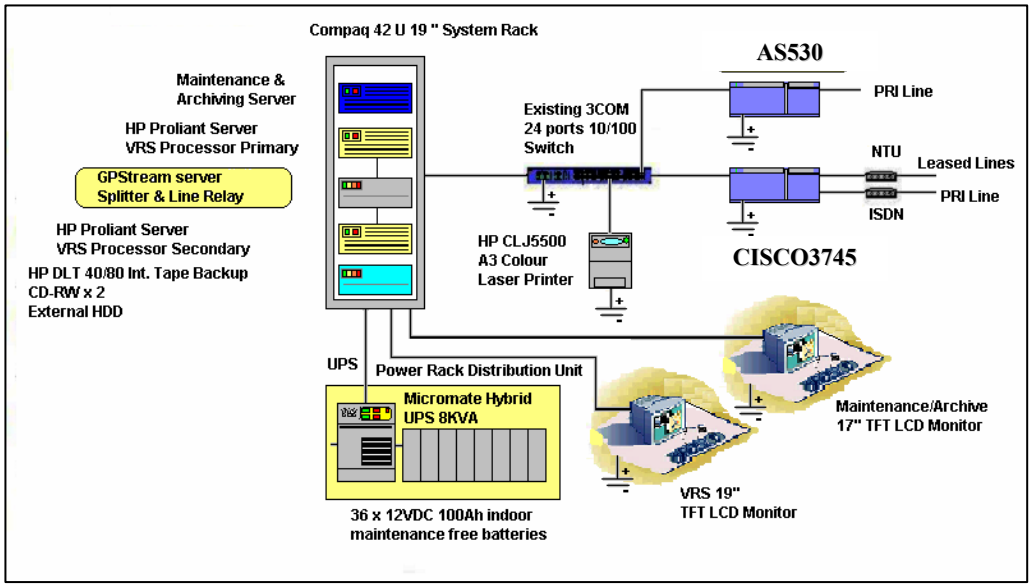

Figure 3.17: Configuration of MyRTKnet control centre (DSMM, 2005)

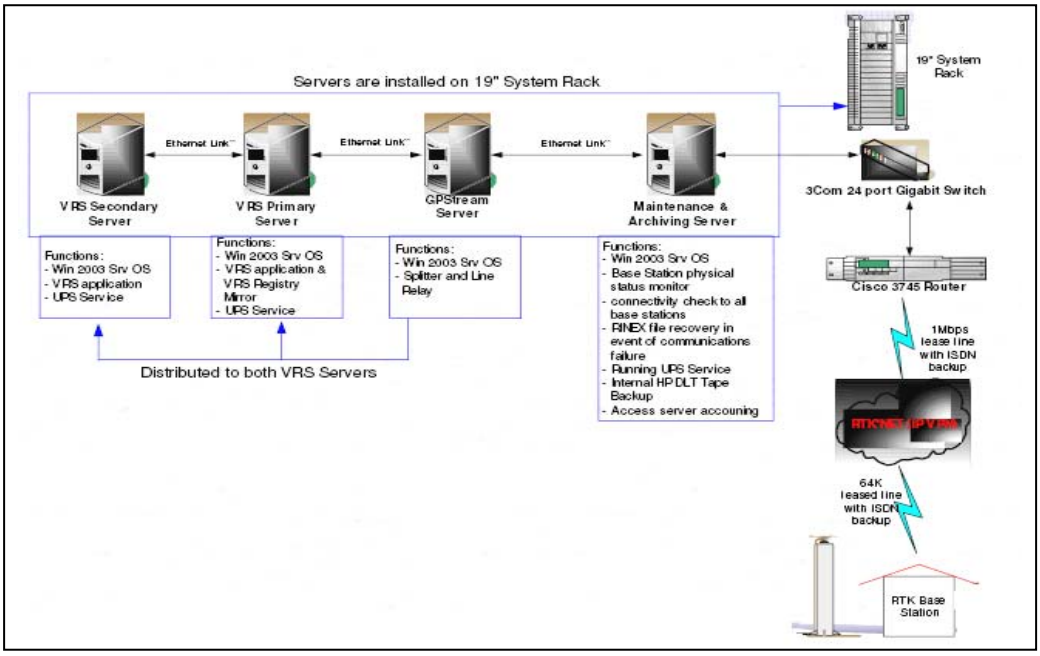

Figure 3.18: MyRTKnet control center networking (DSMM, 2005)

Figure 3.19: MyRTKnet Control Centre and Equipment

3.3.3 MyRTKnet Accuracy Estimation

Network-RTK provides high accuracy within dense network up to centimetre level. This could also be achieved within 30 km of MyRTKnet reference station. The depict information of MyRTKnet accuracy is shows in Table 3.1 and Table 3.2 shows the suitability of positioning methods.

Table 3.1: Design accuracy of MyRTKnet (DSMM 2005)

Operation mode	Design Real-time accuracy @ 95% confident level (single-point positioning mode)	
	Horizontal	Vertical
VRS	4 cm	6 cm
Single Base	4 cm	6 cm
Network DGPS	0.3 m	0.6 m

Table 3.2: Suitability of Positioning Methods (DSMM 2005)

Application	Static & Rapid Static	Stop & Go Kinematic	Real-Time RTK	Network RTK (MyRTKnet)
Geodetic Control	√	*	×	√
Network Densification	√	*	*	√
Cadastral surveys	×	*	*	√
Topographic survey	×	*	*	√
Large scale mapping	×	*	*	√
Building survey	×	×	*	√
Setting-out	×	×	*	√
√ = well suited	* = partly suitable		× = unsuitable	

According to Abu, S. (2006) it is noted that the accuracy of horizontal component for position error in North component (see Figure 3.20) based on VRS data

of 99% confidence level is less 26 mm while the position error in East component (see Figure 3.21) based on VRS data, the error of 99% confidence level is less than 21 mm. The accuracy of vertical component (see Figure 3.22) based on VRS data of 99% confidence level on the other hand is less than 49 mm. Here, it is apparent that the accuracy of the horizontal component is almost twice better compared to the vertical component.

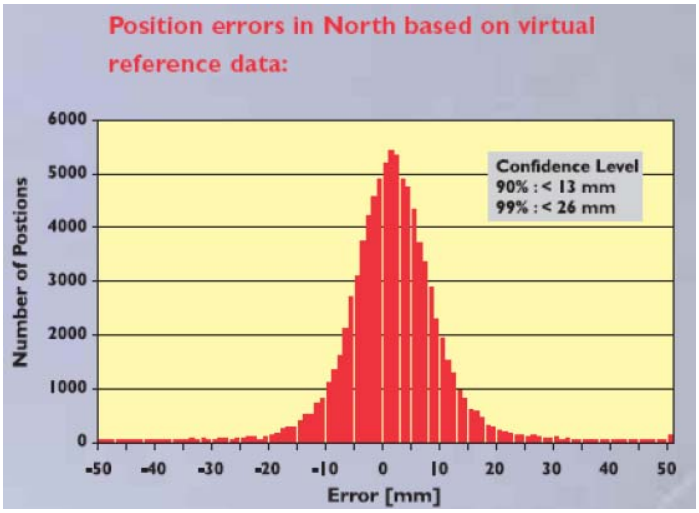

Figure 3.20: Position errors in North (horizontal component) based on VRS data (Abu, S. 2006)

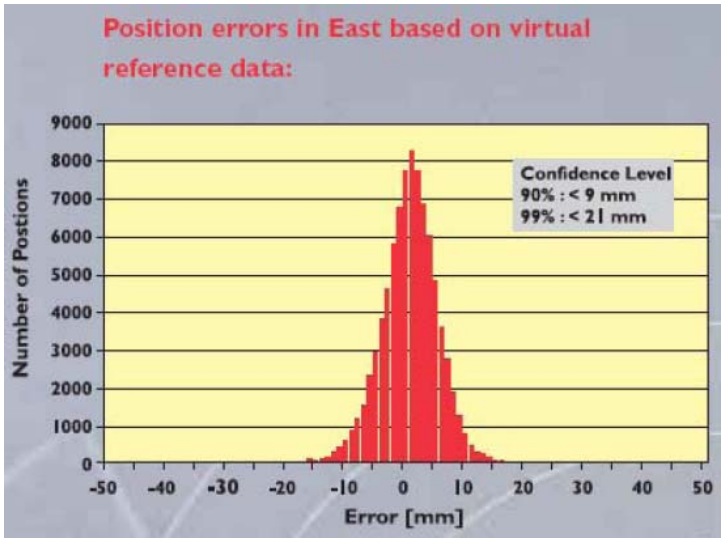

Figure 3.21: Position errors in East (horizontal component) based on VRS data (Abu, S. 2006)

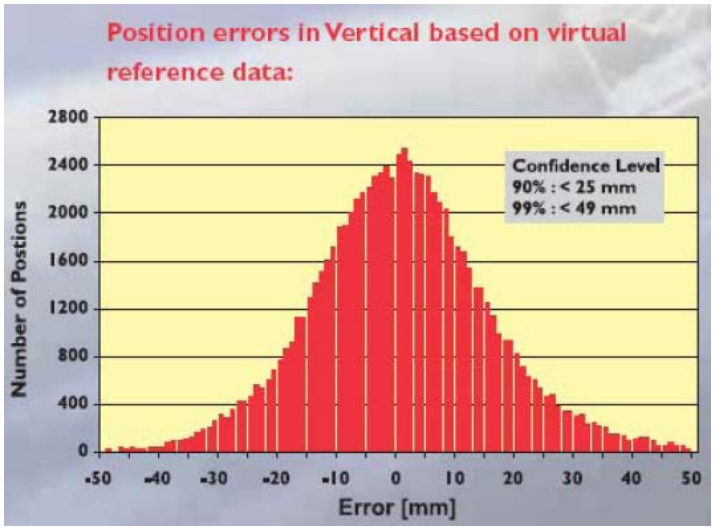

Figure 3.22: Position errors in vertical component based on VRS data (Abu, S. 2006)

Normal distribution trends can also be seen based on the VRS data. As far as the number of position is concerned, it is also notes that the accuracy of each positioning component (Easting, Northing and Height) increases with increases in the number of positions. Further study have also been made by Abu, S. (2006) to study the

initialization times for RTK cold starts based on virtual reference data. As it is apparent that the performance increases when the initialization time increases. Figure 3.23 depict the result of the study.

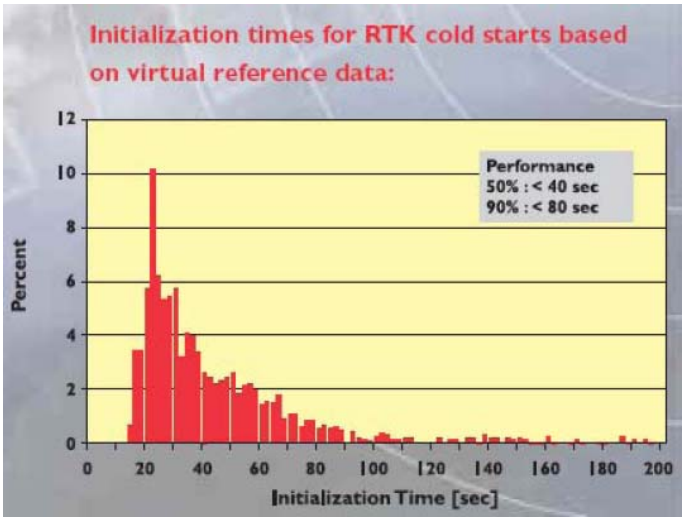

Figure 3.23: Initialization times for RTK cold starts based on VRS data (Abu, S. 2006)

These studies can be divided in dense area and less dense area. The dense areas include of Johor state and Selangor state while less-dense area include of Terengganu state. At present, in Johor (see figure 3.24), nine RTK reference stations are available and well distributed throughout the state. There are seven reference station in Selangor state (see Figure 3.25) and five reference station in Terengganu state (see Figure 3.26). Details on the history, formatting and services of MyRTKnet can be referred via www.rtknet.gov.my (RTKnet server) (see Figure 3.27).

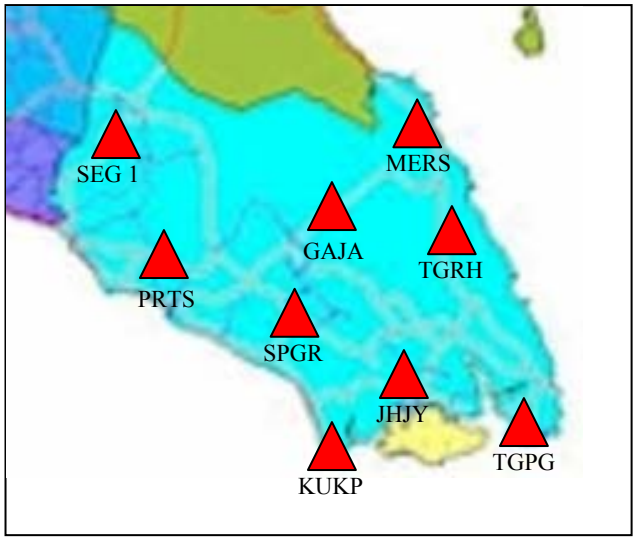

Figure 3.24: Distribution of MyRTKnet reference station in Johor

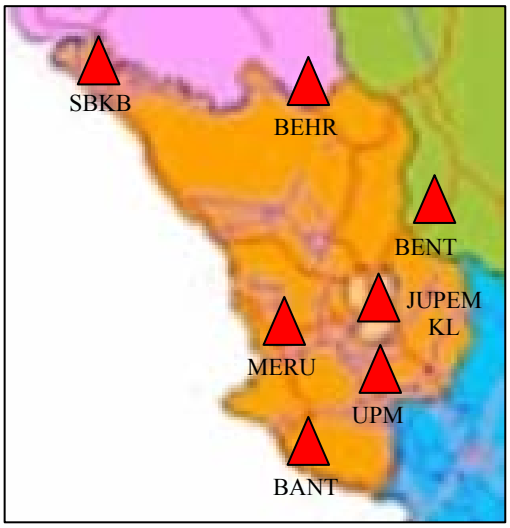

Figure 3.25: Distribution of MyRTKnet reference station in Klang Valley

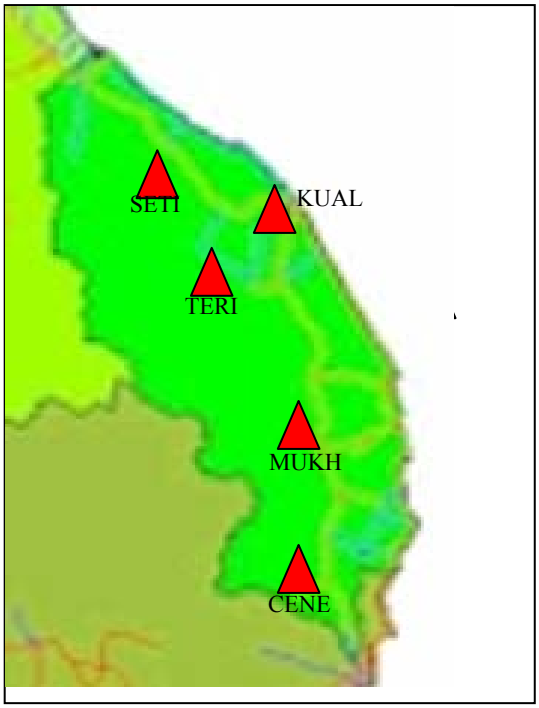

Figure 3.26: Distribution of MyRTKnet reference station in Terenganu

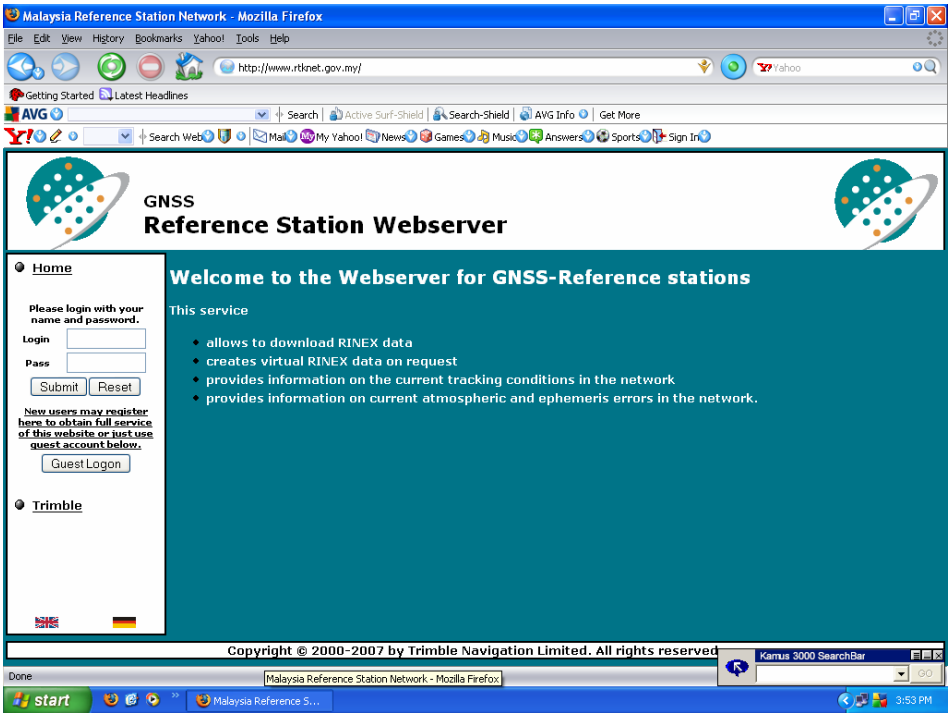

Figure 3.27: RTKnet website references

3.4 Summary

This chapter elaborate the good potential of Malaysian RTK network. This gives a good opportunity for surveyors to use this infrastructure in all survey work. The providing high accuracy is suitable for precise works. The DSMM will upgrade this infrastructure by time to time and the target is by 2015, the number of references station will increase up to 150 stations in Malaysia and this will increase the accuracy. By year 2013 – 2015, the reference station all around the world will be increases more than 4 times of number of reference stations. The best services provided by DSMM of MyRTKnet time to time is not a limitation for user to not to use it. The global trend also allows the surveyor to use this reliable method for all survey work.

CHAPTER 4

GPS CALIBRATION AND SIMULATION OF STUDY

4.1 Introduction

These chapter overviews on the research tools (i.e. Topcon receiver), the calibration test and simulation testing process conducted in this study.

4.2 Instruments

There are a set of instrument that were used for monitoring work. Among others, include as list:

1. Controller FC-200 Rugged
2. Topcon HiPer Ga receiver
3. Cellular phone
4. Download cable and laptop
5. Tripod and tribach or Pole
6. Tape measurement
7. USB download cable

The Controller FC-200 Rugged instructs the GPS receiver that it is going to use a VRS-RTK type of solution with the radio/corrections source connected to serial port 3. Dial the cell phone to connect to GPRS and runs an application to select the NTRIP source and then to decode the NTRIP formatted corrections and output the pure RTCM, CMR or CMR+ to the GPS receiver. To perform VRS-RTK observation mode, numerous surveying tools were used.

The HiPer Ga receiver offers the latest in advanced technology and sophisticated design at an extremely affordable of a small size. Moreover, the HiPer Ga receiver has a lightweight design and dual constellation satellite tracking. This economical RTK base and rover solution features digital radio, Bluetooth wireless technology, and dual constellation upgradeability. Figure 4.1 shows the Topcon Hiper GA instruments.

Figure 4.1: Topcon Hiper GA instrumentation

The HiPer Ga features GPS satellite tracking capability standard, with the add bonus of optional GLONASS satellite tracking. Furthermore, the HiPer Ga can be used as a cable-free base and rover system for traditional application or as two rover receivers

from fixed base station or GNSS network system, via radio or cellular communication. This receiver is a wireless dual constellation GPS System which advanced performance center-mount RTK UHF antenna.

This receiver integrated with 40 channel dual frequency receiver with special features with advanced multi-path mitigation. This added advantage virtually eliminates downtime due to poor satellite coverage or in those difficult environments where satellite obstructions knock out GPS only systems. Table 4.1 shows the physical specification of Topcon HiPer Ga receiver, Table 4.2 shows the satellite tracking specification of Topcon HiPer Ga and Table 4.3 shows the accuracy of Topcon HiPer Ga receiver. Detail specification of Topcon HiPer Ga receiver is attached in Appendix A

Table 4.1: Physical Specification of Topcon HiPer Ga receiver

Physical	
Dimensions(mm)	W:159 x H:173 x D113
Weight	1.65 Kg
Enclosure	Aluminum Extrusion
Antenna	Internal

Table 4.2: Satellite Tracking Specification of Topcon HiPer Ga

Satellite Tracking	
Signal Tracked HiPer GA	GPS and GLONASS L1/L2 C/A, P-Code, Full Code & Carrier
Channels	40 channels L1/L2
WAAS/EGNOS	Available
Cold Start	<60 sec
Warm Start	<10 sec
Reacquisition	<1 sec
Multi-path mitigation	Advanced multi-path mitigation

Table 4.3: Accuracy of Topcon HiPer Ga receiver

Accuracy	
Static, Fast Static L1+L2 L1	 H: 3mm+0.5ppm x D, V: 5mm+0.5ppm x D H: 3mm+0.8ppm x D, V: 4mm+1.0ppm x D”
Kinematic, RTK L1+L2/L1	 H: 10mm+1ppm x D, V: 15mm+1ppm x D”
DGPS	0.3m Post Processing, <0.5m Real-time

While performing VRS-RTK, the controller FC-200 connects the Topcon Hiper Ga receiver and mobile phone. Operating on Windows CE using TOPSURV Field Software, the collected data was downloaded using Topcon Link office software. Topcon Link software also was used to convert the raw data (TPS format) to CSV format (real-time data) or RINEX format (post processing data). Figure 4.2 shows the function of the Topcon HiPer Ga receiver. Figure 4.3 shows the interface of Topcon TopSURV field software and the interface of Topcon Link office software.

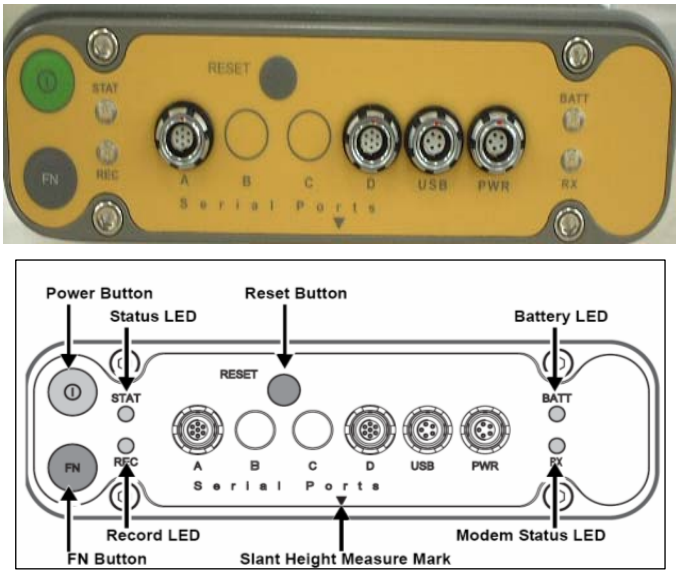

Figure 4.2: Function of the Topcon HiPer Ga receiver

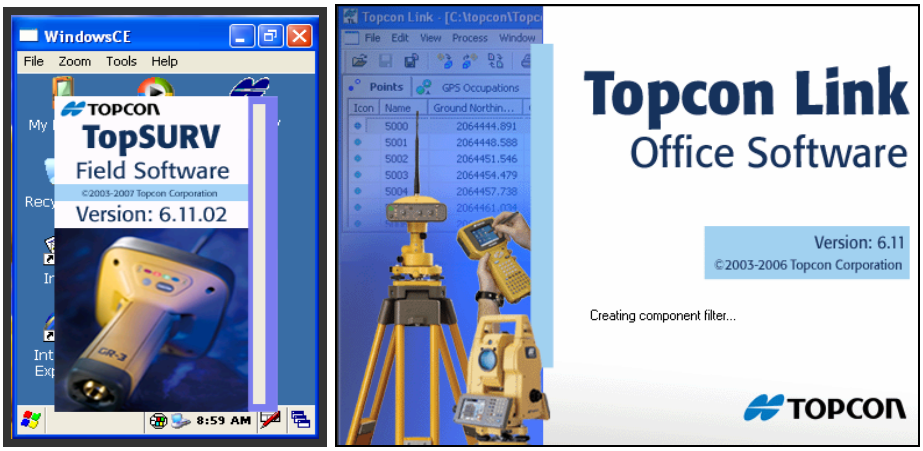

Figure 4.3: Interface of Topcon TopSURV field software and Topcon Link office software

4.3 Calibration Test

In this research, this calibration test was divided in two main conditions: the absolute calibration and the relative calibration. The absolute calibration refers to the true value of existing standard benchmark with the observation value. Relative calibration refers to the comparison of epoch-by-epoch observation value. The following subchapter overviews in the detail of the work procedure and the analysis conducted at both calibrations process.

The calibration test is very important to ensure that the receiver is in good condition. This test must be done every year or after repairing the receiver. The test must be observed using at least three Peninsular Malaysia Primary Geodetic Network (PMPGN) pillars or GNSS calibration pillars that have the accepted GDM2000 coordinates. Currently, there are only two GNSS calibration sites that have GDM2000 coordinate in Peninsular Malaysia: Melaka and Negeri Sembilan.

4.3.1 Absolute calibration

In general, the calibration test was based on the KPU Circular 1/2008. Figure 4.4 shows the flow chart of the calibration tests used in this study.

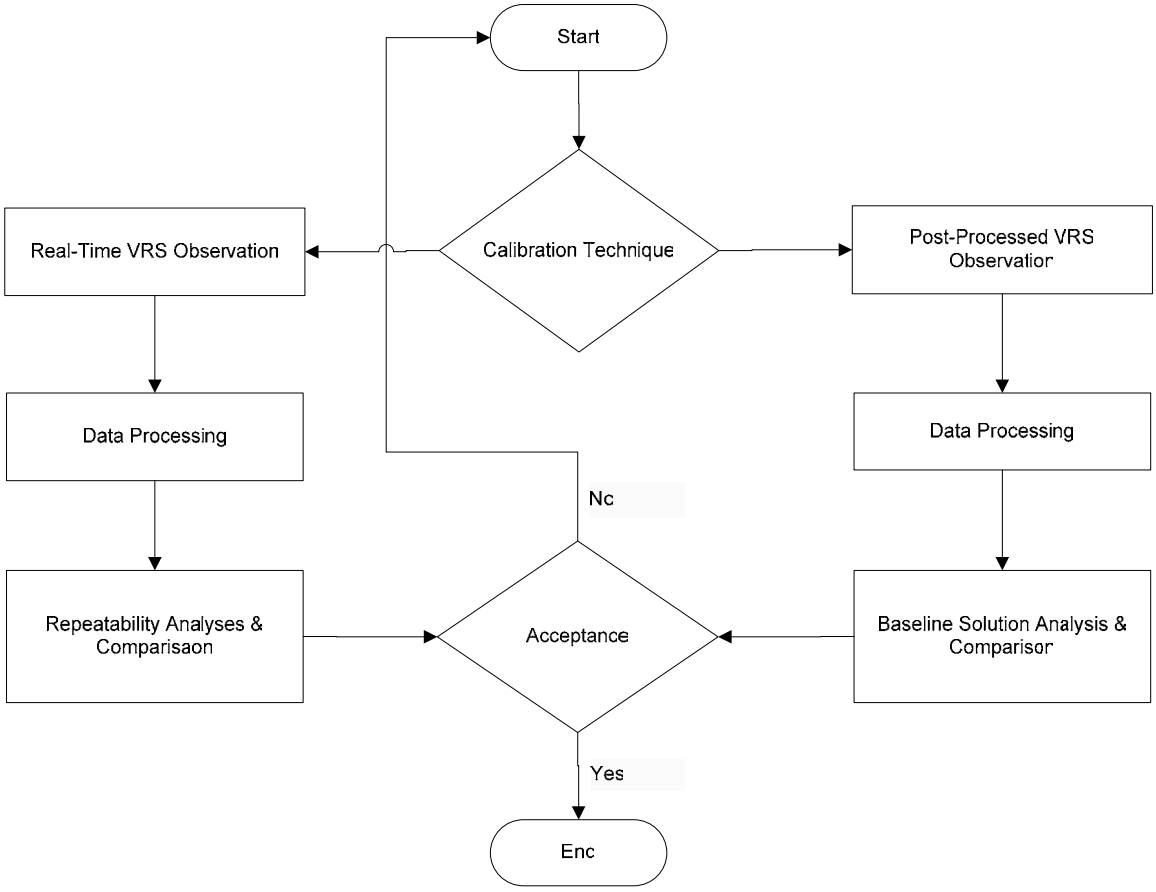

Figure 4.4: Flowchart of GPS Calibration

The GPS calibration was done at JUPEM GPS Test Site, Negeri Sembilan. There are 6 pillars at the calibration site. The coordinate of all the pillars were observed by DSMM and the true coordinates were used as references. Figure 4.5 shows the setting up a receiver on a GPS pillar. Figure 4.6 shows the arrangement of 6 GPS pillars at the calibration site and Figure 4.7 shows the calibration pillar that are used during this work.

Figure 4.5: Setting up receiver at JUPEM GPS Test Site

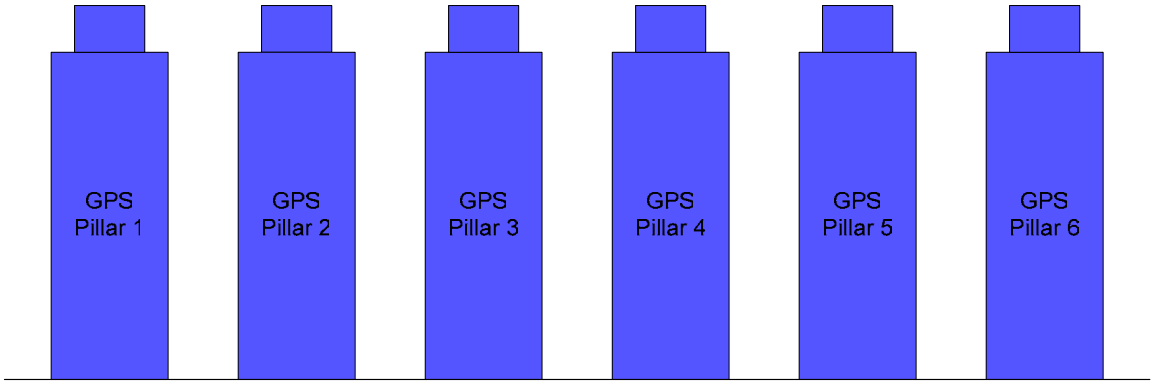

Figure 4.6: GPS Pillars at JUPEM GPS Test Site

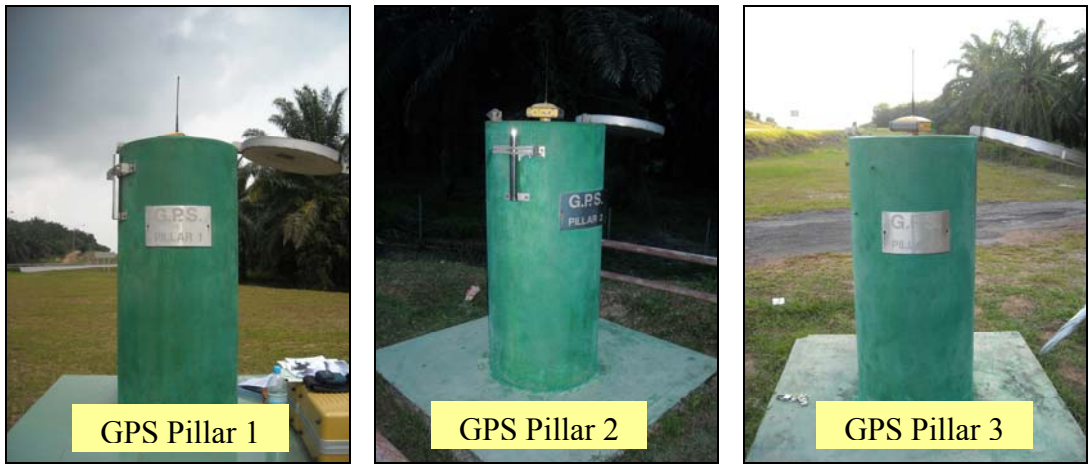

Figure 4.7: GPS Pillars at JUPEM GPS Test Site

A complete set of GNSS instrument consists of 5 main components: receiver, antenna, controller, communication link and processing software. The receiver is a dual-frequency receiver and must be able to receive L1 and L2 carrier phases. Besides that, the receiver is capable of recording raw data and real-time data. It can track at least 6 satellites and the PDOP (Position Dilution of Precision) value should be less than 6.

The real time observation is recorded on average every 5 seconds with 10 observations number for 1 epoch. In static mode, the observation time is at least 3 minutes with 5 seconds interval. The antenna is designed to minimize the electrical phase centre variation and multipath errors. This set of instrument was able to connect with MyRTKnet in real time by using GPRS. In addition, there are other communication links such as EDGE, 3G or GSM that can be used.

In real-time mode calibration, the test was conducted using three sets of epoch at every pillar with difference initialization process. Two epoch of static observations were carried out at every pillar and also through the difference initialization. The differences for every epoch with true value are less than 3 cm for horizontal component and 6 cm for vertical component. Figure 4.8 shows the survey specification for Real-Time Calibration

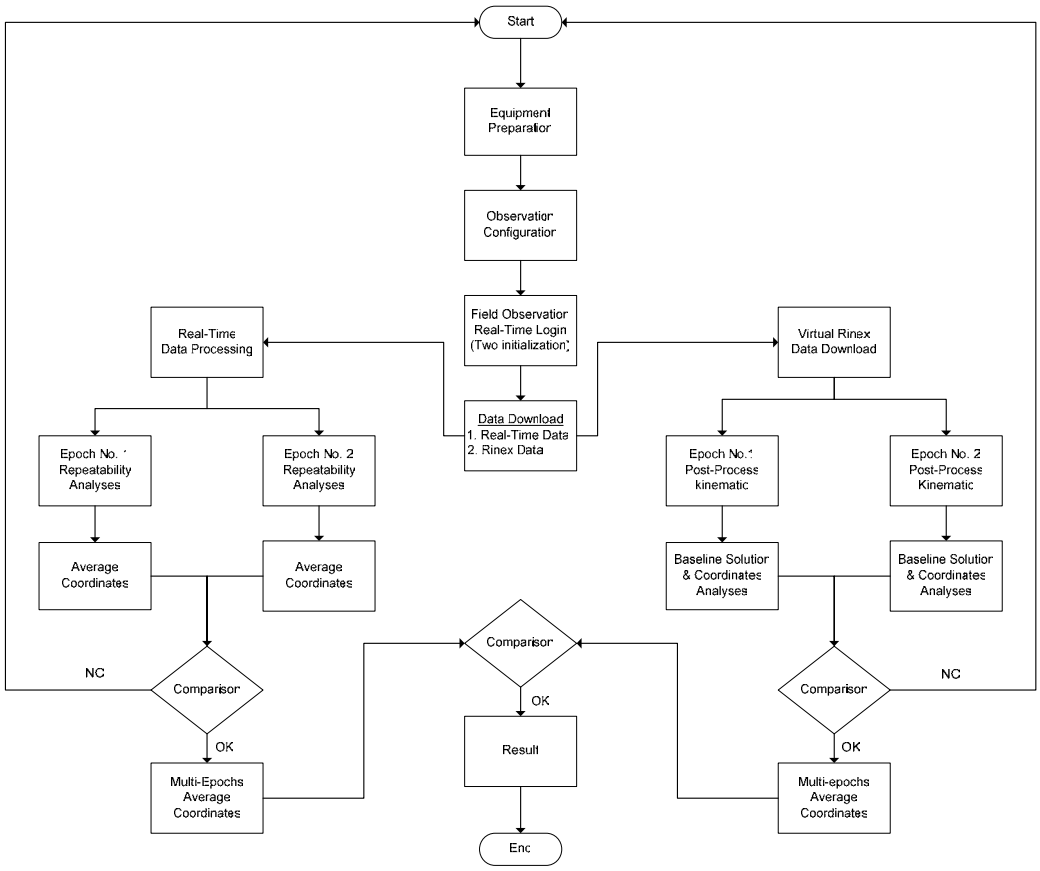

Figure 4.8: Survey specification for Real-Time Calibration

The Real-time observation computation and analysis procedures are as follows:

i. Import the real-time data for all epoch and then export them into comma separated value (CSV) format that is needed for analysis purposes. Using spread sheet in Microsoft Excel will be the most practical way of analyzing real-time data.

ii. Calculate mean for every component. Next, compute observation residuals in meter unit. Formula for observation residuals computation, meter unit conversion and other calculation are shown as follows:

a. Mean for latitude, longitude and ellipsoid height component's computation

$$\overline{Observation} = \frac{\sum_{i-1}^{n} Observation}{n} \quad (4.1)$$

b. Observation residuals (v)'s computation

$$v_i = Observation_i - \overline{Observation} \quad (4.2)$$

c. Residuals Root Mean Square (RMS) computation

$$RMS = \sqrt{\frac{\sum_{i-1}^{n} vi^2}{n}} \quad (4.3)$$

d. Arc distance (degree, minute and seconds) to meter conversion

1 second (arc) = $2\pi R / 1296000$ (4.4)

Where,

R = Central earth radius

π = 3.14159265358979

Value of R can be obtained from this formula:

$R = \sqrt{p.v}$ (4.5)

Where,

ρ = Curvature distance on meridian

v = Curvature distance on ecliptic plane

e. Another simpler way to convert the value of seconds (arc) to meter is by using factor 30. Where,

1 seconds (arc) ≈ 30 meter

iii. Any observation that has residuals value which is three times larger than RMS value should be ignored from average coordinate computation. Total maximum data that can be ignored from the computation is three observations. In the other words, there should be at least seven readings for every epoch of real time observation. Comparison the average coordinate value for every epoch with true value was made.

The analysis of static survey data was done by comparing the true value and the processing result. The true value of the pillars was provided by the geodesy section, DSMM. Table 4.4 shows the true value of all pillars.

Table 4.4: Coordinate of Port Dickson Pillar

Pillar	N	E	h (m)
P001	2° 37′ 38.63962″	101° 53′ 14.69161″	59.660
P002	2° 37′ 38.23322″	101° 53′ 14.18512″	59.357
P003	2° 37′ 36.61218″	101° 53′ 12.15833″	57.598
P004	2° 37′ 34.58521″	101° 53′ 09.62471″	58.472
P005	2° 37′ 32.15211″	101° 53′ 06.58559″	61.508
P006	2° 37′ 28.50330″	101° 53′ 02.02590″	66.574

The static survey was observed for about 30 minutes for two epochs at one pillar. The observation data was processed using Trimble Geomatic Office (TGO) software. In this processing, the virtual rinex data was downloaded from the RTKnet server. Table 4.5 shows the parameters that were selected during the static survey.

Table 4.5: Static observation parameters

No	Items	Assigned Parameter
1	Cut-off angle	15 degrees
2	Data interval	5 seconds
3	Coordinate system	WGS84
4	Datum	GDM 2000
5	Survey style	Static

The objective of real time data analysis is to determine RMS of the observation and comparing with the true value. The statistical analysis of 3 epochs for the 3 pillars, the summary of the post-processing results, and the summary of real-time results are show in following tables and figures.

Table 4.6: The Statistical of real-time result for Pillar 1 Epoch 1

ANALYSIS OF CALIBRATION TEST										
Station no	Pillar 1				Epoch				1	
No of observation	Latitude (U)				Longitude (T)				Ellipsoid height(m)	
	°	‘	″	v (m)	°	‘	″	v (m)	Observation	v (m)
1	2	37	38.63977	-0.0037	101	53	14.69135	-0.0030	59.699	0.002
2	2	37	38.63993	0.0011	101	53	14.69146	0.0003	59.700	0.003
3	2	37	38.63992	0.0008	101	53	14.69151	0.0018	59.689	-0.008
4	2	37	38.63976	-0.0040	101	53	14.69162	0.0051	59.690	-0.007
5	2	37	38.63991	0.0005	101	53	14.69142	-0.0009	59.697	0.000
6	2	37	38.63985	-0.0013	101	53	14.69144	-0.0003	59.698	0.001
7	2	37	38.63993	0.0011	101	53	14.69152	0.0021	59.704	0.007
8	2	37	38.63993	0.0011	101	53	14.69147	0.0006	59.700	0.003
9	2	37	38.63993	0.0011	101	53	14.69142	-0.0009	59.694	-0.003
10	2	37	38.64000	0.0032	101	53	14.69130	-0.0045	59.696	-0.001
Average	2	37	38.63989		101	53	14.69145		59.697	
Minimum	2	37	38.63976		101	53	14.69130		59.689	
Maximum	2	37	38.64000		101	53	14.69162		59.704	
RMS (m)	0.000				0.000				0.000	
Diff coordinate with true value	0.000				0.000				0.037	

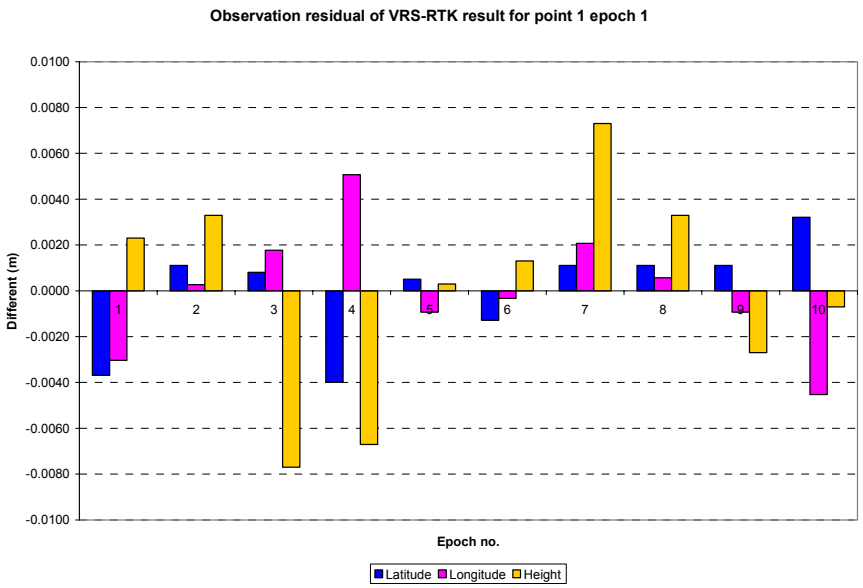

Figure 4.9: Observation residual of VRS-RTK result for Pillar 1 Epoch 1

Table 4.7: The Statistical of real-time result for Pillar 1 Epoch 2

ANALYSIS OF CALIBRATION TEST										
Station no	Pillar 1				Epoch				2	
No of observation	Latitude (U)				Longitude (T)				Ellipsoid height(m)	
	°	‘	”	v (m)	°	‘	”	v (m)	Observation	v (m)
1	2	37	38.64050	0.0017	101	53	14.69195	0.0015	59.690	-0.008
2	2	37	38.64046	0.0005	101	53	14.69195	0.0015	59.689	-0.009
3	2	37	38.64047	0.0008	101	53	14.69189	-0.0003	59.702	0.004
4	2	37	38.64054	0.0029	101	53	14.69183	-0.0021	59.703	0.005
5	2	37	38.64039	-0.0016	101	53	14.69190	0.0000	59.702	0.004
6	2	37	38.64044	-0.0001	101	53	14.69191	0.0003	59.700	0.002
7	2	37	38.64045	0.0002	101	53	14.69184	-0.0018	59.704	0.006
8	2	37	38.64034	-0.0031	101	53	14.69194	0.0012	59.696	-0.002
9	2	37	38.64040	-0.0013	101	53	14.69192	0.0006	59.699	0.001
10	2	37	38.64046	0.0005	101	53	14.69187	-0.0009	59.696	-0.002
Average	2	37	38.64045		101	53	14.69190		59.698	
Minimum	2	37	38.64034		101	53	14.69183		59.689	
Maximum	2	37	38.64054		101	53	14.69195		59.704	
RMS (m)	0.000				0.000				0.000	
Diff coordinate with true value	0.001				0.000				0.038	

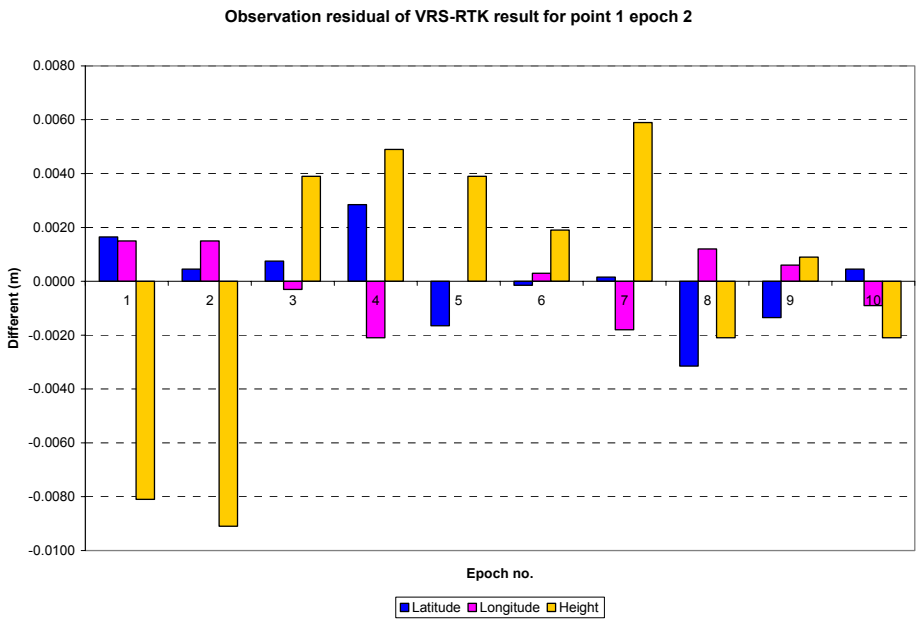

Figure 4.10: Observation residual of VRS-RTK result for Pillar 1 Epoch 2

Table 4.8: The Statistical of real-time result for Pillar 1 Epoch 3

ANALYSIS OF CALIBRATION TEST										
Station no	Pillar 1				Epoch				3	
No of observation	Latitude (U)				Longitude (T)				Ellipsoid height(m)	
	°	‘	”	v (m)	°	‘	”	v (m)	Observation	v (m)
1	2	37	38.63989	-0.0009	101	53	14.69251	-0.0011	59.680	-0.005
2	2	37	38.63992	0.0000	101	53	14.69248	-0.0020	59.687	0.002
3	2	37	38.63982	-0.0030	101	53	14.69251	-0.0011	59.684	-0.001
4	2	37	38.63997	0.0015	101	53	14.69249	-0.0017	59.681	-0.004
5	2	37	38.63996	0.0012	101	53	14.69266	0.0034	59.685	0.000
6	2	37	38.63997	0.0015	101	53	14.69245	-0.0029	59.682	-0.003
7	2	37	38.63995	0.0009	101	53	14.69258	0.0010	59.686	0.001
8	2	37	38.63993	0.0003	101	53	14.69263	0.0025	59.685	0.000
9	2	37	38.63990	-0.0006	101	53	14.69259	0.0013	59.688	0.003
10	2	37	38.63989	-0.0009	101	53	14.69255	0.0001	59.688	0.003
Average	2	37	38.63992		101	53	14.69255		59.685	
Minimum	2	37	38.63982		101	53	14.69245		59.680	
Maximum	2	37	38.63997		101	53	14.69266		59.688	
RMS (m)	0.000				0.000				0.000	
Diff coordinate with true value	0.000				0.001				0.025	

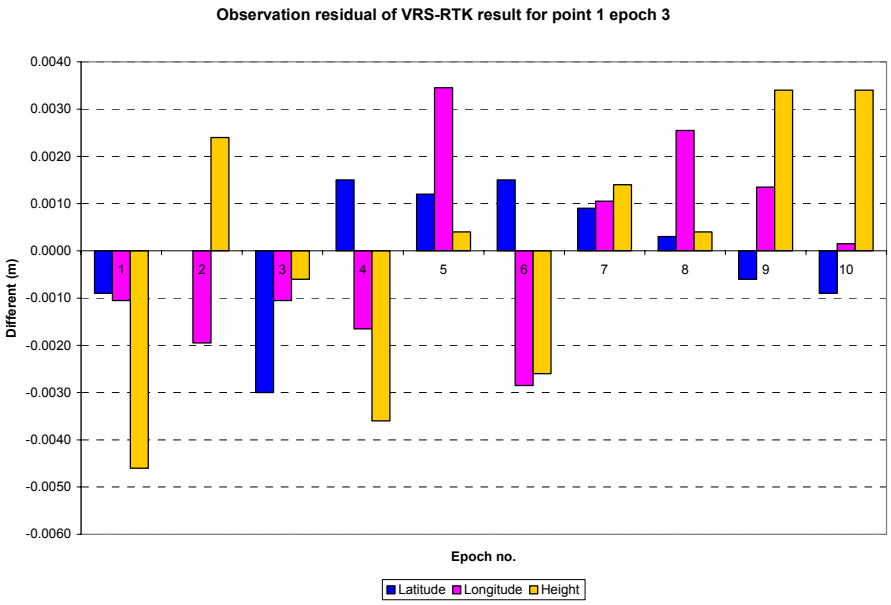

Figure 4.11: Observation residual of VRS-RTK result for Pillar 1 Epoch 3

The calibration at Pillar 1 the observation residual for every observation number are small. The RMS for all three epoch is 0.000 m. The maximum value of differential between true coordinate and average is 0.001 m for horizontal component and 0.038 m for vertical component. So, the result of horizontal component is very precise while the result of vertical component is still within specification.

Table 4.9: The Statistical of real-time result for Pillar 2 Epoch 1

ANALYSIS OF CALIBRATION TEST										
Station no	Pillar 2				Epoch				1	
No of observation	Latitude (U)				Longitude (T)				Ellipsoid height(m)	
	°	‘	”	v (m)	°	‘	”	v (m)	Observation	v (m)
1	2	37	38.23294	-0.00021	101	53	14.18553	0.00099	59.389	0.001
2	2	37	38.23299	0.00129	101	53	14.18544	-0.00171	59.386	-0.002
3	2	37	38.23294	-0.00021	101	53	14.18540	-0.00291	59.390	0.002
4	2	37	38.23296	0.00039	101	53	14.18551	0.00039	59.388	0.000
5	2	37	38.23291	-0.00111	101	53	14.18551	0.00039	59.386	-0.002
6	2	37	38.23300	0.00159	101	53	14.18557	0.00219	59.386	-0.002
7	2	37	38.23295	0.00009	101	53	14.18552	0.00069	59.390	0.002
8	2	37	38.23301	0.00189	101	53	14.18553	0.00099	59.391	0.003
9	2	37	38.23289	-0.00171	101	53	14.18558	0.00249	59.390	0.002
10	2	37	38.23288	-0.00201	101	53	14.18538	-0.00351	59.383	-0.005
Average	2	37	38.23295		101	53	14.18550		59.388	
Minimum	2	37	38.23288		101	53	14.18538		59.383	
Maximum	2	37	38.23301		101	53	14.18558		59.391	
RMS (m)	0.000				0.000				0.000	
Diff coordinate with true value	0.000				0.000				0.031	

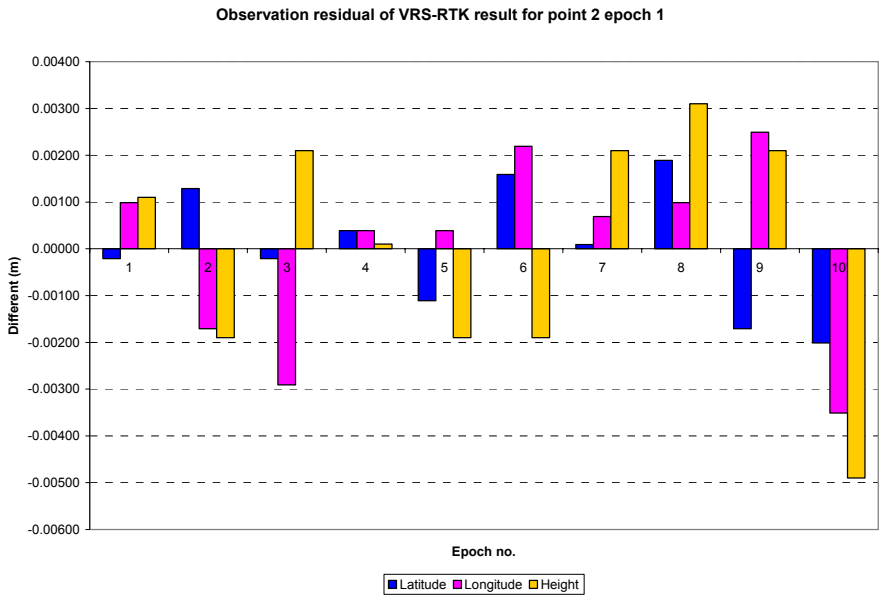

Figure 4.12: Observation residual of VRS-RTK result for Pillar 2 Epoch 1

Table 4.10: The Statistical of real-time result for Pillar 2 Epoch 2

ANALYSIS OF CALIBRATION TEST										
Station no	Pillar 2				Epoch				2	
No of observation	Latitude (U)				Longitude (T)				Ellipsoid height(m)	
	°	‘	”	v (m)	°	‘	”	v (m)	Observation	v (m)
1	2	37	38.23283	0.00108	101	53	14.18544	-0.00009	59.383	0.003
2	2	37	38.23285	0.00168	101	53	14.18546	0.00051	59.375	-0.005
3	2	37	38.23283	0.00108	101	53	14.18548	0.00111	59.381	0.001
4	2	37	38.23286	0.00198	101	53	14.18564	0.00591	59.382	0.002
5	2	37	38.23283	0.00108	101	53	14.18550	0.00171	59.383	0.003
6	2	37	38.23285	0.00168	101	53	14.18535	-0.00279	59.381	0.001
7	2	37	38.23274	-0.00162	101	53	14.18540	-0.00129	59.377	-0.003
8	2	37	38.23266	-0.00402	101	53	14.18543	-0.00039	59.377	-0.003
9	2	37	38.23269	-0.00312	101	53	14.18531	-0.00399	59.383	0.003
10	2	37	38.23280	0.00018	101	53	14.18542	-0.00069	59.381	0.001
Average	2	37	38.23279		101	53	14.18544		59.380	
Minimum	2	37	38.23266		101	53	14.18531		59.375	
Maximum	2	37	38.23286		101	53	14.18564		59.383	
RMS (m)	0.000				0.000				0.000	
Diff coordinate with true value	0.000				0.000				0.023	

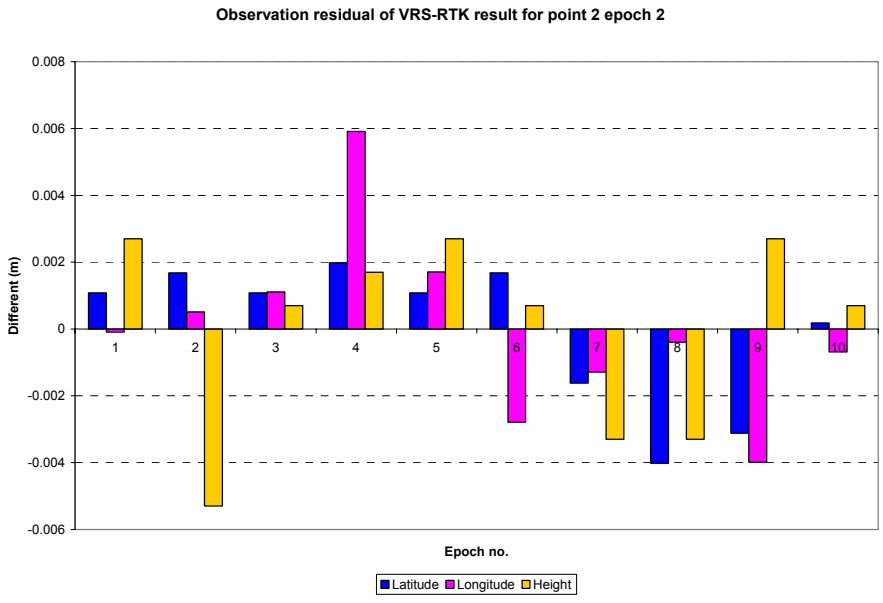

Figure 4.13: Observation residual of VRS-RTK result for Pillar 2 Epoch 2

Table 4.11: The Statistical of real-time result for Pillar 2 Epoch 3

ANALYSIS OF CALIBRATION TEST										
Station no	Pillar 2				Epoch				3	
No of observation	Latitude (U)				Longitude (T)				Ellipsoid height(m)	
	°	‘	”	v (m)	°	‘	”	v (m)	Observation	v (m)
1	2	37	38.23280	-0.00345	101	53	14.18528	-0.00285	59.391	0.003
2	2	37	38.23289	-0.00075	101	53	14.18513	-0.00735	59.389	0.001
3	2	37	38.23282	-0.00285	101	53	14.18505	-0.00975	59.391	0.003
4	2	37	38.23285	-0.00195	101	53	14.18527	-0.00315	59.390	0.002
5	2	37	38.23293	0.00045	101	53	14.18555	0.00525	59.388	0.000
6	2	37	38.23295	0.00105	101	53	14.18554	0.00495	59.385	-0.003
7	2	37	38.23299	0.00225	101	53	14.18557	0.00585	59.385	-0.003
8	2	37	38.23298	0.00195	101	53	14.18548	0.00315	59.385	-0.003
9	2	37	38.23297	0.00165	101	53	14.18542	0.00135	59.386	-0.002
10	2	37	38.23297	0.00165	101	53	14.18546	0.00255	59.388	0.000
Average	2	37	38.23292		101	53	14.18538		59.388	
Minimum	2	37	38.23280		101	53	14.18505		59.385	
Maximum	2	37	38.23299		101	53	14.18557		59.391	
RMS (m)	0.000				0.000				0.000	
Diff coordinate with true value	0.000				0.000				0.031	

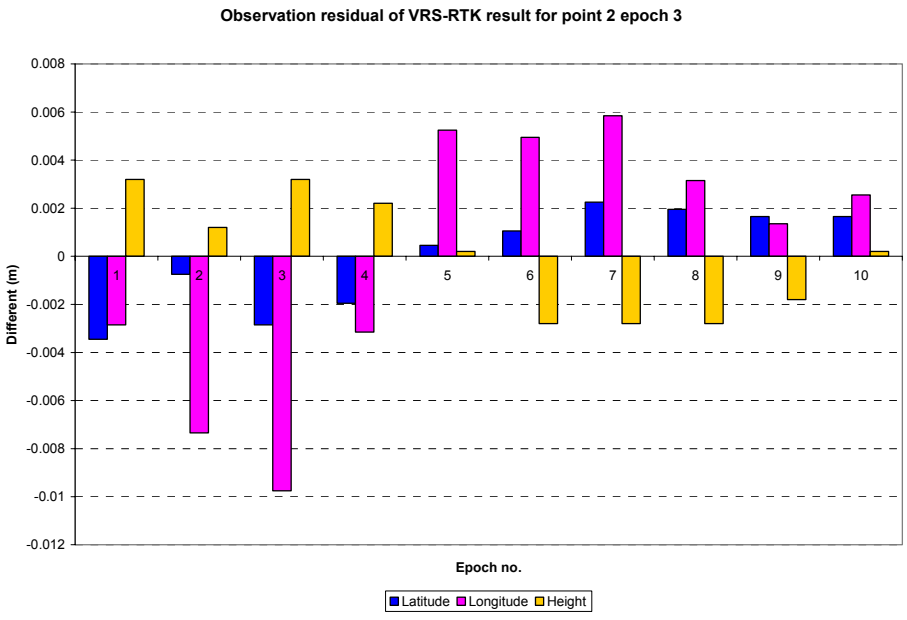

Figure 4.14: Observation residual of VRS-RTK result for Pillar 2 Epoch 3

The calibration at Pillar 2 the observation residual for every observation number are small. The RMS for all three epoch is 0.000 m. The maximum value of differential between true coordinate and average is 0.000 m for horizontal component and 0.031 for vertical component. The differences for all epoch is same as pillar 1 which is the vertical component almost have the differences approximate of 0.030 m.

Table 4.12: The Statistical of real-time result for Pillar 3 Epoch 1

ANALYSIS OF CALIBRATION TEST										
Station no	Pillar 3				Epoch				1	
No of observation	Latitude (U)				Longitude (T)				Ellipsoid height(m)	
	°	‘	″	v (m)	°	‘	″	v (m)	Observation	v (m)
1	2	37	36.61198	-0.00792	101	53	12.15878	0.00948	57.602	-0.002
2	2	37	36.61243	0.00558	101	53	12.15858	0.00348	57.608	0.004
3	2	37	36.61251	0.00798	101	53	12.15829	-0.00522	57.592	-0.012
4	2	37	36.61244	0.00588	101	53	12.15841	-0.00162	57.605	0.001
5	2	37	36.61209	-0.00462	101	53	12.15850	0.00108	57.603	-0.001
6	2	37	36.61207	-0.00522	101	53	12.15800	-0.01392	57.598	-0.006
7	2	37	36.61227	0.00078	101	53	12.15849	0.00078	57.613	0.009
8	2	37	36.61227	0.00078	101	53	12.15834	-0.00372	57.609	0.005
9	2	37	36.61217	-0.00222	101	53	12.15842	-0.00132	57.608	0.004
10	2	37	36.61221	-0.00102	101	53	12.15883	0.01098	57.607	0.003
Average	2	37	36.61224		101	53	12.15846		57.605	
Minimum	2	37	36.61198		101	53	12.15800		57.592	
Maximum	2	37	36.61251		101	53	12.15883		57.613	
RMS (m)	0.000				0.000				0.000	
Diff coordinate with true value	0.000				0.000				0.006	

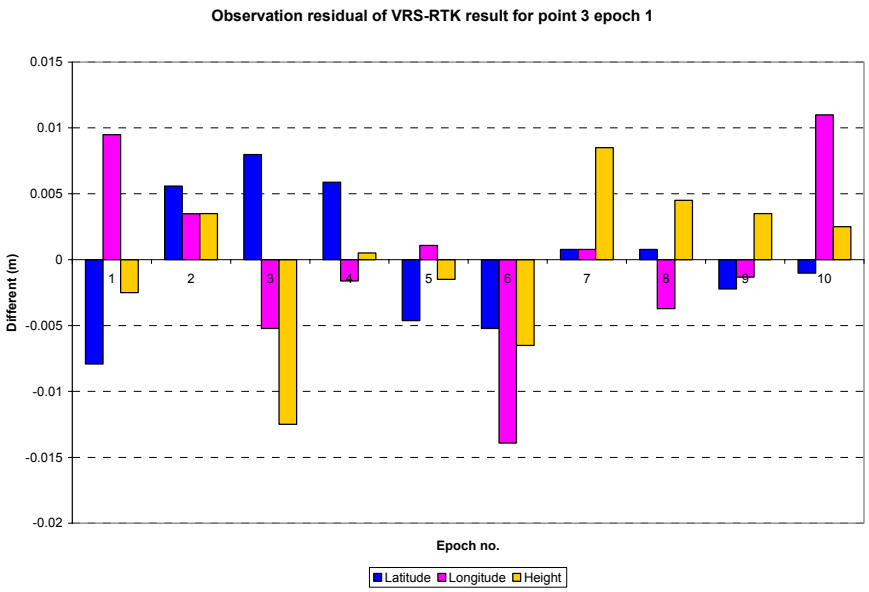

Figure 4.15: Observation residual of VRS-RTK result for Pillar 3 Epoch 1

Table 4.13: The Statistical of real-time result for Pillar 3 Epoch 2

ANALYSIS OF CALIBRATION TEST										
Station no	Pillar 3				Epoch				2	
No of observation	Latitude (U)				Longitude (T)				Ellipsoid height(m)	
	°	‘	”	v (m)	°	‘	”	v (m)	Observation	v (m)
1	2	37	36.61221	0.00498	101	53	12.15861	-0.02583	57.615	0.006
2	2	37	36.61212	0.00228	101	53	12.15857	-0.02703	57.604	-0.005
3	2	37	36.61225	0.00618	101	53	12.15856	-0.02733	57.603	-0.006
4	2	37	36.61249	0.01338	101	53	12.15837	-0.03303	57.613	0.004
5	2	37	36.61218	0.00408	101	53	12.15847	-0.03003	57.609	0.000
6	2	37	36.61207	0.00078	101	53	12.15835	-0.03363	57.615	0.006
7	2	37	36.61229	0.00738	101	53	12.15837	-0.03303	57.619	0.010
8	2	37	36.61238	0.01008	101	53	12.15829	-0.03543	57.625	0.016
9	2	37	36.61237	0.00978	101	53	12.15819	-0.03843	57.597	-0.012
10	2	37	36.61008	-0.05892	101	53	12.16893	0.28377	57.587	-0.022
Average	2	37	36.61204		101	53	12.15947		57.609	
Minimum	2	37	36.61008		101	53	12.15819		57.587	
Maximum	2	37	36.61249		101	53	12.16893		57.625	
RMS (m)	0.001				0.028				0.000	
Diff coordinate with true value	0.000				0.001				0.011	

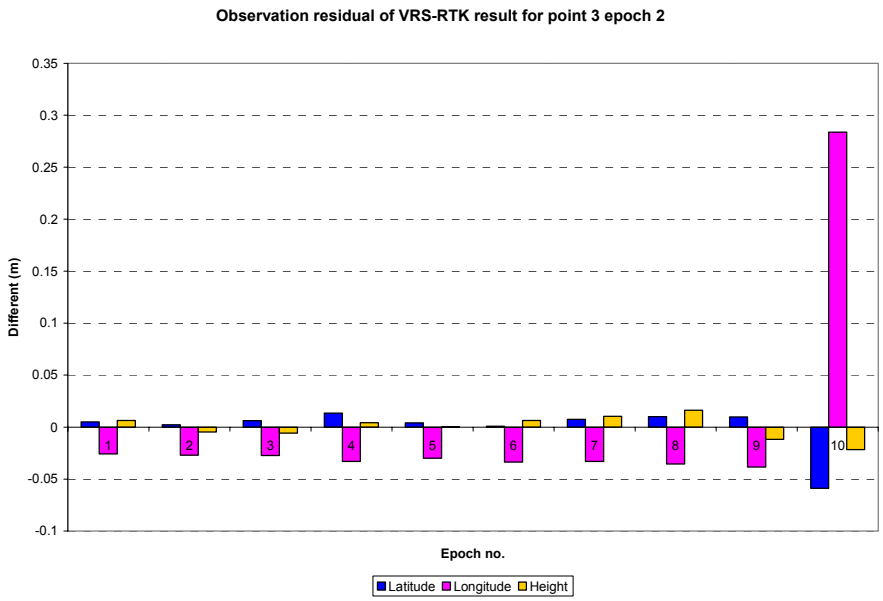

Figure 4.16: Observation residual of VRS-RTK result for Pillar 3 Epoch 2

Table 4.14: The Statistical of real-time result for Pillar 3 Epoch 3

ANALYSIS OF CALIBRATION TEST										
Station no	Pillar 3				Epoch				3	
No of observation	Latitude (U)				Longitude (T)				Ellipsoid height(m)	
	°	‘	″	v (m)	°	‘	″	v (m)	Observation	v (m)
1	2	37	36.61162	-0.00096	101	53	12.15866	0.00363	57.624	0.005
2	2	37	36.61167	0.00054	101	53	12.15863	0.00273	57.617	-0.002
3	2	37	36.61170	0.00144	101	53	12.15868	0.00423	57.626	0.007
4	2	37	36.61170	0.00144	101	53	12.15858	0.00123	57.622	0.003
5	2	37	36.61164	-0.00036	101	53	12.15865	0.00333	57.614	-0.005
6	2	37	36.61172	0.00204	101	53	12.15852	-0.00057	57.613	-0.006
7	2	37	36.61182	0.00504	101	53	12.15824	-0.00897	57.607	-0.012
8	2	37	36.61163	-0.00066	101	53	12.15854	0.00003	57.619	0.000
9	2	37	36.61143	-0.00666	101	53	12.15824	-0.00897	57.625	0.006
10	2	37	36.61159	-0.00186	101	53	12.15865	0.00333	57.621	0.002
Average	2	37	36.61165		101	53	12.15854		57.619	
Minimum	2	37	36.61143		101	53	12.15824		57.607	
Maximum	2	37	36.61182		101	53	12.15868		57.626	
RMS (m)	0.000				0.000				0.000	
Diff coordinate with true value	-0.001				0.000				0.021	

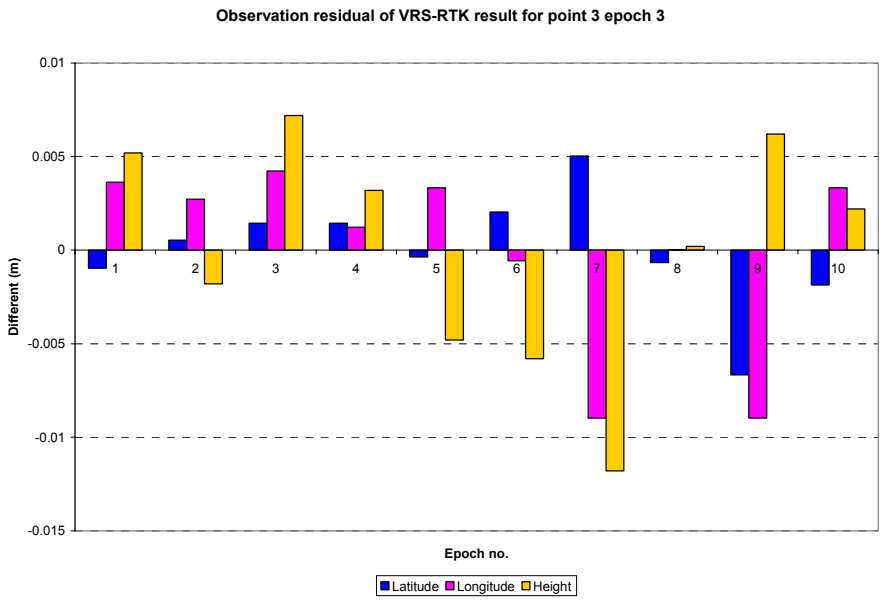

Figure 4.17: Observation residual of VRS-RTK result for Pillar 3 Epoch 3

The calibration at Pillar 3 the observation residual for every observation number are small. The RMS for first epoch and third epoch is 0.000 m while for second epoch, the RMS is 0.001 m for longitude and 0.028 m for longitude. The maximum value of differential between true coordinate and average is 0.001 m for horizontal component and 0.021 m for vertical component. The differences of pillar three are very precise for horizontal component and the vertical component are good which is more better than pillar 1 and pillar 2.

Table 4.15: Summary of the post-processing results

Pillar	Reference Coordinate							Observed Coordinate							Difference (m)		
	Latitude			Longitude			Height (m)	Latitude			Longitude			Height (m)	Latitude	Longitude	Height
1	2	37	38.63962	101	53	14.69161	59.660	2	37	38.63919	101	53	14.69140	59.642	-0.01290	-0.00630	-0.018
								2	37	38.63922	101	53	14.69169	59.642	-0.01200	0.00240	-0.018

Pillar	Reference Coordinate							Observed Coordinate							Difference (m)		
	Latitude			Longitude			Height (m)	Latitude			Longitude			Height (m)	Latitude	Longitude	Height
2	2	37	38.23322	101	53	14.18512	59.357	2	37	38.23310	101	53	14.18529	59.347	-0.00360	0.00510	-0.010
								2	37	38.23314	101	53	14.18546	59.327	-0.00240	0.01020	-0.030

Pillar	Reference Coordinate							Observed Coordinate							Difference (m)		
	Latitude			Longitude			Height (m)	Latitude			Longitude			Height (m)	Latitude	Longitude	Height
3	2	37	36.61218	101	53	12.15833	57.598	2	37	36.61134	101	53	12.15830	57.570	-0.02520	-0.00090	-0.028
								2	37	36.61182	101	53	12.15843	57.582	-0.01080	0.00300	-0.016

Table 4.16: Summary of Real-Time Results

Pillar	Reference Coordinate							Observed Coordinate							Difference (m)		
	Latitude			Longitude			Height (m)	Latitude			Longitude			Height (m)	Latitude	Longitude	Height
1	2	37	38.63962	101	53	14.69161	59.660	2	37	38.63989	101	53	14.69145	59.697	0.00810	-0.00480	0.037
								2	37	38.64045	101	53	14.69190	59.698	0.02490	0.00870	0.038
								2	37	38.63992	101	53	14.69255	59.685	0.00900	0.02820	0.025

Pillar	Reference Coordinate							Observed Coordinate							Difference (m)		
	Latitude			Longitude			Height (m)	Latitude			Longitude			Height (m)	Latitude	Longitude	Height
2	2	37	38.23322	101	53	14.18512	59.357	2	37	38.23295	101	53	14.18550	59.388	-0.00810	0.01140	0.031
								2	37	38.23279	101	53	14.18544	59.380	-0.01290	0.00960	0.023
								2	37	38.23292	101	53	14.18538	59.388	-0.00900	0.00780	0.031

Pillar	Reference Coordinate							Observed Coordinate							Difference (m)		
	Latitude			Longitude			Height (m)	Latitude			Longitude			Height (m)	Latitude	Longitude	Height
3	2	37	36.61218	101	53	12.15833	57.598	2	37	36.61224	101	53	12.15846	57.605	0.00180	0.00390	0.007
								2	37	36.61204	101	53	12.15947	57.609	-0.00420	0.03420	0.011
								2	37	36.61165	101	53	12.15854	57.619	-0.01590	0.00630	0.021

In conclusion, the differences between the observed data and true value are consistence in both horizontal and vertical component. The result for horizontal is very precise which are 0.002 m to 0.024 m while the differences of vertical component are almost 0.020 m to 0.030 m. This indicated that the results for this calibration are not more than the tolerance 3 cm for horizontal component and 6 cm for vertical component. This result shows that the set of calibrated instruments can be used for survey work i.e. structural monitoring.

4.3.2 Relative Calibration

4.3.2.1 Horizontal test

In horizontal test, Northing and Easting axis with centimeter unit interval will be prepared on a blank A4 paper (see figure 4.18). Two axis points were marked as S1 and S2 with coordinate of each point are S1 (0, 0) and S2 (0, 4). The centre (origin) of this paper will be overlapped with the centre point of the GPS monument (see figure 4.19). The Topcon HiPer Ga receiver was at both marked points.

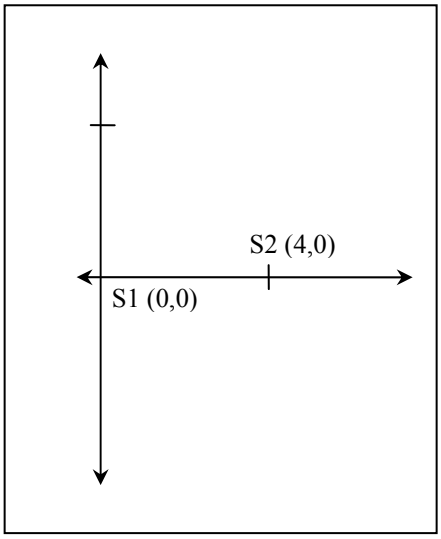

Figure 4.18: Draft of plain paper

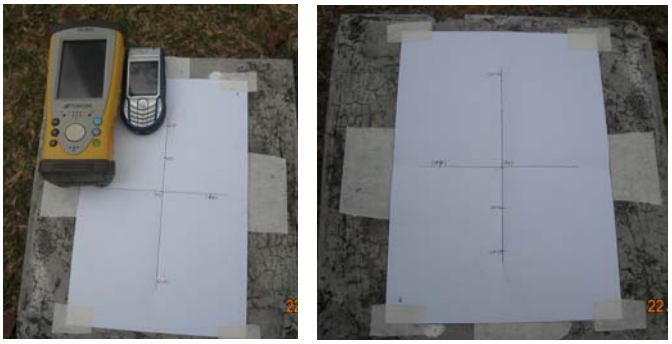

Figure 4.19: Overlap of paper (origin coordinate) and monument

The simulation test was conducted using static survey and VRS-RTK survey modes. In this research, results of static survey were use as a reference. The pole were set at points (S0, and S1) for 10 minute using static survey and VRS-RTK survey mode. Comparison of static result and VRS-RTK were than conducted. Result of static survey is as shown in Table 4.17. Figure 4.20 depicts the differential graph of static data versus VRS-RTK data.

Table 4.17: Result of Static mode

	Latitude (U)			Longitude (T)			Ellipsoid height (m)
ST R1 (0,0)	1	33	54.65310	103	38	8.84818	39.5840
ST R2 (0,0)	1	33	54.65308	103	38	8.84902	39.5740
ST R3 (4,0)	1	33	54.65417	103	38	8.84802	39.5070
ST R4 (4,0)	1	33	54.65460	103	38	8.84846	39.5420
ST R1-ST R2 (m)	0	0	0.00060	0	0	-0.02520	0.01000
ST R3-ST R4 (m)	0	0	-0.01290	0	0	-0.01320	-0.03500

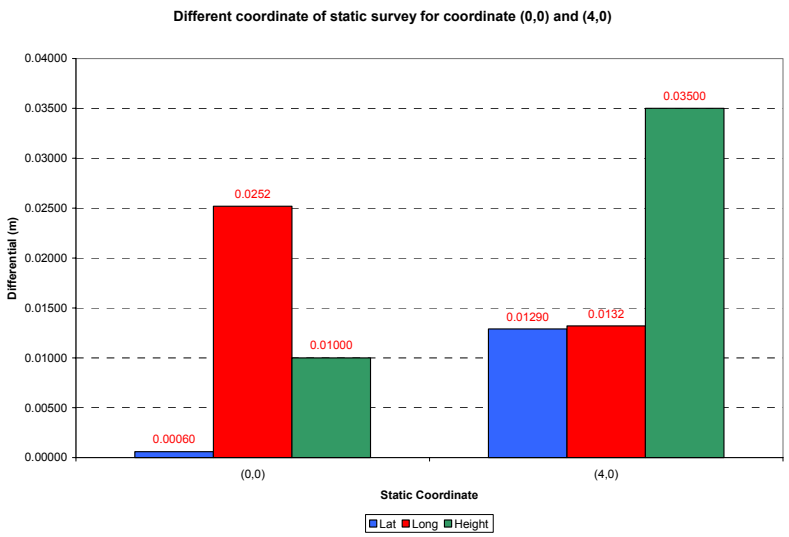

Figure 4.20: Overlap of paper (origin coordinate) and monument

The differences between static observed coordinated at draft paper is about 4 cm on x-axis. Based on static result, differential between latitude of different height for coordinate 0,0 is 25 mm for horizontal component and 10 mm for vertical component while the differential coordinate 4,0 is 13 mm for horizontal component and 10 mm for vertical component.

Difference between static and VRS-RTK results were compare for each observation. Table 4.18 shows the higher value for horizontal component is about 0.0019 cm and smaller value is about 0.0000m.

Table 4.18: Result of Static vs VRS-RTK survey for horizontal test

	Static		VRS-RTK		Diff	
	Latitude (U)	Longitude (T)	Latitude (U)	Longitude (T)	Lat (m)	Long (m)
R1 (0,0)	1 33 54.65310	103 38 8.84818	1 33 54.65311	103 38 8.84808	-0.0004	0.0030
R2 (0,0)	1 33 54.65308	103 38 8.84902	1 33 54.65305	103 38 8.84911	0.0008	-0.0026
R3 (4,0)	1 33 54.65417	103 38 8.84802	1 33 54.65415	103 38 8.84802	0.0005	0.0000
R4 (4,0)	1 33 54.65460	103 38 8.84846	1 33 54.65458	103 38 8.84852	0.0006	-0.0019

4.3.2.3 Vertical test

The purpose of vertical test is to check the potential of VRS-RTK mode for vertical component. The test were conducted at of two different heights (h1, h2) over the same points. The test will be carried out by measuring the same point at two epochs with different setting. Figure 4.21 illustrated the sketch of instrument setting of different height while Figure 4.22 shows the photo of instrument during observation

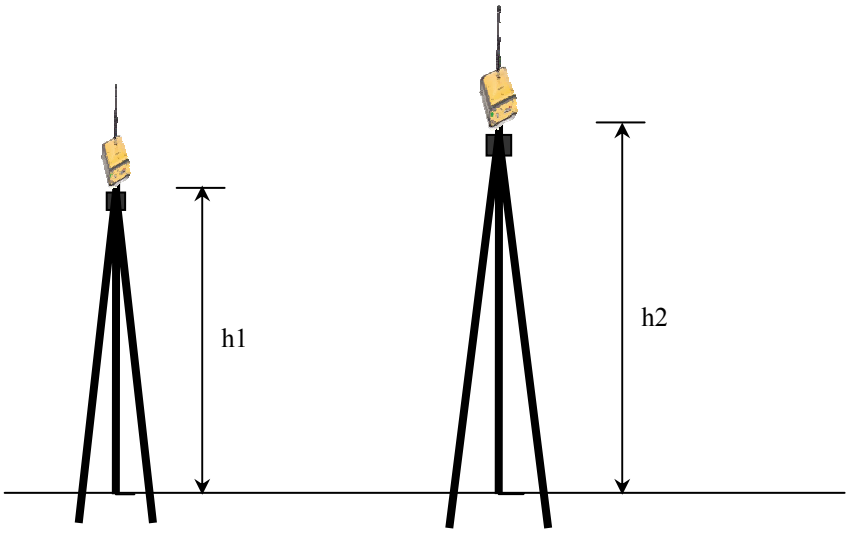

Figure 4.21: Different of height

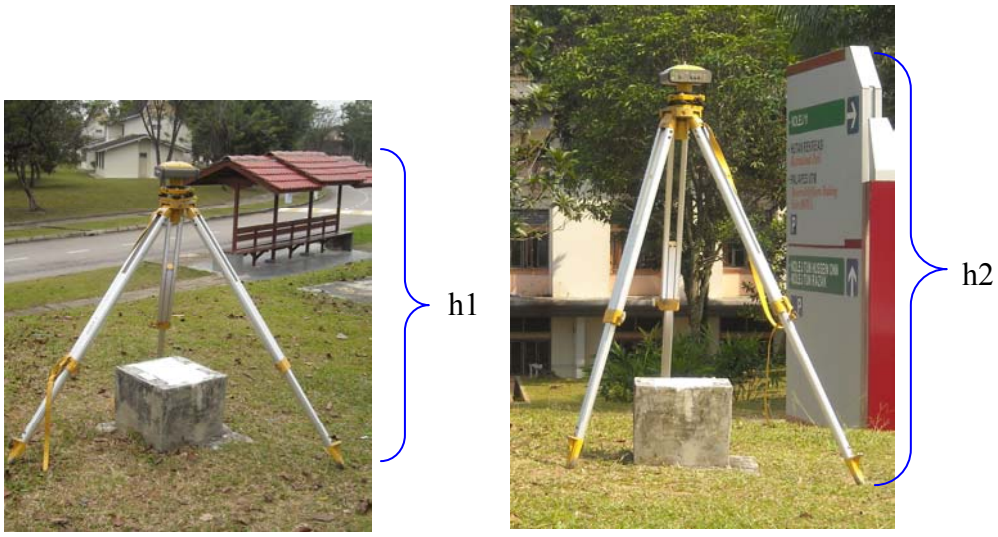

Figure 4.22: Photo of different height

Table 4.19 tabulates the outcome result of the vertical. Height value of static and VRS-RTK data were compared. This result indicates the differential between the result is small. The higher value for this vertical differential is about 5mm. The calibration result of each point and observation residual of every VRS-RTK data shows in following tables and graphs (see Table 4.20 and Figure 4.23 for coordinate 0,0 and h1, Table 4.21 and Figure 4.24 for coordinate 0,0 and h2, Table 4.22 and Figure 4.25 for coordinate 4,0 and h1, and Table 4.23 and Figure 4.26 for coordinate 4,0 and h2).

Table 4.19: Result of Static vs VRS-RTK survey for vertical test

	Static	VRS-RTK	Diff.
	Ellipsoid height (m)	Ellipsoid height (m)	(m)
ST R1 (0,0)	39.5840	39.5885	-0.0045
ST R2 (0,0)	39.5740	39.5793	-0.0053
ST R3 (4,0)	39.5070	39.5052	0.0018
ST R4 (4,0)	39.5420	39.5462	-0.0042

Table 4.20: Calibration result of point R1

ANALYSIS OF SIMULATION TEST IN CONFINED AREA										
Station no	Point R1 (0,0)				Epoch				h1	
	Latitude (U)				Longitude (T)				Ellipsoid height(m)	
No of observation	°	‘	”	v (m)	°	‘	”	v (m)	Observation	v (m)
1	1	33	54.65313	0.001	103	38	8.84827	0.006	39.579	-0.010
2	1	33	54.65311	0.000	103	38	8.84799	-0.003	39.595	0.006
3	1	33	54.65311	0.000	103	38	8.84804	-0.001	39.590	0.002
4	1	33	54.65312	0.000	103	38	8.84786	-0.006	39.603	0.014
5	1	33	54.65301	-0.003	103	38	8.8479	-0.005	39.599	0.010
6	1	33	54.65304	-0.002	103	38	8.84787	-0.006	39.596	0.007
7	1	33	54.65311	0.000	103	38	8.84804	-0.001	39.594	0.005
8	1	33	54.65308	-0.001	103	38	8.84846	0.012	39.574	-0.015
9	1	33	54.65322	0.003	103	38	8.84823	0.005	39.581	-0.008
10	1	33	54.65319	0.002	103	38	8.8481	0.001	39.574	-0.015
Average	1	33	54.65311		103	38	8.84808		39.589	
Minimum	1	33	54.65301		103	38	8.84786		39.574	
Maximum	1	33	54.65322		103	38	8.84846		39.603	
RMS (m)	0.000				0.000				0.000	
Diff between obs coordinate (average) with true value (mm)	0.360				-3.120				4.500	

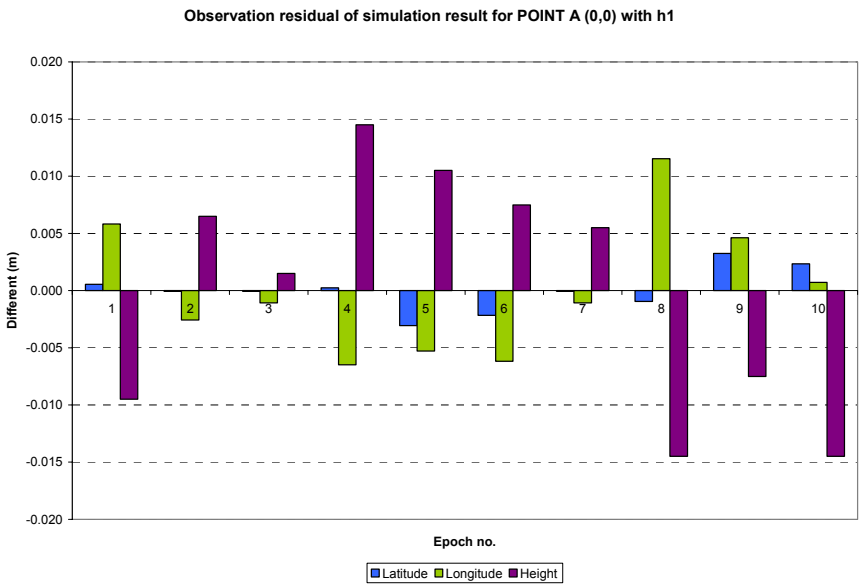

Figure 4.23: Observation residual for point R1 (0,0) of height h1

Table 4.21: Calibration result of point R2

ANALYSIS OF SIMULATION TEST IN CONFINED AREA										
Station no	Point R2 (0,0)				Epoch				h2	
No of observation	Latitude (U)				Longitude (T)				Ellipsoid height(m)	
	°	‘	”	v (m)	°	‘	”	v (m)	Observation	v (m)
1	1	33	54.65311	0.0017	103	38	8.84919	0.0025	39.569	-0.010
2	1	33	54.65295	-0.0031	103	38	8.84906	-0.0014	39.572	-0.007
3	1	33	54.65298	-0.0022	103	38	8.84884	-0.0080	39.576	-0.003
4	1	33	54.65317	0.0035	103	38	8.84895	-0.0047	39.570	-0.009
5	1	33	54.65309	0.0011	103	38	8.84932	0.0064	39.569	-0.010
6	1	33	54.65310	0.0014	103	38	8.84903	-0.0023	39.574	-0.005
7	1	33	54.65327	0.0065	103	38	8.84902	-0.0026	39.577	-0.002
8	1	33	54.65295	-0.0031	103	38	8.84916	0.0016	39.600	0.021
9	1	33	54.65292	-0.0040	103	38	8.84922	0.0034	39.594	0.015
10	1	33	54.65298	-0.0022	103	38	8.84929	0.0055	39.592	0.013
Average	1	33	54.65305		103	38	8.84911		39.579	
Minimum	1	33	54.65292		103	38	8.84884		39.569	
Maximum	1	33	54.65327		103	38	8.84932		39.600	
RMS (m)	0.000				0.000				0.000	
Diff between obs coordinate (average) with true value (mm)	-0.840				2.640				5.300	

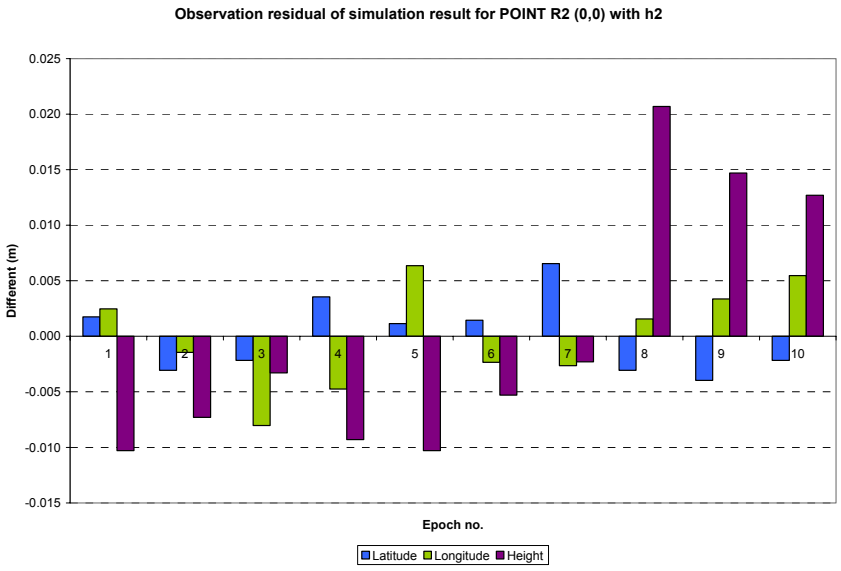

Figure 4.24: Observation residual for point R2 (0,0) of height h2

Table 4.22: Calibration result of point R3

ANALYSIS OF SIMULATION TEST IN CONFINED AREA										
Station no	Point R3 (0,4)				Epoch				h2	
	Latitude (U)				Longitude (T)				Ellipsoid height(m)	
No of observation	°	‘	”	v (m)	°	‘	”	v (m)	Observation	v (m)
1	1	33	54.65408	-0.002	103	38	8.84808	0.002	39.512	0.007
2	1	33	54.65413	-0.001	103	38	8.84800	-0.001	39.502	-0.003
3	1	33	54.65413	-0.001	103	38	8.84808	0.002	39.506	0.001
4	1	33	54.65401	-0.004	103	38	8.84788	-0.004	39.499	-0.006
5	1	33	54.65413	-0.001	103	38	8.84810	0.002	39.511	0.006
6	1	33	54.65420	0.001	103	38	8.84809	0.002	39.512	0.007
7	1	33	54.65419	0.001	103	38	8.84802	0.000	39.510	0.005
8	1	33	54.65420	0.001	103	38	8.84801	0.000	39.501	-0.004
9	1	33	54.65419	0.001	103	38	8.84800	-0.001	39.499	-0.006
10	1	33	54.65428	0.004	103	38	8.84795	-0.002	39.500	-0.005
Average	1	33	54.65415		103	38	8.84802		39.505	
Minimum	1	33	54.65401		103	38	8.84788		39.499	
Maximum	1	33	54.65428		103	38	8.84810		39.512	
RMS (m)	0.000				0.000				0.000	
Diff between obs coordinate (average) with true value (mm)	-0.480				0.030				-1.800	

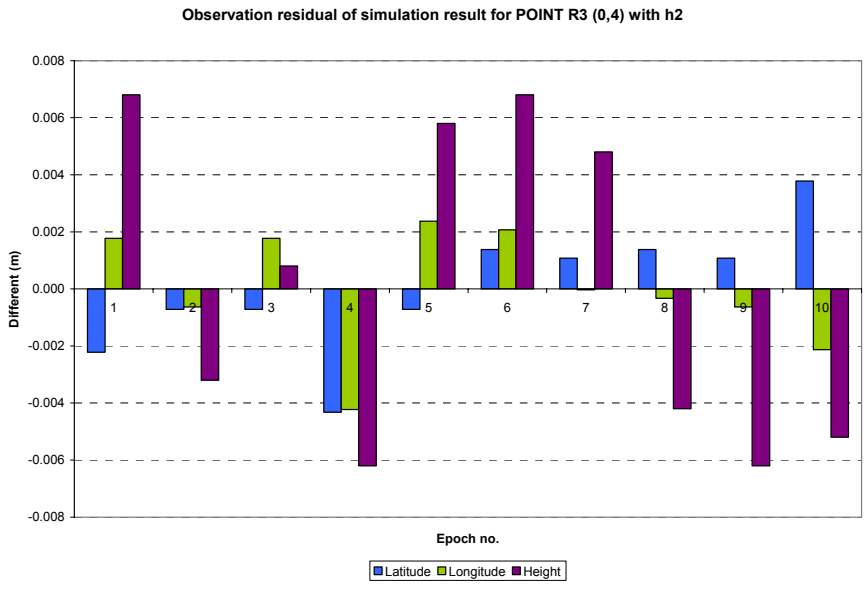

Figure 4.25: Observation residual for point R3 (4,0) of height h2

Table 4.23: Calibration result of point R4

ANALYSIS OF SIMULATION TEST IN CONFINED AREA										
Station no	Point R4 (0,4)				Epoch				h1	
	Latitude (U)				Longitude (T)				Ellipsoid height(m)	
No of observation	°	‘	”	v (m)	°	‘	”	v (m)	Observation	v (m)
1	1	33	54.65452	-0.002	103	38	8.84830	-0.007	39.539	-0.007
2	1	33	54.65434	-0.007	103	38	8.84847	-0.002	39.546	0.000
3	1	33	54.65455	-0.001	103	38	8.84830	-0.007	39.539	-0.007
4	1	33	54.65466	0.002	103	38	8.84834	-0.005	39.546	0.000
5	1	33	54.65464	0.002	103	38	8.84836	-0.005	39.544	-0.002
6	1	33	54.65463	0.002	103	38	8.84849	-0.001	39.551	0.005
7	1	33	54.65460	0.001	103	38	8.84871	0.006	39.548	0.002
8	1	33	54.65451	-0.002	103	38	8.84866	0.004	39.550	0.004
9	1	33	54.65468	0.003	103	38	8.84878	0.008	39.550	0.004
10	1	33	54.65466	0.002	103	38	8.84881	0.009	39.549	0.003
Average	1	33	54.65458		103	38	8.84852		39.546	
Minimum	1	33	54.65434		103	38	8.84830		39.539	
Maximum	1	33	54.65468		103	38	8.84881		39.551	
RMS (m)	0.000				0.000				0.000	
Diff between obs coordinate (average) with true value (mm)	-0.630				1.860				4.200	

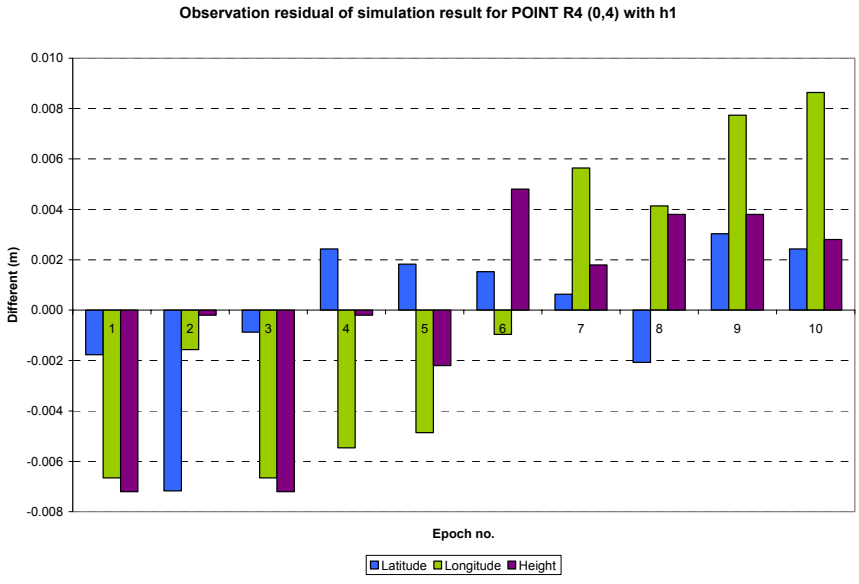

Figure 4.26: Observation residual for point R4 (4,0) of height h1

From the calibration result, the observation residual for all observation are small. The RMS for each coordinate component (horizontal and vertical) of this result is 0.000 m. The maximum value of differential between true value (static coordinate) and average coordinate is 3.1 mm for horizontal component and 5.3 mm for vertical component.

4.4 VRS-RTK Simulation Test

The aim of the simulation is to provide the acquainted with instrument that will be used and for better understanding on VRS-RTK through simulation test made on a bridge in UTM campus. For the purpose of real-time structural health detection, well-calibrated Topcon HiPer Ga dual-frequency receivers with internal radio modem were used in this study. By applying static survey mode to determine true coordinates in which will be used latter as reference, the test was then conducted in real-time using VRS-RTK mode. Figure 4.27 shows the setting up of the Topcon HiPer Ga instrument.

Figure 4.27: Setting up Topcon HiPer Ga Instrument

This survey involved with Topcon HiPer Ga receivers and the field observation was carried out for about one 20 minute per epoch with 10 degrees cut-of angle and 15 seconds

interval. Two epochs of static surveying method is applied to determine the position (true coordinate) of two selected reference points namely P1 and P2 (see Figure 4.28) and the instrument set-up at rover station shows in Figure 4.29.

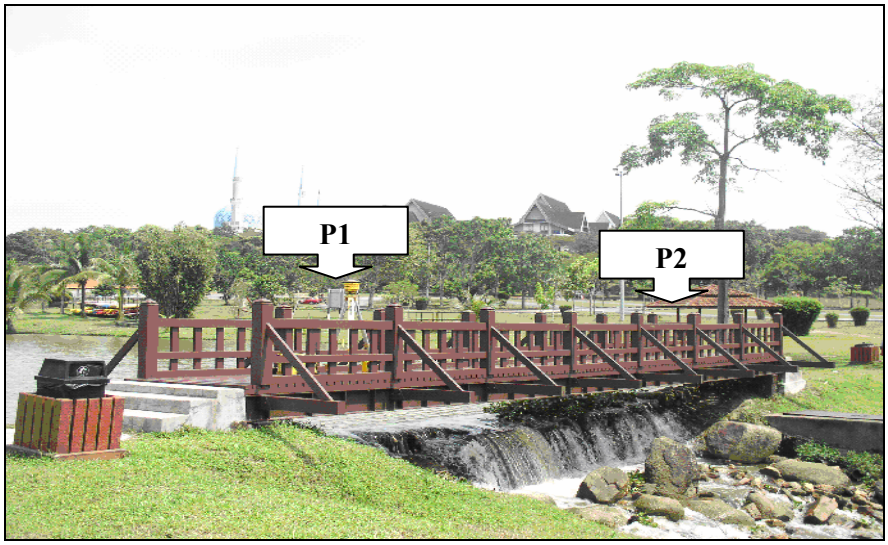

Figure 4.28: Location of Point P1 and P2

Figure 4.29: Instrument set-up at Rovers station (Point P1 and P2)

For the VRS-RTK technique, the data was collected in real time for 10 epochs. For VRS-RTK survey parameter, the solution type was set up a Fix only. During the survey, the Fixed in green box will appear (see Figure 4.30), and the radio link should received 100%

by checked the system status of radio link. Figure 4.31 shows the overview of positioning status checking. PDOP represents the contribution of the satellite geometry to the 3D positioning. It is better to get PDOP value less than 6. Checking up of system and satellite tracking status to know the position type, number of satellite tracking, number of initialized satellite, and percent of radio link signal that shows the strength of VRS signal received (see Figure 4.32).

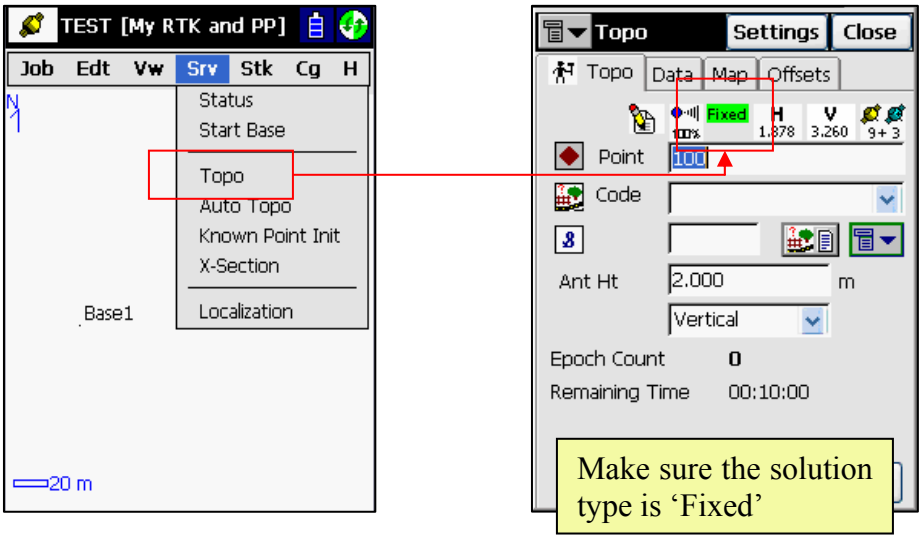

Figure 4.30: Fixed solution

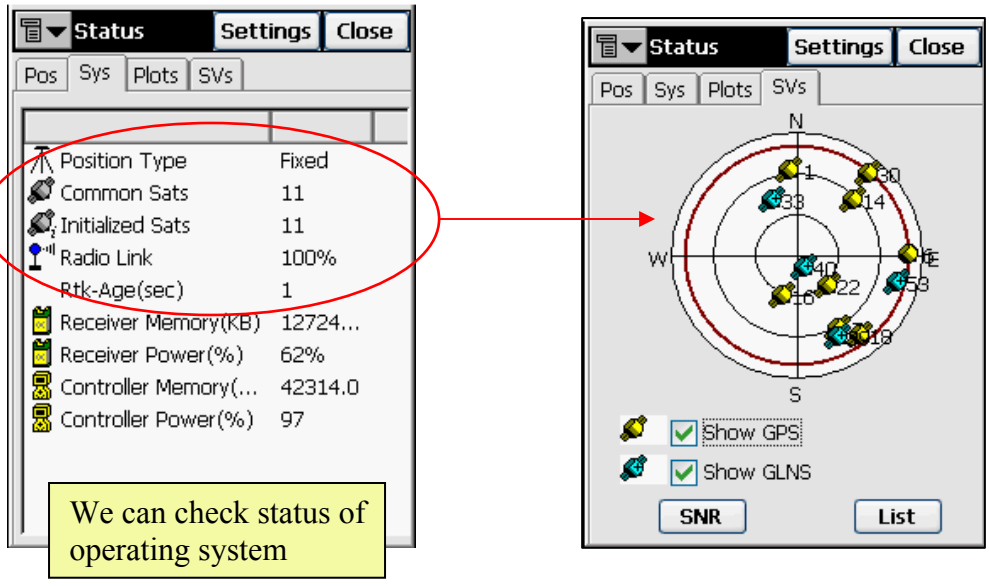

Figure 4.31: Overview of positioning status

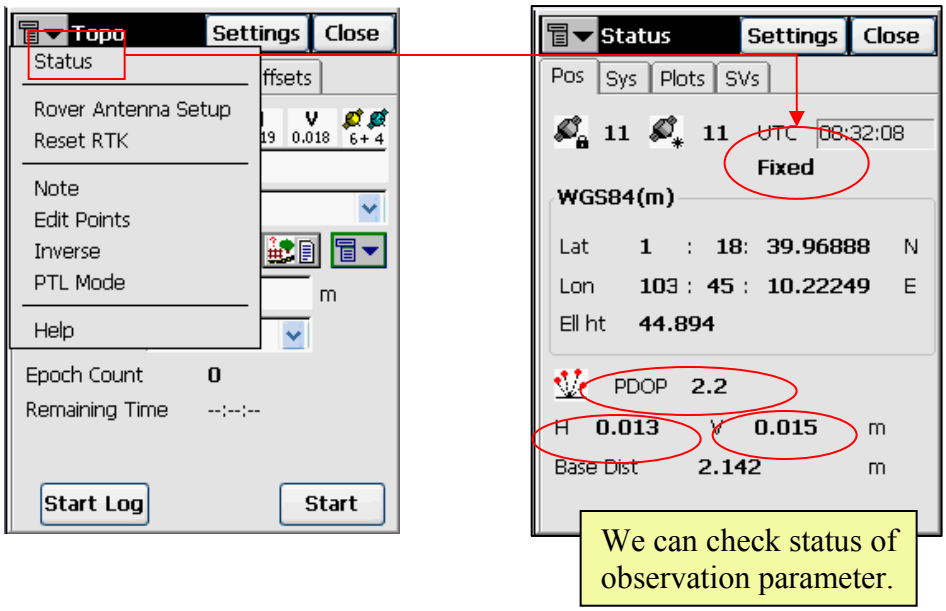

Figure 4.32: Overview of system and satellite tracking status

The data was collected in real-time with fixed solution type. Figure 4.33 shows the solution type data for VRS-RTK data collection. The precision of observed data are given automatically. Figure 4.34 shows the precision of horizontal component and precision of vertical component for P1 and P2 that are obtained during observation.

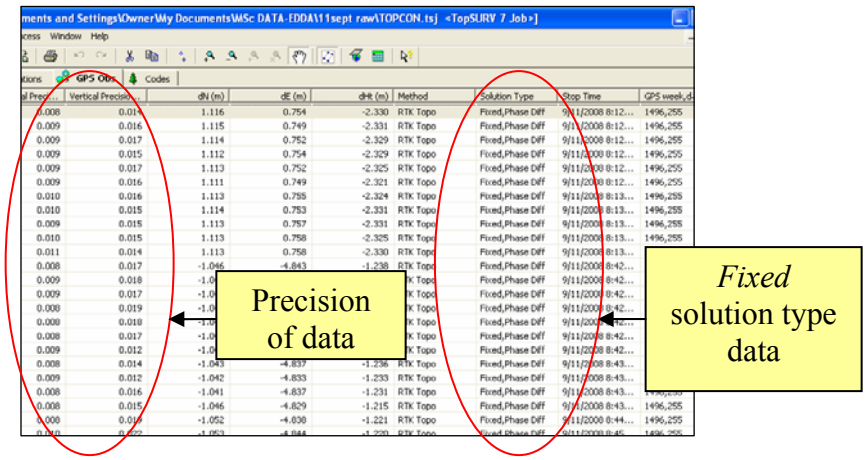

Figure 4.33: Checking up of system and satellite tracking status

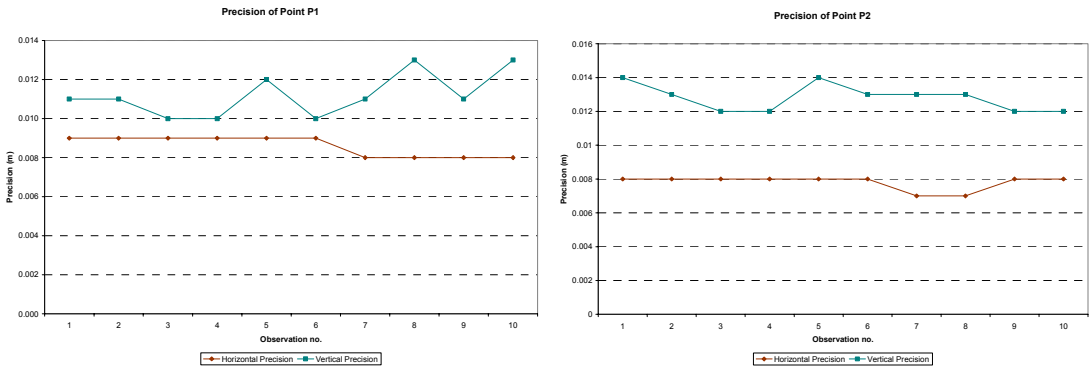

Figure 4.34: Precision for Point P1 and P2

The precision of this result shows the accuracy of the observation. Precision of point P1 and P2 in this simulation test is below 0.008 m for horizontal component and precision of vertical component is below than 0.015 m. Smaller precision provided better result and high precision is instead of that.

As mentioned earlier, two epochs of static surveying technique have been conducted to establish the true positions (coordinates) of the monitoring points on the bridge (P1 and P2). The base station was set at UTM11 benchmark beside UTM helipad. The static survey was then processed and adjusted using Trimble™ Geomatic Office v1.6 software. The adjusted geodetic coordinates from the network adjustment is as tabulated as

True value (TV). These tables show the variation of coordinates at the two monitoring points (P1 and P2) compared to the true values. The results for RTK-GPS and simple analysis for point P1 and P2 were illustrated in Table 4.24.

Table 4.24: Analysis of Static vs VRS-RTK data for Point P1 and P2

	Latitude (U)			Longitude (T)			Ellipsoid height (m)
P1 STATIC	1	33	17.86713	103	38	23.35866	11.424
P2 STATIC	1	33	18.00324	103	38	23.47522	11.393
P1 VRS-RTK	1	33	17.86719	103	38	23.35869	11.426
P2 VRS-RTK	1	33	18.00329	103	38	23.47521	11.3987
Diff P1 ST-P1 VRS (mm)	0	0	1.65	0	0	1.02	2.3
Diff P2 ST-P2 VRS (mm)	0	0	1.44	0	0	0.24	5.7

Based on the results, it is noted that the differences between the static data and the VRS-RTK data for point P1 and P2 significantly small. Based on the analyses, conclusion can be made that there is no structural displacement detected at the bridge. It is also suggested that the structural health of the bridge was in a satisfactory condition. Figure 4.35 shows the graph of differential value of static data and VRS-RTK data for P1 and P2, followed the observation residual graph of VRS-RTK data for point P1 (see Figure 4.36) and P2 (Figure 4.37). The details on VRS-RTK data for this simulation test are attached in Appendix B.

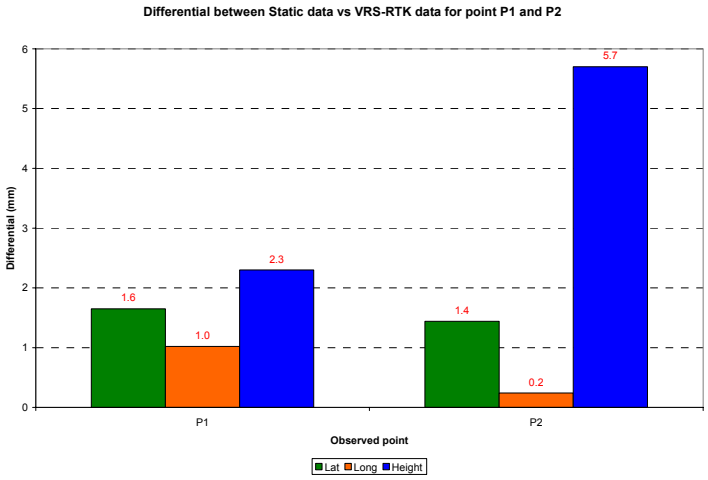

Figure 4.35: Differential value of static data and VRS-RTK data for P1 and P2

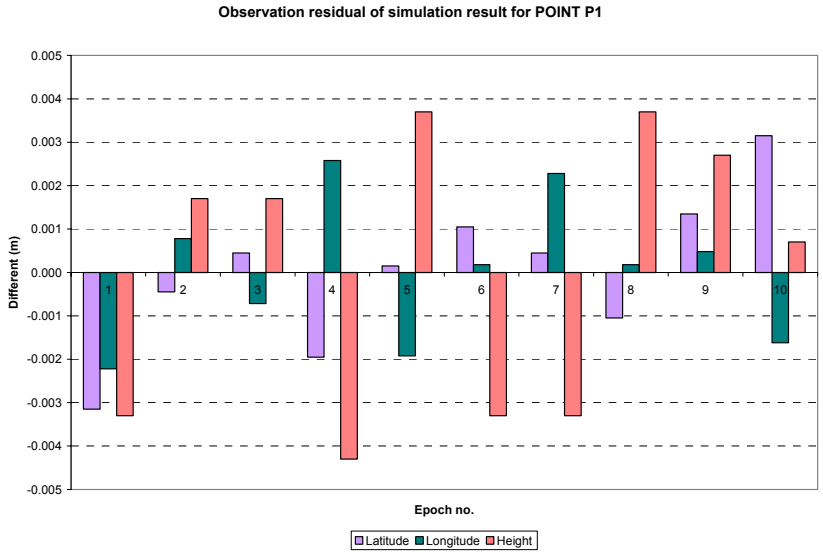

Figure 4.36: Observation residual of VRS-RTK data for point P1

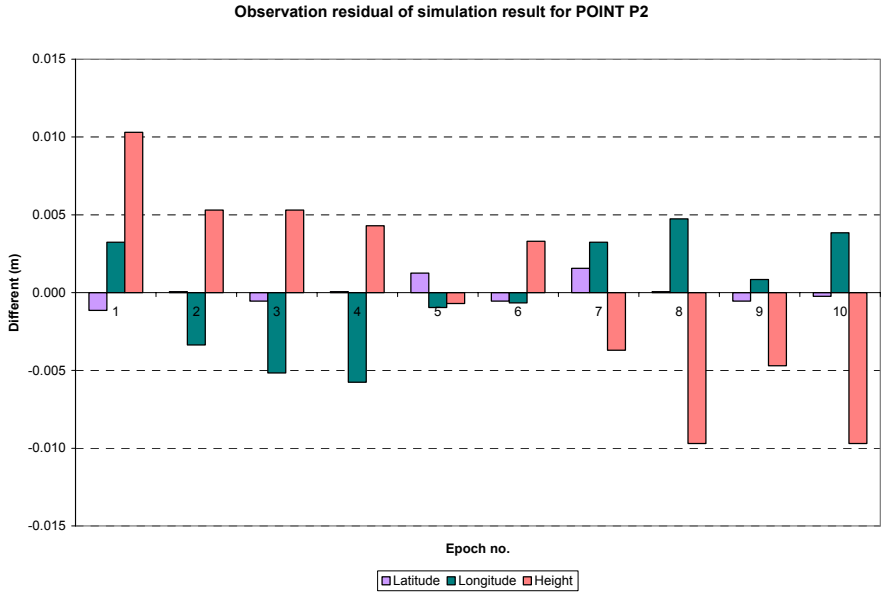

Figure 4.37: Observation residual of VRS-RTK data for point P2

The observation residual for point P1 is less than 0.005 m for both horizontal and vertical component. While the observation residual for point P2, the maximum value for horizontal component is below than 0.006 m and less than 0.010 m for vertical component.

4.5 VRS-RTK performance: Assisted – GPS Indoor Monitoring

This campaign focuses on real-time GPS indoor SHM performed at TOPCON Malaysia building at Taman Ampang Hilir, Kuala Lumpur. Conducted using VRS-RTK technique, this case study is setting to study the VRS-RTK signal strength in indoor environment and the potential of this technique for SHM inside the building. Figure 4.38 shows the location of the study area. This campaign included with real-time monitoring.

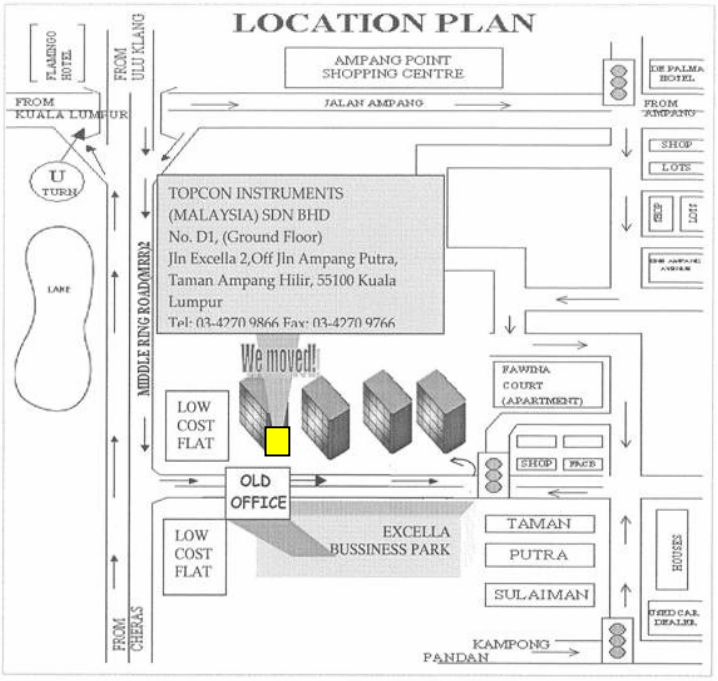

Figure 4.38: Study area, Topcon Malaysia, Taman Ampang Hilir, Kuala Lumpur

4.5.1 The Methodology

Satellite navigation system the GPS are traditionally considered suitable for outdoor use. To provide reliable, accurate navigation monitoring buildings, such system must be combined with external complements such as sensors, WLAN, Bluetooth and RFID. The indoor GPS-based system used in this study is based on a dual frequency receiver's antenna located on top of Topcon Malaysia Building connected to a splitter that connects radiator and Topcon GB-1000 main controller place inside the building. GPS retrieved system were then transmitted indoors to user equipped with appropriate GPS receiver. Figure 4.39 illustrates the assisted GPS indoor monitoring approach used in this study.

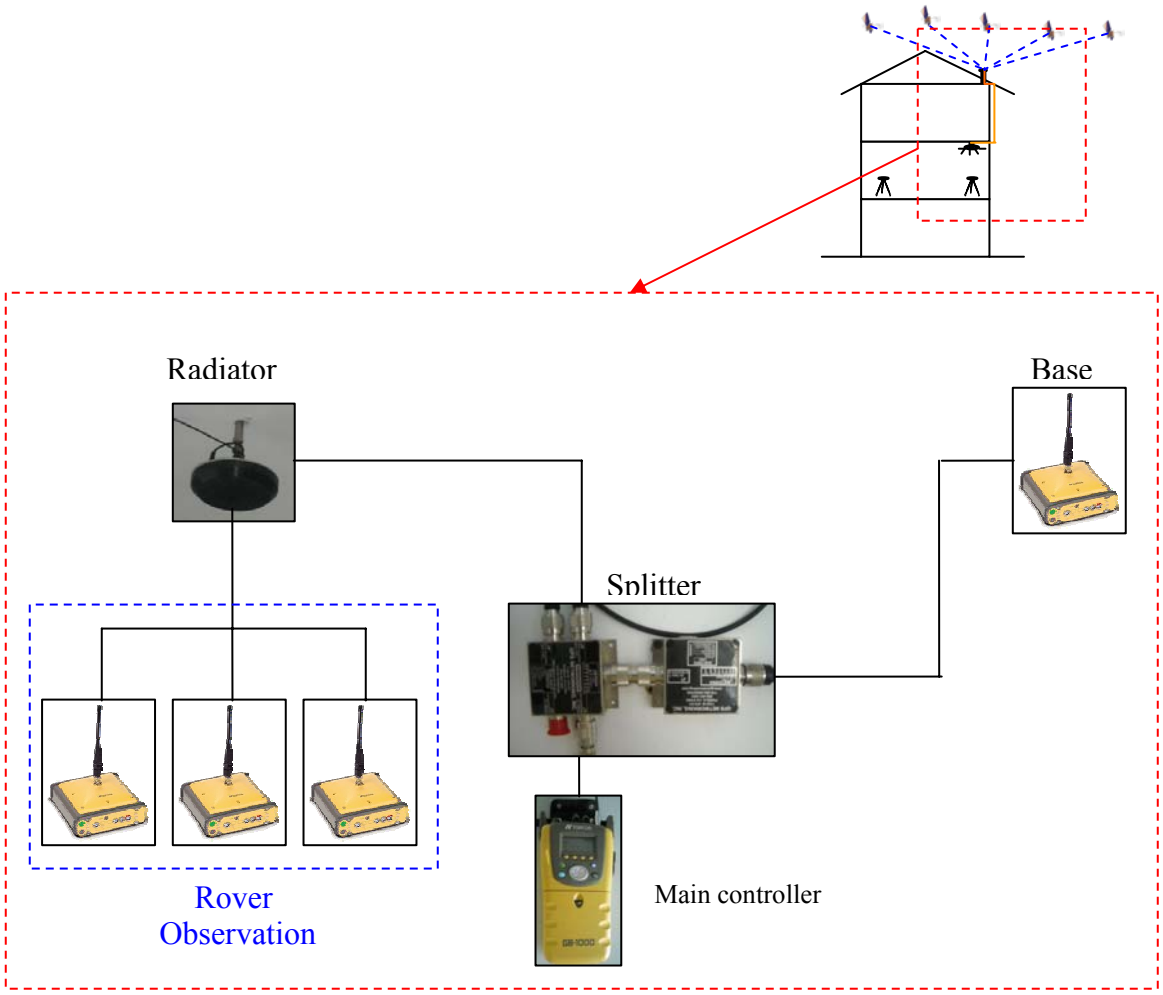

Figure 4.39: Assisted-GPS indoor SHM

Similar to the previous case study, GPS static survey was firstly conducted to obtain a reference to VRS-RTK technique conducted for SHM. Four reference points (A, B, C and D) were observed using static survey. Performance at a cut- off angle of 15 degree with 5 second data interval, three reference points (A, B, C and D) were observed using static survey. VRS-RTK was then conducted at similar reference points. There are four observation point were observed during this study. Each of this point was observed in five epochs. One epoch observation will be having 10 observation data. Figure 4.40 illustrates the overview of the instrumentation setup in the work area.

Figure 4.40: Instrument setup inside building

4.5.2 Result and Analysis

As mention earlier, GPS observation campaigns were performance at A, B, C, and D at three episodic intervals. Accordingly, Figure 4.41 – Figure 4.43 illustrates the observation residual of first epoch at observed points. Figure 4.44 illustrates the coordinate precision of point A obtained at Epoch 1.

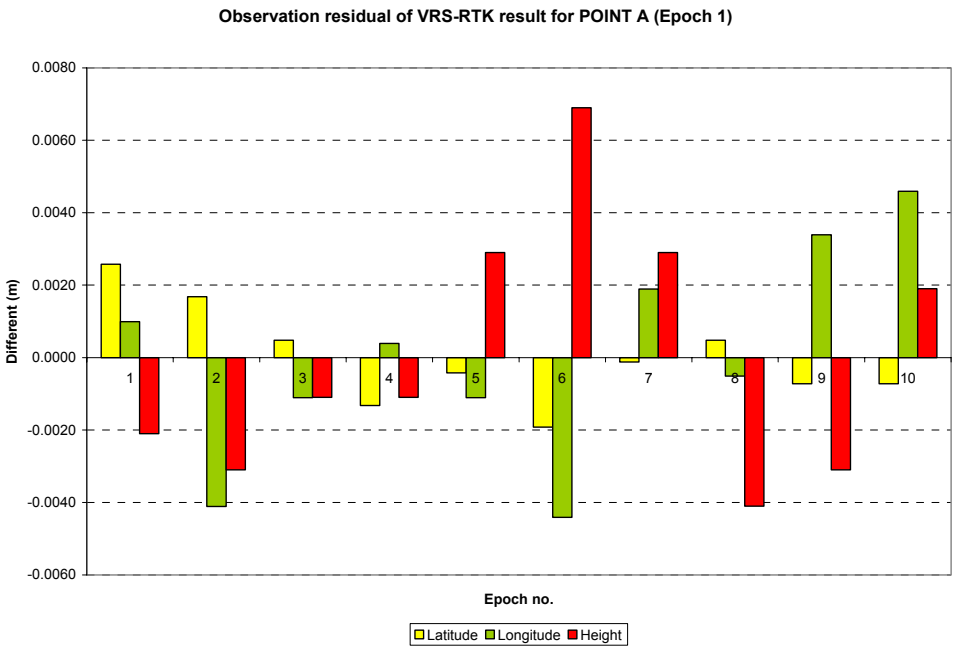

Figure 4.41: Observation residual at point A Epoch 1

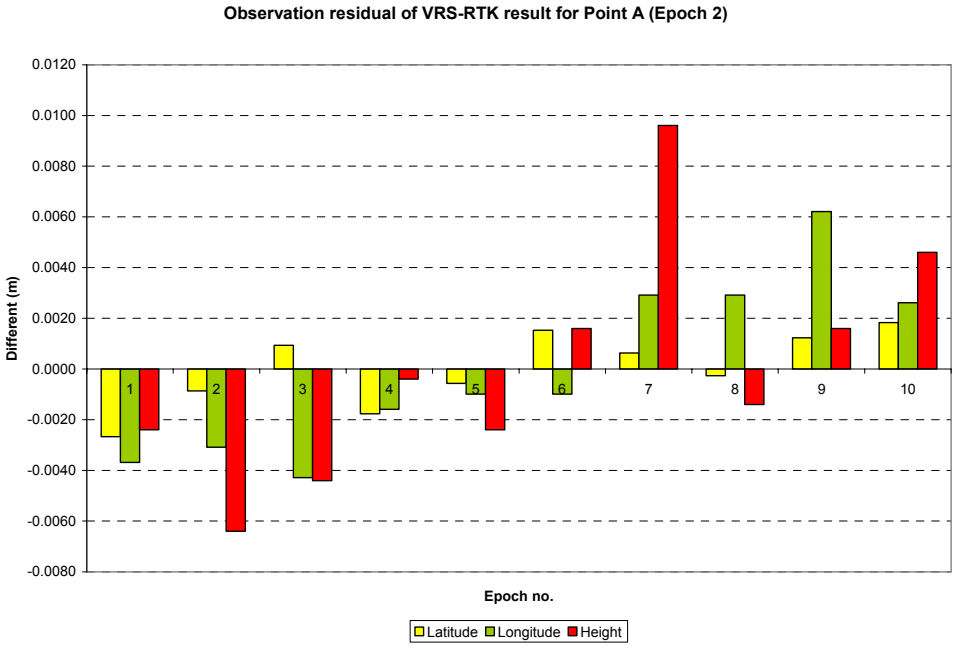

Figure 4.42: Observation residual at point A Epoch 2

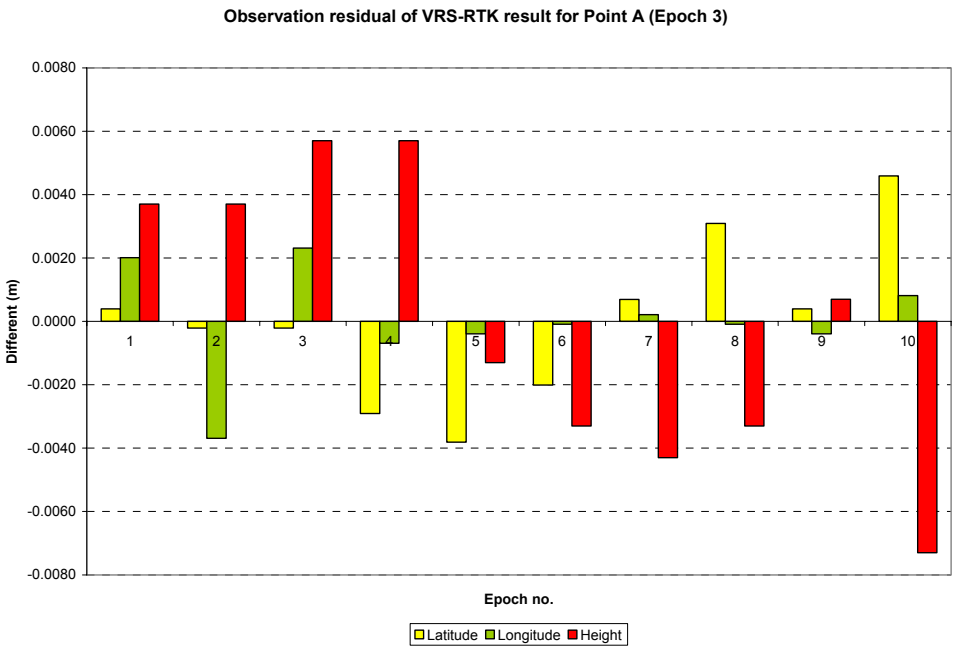

Figure 4.43: Observation residual at point A Epoch 3

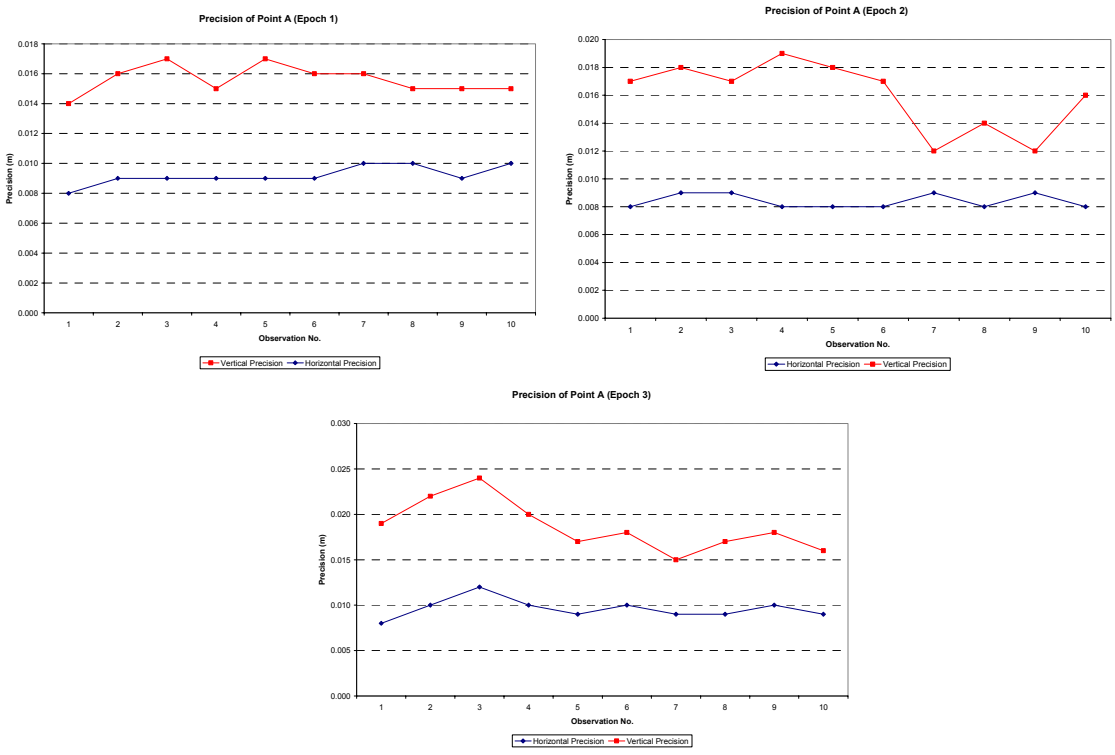

Figure 4.44: Precision analysis at point A for Epoch 1, 2 and 3

Based on the result, it is apparent that the maximum observation residual detected at point A on the basis of horizontal and vertical components were 0.005 m and 0.007 m respectively. For epoch 2, the maximum observation residual detected on the basic of horizontal and vertical component were 0.006 m and 0.006 m. For epoch 3 the maximum observation residual detected on the basic of horizontal and vertical component were 0.005 m and 0.007 m. As far as the horizontal precision analysis conducted of epoch 1, epoch 2 and epoch 3, it is noted that the maximum and the minimum residual range from 0.008 m to 0.010 m, 0.008 m to 0.009 m, and 0.008 m to 0.012 m respectively. As far as the vertical precision analysis conducted of epoch 1, epoch 2 and epoch 3, it is noted that the maximum and the minimum residual range from 0.014 m to 0.017 m, 0.012 m to 0.019 m, and 0.015 m to 0.024 m. Figure 4.45 – Figure 4.47 illustrates the observation residual at point B respectively. Figure 4.48 on the other hand illustrates the precision analysis at point B for every epoch.

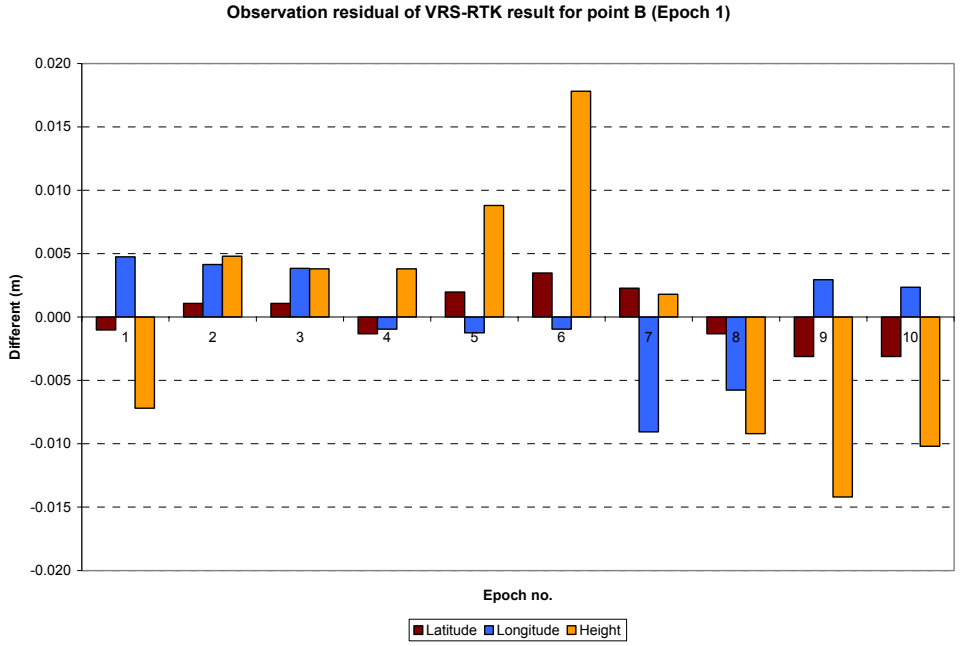

Figure 4.45: Observation residual at point B Epoch 1

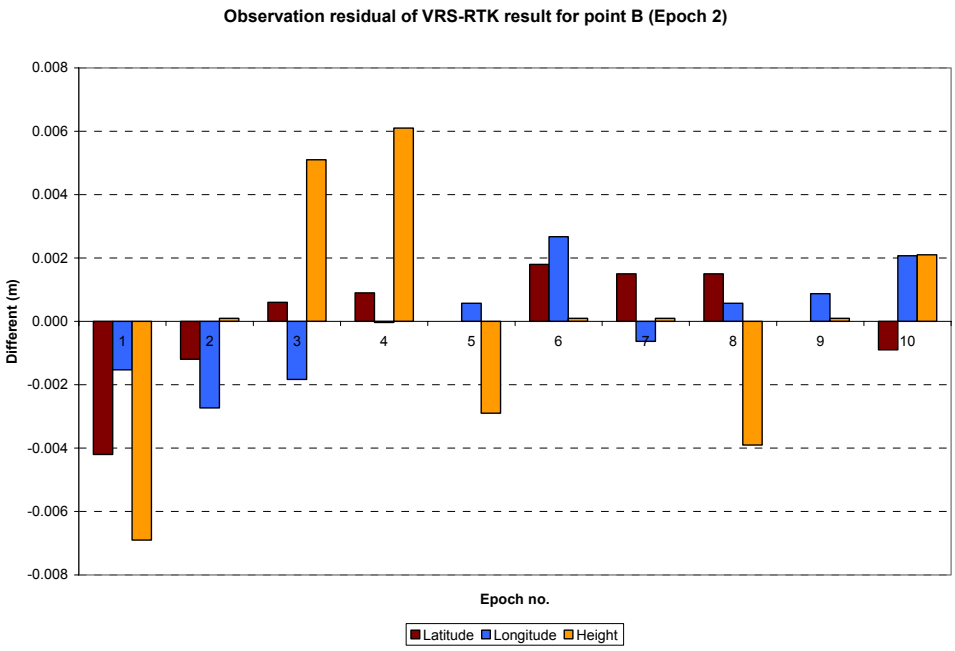

Figure 4.46: Observation residual at point B Epoch 2

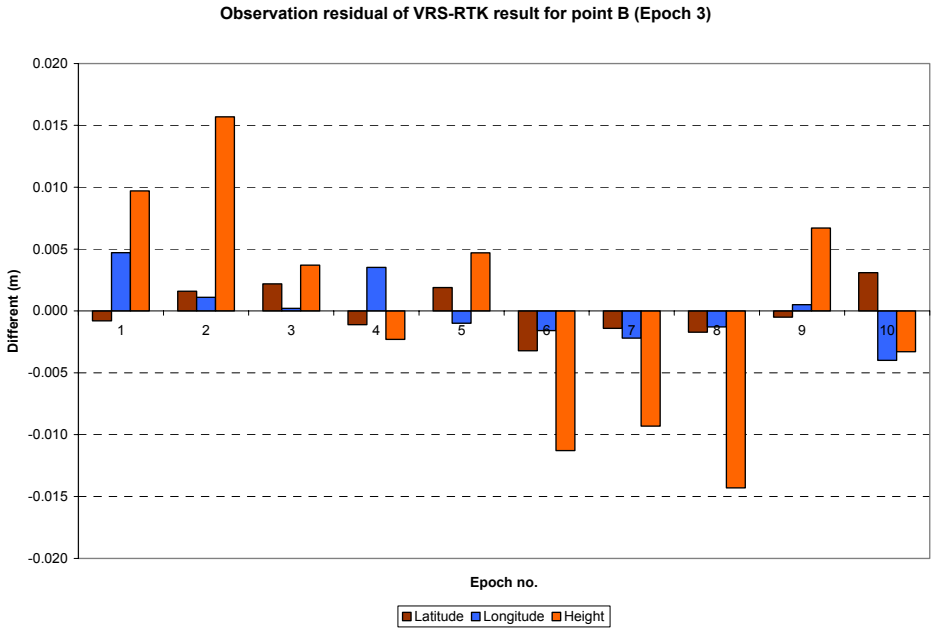

Figure 4.47: Observation residual at point B Epoch 3

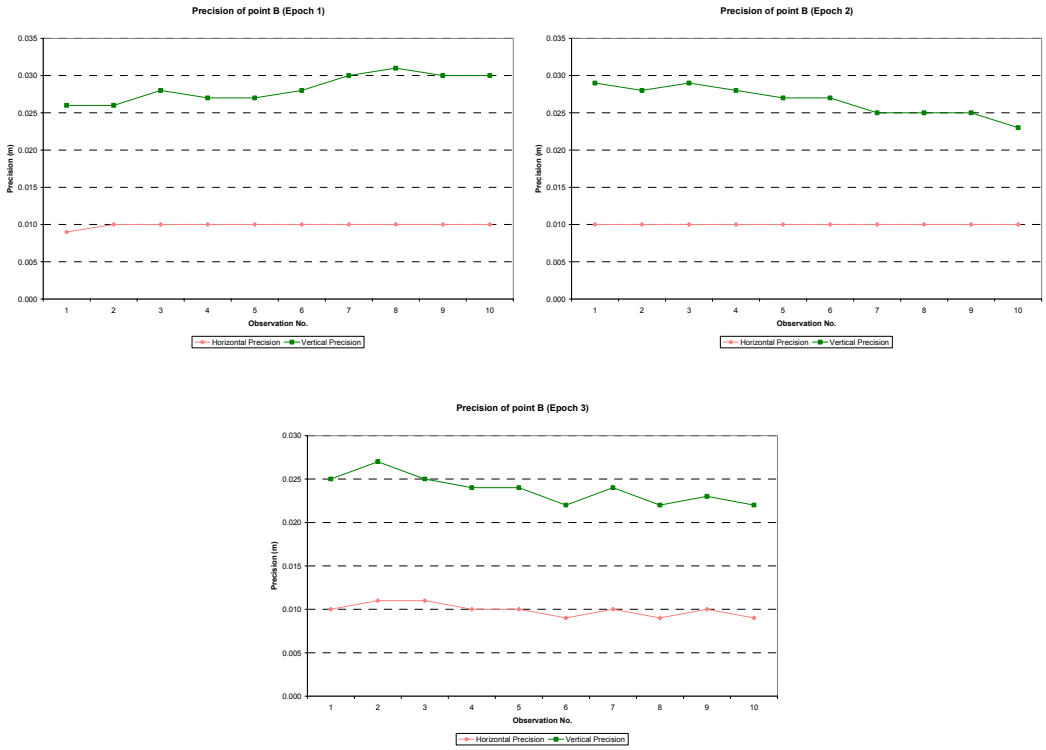

Figure 4.48: Precision graph of point B at Epoch 1, 2 and 3

Based on the result, the maximum observation residual detected at point B on the basis of horizontal and vertical components were 0.009 m and 0.018 m respectively. For epoch 2, the maximum observation residual detected on the basic of horizontal and vertical component were 0.004 m and 0.007 m. For epoch 3 the maximum observation residual detected on the basic of horizontal and vertical component were 0.005 m and 0.016 m. As far as the horizontal precision analysis conducted of epoch 1, epoch 2 and epoch 3, it is noted that the maximum and the minimum residual range from 0.009 m to 0.010 m, 0.010 m, and 0.008 m to 0.010 m respectively. As far as the vertical precision analysis conducted of epoch 1, epoch 2 and epoch 3, it is noted that the maximum and the minimum residual range from 0.026 m to 0.031 m, 0.023 m to 0.029 m, and 0.018 m to 0.025 m. Figure 4.49 – Figure 4.51 illustrates the observation residual at point C respectively. Figure 4.52 on the other hand illustrates the precision analysis at point C for every epoch.

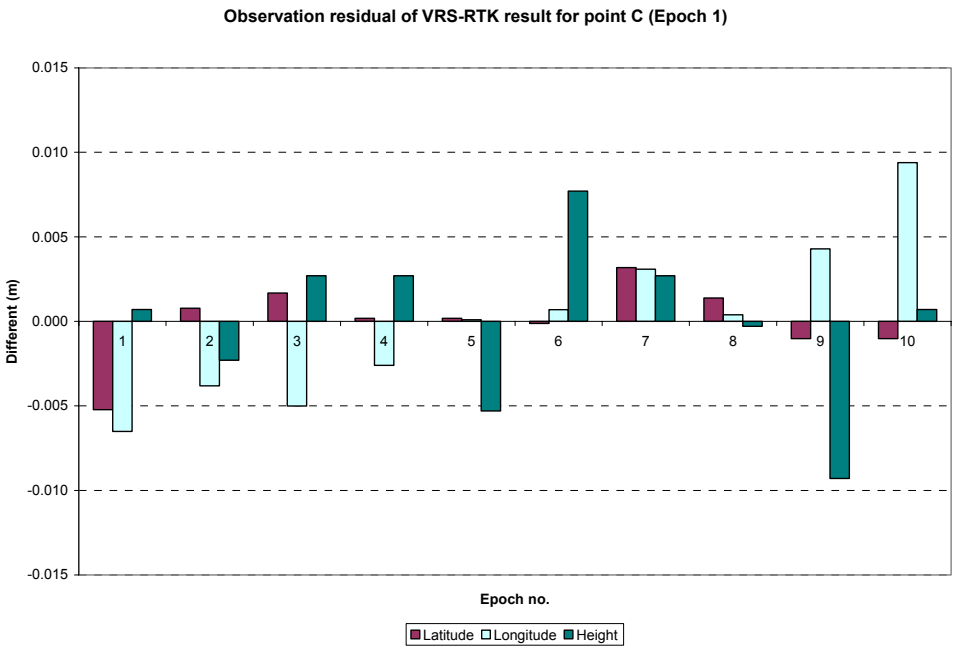

Figure 4.49: Observation residual at point C Epoch 1

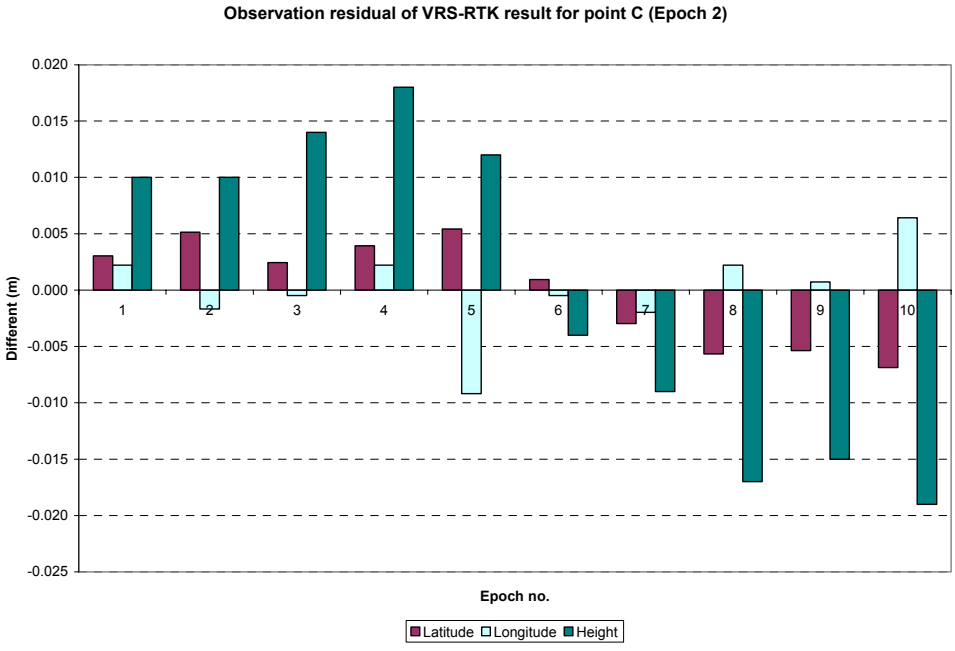

Figure 4.50: Observation residual at point C Epoch 2

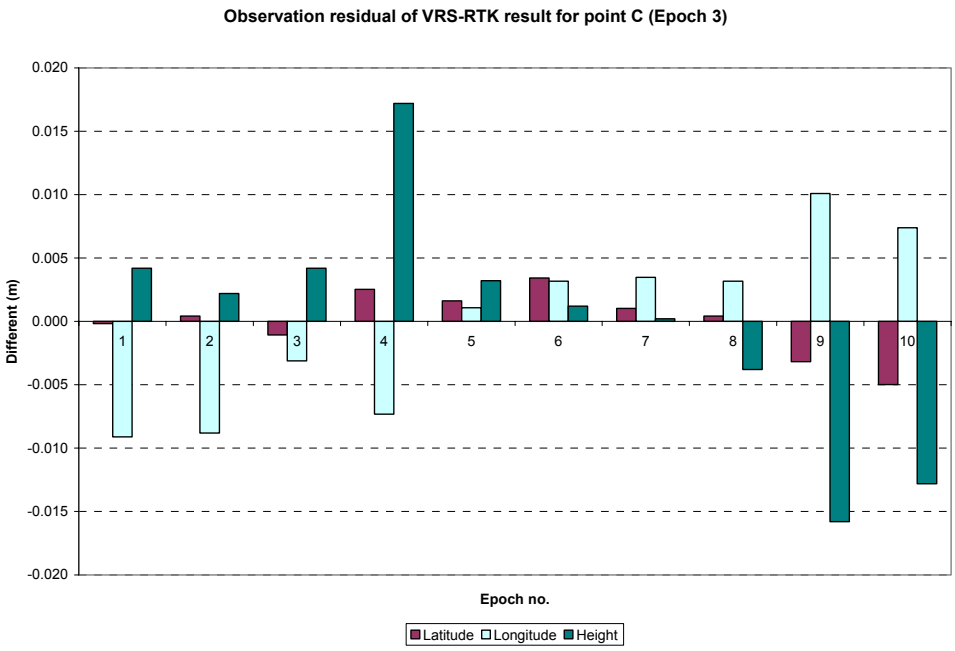

Figure 4.51: Observation residual at point C Epoch 3

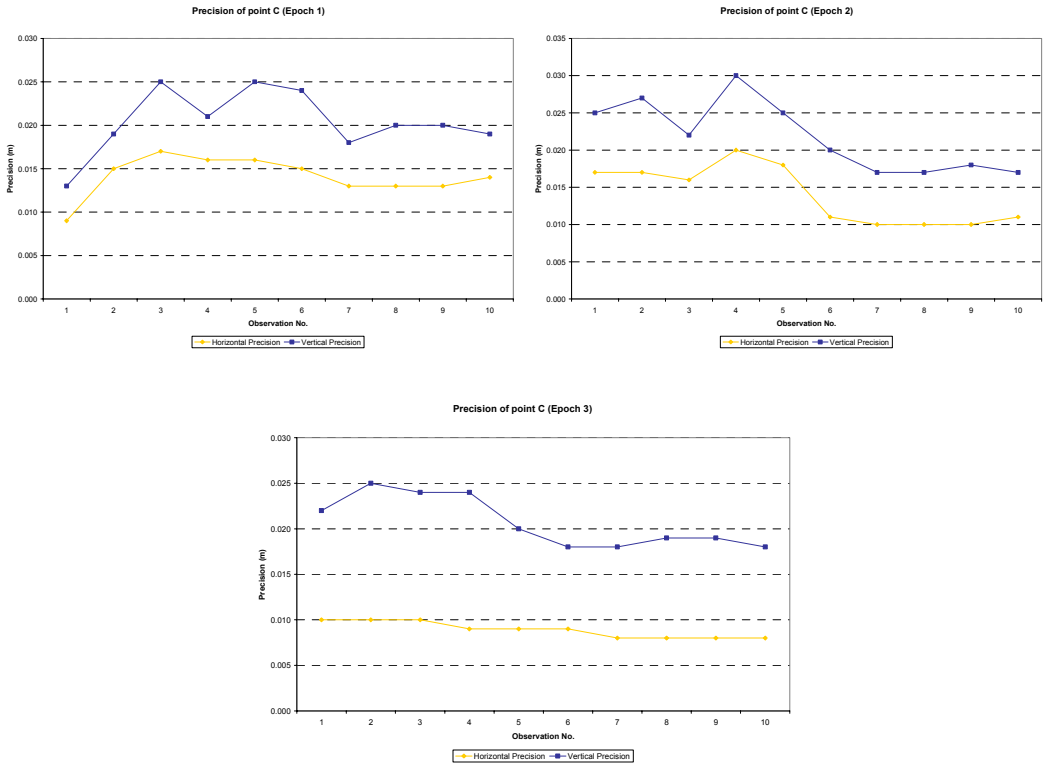

Figure 4.52: Precision analysis graph of point C at Epoch 1, 2 and 3

The result show that the maximum observation residual detected at point C on the basis of horizontal and vertical components were 0.009 m for both components respectively. For epoch 2, the maximum observation residual detected on the basic of horizontal and vertical component were 0.009 m and 0.019 m. For epoch 3 the maximum observation residual detected on the basic of horizontal and vertical component were 0.010 m and 0.017 m. As far as the horizontal precision analysis conducted of epoch 1, epoch 2 and epoch 3, it is noted that the maximum and the minimum residual range from 0.009 m to 0.017 m, 0.010 m to 0.020 m, and 0.009 m to 0.013 m respectively. As far as the vertical precision analysis conducted of epoch 1, epoch 2 and epoch 3, it is noted that the maximum and the minimum residual range from 0.013 m to 0.025 m, 0.017 m to 0.027 m, and 0.012 m to 0.015 m. Figure 4.53 – Figure 4.55 illustrates the observation residual at point D respectively. Figure 4.56 on the other hand illustrates the precision analysis at point D for every epoch.

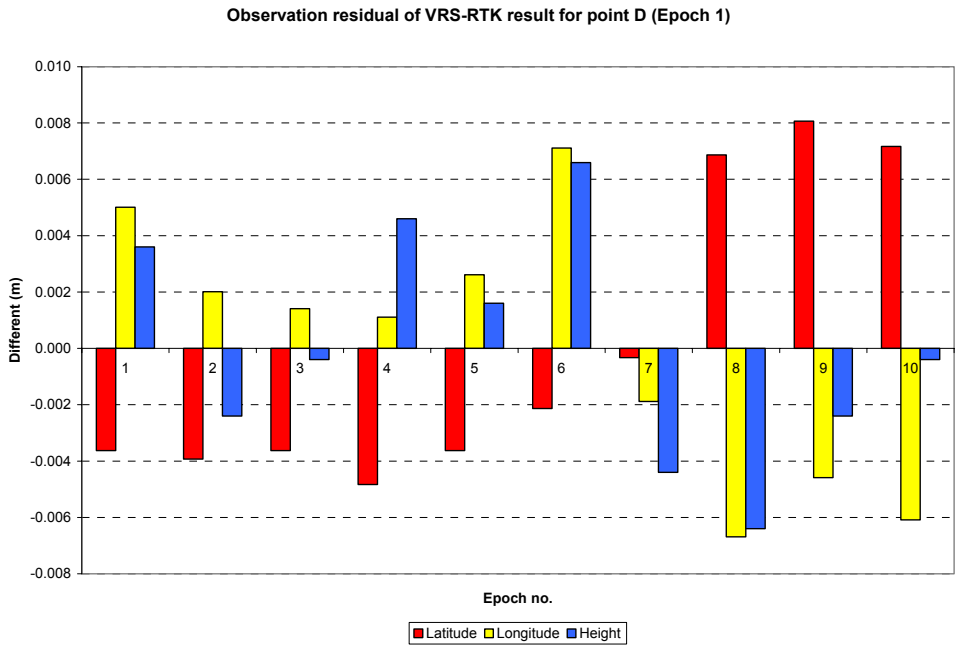

Figure 4.53: Observation residual at point D Epoch 1

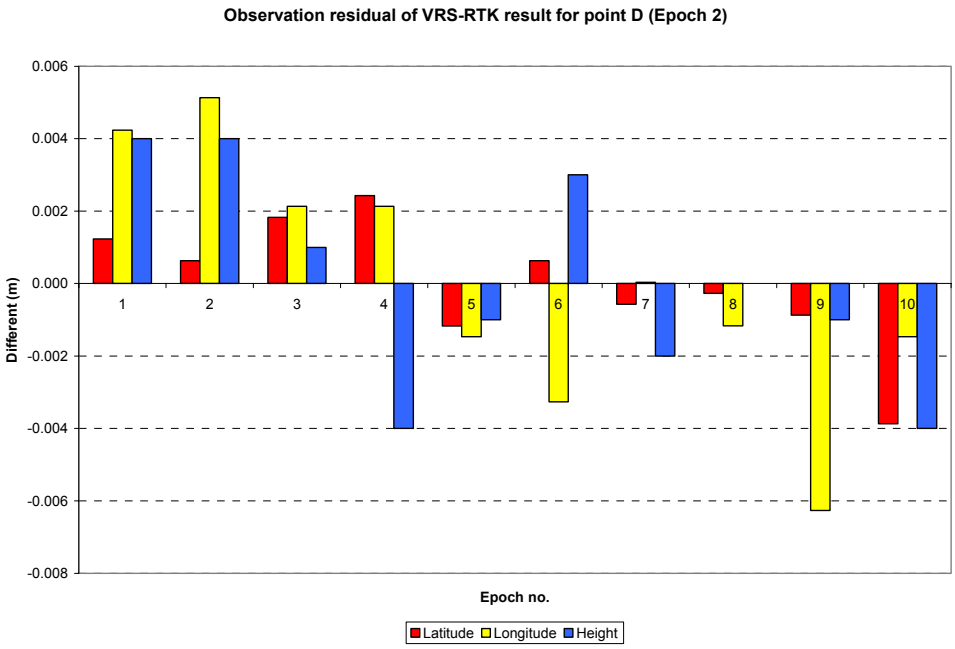

Figure 4.54: Observation residual at point D Epoch 2

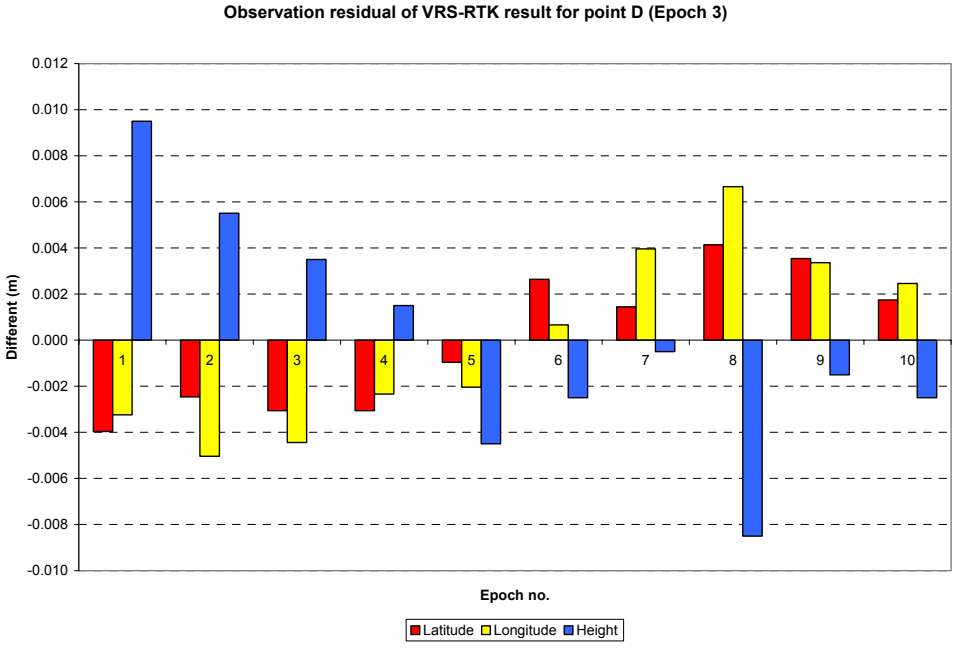

Figure 4.55: Observation residual at point D Epoch 3

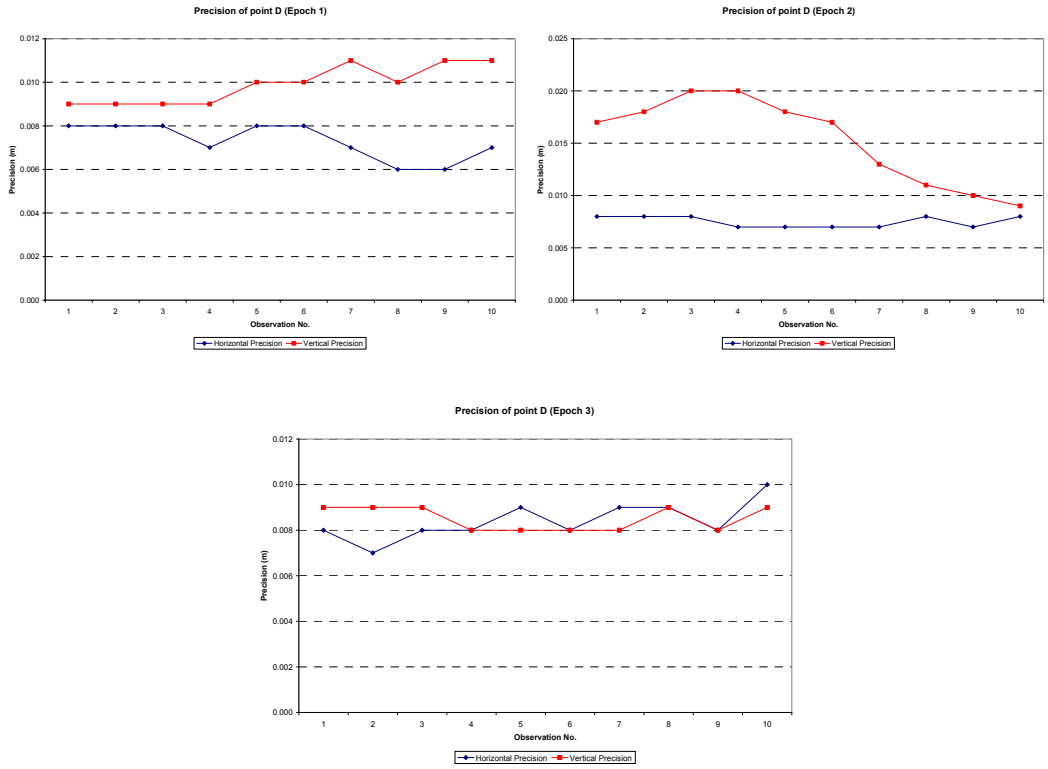

Figure 4.56: Precision analysis graph of point D at Epoch 1, 2 and 3

Based on the result, the maximum observation residual detected at point D on the basis of horizontal and vertical components at epoch 1 were 0.008 m and 0.006 m respectively. For epoch 2, the maximum observation residual detected on the basic of horizontal and vertical component were 0.006 m and 0.004 m. For epoch 3 the maximum observation residual detected on the basic of horizontal and vertical component were 0.005 m and 0.010 m. As far as the horizontal precision analysis conducted of epoch 1, epoch 2 and epoch 3, it is noted that the maximum and the minimum residual range from 0.006 m to 0.008 m, 0.007 m to 0.008 m, and 0.007 m to 0.010 m respectively. As far as the vertical precision analysis conducted of epoch 1, epoch 2 and epoch 3, it is noted that the maximum and the minimum residual range from 0.009 m to 0.011 m, 0.009 m to 0.020 m, and 0.008 m to 0.009 m. Detail on VRS-RTK data for every epoch is attached in Appendix C. The result for static data is shows in Table 4.25. The differences between the static data and the average of every epoch are shows in Table 4.26.

Table 4.25: Static Result for point A, B, C, and D

	Latitude (U)			Longitude (T)			Ellipsoid height(m)
A	3	9	1.85602	101	44	49.27562	61.784
B	3	9	1.85583	101	44	49.27474	61.496
C	3	9	1.85566	101	44	49.27527	61.523
D	3	9	1.85574	101	44	49.27557	61.722

Table 4.26: Differences of static data vs. VRS-RTK data for every epoch

	Latitude (U)			Longitude (T)			Height (m)
A	3	9	1.85602	101	44	49.27562	61.784
A E1	3	9	1.85560	101	44	49.27621	61.748
A E2	3	9	1.85622	101	44	49.27555	61.782
A E3	3	9	1.85591	101	44	49.27555	61.793
A - A E1(mm)			12.480			17.580	35.900
A - A E2 (mm)			5.970			2.040	1.600
A - A E3 (mm)			3.390			2.040	9.300
B	3	9	1.85583	101	44	49.27474	61.496
B E1	3	9	1.85587	101	44	49.27470	61.499
B E2	3	9	1.85589	101	44	49.27469	61.495
B E3	3	9	1.85578	101	44	49.27511	61.495
B - B E1(mm)			1.410			1.000	2.733
B - B E2 (mm)			1.890			1.330	1.567

B - B E3 (mm)			1.500			11.330	1.167
C	3	9	1.85566	101	44	49.27527	61.523
C E1	3	9	1.85569	101	44	49.27528	61.526
C E2	3	9	1.85576	101	44	49.27543	61.533
C E3	3	9	1.85560	101	44	49.27497	61.518
C - C E1(mm)			0.930			0.340	3.600
C - C E2 (mm)			2.880			4.810	10.300
C - C E3 (mm)			2.010			8.750	4.900
D	3	9	1.85574	101	44	49.27557	61.722
D E1	3	9	1.85566	101	44	49.27560	61.706
D E2	3	9	1.85580	101	44	49.27535	61.725
D E3	3	9	1.85573	101	44	49.27556	61.714
D - D E1(mm)			2.390			0.891	15.567
D - D E2 (mm)			1.750			6.732	3.033
D - D E3 (mm)			0.260			0.459	8.467

The differences between static data of point A and VRS-RTK data of point A for first epoch are 12.480 mm in latitude component, 17.580 mm for longitude component and 35.900 mm for height component. The differences of point A for second epoch are 5.970 mm in latitude component, 2.040 mm for longitude component and 1.600 mm for height component and the differences of static data for point A and VRS-RTK data for third epoch of point A are 3.390 mm in latitude component, 2.040 mm for longitude component and 1.600 mm for height component. The differences between static data of point B vs. VRS-RTK data of first epoch are 1.410 mm in latitude component, 1.000 mm for longitude component and 2.733 mm for height component, the differences of second epoch are 1.890 mm in latitude component, 1.330 mm for longitude component and 1.567 mm for height component, for the third epoch, the differences are 1.500 mm for latitude component, 11.330 mm for longitude component and 1.167 mm for height component.

Beside that, the differences between static data of point C and VRS-RTK data for epoch 1 are 0.930 mm in latitude component, 0.340 mm for longitude component and 3.600

mm for height component, the differences for epoch 2 are 2.880 mm for latitude component, 4.810 mm for longitude component and 10.300 mm for height component while the differences for epoch 3 are 2.010 mm for latitude component, 8.750 mm for longitude component and 4.900 mm for height component. For the point D, the differences for first epoch are 2.390 mm for latitude component, 0.891 mm for longitude component and 15.567 mm for height component. The differences for of second epoch are 1.750 mm for latitude component, 6.732 mm for longitude component and 3.033 mm for height component and the differences for third epoch of point D are 0.260 mm for latitude component, 0.459 mm for longitude component and 8.467 mm for height component. These differences of all point between true value and VRS-RTK data for every epoch shows in Figure 4.57.

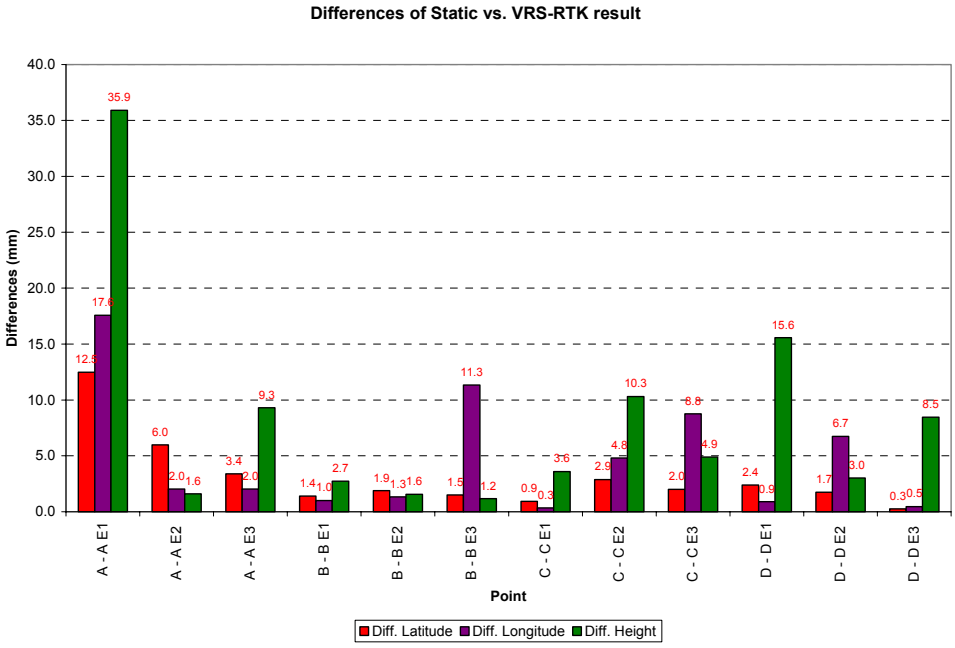

Figure 4.57: Differences static vs. VRS-RTK result

Differential coordinate of VRS-RTK result for all point observed between epochs are illustrate in the graph for point A (see Figure 4.58), point B (see Figure 4.59), point C

(see Figure 4.60) and point D (see Figure 4.61). The differential is between first epoch with second epoch and first epoch with third epoch.

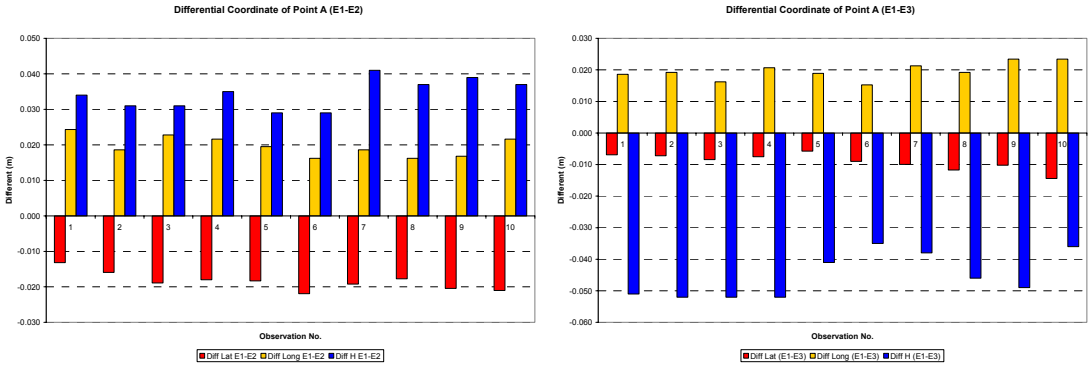

Figure 4.58: Differential Coordinate of Point A

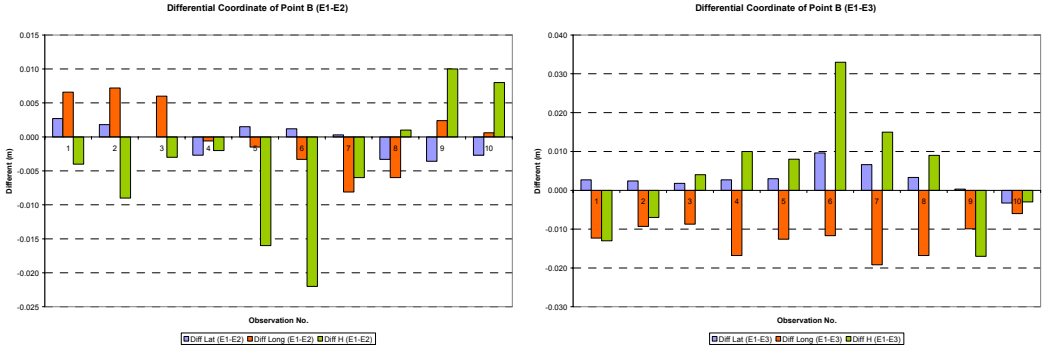

Figure 4.59: Differential Coordinate of Point B

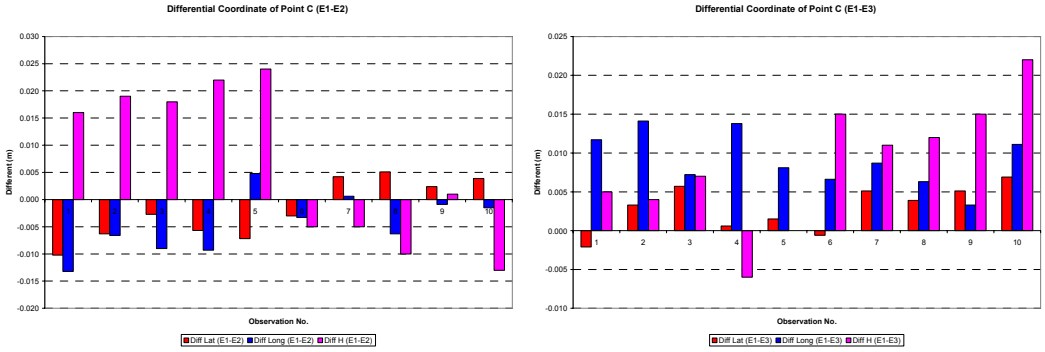

Figure 4.60: Differential Coordinate of Point C

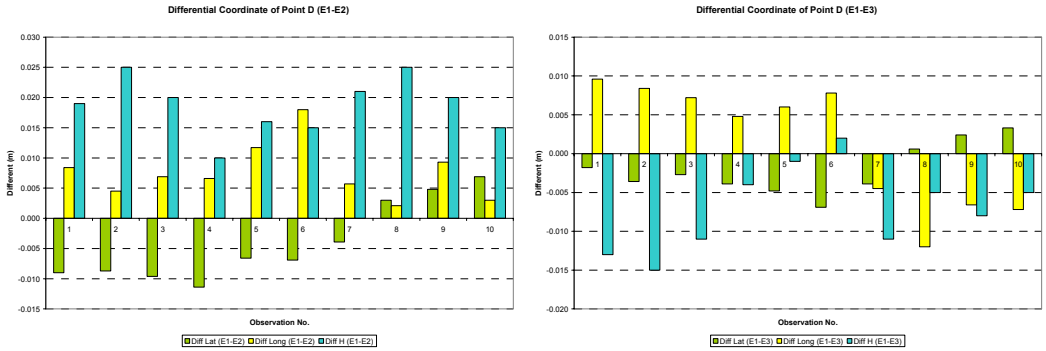

Figure 4.61: Differential Coordinate of Point D

The maximum differences of VRS-RTK result between epoch 1 and epoch 2 for point A are 0.024 m of horizontal component and 0.041 m of height component while the differences between epoch 1 and epoch 3 are 0.023 m of horizontal component and 0.052 m for vertical component. For point B, the maximum differences between epoch 1 and epoch 2 are 0.008 m of horizontal component and 0.022 m of vertical component while the maximum differences between epoch 1 and epoch 3 are 0.009 m of horizontal component and 0.033 m of vertical component. Beside that, the maximum differences between first epoch and second epoch for point C are 0.013 m of horizontal component and 0.024 m of vertical component and the maximum differences between first epoch and third epoch for point C are 0.012 m of horizontal component and 0.022 m of vertical component. The maximum differences between first epoch and second epoch for point D are 0.011 m of horizontal component and 0.025 m of vertical component and the maximum differences between first epoch and third epoch for point D are 0.012 m of horizontal component and 0.015 m of vertical component.

Initialization time is a time required to solve ambiguities of the VRS-RTK system. In this study, the initialization time or time to first fix (TTFF) of all epoch observation for this study was recorded (see Figure 4.62). Based on the result, it is noted that the GPS

signal strength inside the building are good whereby TTFF for all observation campaigns were less than 15 second. For point A, C and D, the TTFF for epoch 2 and epoch 3 are less than TTFF of epoch 1. The TTFF for epoch 2 of point B is more than TTFF of epoch 1.

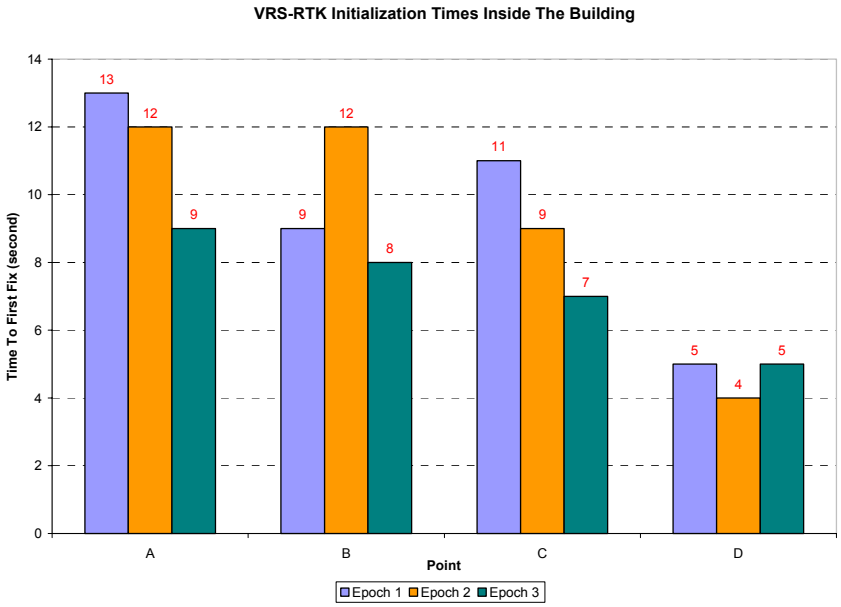

Figure 4.62: TTFF of VRS-RTK technique inside the building

Based on this study, several conclusions can be made based on the results obtained from the study. Divided on the basic of the structural health and GPS positioning performance amongst other conclusion includes:

1. Topcon Building was in a stable condition with no significance deformation detected during the GPS observation campaigns.

2. The VRS-RTK technique can be used for indoor monitoring if all the component is proper setup.

This case study gives the great idea which can prevent the observed point from the obstruction. This is because this assisted GPS can make monitoring the structural in indoor area are possible.

4.6 Summary

The purpose of this calibration is to test the instrument used in this research. Beside that, this calibration was needed because the proposed method is new in SHM. The simulation test was tested to study the received data during the observation. Both calibration and simulation test is important for first stage in proposed the new method in SHM. All the calibration result shows that the results are less than 3 cm tolerance for horizontal component and 6 cm tolerance for vertical component. The case study that is performed in indoor area shows that the VRS-RTK technique is capable to apply inside the building and have a good potential. The integrated stuff inside the building with outside receiver proves that the signal strength that is received by outside receiver can be exactly same with inside receiver.

CHAPTER 5

CASE STUDIES: SHM DATA COLLECTION AND ANALYSIS

5.1 Introduction

This chapter explains SHM data collection and analysis approaches at different environments and infrastructures. Conducted using VRS-RTK technique, the analyses of the measurements was discussed. On the basis of two case studies: the GPS-based breakwater monitoring and GPS-based building monitoring.

5.2 Case Study I: GPS-Based Breakwater Monitoring

This study presents the GPS survey measurements performed at the South Breakwater of the Export Terminal, Tanjung Sulong, Kemaman, Terengganu Darul Iman (Figure 5.1). The South Breakwater was constructed between 1981 and 1985 to accommodate the safeties of the navigable vessels to the Export Terminal of the Plant Operation Division of PETRONAS Gas Berhad (PGB) the nation's premier transshipment hub. Measuring of about 1525 m, the breakwater is of rubble mound type armoured with stone of igneous rock, weighing 5-10.5 tonnes. In order to monitor the performance of the structure due potential movements subsequently induced by wave motions and seepage,

monitoring survey using GPS were conducted. The flow of GPS campaign is as illustrated in Figure 5.2 and Figure 5.3 shows the monitoring concept of VRS-RTK at Breakwater.

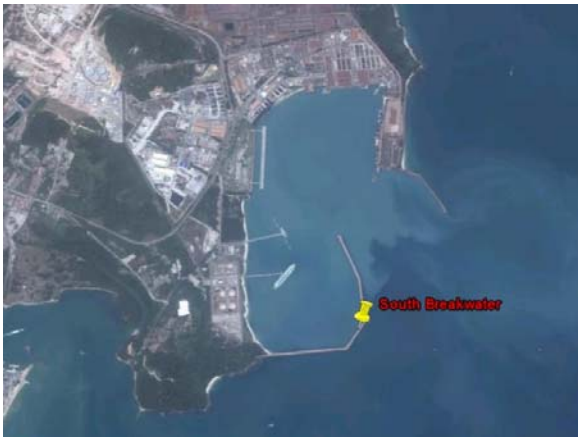

Figure 5.1: South Breakwater at Export Terminal Tanjung Sulong, Kemaman, Terengganu

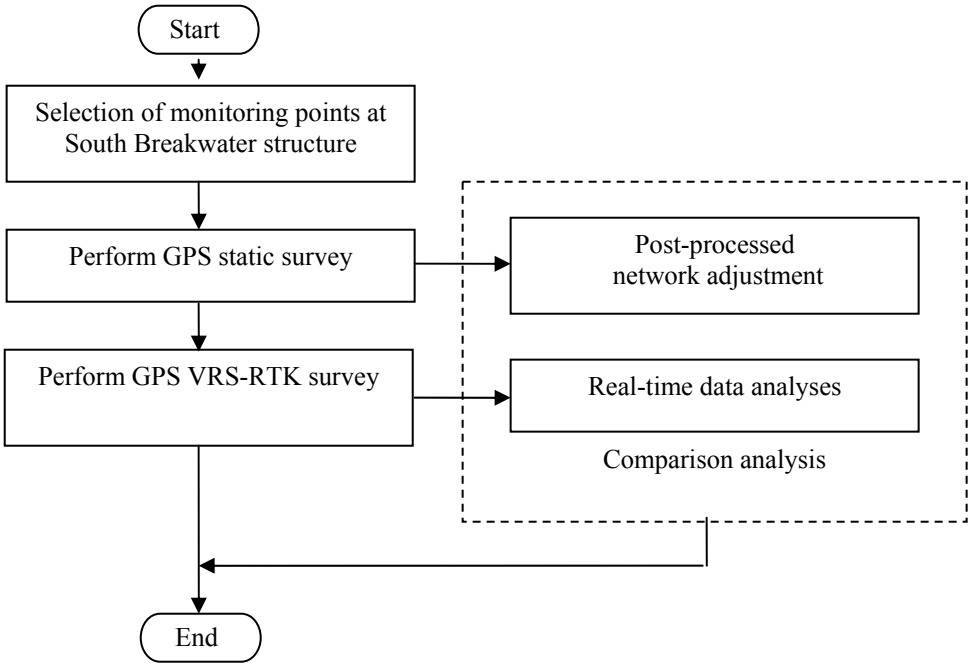

Figure 5.2: Flow of GPS campaign

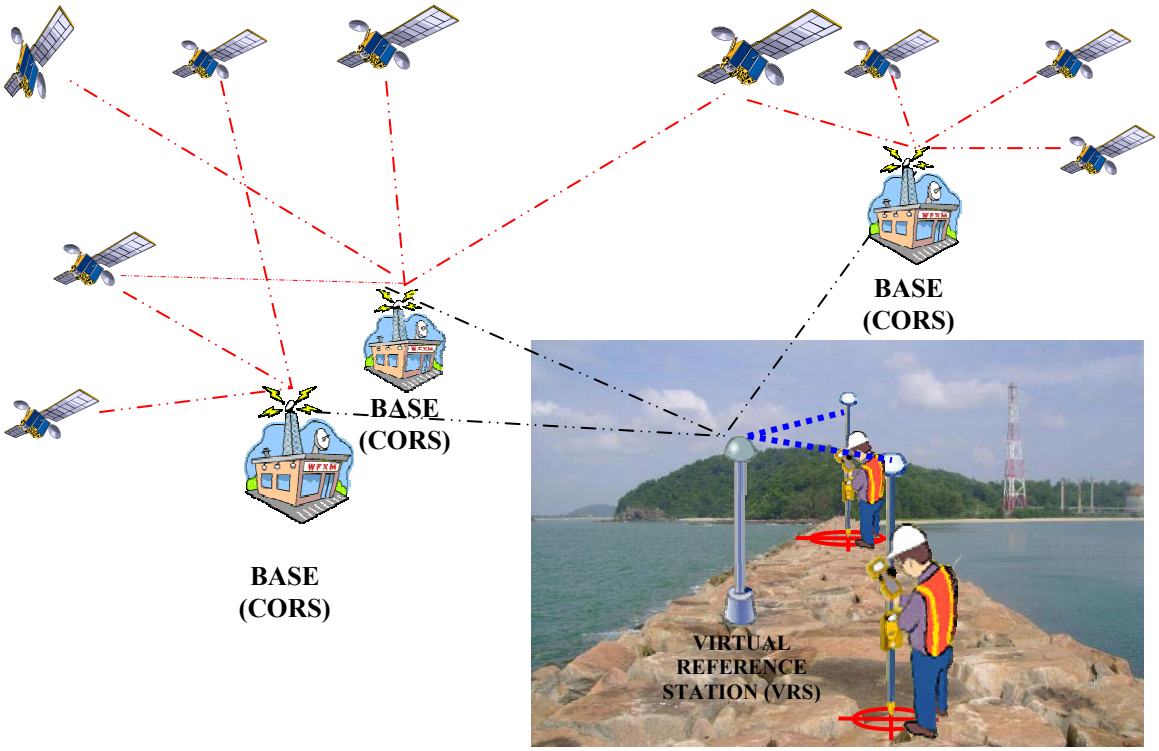

Figure 5.3: Concept of VRS-RTK at Breakwater

5.2.1 The Methodology

TRIMBLE 4800 and Topcon HiPer GA receivers were used (Figure 5.4). As both receiver are dual-frequency receivers the advantages of dual-frequency receivers include, the ability to survey with higher accuracy for longer baselines and less occupation time spent at each survey (monitoring) points.

Figure 5.4: TRIMBLE 4800 GPS Receiver and Topcon HiPer GA Receiver

Two GPS campaign using static survey and VRS-RTK survey were performed. In addition to the Department of Surveying and Mapping's GPS reference point (P227) located at about 10.5 km from the South Breakwater. The following points were observed during the GPS campaign:

i. One control station (UTM01) near the Export Terminal. This point served as an additional reference station to support GPS-based breakwater monitoring.

ii. Six monitoring points (A, X, B, C, D and E) on the breakwater (Figure 5.5)

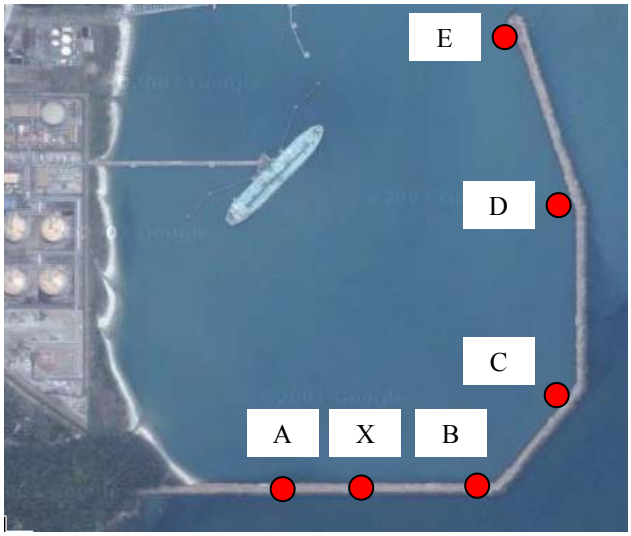

Figure 5.5: Monitoring point at South Breakwater

Two dual-frequency TRIMBLE 4800 receivers were used to conduct observations in static mode. For the purpose of this study one receiver was configured as a reference station whilst the other as a rover. Figure 5.6 and Figure 5.7 illustrates the set up of GPS reference station and rover station respectively.

Figure 5.6: Reference Station (Point P227)

Figure 5.7: Rover Station

Static surveying technique has been conducted to establish the true positions (coordinates) of the monitoring points. During the static survey, carrier phase observations were recorded every 15 second for about half an hour. A minimum of four satellites were observed during the whole observation period.

GPS post-processed relative data processing and network adjustment were performed using Trimble Geomatic Office (TGO) software. Output from this software consists of adjusted coordinates at two stations for each observation session, along with the associated covariance information. Since, the GPS positioning provides position in geocentric World Geodetic System 1984 (WGS84), the transformation of these coordinates

to the local geodetic system is needed. In this case, the GPS data processing and reduction of the three dimensional WGS84 coordinates were performed to obtain Rectified Skew Orthomorphic (RSO) coordinates. The results of static GPS measurements for the six monitoring points were summarized in Table 5.1.

Table 5.1: Coordinates of Static Monitoring

Points	Latitude	Longitude	Height
A	4°14'20.33982"N	103°27'42.84803"E	9.608
X	4°14'20.33910"N	103°27'49.72737"E	9.703
B	4°14'20.32691"N	103°27'56.11772"E	9.645
C	4°14'25.88993"N	103°28'00.71422"E	6.887
D	4°14'35.74752"N	103°28'00.70558"E	6.728
E	4°14'46.22207"N	103°27'57.13856"E	7.100

In order to perform SHM using VRS-RTK technique, Topcon HiPer GA receiver was used. Similar to the Trimble 4800 receiver, Topcon HiPer GA receiver is a tightly integrated instrument in which all components (antenna, receiver and UHF radio link) are in one unit that sits atop a pole (which cleverly contains the batteries in its base) or a tripod VRS-RTK measurements were performed at 1 epoch for every monitoring point. Each epoch consists of 10 observations at an average of 5 second per observation. VRS-RTK provide the position in real-time. Table 5.2 illustrates the result of VRS-RTK survey.

Table 5.2: Coordinates of VRS-RTK monitoring

Points	Latitude	Longitude	Height (m)
A	4°14'20.33985"N	103°27'42.84810"E	9.614
X	4°14'20.33914"N	103°27'49.72740"E	9.700
B	4°14'20.32692"N	103°27'56.11774"E	9.650
C	4°14'25.88997"N	103°28'00.71422"E	6.891
D	4°14'35.74749"N	103°28'00.70553"E	6.734
E	4°14'46.22208"N	103°27'57.13861"E	7.104

5.2.2 Result and Analysis

The mean of 10 VRS-RTK results were compared with 10 individual GPS observation result. To estimate the error deviation detected of each GPS observation data, statistical analysis was then conducted using Root mean square (RMS). The different value of VRS-RTK result with the average coordinate for each point illustrated in Figure 5.8. Table 5.3 on the other hand is illustrates the RMS for point A. Further details other points are as shown in Appendix D.

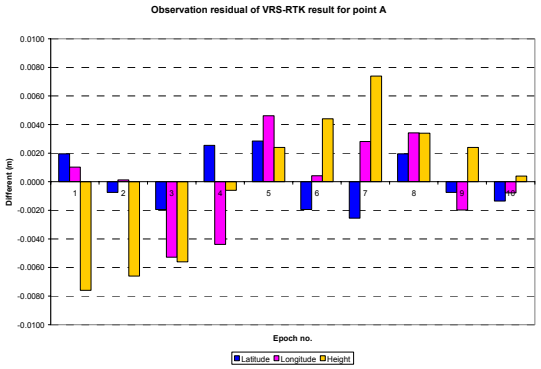

Point A

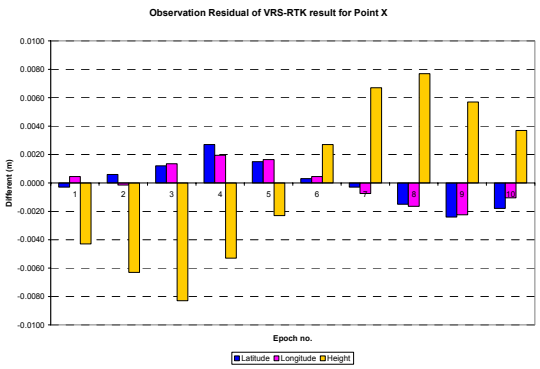

Point X

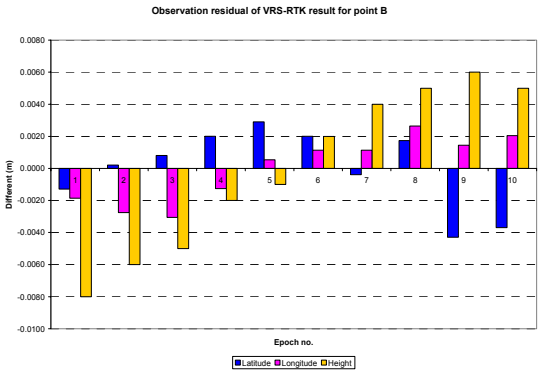

Point B

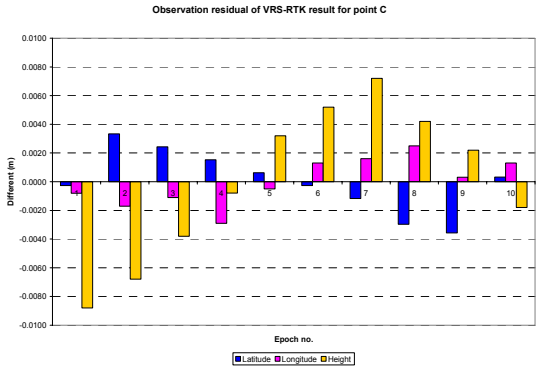

Point C

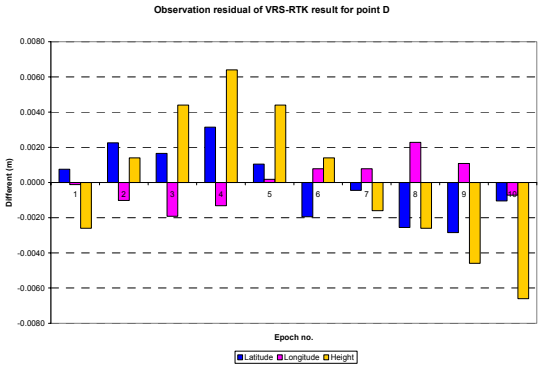

Point D

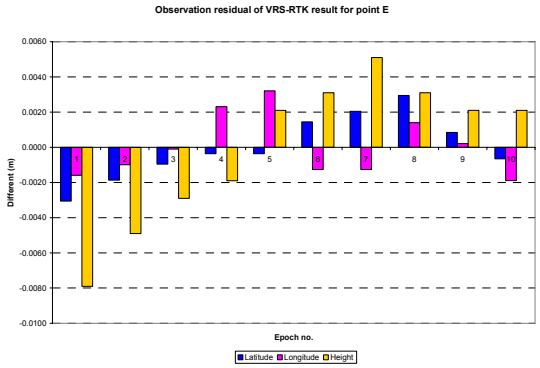

Point E

Figure 5.8: Observation residual of VRS-RTK result for point A, X, B, C, D and E

Table 5.3: RMS of Point A

ANALYSIS OF VRS-RTK										
Station no	A				Epoch				1	
	Latitude (U)				Longitude (T)				Ellipsoid height(m)	
No of observation	°	‘	”	v (m)	°	‘	”	v (m)	Observation	v (m)
1	4	14	20.33991	0.0019	103	27	42.84813	0.0010	9.606	-0.008
2	4	14	20.33982	-0.0008	103	27	42.8481	0.0001	9.607	-0.007
3	4	14	20.33978	-0.0019	103	27	42.84792	-0.0053	9.608	-0.006
4	4	14	20.33993	0.0025	103	27	42.84795	-0.0044	9.613	-0.001
5	4	14	20.33994	0.0028	103	27	42.84825	0.0046	9.616	0.002
6	4	14	20.33978	-0.0019	103	27	42.84811	0.0004	9.618	0.004
7	4	14	20.33976	-0.0026	103	27	42.84819	0.0028	9.621	0.007
8	4	14	20.33991	0.0019	103	27	42.84821	0.0034	9.617	0.003
9	4	14	20.33982	-0.0008	103	27	42.84803	-0.0020	9.616	0.002
10	4	14	20.33980	-0.0014	103	27	42.84807	-0.0008	9.614	0.000
Average	4	14	20.33985		103	27	42.84810		9.614	
Minimum	4	14	20.33976		103	27	42.84792		9.606	
Maximum	4	14	20.33994		103	27	42.84825		9.621	
RMS (m)	0.000				0.000				0.000	
Diff between obs coordinate (average) with true value (mm)	0.075				0.198				5.600	

RMS for Point A

Small variation can be detected on the observed positioning component using VRS-RTK especially on the height component. Based on the result, the height variations at point A, X, B, C, D and E were 0.000 -0.008 m, 0.000 – 0.003 m, 0.000 – 0.004 m, 0.000 – 0.004 m, 0.000 – 0.003 m, and 0.000 – 0.003 m. As far as the Northing component is concerned, the variations range from about 0.000 – 0.003 m, 0.000 – 0.002 m, 0.000 – 0.003 m, 0.000 – 0.003 m, 0.000 – 0.002 m and 0.001 – 0.003 m. for point A, X, B, C, D and E respectively. The variations on the Easting component is about 0.001 – 0.005 m, 0.002 – 0.008 m, 0.001 – 0.008 m, 0.001 – 0.009 m, 0.001 – 0.007 m and 0.002 – 0.008 m for point A, X, B, C, D and E respectively.

For the purpose of South Breakwater monitoring, observations campaign of static and VRS-RTK were then analyzed. The adjusted coordinates and reduced levels between

two different campaigns (observation mode) were compared and investigated. Figure 5.9 shows the differences coordinates (lat, long, height) of the monitoring points in the RSO coordinates system between two observation modes.

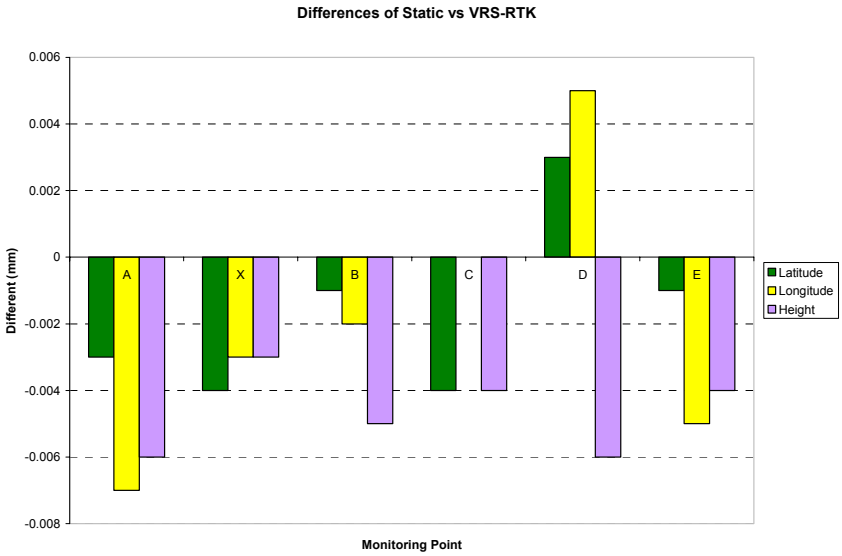

Figure 5.9: Difference of Static vs VRS-RTK in Horizontal and Vertical Component

Based on the result, the differences of static and VRS-RTK technique at northing, easting and height component in SHM can be expected. The coordinate differences for nothing component is about 4 mm. As far as the easting positioning component is concerned, the differences between the static and VRS-RTK is about 7 mm. In regards to the vertical movement, the difference between these two observation modes on the other hand is about 6 mm.

The initialization time of all points for this campaign was recorded (see Figure 5.10). Based on the result, TTFF for all observation campaigns were typically less than 45 seconds. The TTFF for point A was 24 second, point X was 29 second, point B was 34 second, point C was 38 second, point D was 35 second and point E is 41 second. These initialization times were somewhat poor compare to previous indoor monitoring work

where the TTFF of indoor monitoring was less than 15 seconds. This raises the possibility of multipath effect because the breakwater environment it self is at sea site.

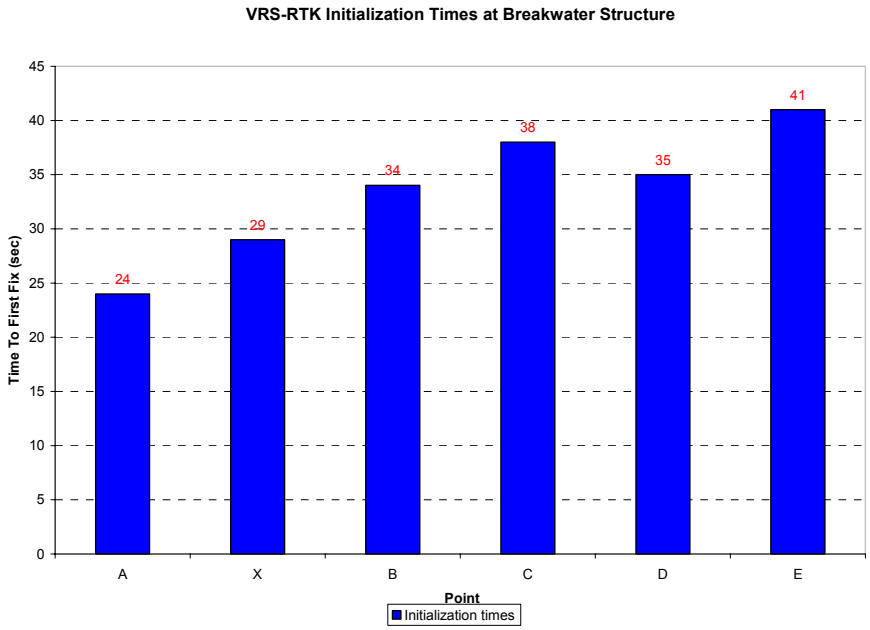

Figure 5.10: TTFF of VRS-RTK technique at Breakwater Structure

Several conclusions can be made based on the results obtained from the study. Divided on the basic of the structural health and GPS positioning performance amongst other conclusion includes:

1. South Breakwater was in a stable condition with no significance deformation detected during the GPS observation campaigns.

2. Though discrepancies in the GPS measurement using two differences method (static and VRS-RTK) can be expected, it is apparent that these variations were at a minimal value of 0.004 m N, 0.007 m E and 0.006 H only.

5.3 Case Study II: GPS – Based Building Monitoring

This study focuses on SHM conducted at Composite Lab, Block P23, three storey building Faculty of Mechanical Engineering, Universiti Teknologi Malaysia. As Figure 5.11 illustrates the layout of the study area, Figure 5.12 shows the overview of the building.

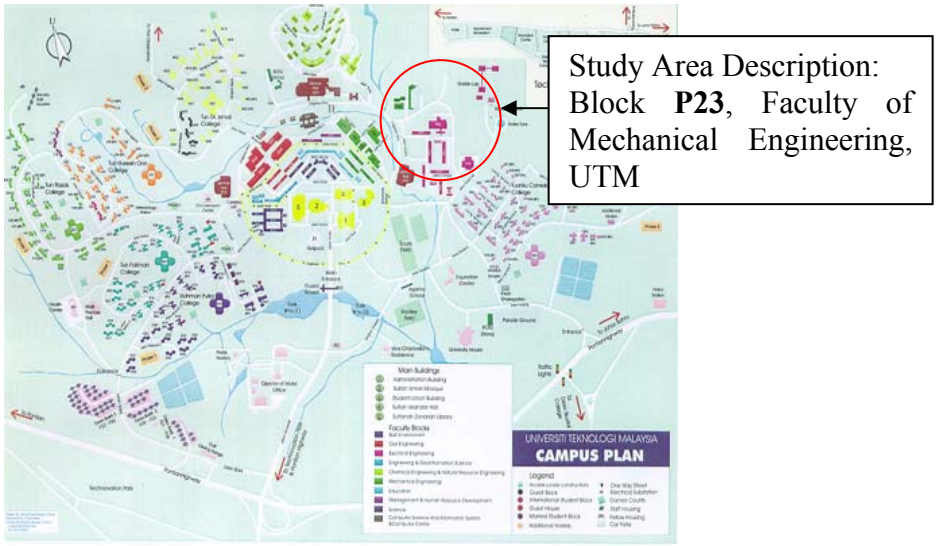

Figure 5.11: Layout of the study area

Figure 5.12: Overview of P23 Building

5.3.1 The Methodology

Similar to the GPS observation campaign conducted during Case Study 1, this study focuses on the SHM VRS-RTK technique using Topcon HiPer GA dual- frequency receivers. In addition to three monitoring station (P1, P2 and P3) located at the top of P23 building, three ground station (B001, B002 and B003) were established to be used as the reference station. Figure 5.13 illustrated Sketch of control station and monitoring station in study area and Figure 5.14 illustrated VRS-RTK observation at building P23. There is restricted area which was not allowed any one to use that area because there are many cracks on the wall at that side.

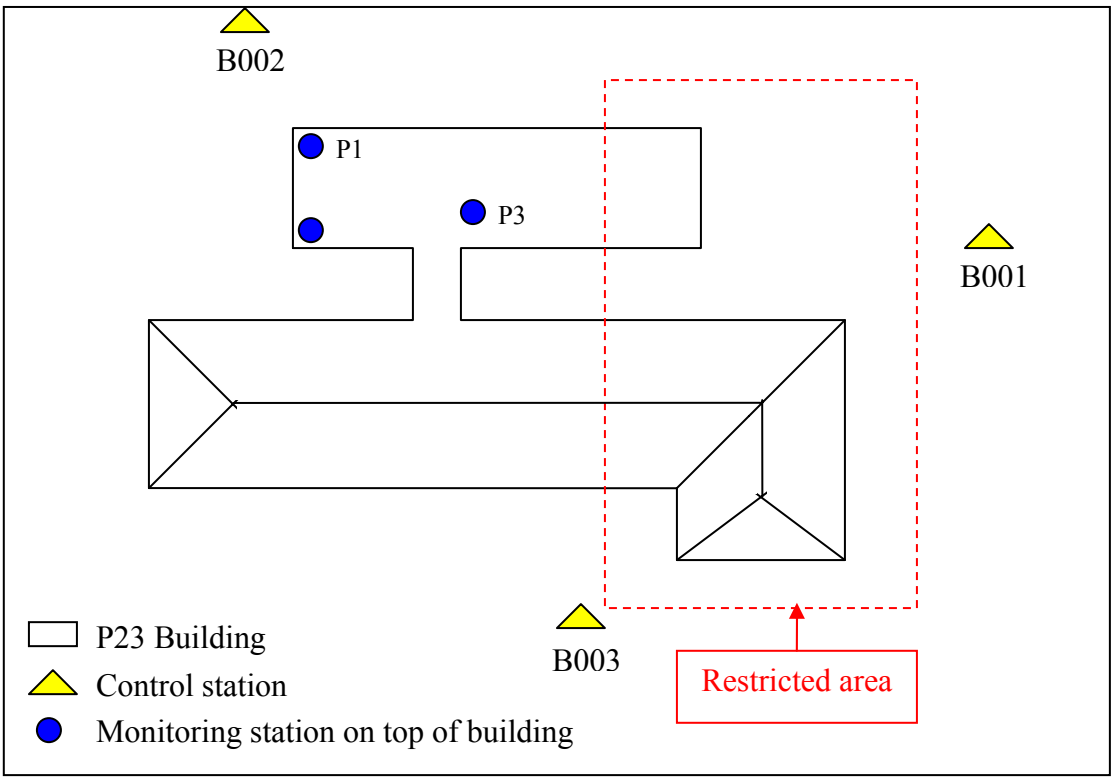

Figure 5.13: Distribution of GPS point at P23 building

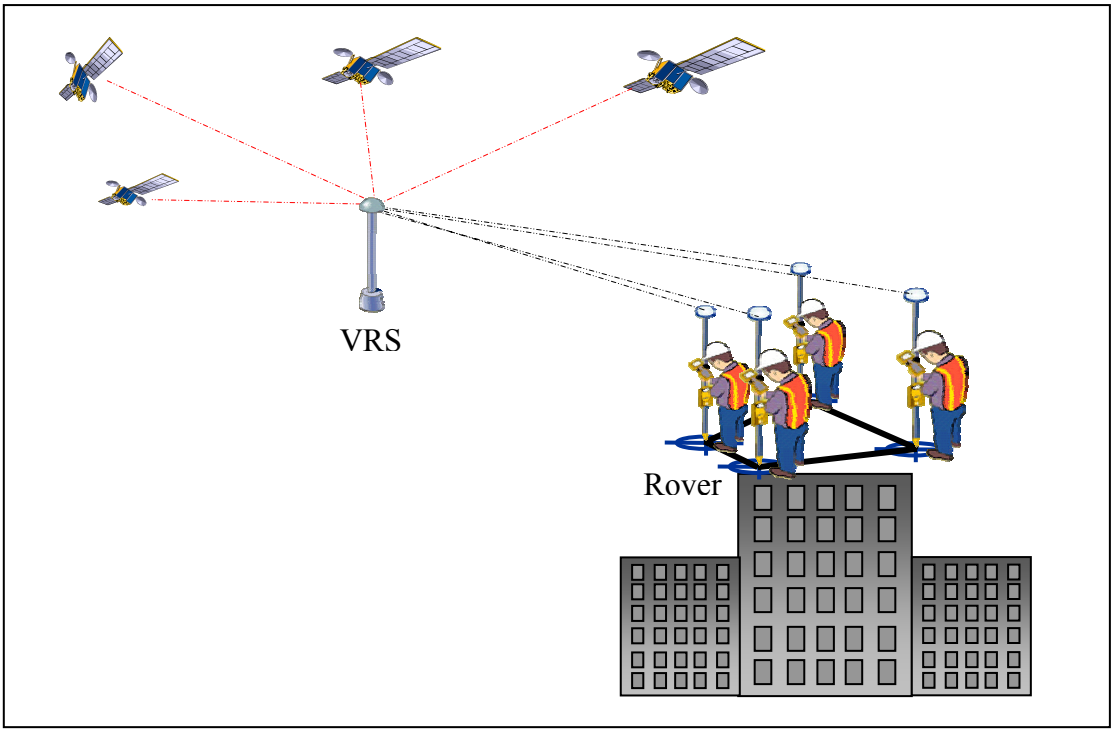

Figure 5.14: VRS-RTK observation at building P23

The establishment of B001, B002 and B003 were based on GPS static survey performance in relative to UTM GPS station (UTM 01) situated near Balai Cerap, UTM. The static survey was carried at half an hour interval. Figure 5.15 shows the overview of B001, B002 and B003 reference station mark. Figure 5.16 shows the base station at UTM 01 and Figure 5.17 shows the instrumentation set up at point B001, B002, and B003. Figure 5.18 shows the instrumentation set up at points P1, P2 and P3.

Figure 5.15: Overview of B001, B002 and B003 reference station mark.

Figure 5.16: Base Station at UTM 01

Figure 5.17: Instrumentation set up at point B001, B002, and B003

Figure 5.18: Instrumentation set up at points P1, P2 and P3

5.3.2 Result and Analysis

As mention earlier, GPS observation campaign were performance at P1, P2, P3 (top on the building) and points B001, B002 and B003 (on the ground as control point) at two episodic interval. The details on VRS-RTK data for this simulation test are attached in Appendix E. Accordingly, Figure 5.19 – Figure 5.21 illustrates the observation residual of first epoch at P1, P2 and P3. Figure 5.22 illustrates the coordinate precision obtained at Epoch 1.

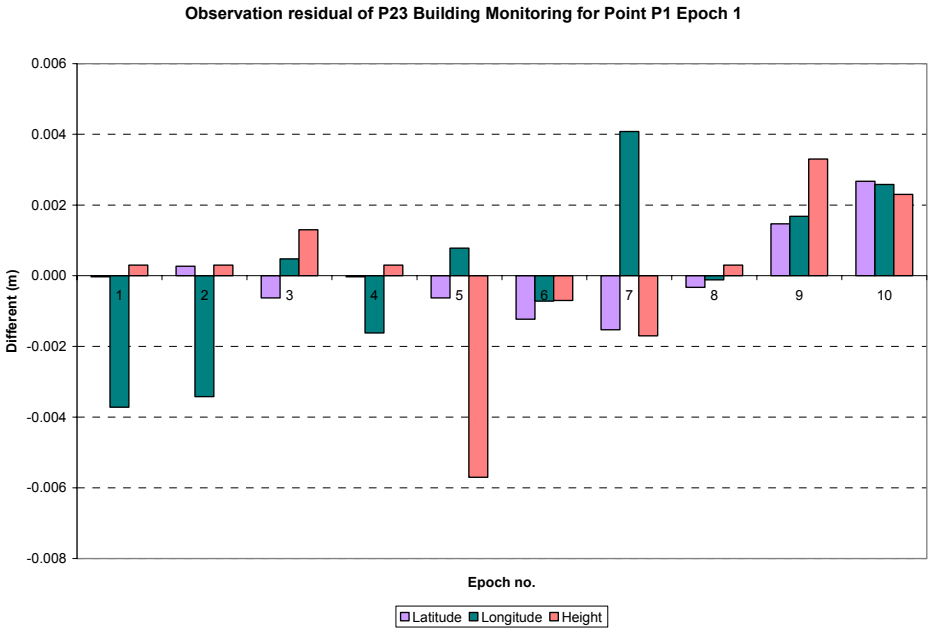

Figure 5.19: Observation residual at Point P1 Epoch 1

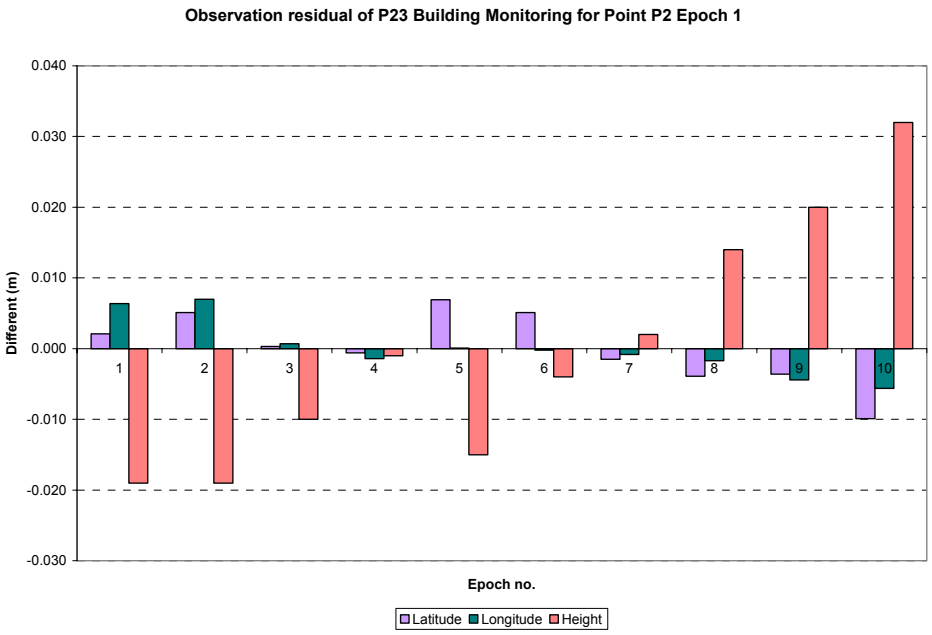

Figure 5.20: Observation residual at Point P2 Epoch 1

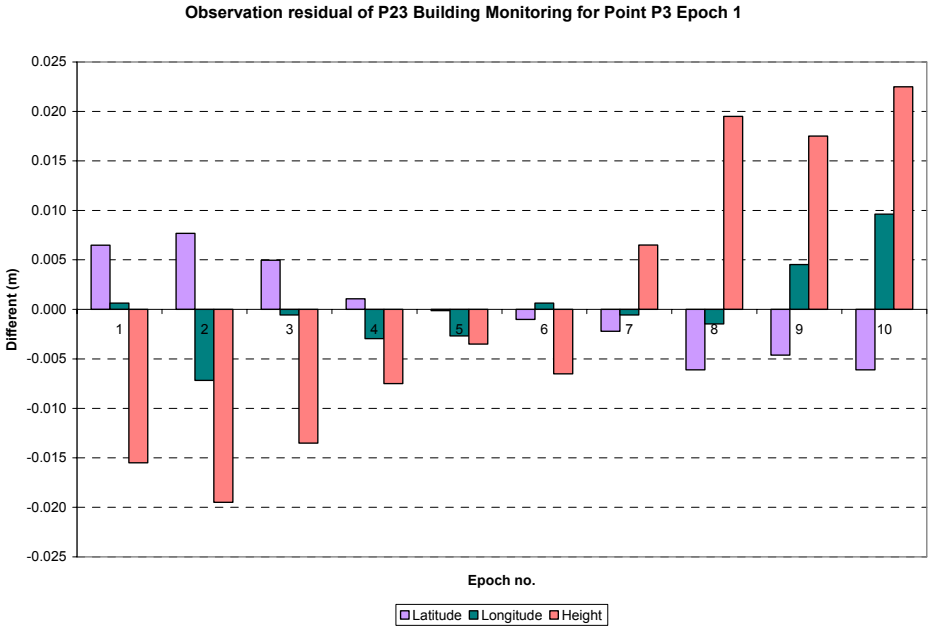

Figure 5.21: Observation residual at Point P3 Epoch 1

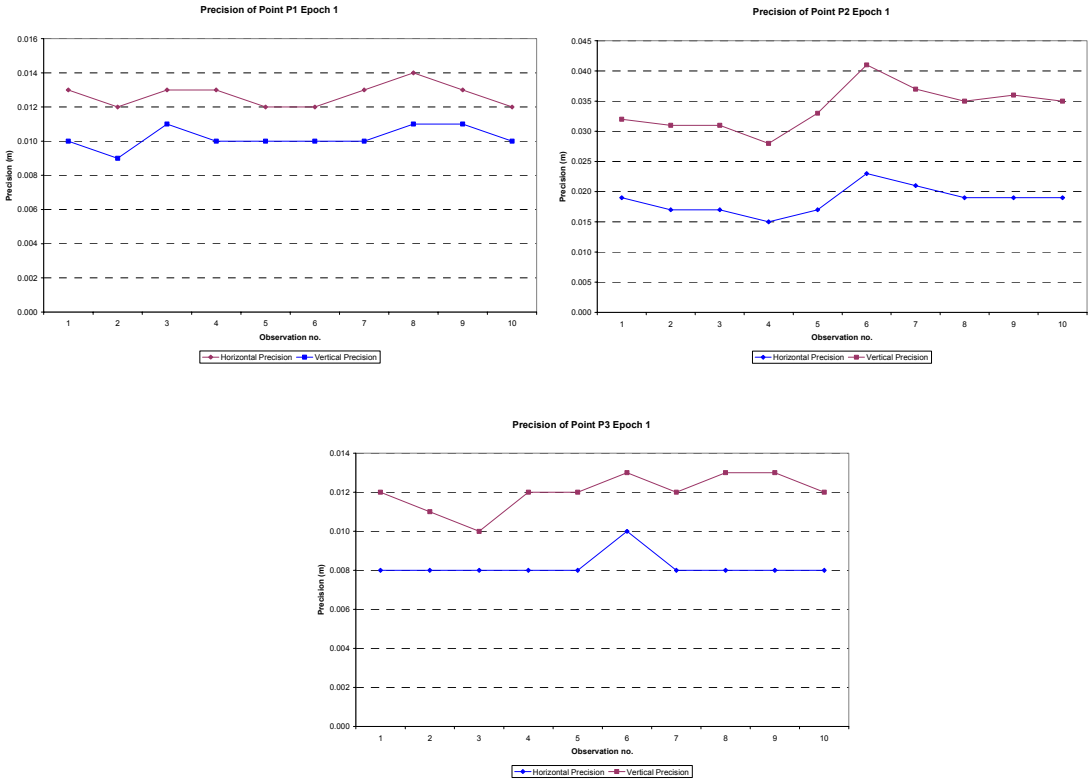

Figure 5.22: Precision analysis at Point P1, P2 and P3 Epoch 1

Based on the result, it is noted that the maximum observation residual detected at P1 on the basis of horizontal and vertical components were 0.004 m and 0.006 m respectively. For point P2, the maximum observation residual detected on the basic of horizontal and vertical component were 0.010 m and 0.032 m. For point P3 the maximum observation residual detected on the basic of horizontal and vertical component were 0.010 m and 0.023 m. As far as the horizontal precision analysis conducted of P1, P2 and P3, it is noted that the maximum and the minimum residual range from 0.009 m to 0.011 m, 0.015 m to 0.023 m, and 0.008 m to 0.010 m respectively. As far as the vertical precision analysis conducted of P1, P2 and P3, it is noted that the maximum and the minimum residual range from 0.009 m to 0.011 m, 0.028 m to 0.041 m, and 0.010 m to 0.013 m. Figure 5.23 – Figure 5.25 illustrates the observation residual at P1, P2 and P3 Epoch 2 respectively. Figure 5.26 on the other hand illustrates the precision analysis at P1, P2 and P3.

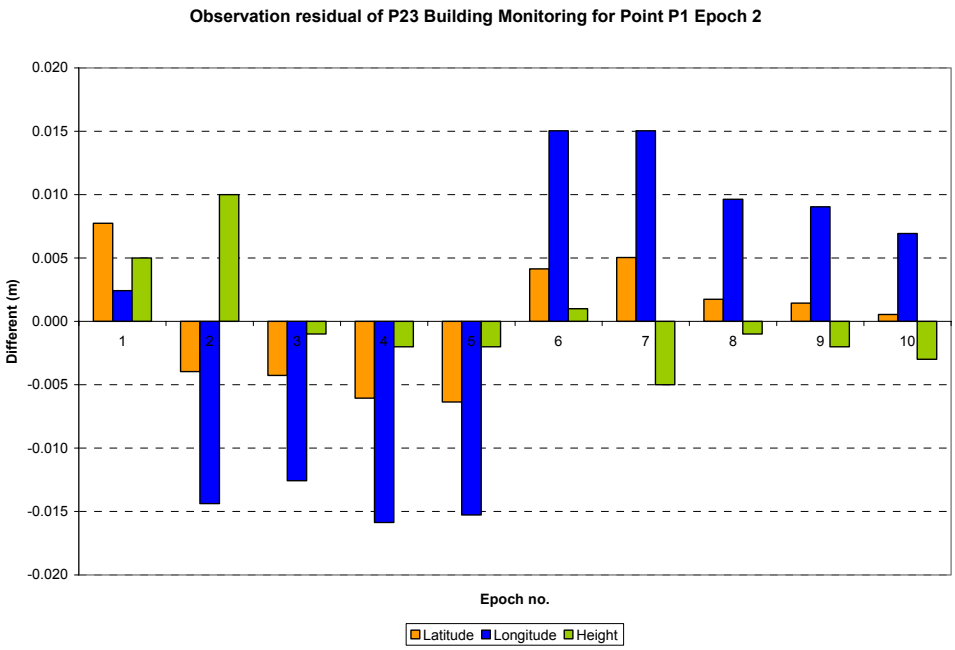

Figure 5.23: Observation residual at Point P1 Epoch 2

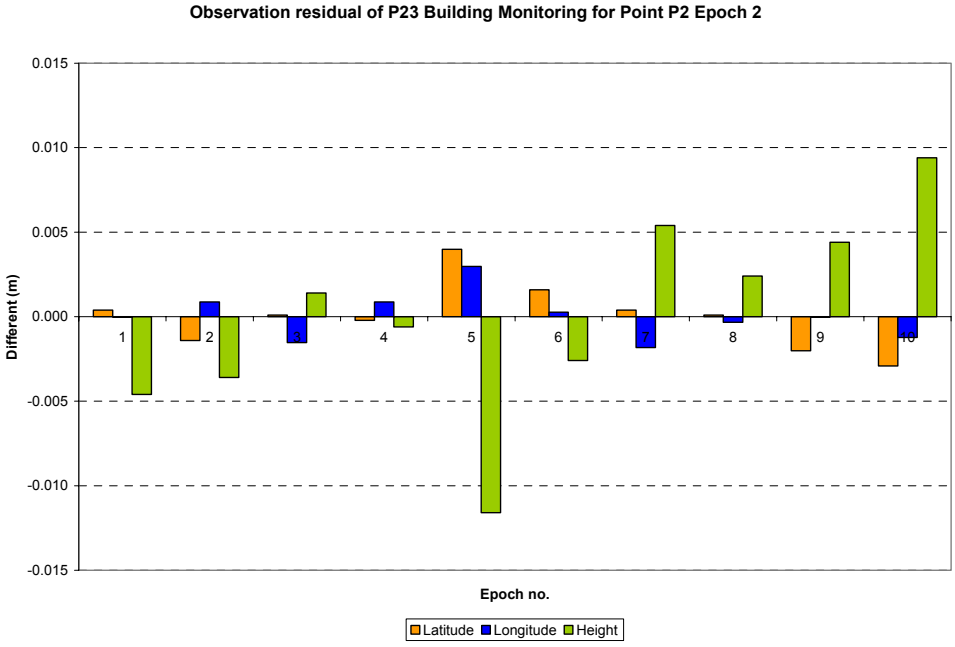

Figure 5.24: Observation residual at Point P2 Epoch 2

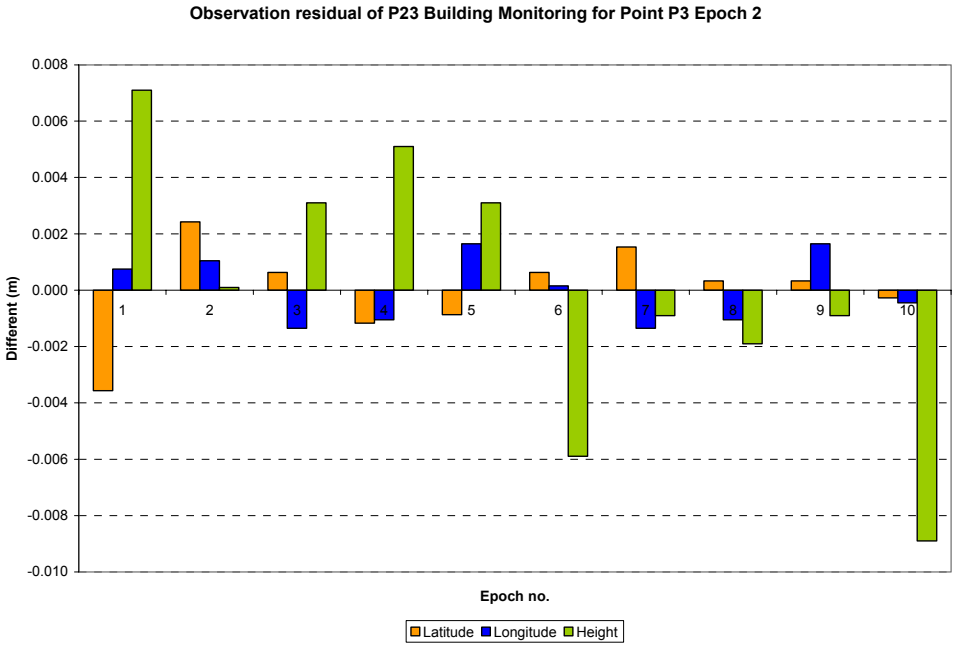

Figure 5.25: Observation residual at Point P3 Epoch 2

Figure 5.26: Precision analysis at Point P1, P2 and P3 Epoch 2

The result shows that the maximum observation residual detected at P1 on the basis of horizontal and vertical components were 0.016 m and 0.010 m respectively. For point P2, the maximum observation residual detected on the basic of horizontal and vertical component were 0.004 m and 0.012 m. For point P3 the maximum observation residual detected on the basic of horizontal and vertical component were 0.004 m and 0.009 m. As far as the horizontal precision analysis conducted of P1, P2 and P3, it is noted that the maximum and the minimum residual range from 0.006 m to 0.009 m, 0.008 m to 0.011 m, and 0.006 m to 0.007 m respectively. As far as the vertical precision analysis conducted of P1, P2 and P3, it is noted that the maximum and the minimum residual range from 0.010 m to 0.015 m, 0.022 m to 0.034 m, and 0.012 m to 0.015 m. Figure 5.27 – Figure 5.29 illustrates the observation residual at B001, B002 and B003 Epoch 1 respectively. Figure 5.30 on the other hand illustrates the precision analysis at B001, B002 and B003.

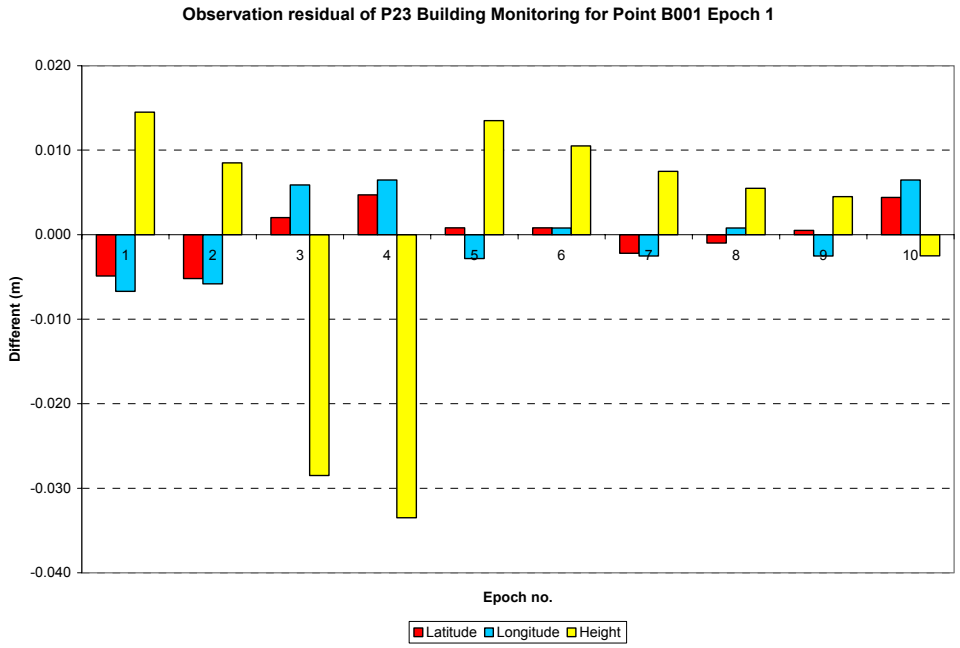

Figure 5.27: Observation residual at Point B001 Epoch 1

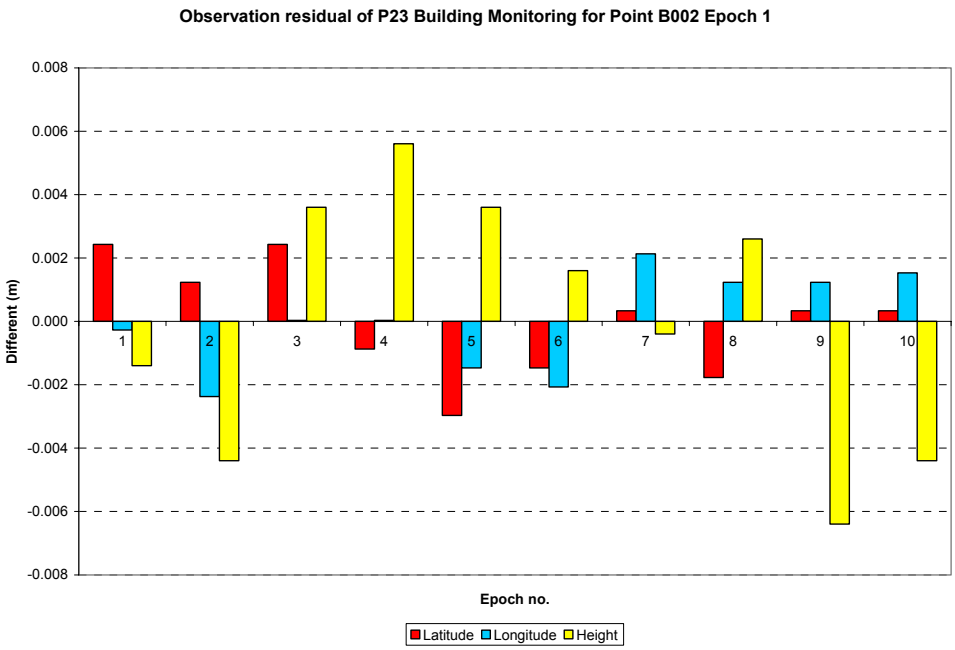

Figure 5.28: Observation residual at Point B002 Epoch 1

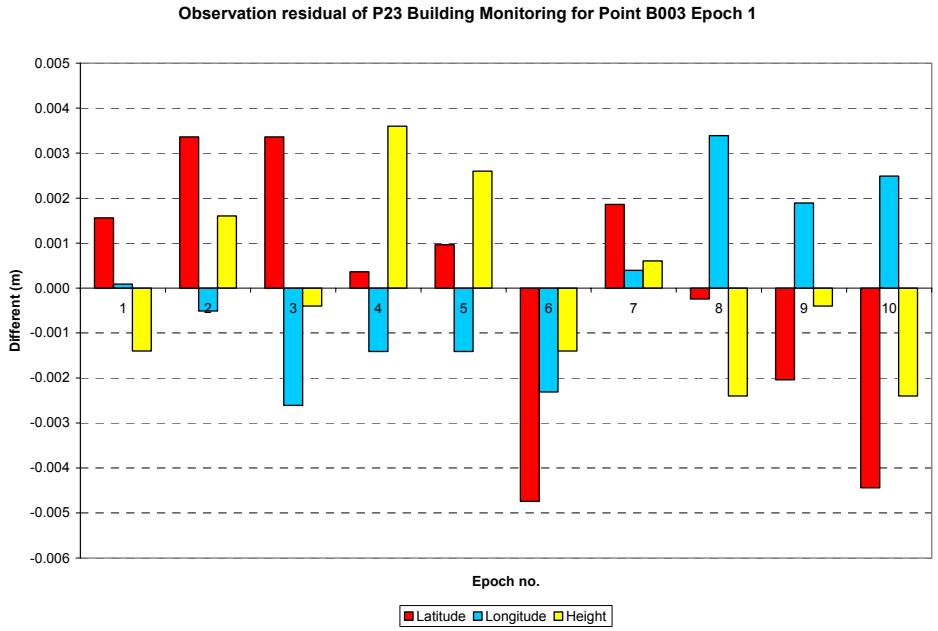

Figure 5.29: Observation residual at Point B003 Epoch 1

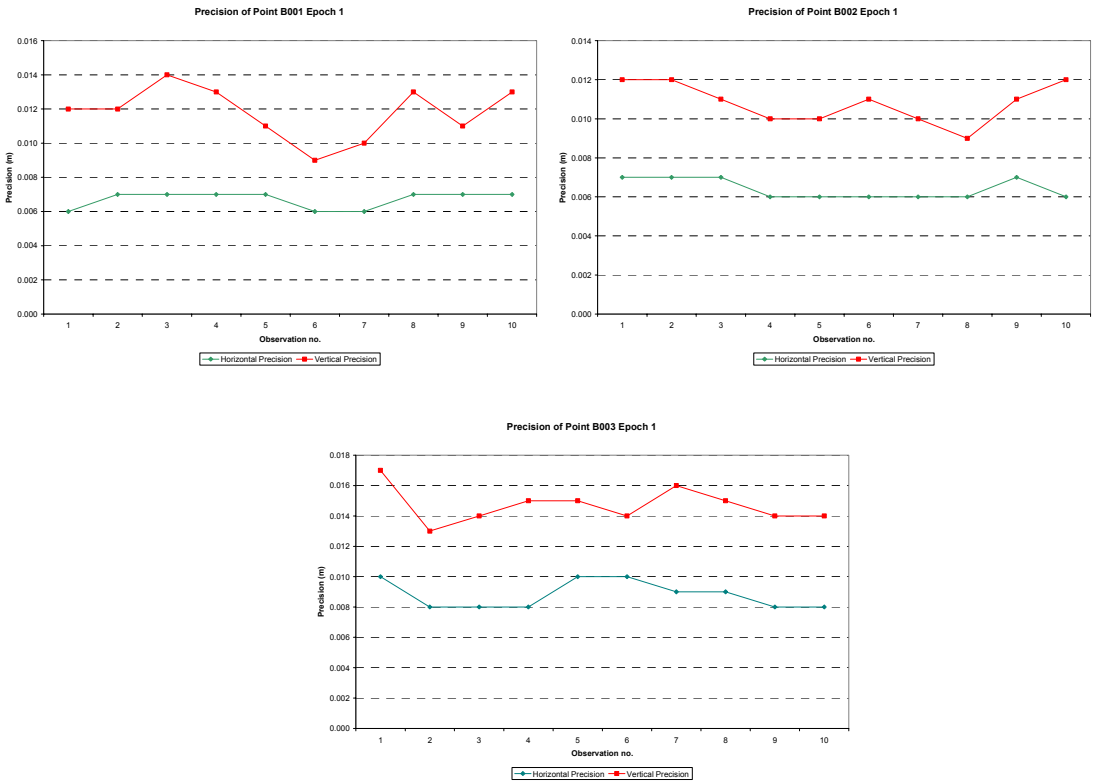

Figure 5.30: Precision analysis at Point B001, B002 and B003 Epoch 1

The maximum observation residual detected at B001 on the basis of horizontal and vertical components were 0.007 m and 0.033 m respectively. For point B002, the maximum observation residual detected on the basic of horizontal and vertical component were 0.003 m and 0.006 m. For point B003 the maximum observation residual detected on the basic of horizontal and vertical component were 0.005 m and 0.004 m. As far as the horizontal precision analysis conducted of B001, B002 and B003, it is noted that the maximum and the minimum residual range from 0.006 m to 0.007 m, 0.006 m to 0.007 m, and 0.008 m to 0.010 m respectively. As far as the vertical precision analysis conducted of B001, B002 and B003, it is noted that the maximum and the minimum residual range from 0.009 m to 0.014 m, 0.009 m to 0.012 m, and 0.013 m to 0.017 m. Figure 5.31 – Figure 5.33 illustrates the observation residual at B001, B002 and B003 Epoch 2 respectively. Figure 5.34 on the other hand illustrates the precision analysis at B001, B002 and B003.

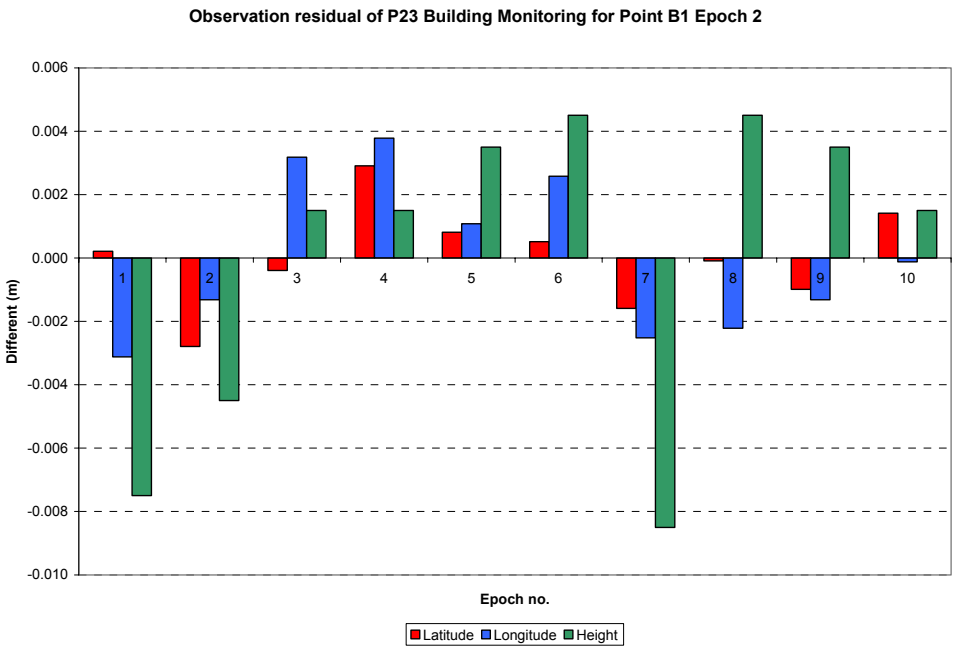

Figure 5.31: Observation residual at Point B001 Epoch 2

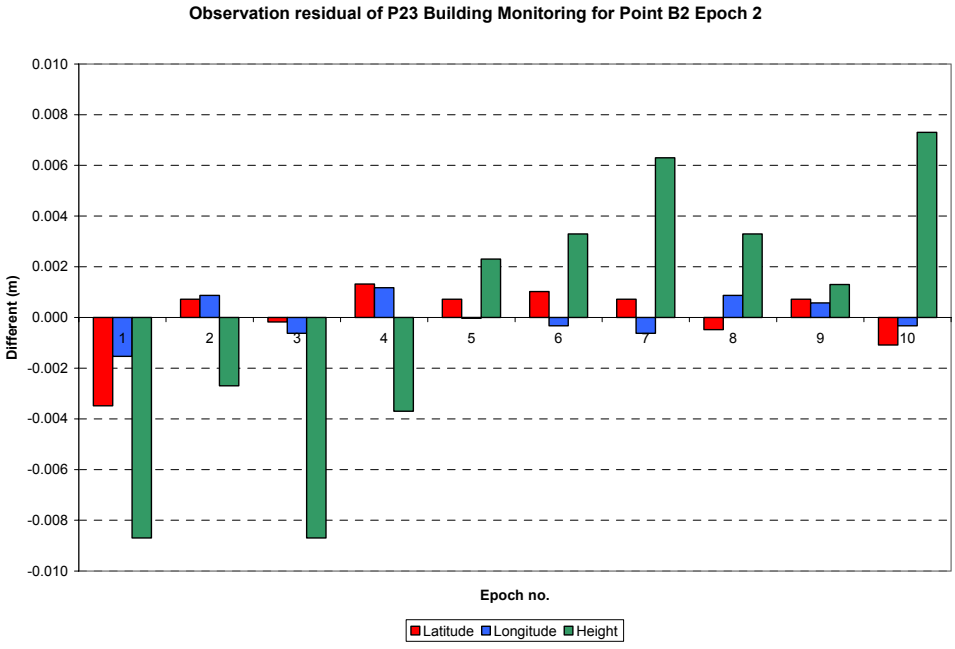

Figure 5.32: Observation residual at Point B002 Epoch 2

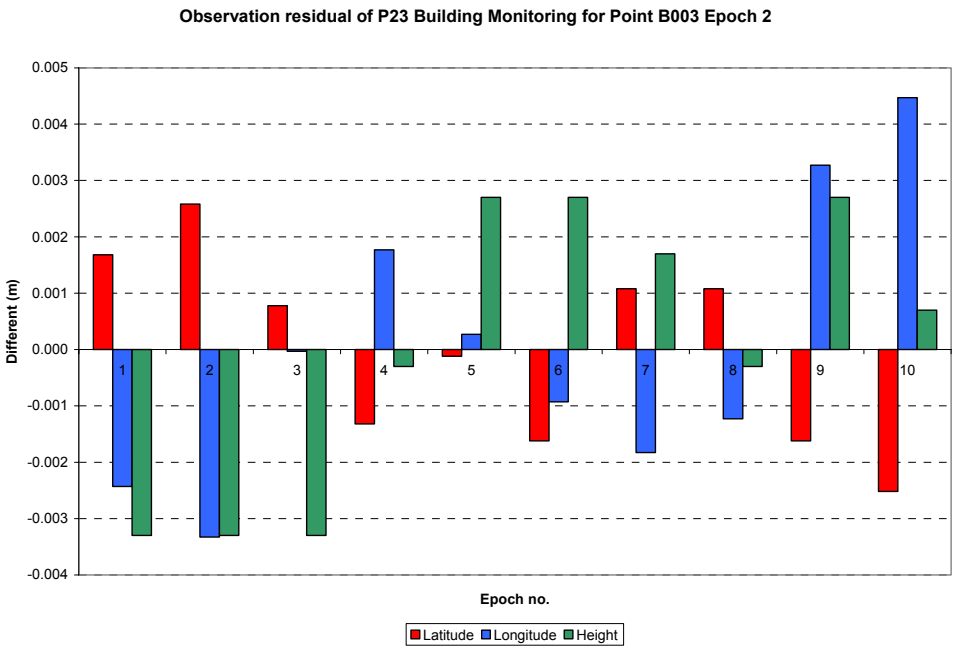

Figure 5.33: Observation residual at Point B003 Epoch 2

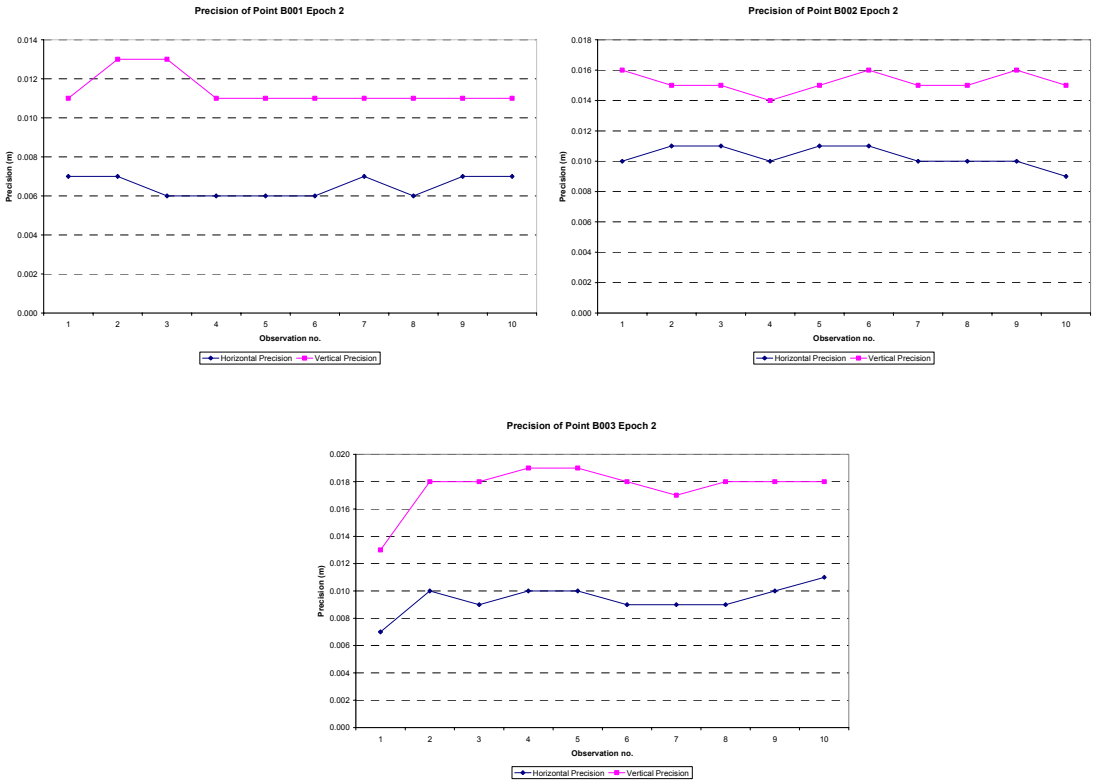

Figure 5.34: Precision analysis at Point B001, B002 and B003 Epoch 2

Based on the result, it is noted that the maximum observation residual detected at B001 on the basis of horizontal and vertical components were 0.004 m and 0.008 m respectively. For point B002, the maximum observation residual detected on the basic of horizontal and vertical component were 0.003 m and 0.009 m. For point B003 the maximum observation residual detected on the basic of horizontal and vertical component were 0.004 m and 0.003 m. As far as the horizontal precision analysis conducted of B001, B002 and B003, it is noted that the maximum and the minimum residual range from 0.006 m to 0.007 m, 0.009 m to 0.011 m, and 0.007 m to 0.011 m respectively. As far as the vertical precision analysis conducted of B001, B002 and B003, it is noted that the maximum and the minimum residual range from 0.011 m to 0.013 m, 0.014 m to 0.016 m, and 0.013 m to 0.019 m. Figure 5.35 illustrates inter epochs analysis at P1, P2 and P3 – static data.

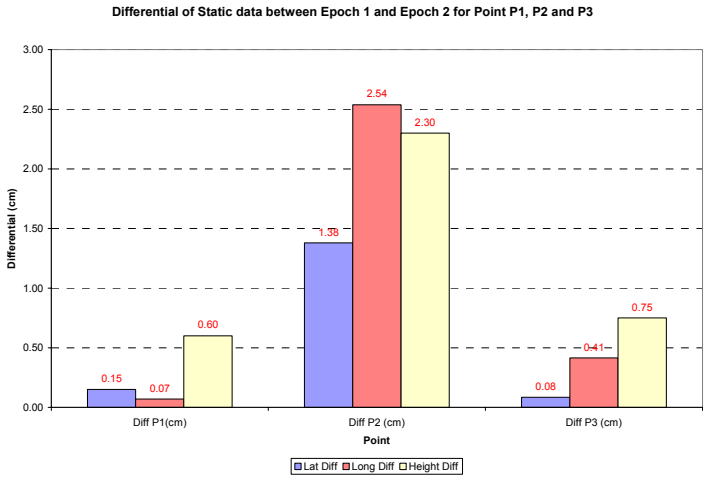

Figure 5.35: Inter epochs analysis at P1, P2 and P3 – static data.

The difference between epochs for point P1 is less than 1 cm that is 0.15 cm for latitude component, 0.07 cm for longitude component and 0.6 cm for height component. The difference of point P2 is 1.38 cm for latitude component, 2.54 cm for longitude component and 2.30 cm for height component. The difference of point P3 is less than 1 cm, which is 0.08 cm for latitude component, 0.41 cm for longitude component and 0.75 for

height component. Figure 5.36 illustrates inter epochs analysis at B001, B002 and B003 – static data.

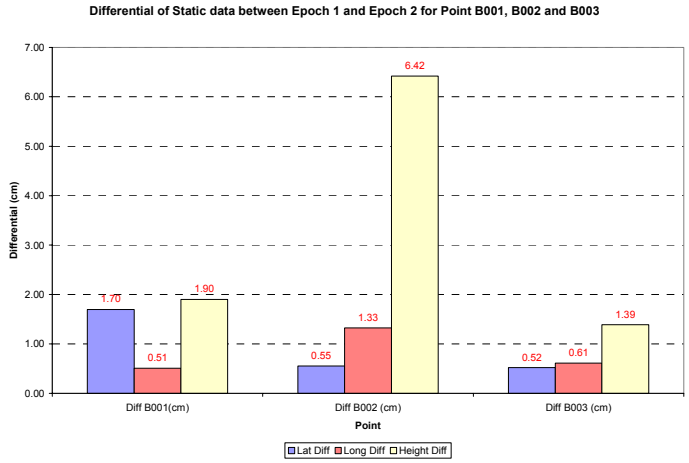

Figure 5.36: Inter epochs analysis at B001, B002 and B003 – static data.

Differences between two epochs of point B001 indicated there are 1.7 cm of latitude component, 0.51 cm of longitude component and 1.9 cm of height component. The differences of point B002 are 0.55 cm for latitude component, 1.33 cm for longitude and 6.42 cm for height component. The differences of point B003 are 0.52 cm of latitude component, 0.61 cm of longitude component and 1.39 of height component. Figure 5.37 shows inter epochs analysis at P1, P2 and P3 –VRS-RTK data.

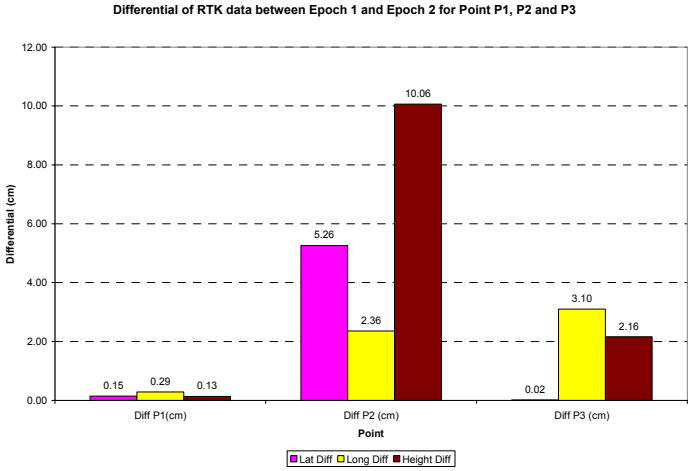

Figure 5.37: Inter epochs analysis at P1, P2 and P3 –VRS-RTK data.

The differences of point P1 are less than 1 cm, which is 0.15 cm of latitude component, 0.29 cm of latitude component and 0.13 cm of height component. Differences of point P2 are 5.26 cm of latitude component, 2.36 cm of longitude component and 10.06 cm of height component. For point P3, the differences are 0.02 cm of latitude component, 3.10 cm of longitude component and 2.16 cm of height component. Figure 5.38 shows inter epochs analysis at B001, B002 and B003 –VRS-RTK data.

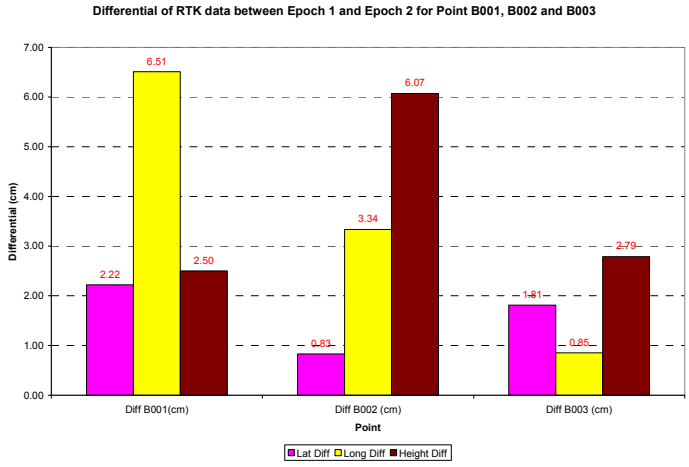

Figure 5.38: Inter epochs analysis at B001, B002 and B003 –VRS-RTK data.

This VRS-RTK result is the average of ten observations per epoch. The differences for point B001 are 2.22 cm of latitude component, 6.51 cm of longitude component and 2.50 cm of height component. For point B002, there are 0.83 cm differences of latitude component, 3.34 cm of longitude component and 6.07 cm of height component. The differences of point B003 are 1.81 cm of latitude component, 0.85 cm of longitude component and 2.79 cm of height component. Figure 5.39 illustrates the differential of Static data vs. VRS-RTK data for point P1, P2 and P3

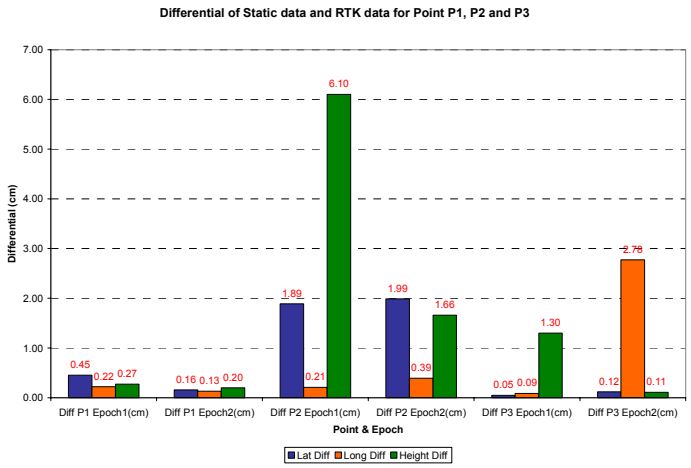

Figure 5.39: Differential of Static data vs. VRS-RTK data for point P1, P2 and P3

The differences for point P1 epoch 1 are 0.45 cm of latitude component, 0.22 cm of longitude component and 0.27 cm of height component. The differences for epoch 2 of point P1 are 0.16 cm for latitude component, 0.13 cm of longitude component and 0.20 cm of height component. The differences of first epoch for point P2 are 1.89 cm for latitude component, 0.21 cm of longitude component and 6.10 cm of height component while the differences of second epoch are 1.99 cm for latitude component, 0.39 cm of longitude component and 1.66 cm of height component. The differences for first epoch of point P3 1 are 0.05 cm of latitude component, 0.09 cm of longitude component and 1.30 cm of height component. The differences for second epoch of point P3 are 0.12 cm for latitude component, 2.78 cm of longitude component and 0.11 cm of height component. Figure 5.40 illustrates the differential of Static data vs. VRS-RTK data for point B001, B002 and B003

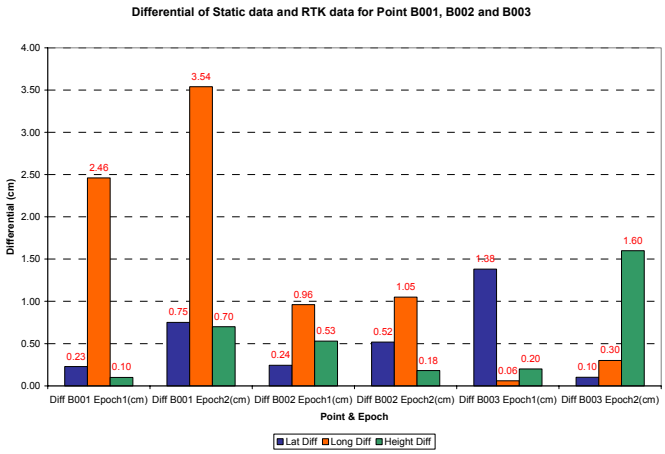

Figure 5.40: Differences of Static data vs. VRS-RTK data for point B001, B002 and B003

The differences for first epoch of point B001 are 0.23 cm of latitude component, 2.46 cm of longitude component and 0.10 cm of height component. The differences for second epoch of point B001 are 0.75 cm for latitude component, 3.54 cm of longitude component and 0.70 cm of height component. The differences of first epoch for point B002 are 0.24 cm for latitude component, 0.96 cm of longitude component and 0.53 cm of height component while the differences of second epoch are 0.52 cm for latitude component, 1.05 cm of longitude component and 0.18 cm of height component. The differences for first epoch of point B003 1 are 1.38 cm of latitude component, 0.06 cm of longitude component and 0.20 cm of height component. The differences for second epoch of point B003 are 0.10 cm for latitude component, 0.30 cm of longitude component and 1.60 cm of height component.

Figure 5.41 illustrates the result for TTFF of VRS-RTK technique observed at P23 building. Based on the result, TTFF for all point at P23 building were less than 25 seconds. The TTFF for points P1, P3, B001, B002 and B003 were less than 14 second while TTFF of point P2 was 21 second for the first epoch and 19 second for the second epoch. This might be due to the roof obstruction located at point P2.

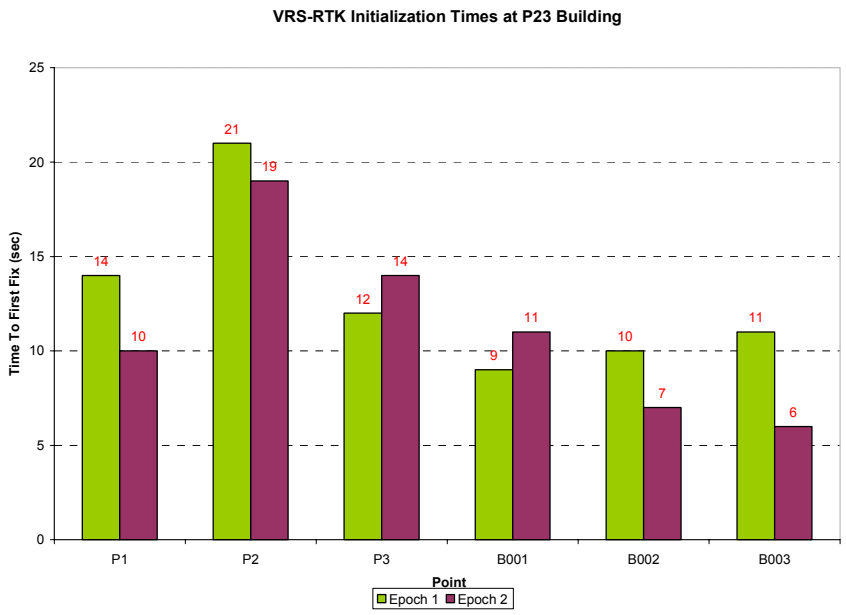

Figure 5.41: TTFF of VRS-RTK technique at P23 Building

Several conclusions can be made based on the results obtained from the study. Divided on the basic of the structural health and GPS positioning performance amongst other conclusion includes:

1. Building P23 was in a stable condition with no significance deformation detected during the GPS observation campaigns.

2. Point P2 shows the big value of differences in both static mode result and VRS-RTK mode result. The maximum value for static data are 1.38 cm of latitude, 2.54 cm of longitude and 2.30 of height while the maximum differences value for VRS-RTK data are 5.26 cm of latitude, 2.36 of longitude, and 10.06 cm of height.

5.5 Discussion

Based on the result from all three case study, the discussion will include the aspect of instrument that are used, the RTKnet reference station, cell-phone coverage, work environment, TTFF and etc. The used of this VRS-RTK mode have pro and cont. The following discussion may give the guides for engineers and surveyors the used this VRS-RTK for SHM.

To perform this VRS-RTK mode, the instrument should able to receive the correction from VRS and should make sure that the study area is with mobile coverage. This is because, the surveyor used the mobile phone as a modem to received the correction from VRS in real-time. The result of VRS-RTK data shows mostly the vertical component is less accuracy compare to horizontal component. This is also depends on the distance from VRS (that we can't be able to see the exactly position of this VRS). Figure 5.42 shows the two situations of VRS from observed point.

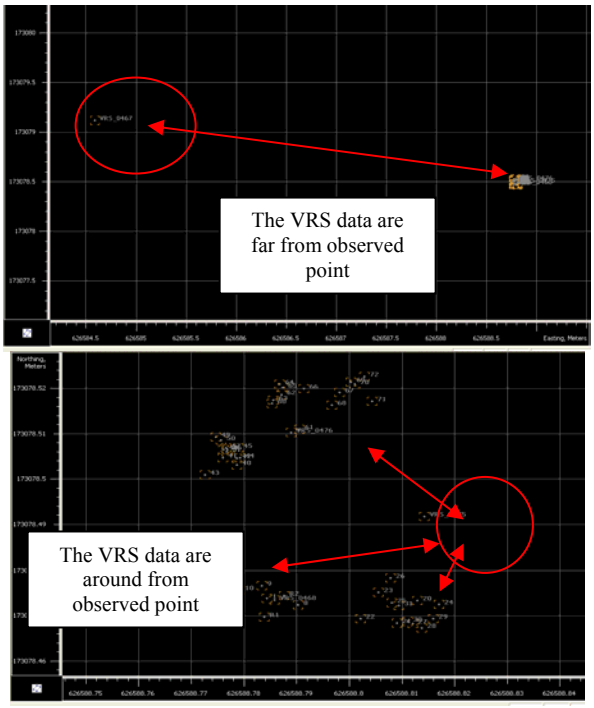

Figure 5.42: Differences case of VRS from observed point

The first figure shows that the position of VRS is far from observed point depends on second figure. The nearest position of VRS position from observed point is better. The position of VRS affected the VRS-RTK result. This means that even the data is fixed, but the accuracy is not really good. During this survey monitoring, normally the VRS location is around below than 7 m radius from observed point. Figure 5.43 shows the screenshot of controller that shows the distance of VRS.

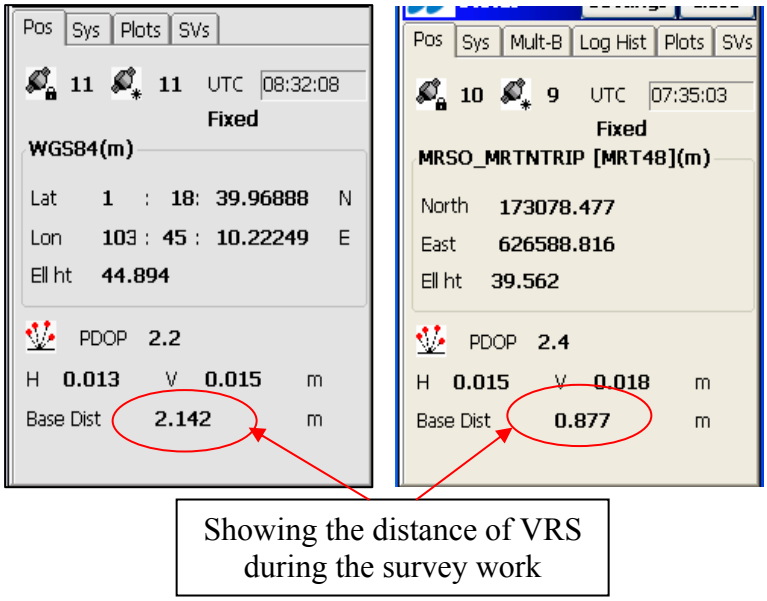

Figure 5.43: VRS distance around survey work

Moreover, there are some disadvantage by using this VRS-RTK mode, it's take many time for initialization if the work environment is not really clear, for example if the observed point are obstruction by canopy and etc. During this survey campaign at building monitoring at P23, point P2 shows of the precision for both horizontal and vertical are high compare the other point. This is because the point is near and covered or obstruct by the roof of the building. Figure 5.44 shows the observed point that covered by the roof.

Figure 5.44: The observed point that obstruct by the roof

This problem has been proofed by another simple research that was held at the *Lembaga Jurukur Tanah* (LJT) field at Kuala Lumpur. The tests are made in two conditions which are observation at center of the field which have very good sky view and the other in below the tree which is bad sky view. This test therefore to identify this factor is some of the limitation of RTK system.

The time was recorded upon star-up the receiver till the initialization was gain which is the solution data type is fixed. This successful initialization also can be recognized by the 'bit' sound (the first fixed data). The time is recorded manually. Figure 5.45 shows

the observation points which have good sky view and bad sky view and the result of this test is showing in Table 5.4 and Figure 5.46.

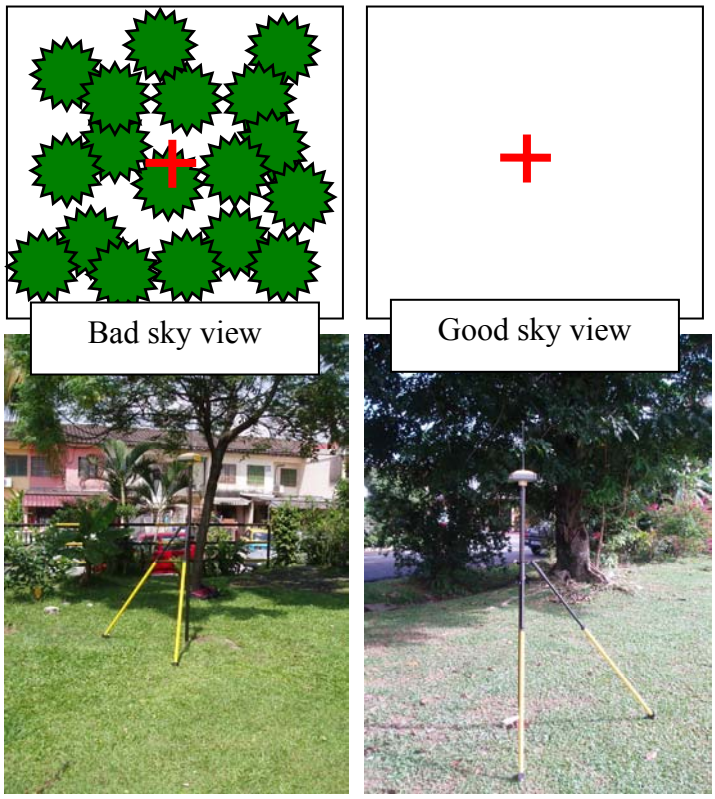

Figure 5.45: Observed point in difference sky view

Table 5.4: Time To First Fix (TTFF) of VRS-RTK in various conditions

	Good sky view initialization time (sec)	Obstruction sky view initialization time (sec)
Test 1	12	nil
Test 2	16	220
Test 3	9	nil

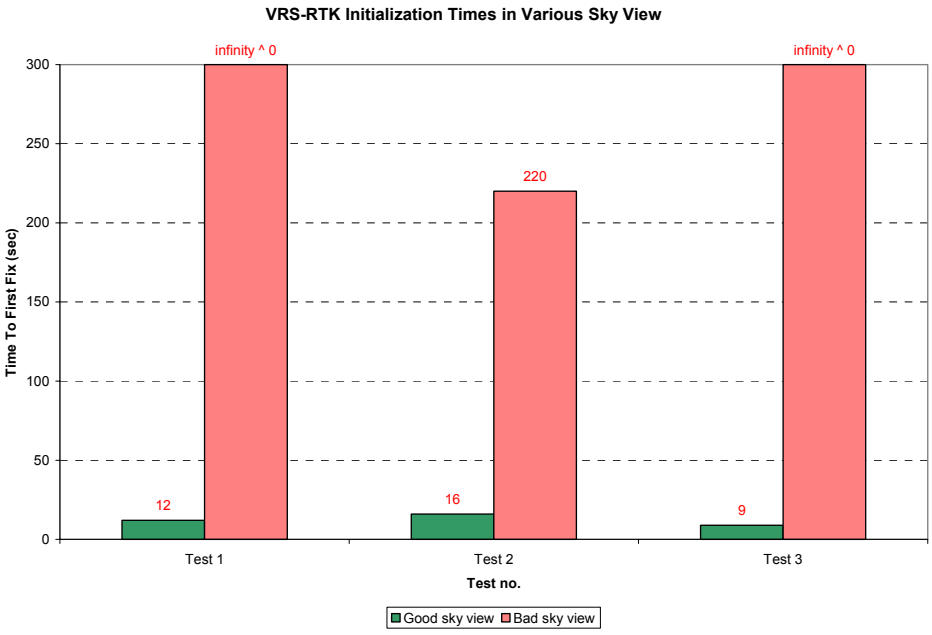

Figure 5.46: TTFF of VRS-RTK in Various Sky View

The results of TTFF under ideal sky view were 12 second for the first test, 19 second for the second test and 9 second for the third test. The TTFF under bad sky view for the first and the third test are nil, given that more than 5 minute were needed for initialization process. In most cases it is hard to solve ambiguity under bad sky view. As shown in Test 1 and Test 3, even after long observation, the fixed solution can be easily disconnected because of the weak signal. The initialization process also can be affected by number of satellites, satellite geometry, multipath, ionospheric interference, signal strength and radio interference. It is as well suggested that a good sky view is merely essential to perform SHM using GPS. As far as the configuration setup is concerned, during the observation one can check the sky visibility using the controller (as in this case using the Topcon FC-200 instrument) by checking the 'Mutl-B' status or 'Topo' screenshot (see Figure 5.47).

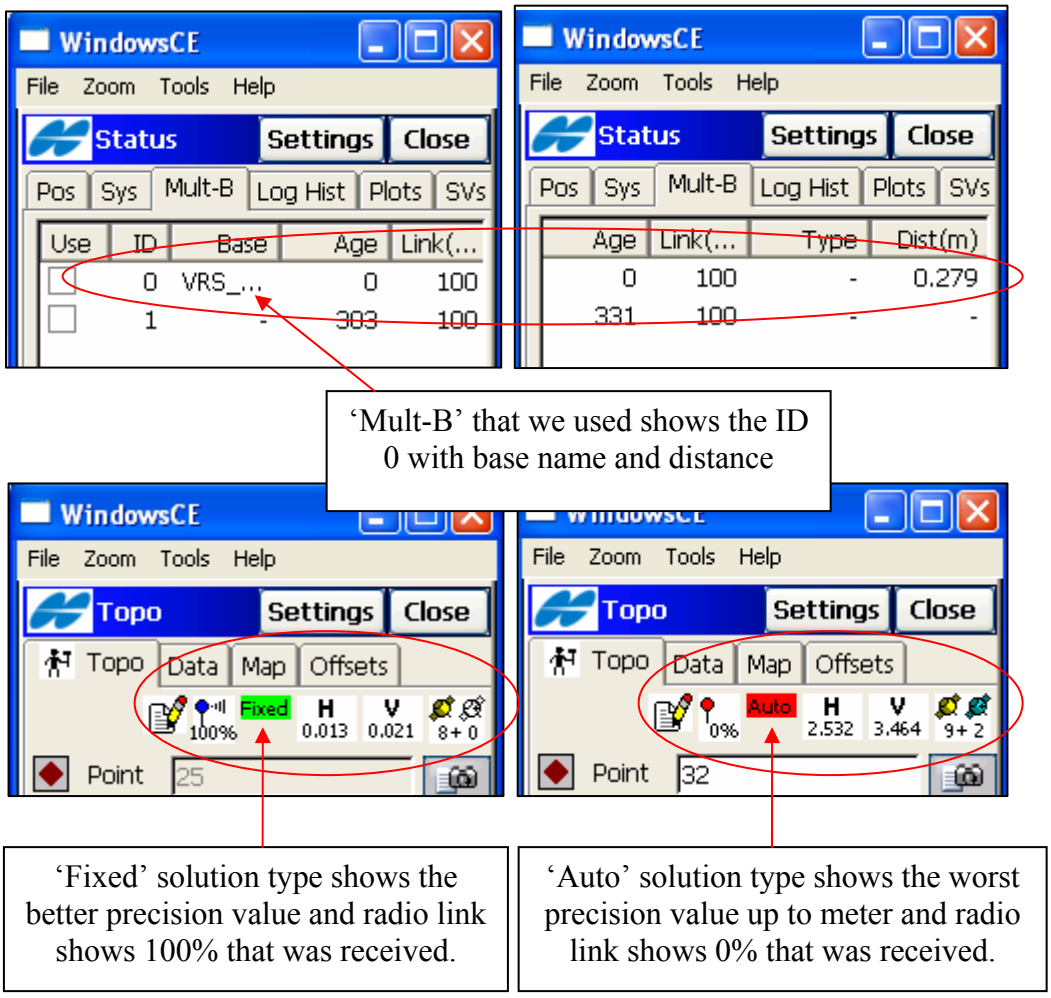

Figure 5.47: Status checking at controller

Moreover, the correction of VRS are hard to received at time around noon which is 11.30 am – 1.30 pm. This is because the connection to server is always disconnected. The ambiguity resolution in VRS-RTK mode when operating with no obstruction is no recorded of initialization failure while instead of that which are under obstruction, its take many minute to initialize for fixed solution and sometime can't get the fixed solution cause of no initialization. In addition, the precision of the data is inconsistence if the signals are always on-off, which is for one epoch there are more than one VRS, the Figure 5.48 show the number of VRS in one epoch.

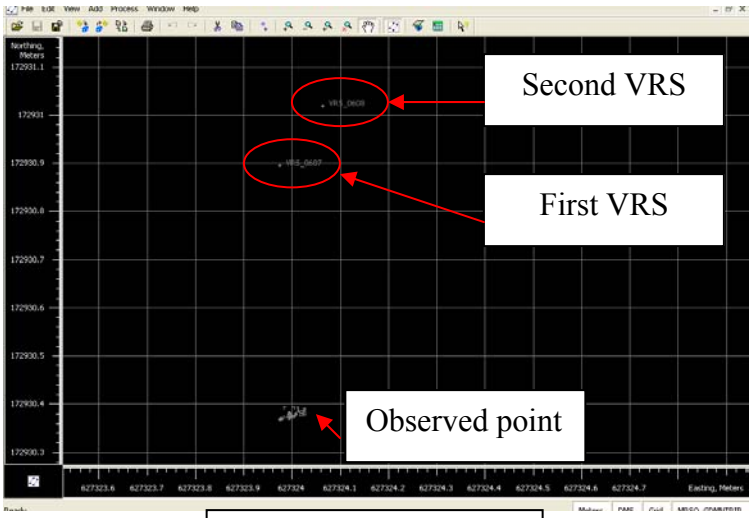

Epoch with 2 VRS

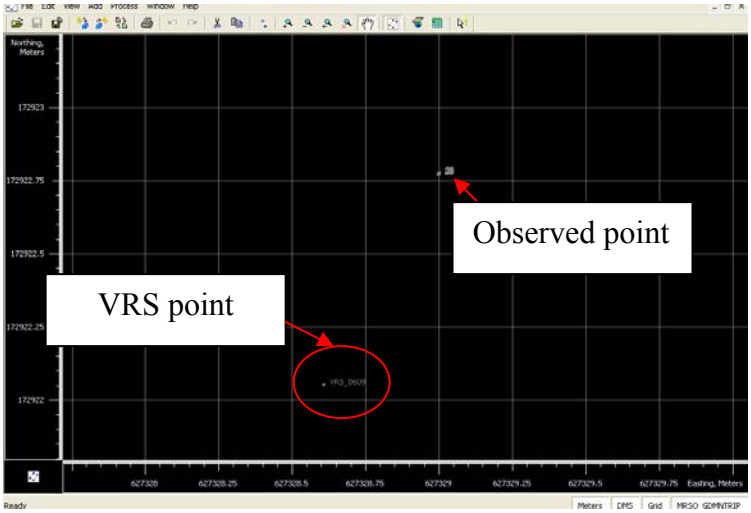

Epoch with 1 VRS

Figure 5.48: VRS no. in one epoch

Therefore, the result and statistical analysis from all these case study are interpreted. The movement or displacements are calculated by differencing of difference epoch and true value. Figure 5.49 shows the displacement geometric modeling.

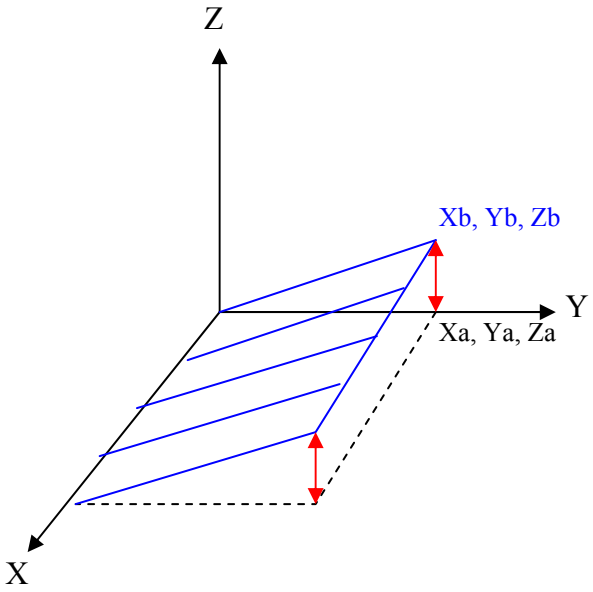

Figure 5.49: Displacement geometric modeling

The movement can be described as point displacement of all components ($d_{n;}$: ΔX, ΔY, ΔZ) for all point which ΔX is X coordinate displacement, ΔY is Y coordinate displacement and ΔZ is Z coordinate displacement. The coordinate differences of each movement vector have direction and magnitude.

Whereas:

$$\Delta X = Xb - Xa$$

$$\Delta Y = Yb - Ya$$

$$\Delta Z = Zb - Za$$

CHAPTER 6

CONCLUSIONS AND RECOMMENDATIONS

6.1 Introduction

This chapter draws the conclusion of the research based on the SHM study conducted using VRS-RTK and analysis technique. In addition, recommendations for future works were discussed.

6.2 Conclusions

This research starts with calibration work which include of absolute calibration and relative calibration held at GNSS calibration site at Port Dickson, Negeri Sembilan and at existing bench mark in Universiti Teknologi Malaysia. The result shows that the instrument is in good condition to perform VRS-RTK technique for SHM. The simulation test is also perform to study the potential of VRS-RTK technique for SHM based on this, the procedure of SHM is apply during the simulation test. The VRS-RTK technique also performed in indoor monitoring area which is at Topcon Lab, Topcon building area. Ampang Hilir, Kuala Lumpur. The use of this technique proved that the VRS-RTK technique is able to apply in various environments either at outdoor or indoor area. The

finding of this work is that the Topcon Building was in a stable condition with no significance deformation detected during the GPS observation campaigns. Moreover, VRS-RTK technique can be used for indoor monitoring if all the component is proper setup.

The network-RTK (VRS-RTK) technique has more advantage instead of using single-base RTK-GPS. This VRS-RTK technique deployed the distance-dependent errors and are well suggested especially for SHM in urban area which can overcome the problem of distance between the monitor and reference receiver. Moreover, since there are more reference stations are currently available, the network-RTK offers significant advantages over the single-RTK in term of improved accuracy and redundancy.

This study focuses on SHM using VRS-RTK based on two case studies: the GPS-based breakwater monitoring at Kemaman, Terengganu, and the GPS-based building monitoring at block P23, Faculty of Mechanical, Universiti Teknologi Malaysia. The statistical analysis for VRS-RTK data has demonstrated the advantage of network-RTK to be use as tool for SHM. Based on the result, there are no deformation detected at Kemaman Breakwater and Topcon Building but there is small movement in easting component for building P23 at Faculty of Mechanical, Universiti Teknologi Malaysia.

Several conclusions can be made based on the results obtained from the study. Divided on the basis of the structural health and GPS positioning performance amongst other conclusion includes:

Case study 1:

1. South Breakwater was in a stable condition with no significance deformation detected during the GPS observation campaigns.

2. Though discrepancies in the GPS measurement using two differences method (static and VRS-RTK) can be expected, it is apparent that these

variations were at a minimal value of 0.004 m N, 0.007 m E and 0.006 H only.

Case study 2:

1. Building P23 was in a stable condition with no significance deformation detected during the GPS observation campaigns.

2. Point P2 shows big differences in both static mode result VRS-RTK mode result. The maximum value for static data are 1.38 cm of latitude, 2.54 cm of longitude and 2.30 of height while the maximum differences value for VRS-RTK data are 5.26 cm of latitude, 2.36 of longitude, and 10.06 cm of height.

6.3 Recommendations

VRS-RTK technique has the potential to be employed as one of the effective yet practical monitoring tools for SHM practice. To further utilize this space-based technology for continuous deformation monitoring, this VRS-RTK technique could be extended for other research area for example landslide monitoring.

Internet-based online VRS-RTK SHM system can also be developed. The fully on-line integrity monitoring system which can be installed permanently at monitoring object to allow direct data transfer from monitoring sensor to data server, advance wireless technology approach can be integrated. The wireless sensor can directly transfer the data to centralized data storage, thus reducing the price and time of operations.

It also recommended to test the VRS-RTK technique in dynamic base platform with difference velocity. This is because to apply this technique especially at high-rise building

for example more than 50 storeys building, the wind effect could be an external nuisance factor. The global trends allow this VRS-RTK technique is interesting topic for future research.

REFERENCES

Ahmad, A. (2005). *Analisis ke Atas Prestasi Kamera Digital Kompak untuk Aplikasi Fotogrametri Jarak Dekat*. Ph. D. Thesis, Universiti Teknologi Malaysia, Johor, Malaysia.

Abu, S. H. (2006). *JUPEM Geodetic Infrastructure for GNSS Application*. Unpublished Note. Geodesy Section. Mapping Division. Department of Survey and Mapping Malaysia.

Ali, H., Nordin, A. F., Abu, S. H. and L. H., Chang, (2005). MyRTKnet: Get set and go! *MyCoordinate*. Retrieved August 25, 2007, from http://mycoordinates.org/pdf

Al Marzooqi, Y., Fashir, H., Babiker, T., (2005). Establishment & Testing of Dubai Virtual Reference Syatem (DVRS) National GPS-RTK Network. *FIG Working Week 2005 and GSDI-8*, 16-21 April 2005. Cairo, Egypt,

Ashkenazi, V., Dodson, A. H., and Roberts, G. W.(1998). Real-Time Monitoring of Bridges by GPS. *FIG XXI International Congress*, 1998. Brighton, England, 503-512.

Balageas, D. L., (2001). *Structural Health Monitoring R & D at the European Research Establishments in Aerospace (EREA)*, Fu – Kuo Chang (Ed.) *Structural Health Monitoring - The Demands and Challenges, Third International Workshop on Structural Health Monitoring.* (pp. 12-29.) September 12-14, 2001, Stanford, CA, CRC Press, Boca Raton, London, New York, Washinton D. C.

Balageas, D. L., (2006). *Introduction to Structural Health Monitoring, Proceeding of the Second International Conference on Structural Health Monitoring of Intelligent Infrastructure,* November 16-18, 2005 J. P. Ou, H. Li, and Z. D. Duan (Eds.) *Structural Health Monitoring and Intelligent Infrastructure Vol. 1*. (pp. 13-43.), Taylor & Francis, Taylor & Francis Group, London.

Breuer, P., Chmielewski, T., Gorski, P., and Konopka, E. (2002). Application of GPS technology to measurements of displacements of high-rise structures due to weak winds. *Journal of Wind Engineering and Industrial Aerodynamics*, 90(3), 223-230.

Celebi, M., W. Prescott, R. Stein, K. Hudnut, J. Behr, and S. Wilson (1998). GPS Monitoring of Structures: Recent advances. *Proceedings of the 30th Joint Meeting of the U.S.-Japan Cooperative Program in Natural Resources Panel on Wind and Seismic Effects*.

Celebi, M. (2000). GPS in dynamic monitoring of long-period structures. *Soil Dynamics and Earthquake Engineering*, 20(5-8), 477-483.

Chang, F. –K., (1999). *Structural Health Monitoring: a summary report on the First International Workshop on Structural Health Monitoring*, September 18-20, 1997, *Structural Health Monitoring 2000, Proceeding of the Second International Workshop on Structural Health Monitoring*, (pp. xix-xxiv) Stanford, CA, September 8-10, 1999, Lancaster – Basel, Technomic Publishing Co, Inc.

Chrzanowski, A., Chen, Y. Q. and Secord, J. M (1986). *Geometrical Analysis of Deformation Survey*, Deformation Measurement Workshop (Massachusetts Institute of Technology). Bock, Yehuda (Ed.). *Modern methodology in precise engineering and deformation survey-II* (pp.170-206.). Cambridge: Massachusetts Institute of Technology.

Department of Survey and Mapping Malaysia (1999). *GPS Cadastral Survey Guidelines*. Kuala Lumpur: KPU Circular vol 6-1999.

Department of Survey and Mapping Malaysia (2005). *Garis Panduan Mengenai Penggunaan Perkhidmatan Malaysia RTK GPS Network (MyRTknet)*. Kuala Lumpur: KPU Circular vol 9-2005

Department of Survey and Mapping Malaysia (2008). *Garis Panduan Mengenai Ujian Alat Sistem Penentududukan Sejagat (GNSS) yang Menggunakan RTK GNSS Network (MyRTknet)*. Kuala Lumpur: KPU Circular vol 1-2008

Duff, K., and Hyzak, M. (1997). Structural Monitoring with GPS. *Public Roads.* Spring 1997.

El-Rabbany, A. (2002). *Introduction to GPS: The Global Positioning System*. Artech House.

Gunter Seeber, (2003). *Satellite Geodesy 2nd completely revised and extended edition*, Walter de Gruyter, Berlin, New York.

Guo, J., and Ge, S.(1997). Research of Displacement and Frequency of Tall Building under Wind Load Using GPS. *The 10th International Technical Meeting of the Satellite Division of the Institute of Navigation*, Kansas City, 1385-1388.

Guo, J., Xu, L., Dai, L., McDonald, M., Wu, J., and Li, Y. (2005). Application of the Real-Time Kinematic Global Positioning System in Bridge Safety Monitoring. *Journal of Bridge Engineering*, 10(2), 163-168.

Henning, W. (2006). The New RTK-Changing Techniques for GPS Surveying in the USA. *Surveying and Land Information Science*, Vol. 66, No. 2, 2006, pp. 107-110

Hofmann-Wellenhof, B., and Lichtenegger, H. (1997). *GPS Theory and Practice*, Springer-Verlag, Wien Austria.

Hofmann-Wellenhof, B; Lichtenegger and Collins, J. (1994). *GPS – Theory and Practise.* 3rd Edition, Spriger-Verlag.

Kaplan, E. D., and Hegarty, C. J. (2006). *Understanding GPS: Principles and Applications, 2nd Edition*. Artech House, Boston, USA, 703.

Kijewski-Correa, T., Kareem, A., and Kochly, M. (2006). Experimental Verification and Full-Scale Deployment of Global Positioning Systems to Monitor the Dynamic Response of Tall Buildings. *Journal of Structural Engineering*, 132(8), 1242-1253.

Landau, H., Vollath, U., Chen, X., (2003). *Virtual Reference Stations versus Broadcast Solutions in Network RTK – Advantages and Limitations.* Trimble Terrasat GmbH. Retrieved December 15, 2007 from http://www.gpsnet.dk/showing.php?ID=376

Landau, H., Vollath, U., and Chen, X., (2002). Virtual Reference Station Systems. *Journal of Global Positioning Systems* (2002) Vol. 1, No. 2: 137-143

Leick, A. (1995). *GPS Satellite Surveying*, Wiley, New York , Chichester,Brisbane, Toronto and Singapore.

Leach, M. P., and Hyzak, M. D.(1994). GPS Structural Monitoring as Applied to a Cable-Stayed Suspension Bridge. *FIG XX-International Congress*, Melbourne,Australia, 606.2/1-606.2/12.

Lovse, J. W., Teskey, W. F., and Lachapelle, G. (1995). Dynamic Deformation Monitoring of Tall Structure Using GPS Technology. *Journal of Surveying Engineering*, 121(1), 35-40

Mat Amin, Z, Wan Akib, W. A and Twigg, D.R. (2002). The Time Series Analysis in GPS Structural Monitoring Schemes. *Map Asia 2002.* Bangkok.

Mat Amin, Z, Wan Akib W. A. & Setan, H, (2003). Experimental Works on the Use of Kinematic GPS Positioning in Continuous Monitoring Applications. *International & Exhibition on Geoinformation 2003*, Shah Alam.

Mat Amin, Z. and Wan Aziz W.A. (2003). Experimental Detection Of The Penang Bridge Vibration With Real Time Kinematic *GPS*, *Proc. International Symposium & Exhibition on Geoinformation, 2003,* Shah Alam, Selangor, October 2003, p.241-246.

Mat Amin, Z, Wan Akib, W. A and Zuhaidah, N (2007). A Study on the Instrumentation Control between Global Positioning System and LabVIEW software for Real-Time Applications. *Persidangan Kejuruteraan Awam: 50 Kemerdekaan.* May 29 – 31, 2007. Langkawi, Kedah.

Nakamura, S.-i. (2000). GPS Measurement of Wind-Induced Suspension Bridge Girder Displacements. *Journal of Structural Engineering*. 126(12), 1413-1419.

Nordin, Z., Yahya, M. H, Wan Akib, W. A. and Mat Amin, Z., (2008). The Utilization of RTK-GPS for Real-Time Kinematic Structural Health Detection. *International Conference on Civil Engineering (ICCE' 08)*, May 12-14, 2008. Kuantan, Pahang, Malaysia.

Ogaja, C. (2001). On-line GPS integrity monitoring and deformation analysis for structural monitoring applications. To be pres. 14th Int. Tech. *Meeting of the Satellite Division of the U.S. Inst. of Navigation,* Salt Lake City, Utah, 11-14 September.

Ogaja, C., C. Rizos, J. Wang, & J. Brownjohn. (2001). High precision dynamic GPS system for on-line structural monitoring. *5th Int. Symp. on Satellite Navigation Technology & Applications*, Canberra, Australia, 24-27 July, paper 35.

Ogaja, C., C. Rizos, and S. Han (2000). Is GPS Good Enough for Monitoring The Dynamics of High-rise Buildings? *2nd Trans Tasman Survey Congress*, Queenstown, New Zealand, 20-26 August, 150-164.

Qu, W. Z., Zeng, Y. L. And Jiang, Y. J (2006). *Structural Damage Detection Using Wavelet Approach for Two Kinds of Spike in the Wavelet Details*. Ou, Li & Duan (Eds.) *Structural Health Monitoring and Intelligent Infrastructure Volume 2* (pp. 1029 – 1036). Taylor & Francis Group, London. UK

Ou, J. P., Li, H., and Duan, Z. D., (2006). *Structural Health Monitoring and Intelligent Infrastructure Volume 2.* Taylor and Francis, London, UK.

Parkinson, B. W., and Spilker, J. J. (1996). *Global Positioning System: Theory and Applications Volume 1*. Progress in Astronautics and Aeronautics, American Institute of Aeronautics and Astronautics, Inc., Washington, USA, 793.

Retscher, G. (2002). Accuracy Performance of Virtual Reference Station (VRS) Networks. *Journal of Global Positioning System 2002*. Vol. 1, No. 1:40-47

Rizos, C (1999). *Basic GPS Positioning Notes. Chapter 1 – 3*, University of New South Wales, 1999.

Santala, J. and Totterstrom, S. (2002). On Testing of RTK-Network Virtual Concept. Congress on The Status of Virtual Reference Station, *FIG XXII International. Congress 2002*, Washington, D.C.

Salleh. C. Z, (2007). *Monitoring Survey of Breakwater Structure Using Total Station at Pangkalan Laut 1, TLDM, Tanjung Gelang, Apart of Kuantan Port, Kuantan*. B. Eng (Geomatic) Thesis, Universiti Technologi Malaysia, Johor, Malaysia.

Tamura, Y., Matsui, M., Pagnini, L.-C., Ishibashi, R., and Yoshida, A. (2002). Measurement of wind-induced response of buildings using RTK-GPS. *Journal of Wind Engineering and Industrial Aerodynamics*, 90(12-15), 1783-1793.

Teskey, W. F., and Porter, T. R. (1988). An Integrated Method for Monitoring the Deformation Behavior of Engineering Structures. *5th International FIG Symposium on Deformation Measurement,* New Brunswick, Canada.

Trimble Navigation Limited (2001). *Trimble Virtual Reference Station VRS*. [Brochure] Trimble Terrasat GmbH. Retrieved July 15, 2007. From http://www.trimble.com.html

USACE (2003). NAVSTAR Global Positioning System Surveying. Engineering and Design, US Army Corps of Engineers, July 2003.

Vollath U., Buecherl A., Landau H., Pagels C. and Wagner B. (2000). Long-RangeRTK Positioning Using Virtual Reference Stations. *In: Proceedings of IONGPS 2000. The 13th International Technical Meeting of the Satellite Division of the Institute of Navigation,* Salt Lake City, Utah, September 19-22, pp.1143-1147.

Wahlund, S. (2002). Production measurements with Network RTK – Tests and analyses, LMV-rapport 2002:2, Gävle

Wan Akib, W. A., Othman Z. and Najib H (2001). Monitoring high-rise building deformation using Global Posoitioning System. *The Asian GPS Conference 2001 Proceedings.*

Wan Akib, W. A., Ghazali, M. D, (2003). The application of real-time kinematic GPS in long span bridge deformation studied, *Asia Pacific Structural Engineering and Construction Conference (ASPEC 2003)*, Johor Bahru, 2-4 September 2003.

Wan Akib W.A., Mat Amin, Z. and Shu, K.K. (2005). The Deformation Study of High Building Using RTK-GPS: A First Experience in Malaysia. *FIG Working Week*, Cairo, Egypt.

Wanninger, L. (2004). Introduction to Network RTK. *IAG Working Group 4.5.1*: Network RTK Internet: http://www.network –rtk.info/intro/introduction.html

Wells, D., N. Beck, D. Delikaraoglou, A. Kkleusberg, E.J. Krakiwsky, G. Lachapelle, R.B. Langley, M. Nakiboglu, K.P. Schwarz, J.M. Tranquilla and P. Vanicek (1999). *Guide to GPS Positioning*. Lecture Notes No. 58, University of New Brunswick, November 1999.

Xiolin, M., Roberts, G., Dodson, A., Andreotti, M., Cosser, E., and Meo, M (2004). Development of a Prototype Remote Structural Health Monitoring System. *In Proceeding 1st FIG International Symposium on Engineering Surveys for Construction Works and Structural Engineering*. Nottingham, United Kingdom.

Y. M. Xie and I. Patnaikuni (2008). *Innovations in Structural Engineering and Construction Volume 1*. Taylor and Francis. London, UK

APPENDIX A

Specification of Topcon HiPer Ga Receiver

SATELLITE TRACKING	
Signal Tracked HiPer GA	GPS and GLONASS L1/L2 C/A, P-Code, Full Code & Carrier
Channels	40 channels L1/L2
WAAS/EGNOS	Available
Cold Start	<60 sec
Warm Start	<10 sec
Reacquisition	<1 sec
Multi-path mitigation	Advanced multi-path mitigation
ACCURACY	
Static, Fast Static L1+L2 L1	 H: 3mm+0.5ppm x D, V: 5mm+0.5ppm x D H: 3mm+0.8ppm x D, V: 4mm+1.0ppm x D"
Kinematic, RTK L1+L2/L1	 H: 10mm+1ppm x D, V: 15mm+1ppm x D"
WAAS/EGNOS	
Differential Accuracy	< 5m 3DMRMS
PHYSICAL	
Dimensions(mm)	W:159 x H:173 x D113
Weight	1.65 Kg
Enclosure	Aluminum Extrusion
Antenna	Internal
RTK COMMUNICATIONS	
Modem Type	Internal Digital TX/RX/DSP
Output Power	Selectable up to 1W (in 1 dB steps)
Frequency Range	410-470 MHz programmable
Maximum Range	3.5 to 5 miles with optimal conditions
Channel Spacing	25kHz or 12.5kHz selectable
RTK Update rate	5Hz, upgradeable to 20Hz
Latency	25msec
Format	CMR2, CMR+, RTCM 2.1, 2.3, 3.0, TPS
Cellular Modem Support External capable	

APPENDIX B

DATA SIMULATION TESTING AT BRIDGE NEAR UTM LAKE

ANALYSIS OF SIMULATION TEST IN CONFINED AREA										
Station no	Point P1				Epoch					
	Latitude (U)				Longitude (T)				Ellipsoid height(m)	
No of observation	°	‘	″	v (m)	°	‘	″	v (m)	Observation	v (m)
1	1	33	17.86708	-0.003	103	38	23.35862	-0.002	11.423	-0.003
2	1	33	17.86717	0.000	103	38	23.35872	0.001	11.428	0.002
3	1	33	17.86720	0.000	103	38	23.35867	-0.001	11.428	0.002
4	1	33	17.86712	-0.002	103	38	23.35878	0.003	11.422	-0.004
5	1	33	17.86719	0.000	103	38	23.35863	-0.002	11.430	0.004
6	1	33	17.86722	0.001	103	38	23.35870	0.000	11.423	-0.003
7	1	33	17.86720	0.000	103	38	23.35877	0.002	11.423	-0.003
8	1	33	17.86715	-0.001	103	38	23.35870	0.000	11.430	0.004
9	1	33	17.86723	0.001	103	38	23.35871	0.000	11.429	0.003
10	1	33	17.86729	0.003	103	38	23.35864	-0.002	11.427	0.001
Average	1	33	17.86719		103	38	23.35869		11.426	
Minimum	1	33	17.86708		103	38	23.35862		11.422	
Maximum	1	33	17.86729		103	38	23.35878		11.430	
RMS (m)	0.000				0.000				0.000	
Diff coordinate with true value	1.650				1.020				2.300	

ANALYSIS OF SIMULATION TEST IN CONFINED AREA										
Station no	Point P2				Epoch					
	Latitude (U)				Longitude (T)				Ellipsoid height(m)	
No of observation	°	‘	″	v (m)	°	‘	″	v (m)	Observation	v (m)
1	1	33	18.00325	-0.001	103	38	23.47532	0.003	11.409	0.010
2	1	33	18.00329	0.000	103	38	23.47510	-0.003	11.404	0.005
3	1	33	18.00327	-0.001	103	38	23.47504	-0.005	11.404	0.005
4	1	33	18.00329	0.000	103	38	23.47502	-0.006	11.403	0.004
5	1	33	18.00333	0.001	103	38	23.47518	-0.001	11.398	-0.001
6	1	33	18.00327	-0.001	103	38	23.47519	-0.001	11.402	0.003
7	1	33	18.00334	0.002	103	38	23.47532	0.003	11.395	-0.004
8	1	33	18.00329	0.000	103	38	23.47537	0.005	11.389	-0.010
9	1	33	18.00327	-0.001	103	38	23.47524	0.001	11.394	-0.005
10	1	33	18.00328	0.000	103	38	23.47534	0.004	11.389	-0.010
Average	1	33	18.00329		103	38	23.47521		11.399	
Minimum	1	33	18.00325		103	38	23.47502		11.389	
Maximum	1	33	18.00334		103	38	23.47537		11.409	
RMS (m)	0.000				0.000				0.000	
Diff coordinate with true value	1.440				-0.240				5.700	

APPENDIX C

ASSISTED- GPS INDOOR MONITORING

ANALYSIS OF SIMULATION TEST IN CONFINED AREA										
Station no	Point A				Epoch				1	
	Latitude (U)				Longitude (T)				Ellipsoid height(m)	
No of observation	°	‘	″	v (m)	°	‘	″	v (m)	Observation	v (m)
1	3	9	1.85569	0.003	101	44	49.27624	0.001	61.746	-0.002
2	3	9	1.85566	0.002	101	44	49.27607	-0.004	61.745	-0.003
3	3	9	1.85562	0.000	101	44	49.27617	-0.001	61.747	-0.001
4	3	9	1.85556	-0.001	101	44	49.27622	0.000	61.747	-0.001
5	3	9	1.85559	0.000	101	44	49.27617	-0.001	61.751	0.003
6	3	9	1.85554	-0.002	101	44	49.27606	-0.004	61.755	0.007
7	3	9	1.85560	0.000	101	44	49.27627	0.002	61.751	0.003
8	3	9	1.85562	0.000	101	44	49.27619	-0.001	61.744	-0.004
9	3	9	1.85558	-0.001	101	44	49.27632	0.003	61.745	-0.003
10	3	9	1.85558	-0.001	101	44	49.27636	0.005	61.750	0.002
Average	3	9	1.85560		101	44	49.27621		61.748	
Minimum	3	9	1.85554		101	44	49.27606		61.744	
Maximum	3	9	1.85569		101	44	49.27636		61.755	
RMS (m)	0.000				0.000				0.000	
Diff between obs coordinate (average) with true value (mm)	-12.480				17.610				-35.900	

ANALYSIS OF SIMULATION TEST IN CONFINED AREA										
Station no	Point A				Epoch				2	
	Latitude (U)				Longitude (T)				Ellipsoid height(m)	
No of observation	°	‘	″	v (m)	°	‘	″	v (m)	Observation	v (m)
1	3	9	1.85613	-0.003	101	44	49.27543	-0.004	61.780	-0.002
2	3	9	1.85619	-0.001	101	44	49.27545	-0.003	61.776	-0.006
3	3	9	1.85625	0.001	101	44	49.27541	-0.004	61.778	-0.004
4	3	9	1.85616	-0.002	101	44	49.27550	-0.002	61.782	0.000
5	3	9	1.85620	-0.001	101	44	49.27552	-0.001	61.780	-0.002
6	3	9	1.85627	0.002	101	44	49.27552	-0.001	61.784	0.002
7	3	9	1.85624	0.001	101	44	49.27565	0.003	61.792	0.010
8	3	9	1.85621	0.000	101	44	49.27565	0.003	61.781	-0.001
9	3	9	1.85626	0.001	101	44	49.27576	0.006	61.784	0.002
10	3	9	1.85628	0.002	101	44	49.27564	0.003	61.787	0.005
Average	3	9	1.85622		101	44	49.27555		61.782	
Minimum	3	9	1.85613		101	44	49.27541		61.776	
Maximum	3	9	1.85628		101	44	49.27576		61.792	
RMS (m)	0.000				0.000				0.000	
Diff between obs coordinate (average) with true value (mm)	5.970				-2.010				-1.600	

ANALYSIS OF SIMULATION TEST IN CONFINED AREA										
Station no	Point A				Epoch				3	
	Latitude (U)				Longitude (T)				Ellipsoid height(m)	
No of observation	°	‘	″	v (m)	°	‘	″	v (m)	Observation	v (m)
1	3	9	1.85592	0.000	101	44	49.27562	0.002	61.797	0.004
2	3	9	1.85590	0.000	101	44	49.27543	-0.004	61.797	0.004
3	3	9	1.85590	0.000	101	44	49.27563	0.002	61.799	0.006
4	3	9	1.85581	-0.003	101	44	49.27553	-0.001	61.799	0.006
5	3	9	1.85578	-0.004	101	44	49.27554	0.000	61.792	-0.001
6	3	9	1.85584	-0.002	101	44	49.27555	0.000	61.790	-0.003
7	3	9	1.85593	0.001	101	44	49.27556	0.000	61.789	-0.004
8	3	9	1.85601	0.003	101	44	49.27555	0.000	61.790	-0.003
9	3	9	1.85592	0.000	101	44	49.27554	0.000	61.794	0.001
10	3	9	1.85606	0.005	101	44	49.27558	0.001	61.786	-0.007
Average	3	9	1.85591		101	44	49.27555		61.793	
Minimum	3	9	1.85578		101	44	49.27543		61.786	
Maxsimum	3	9	1.85606		101	44	49.27563		61.799	
RMS (m)	0.000				0.000				0.000	
Diff between obs coordinate (average) with true value (mm)	-3.390				-2.010				9.300	

ANALYSIS OF SIMULATION TEST IN CONFINED AREA										
Station no	Point B				Epoch				1	
	Latitude (U)				Longitude (T)				Ellipsoid height(m)	
No of observation	°	‘	″	v (m)	°	‘	″	v (m)	Observation	v (m)
1	3	9	1.85584	-0.001	101	44	49.27486	0.005	61.492	-0.007
2	3	9	1.85591	0.001	101	44	49.27484	0.004	61.504	0.005
3	3	9	1.85591	0.001	101	44	49.27483	0.004	61.503	0.004
4	3	9	1.85583	-0.001	101	44	49.27467	-0.001	61.503	0.004
5	3	9	1.85594	0.002	101	44	49.27466	-0.001	61.508	0.009
6	3	9	1.85599	0.003	101	44	49.27467	-0.001	61.517	0.018
7	3	9	1.85595	0.002	101	44	49.27440	-0.009	61.501	0.002
8	3	9	1.85583	-0.001	101	44	49.27451	-0.006	61.490	-0.009
9	3	9	1.85577	-0.003	101	44	49.27480	0.003	61.485	-0.014
10	3	9	1.85577	-0.003	101	44	49.27478	0.002	61.489	-0.010
Average	3	9	1.85587		101	44	49.27470		61.499	
Minimum	3	9	1.85577		101	44	49.27440		61.485	
Maximum	3	9	1.85599		101	44	49.27486		61.517	
RMS (m)	0.000				0.000				0.000	
Diff between obs coordinate (average) with true value (mm)	1.320				-1.140				3.200	

ANALYSIS OF SIMULATION TEST IN CONFINED AREA										
Station no	Point B				Epoch				2	
	Latitude (U)				Longitude (T)				Ellipsoid height(m)	
No of observation	°	‘	″	v (m)	°	‘	″	v (m)	Observation	v (m)
1	3	9	1.85575	-0.004	101	44	49.27464	-0.002	61.488	-0.007
2	3	9	1.85585	-0.001	101	44	49.27460	-0.003	61.495	0.000
3	3	9	1.85591	0.001	101	44	49.27463	-0.002	61.500	0.005
4	3	9	1.85592	0.001	101	44	49.27469	0.000	61.501	0.006
5	3	9	1.85589	0.000	101	44	49.27471	0.001	61.492	-0.003
6	3	9	1.85595	0.002	101	44	49.27478	0.003	61.495	0.000
7	3	9	1.85594	0.001	101	44	49.27467	-0.001	61.495	0.000
8	3	9	1.85594	0.001	101	44	49.27471	0.001	61.491	-0.004
9	3	9	1.85589	0.000	101	44	49.27472	0.001	61.495	0.000
10	3	9	1.85586	-0.001	101	44	49.27476	0.002	61.497	0.002
Average	3	9	1.85589		101	44	49.27469		61.495	
Minimum	3	9	1.85575		101	44	49.27460		61.488	
Maximum	3	9	1.85595		101	44	49.27478		61.501	
RMS (m)	0.000				0.000				0.000	
Diff between obs coordinate (average) with true value (mm)	1.800				-1.470				-1.100	

ANALYSIS OF SIMULATION TEST IN CONFINED AREA										
Station no	Point B				Epoch				3	
	Latitude (U)				Longitude (T)				Ellipsoid height(m)	
No of observation	°	‘	″	v (m)	°	‘	″	v (m)	Observation	v (m)
1	3	9	1.85575	-0.001	101	44	49.27527	0.005	61.505	0.010
2	3	9	1.85583	0.002	101	44	49.27515	0.001	61.511	0.016
3	3	9	1.85585	0.002	101	44	49.27512	0.000	61.499	0.004
4	3	9	1.85574	-0.001	101	44	49.27523	0.004	61.493	-0.002
5	3	9	1.85584	0.002	101	44	49.27508	-0.001	61.500	0.005
6	3	9	1.85567	-0.003	101	44	49.27506	-0.002	61.484	-0.011
7	3	9	1.85573	-0.001	101	44	49.27504	-0.002	61.486	-0.009
8	3	9	1.85572	-0.002	101	44	49.27507	-0.001	61.481	-0.014
9	3	9	1.85576	-0.001	101	44	49.27513	0.001	61.502	0.007
10	3	9	1.85588	0.003	101	44	49.27498	-0.004	61.492	-0.003
Average	3	9	1.85578		101	44	49.27511		61.495	
Minimum	3	9	1.85567		101	44	49.27498		61.481	
Maximum	3	9	1.85588		101	44	49.27527		61.511	
RMS (m)	0.000				0.000				0.000	
Diff between obs coordinate (average) with true value (mm)	-1.590				11.190				-0.700	

ANALYSIS OF SIMULATION TEST IN CONFINED AREA										
Station no	Point C				Epoch				1	
	Latitude (U)				Longitude (T)				Ellipsoid height(m)	
No of observation	°	‘	″	v (m)	°	‘	″	v (m)	Observation	v (m)
1	3	9	1.85552	-0.005	101	44	49.27506	-0.007	61.527	0.001
2	3	9	1.85572	0.001	101	44	49.27515	-0.004	61.524	-0.002
3	3	9	1.85575	0.002	101	44	49.27511	-0.005	61.529	0.003
4	3	9	1.85570	0.000	101	44	49.27519	-0.003	61.529	0.003
5	3	9	1.85570	0.000	101	44	49.27528	0.000	61.521	-0.005
6	3	9	1.85569	0.000	101	44	49.27530	0.001	61.534	0.008
7	3	9	1.85580	0.003	101	44	49.27538	0.003	61.529	0.003
8	3	9	1.85574	0.001	101	44	49.27529	0.000	61.526	0.000
9	3	9	1.85566	-0.001	101	44	49.27542	0.004	61.517	-0.009
10	3	9	1.85566	-0.001	101	44	49.27559	0.009	61.527	0.001
Average	3	9	1.85569		101	44	49.27528		61.526	
Minimum	3	9	1.85552		101	44	49.27506		61.517	
Maximum	3	9	1.85580		101	44	49.27559		61.534	
RMS (m)	0.000				0.000				0.000	
Diff between obs coordinate (average) with true value (mm)	1.020				0.210				3.300	

ANALYSIS OF SIMULATION TEST IN CONFINED AREA										
Station no	Point C				Epoch				2	
	Latitude (U)				Longitude (T)				Ellipsoid height(m)	
No of observation	°	‘	″	v (m)	°	‘	″	v (m)	Observation	v (m)
1	3	9	1.85586	0.003	101	44	49.27550	0.002	61.543	0.010
2	3	9	1.85593	0.005	101	44	49.27537	-0.002	61.543	0.010
3	3	9	1.85584	0.002	101	44	49.27541	0.000	61.547	0.014
4	3	9	1.85589	0.004	101	44	49.27550	0.002	61.551	0.018
5	3	9	1.85594	0.005	101	44	49.27512	-0.009	61.545	0.012
6	3	9	1.85579	0.001	101	44	49.27541	0.000	61.529	-0.004
7	3	9	1.85566	-0.003	101	44	49.27536	-0.002	61.524	-0.009
8	3	9	1.85557	-0.006	101	44	49.27550	0.002	61.516	-0.017
9	3	9	1.85558	-0.005	101	44	49.27545	0.001	61.518	-0.015
10	3	9	1.85553	-0.007	101	44	49.27564	0.006	61.514	-0.019
Average	3	9	1.85576		101	44	49.27543		61.533	
Minimum	3	9	1.85553		101	44	49.27512		61.514	
Maximum	3	9	1.85594		101	44	49.27564		61.551	
RMS (m)	0.000				0.000				0.001	
Diff between obs coordinate (average) with true value (mm)	2.970				4.680				10.000	

ANALYSIS OF SIMULATION TEST IN CONFINED AREA										
Station no	Point C				Epoch				3	
	Latitude (U)				Longitude (T)				Ellipsoid height(m)	
No of observation	°	‘	″	v (m)	°	‘	″	v (m)	Observation	v (m)
1	3	9	1.85559	0.000	101	44	49.27467	-0.009	61.522	0.004
2	3	9	1.85561	0.000	101	44	49.27468	-0.009	61.520	0.002
3	3	9	1.85556	-0.001	101	44	49.27487	-0.003	61.522	0.004
4	3	9	1.85568	0.003	101	44	49.27473	-0.007	61.535	0.017
5	3	9	1.85565	0.002	101	44	49.27501	0.001	61.521	0.003
6	3	9	1.85571	0.003	101	44	49.27508	0.003	61.519	0.001
7	3	9	1.85563	0.001	101	44	49.27509	0.003	61.518	0.000
8	3	9	1.85561	0.000	101	44	49.27508	0.003	61.514	-0.004
9	3	9	1.85549	-0.003	101	44	49.27531	0.010	61.502	-0.016
10	3	9	1.85543	-0.005	101	44	49.27522	0.007	61.505	-0.013
Average	3	9	1.85560		101	44	49.27497		61.518	
Minimum	3	9	1.85543		101	44	49.27467		61.502	
Maximum	3	9	1.85571		101	44	49.27531		61.535	
RMS (m)	0.000				0.000				0.000	
Diff between obs coordinate (average) with true value (mm)	-1.920				-8.880				-5.200	

ANALYSIS OF SIMULATION TEST IN CONFINED AREA										
Station no	Point D				Epoch				1	
	Latitude (U)				Longitude (T)				Ellipsoid height(m)	
No of observation	°	‘	″	v (m)	°	‘	″	v (m)	Observation	v (m)
1	3	9	1.85554	-0.004	101	44	49.27577	0.005	61.710	0.004
2	3	9	1.85553	-0.004	101	44	49.27567	0.002	61.704	-0.002
3	3	9	1.85554	-0.004	101	44	49.27565	0.001	61.706	0.000
4	3	9	1.85550	-0.005	101	44	49.27564	0.001	61.711	0.005
5	3	9	1.85554	-0.004	101	44	49.27569	0.003	61.708	0.002
6	3	9	1.85559	-0.002	101	44	49.27584	0.007	61.713	0.007
7	3	9	1.85565	0.000	101	44	49.27554	-0.002	61.702	-0.004
8	3	9	1.85589	0.007	101	44	49.27538	-0.007	61.700	-0.006
9	3	9	1.85593	0.008	101	44	49.27545	-0.005	61.704	-0.002
10	3	9	1.85590	0.007	101	44	49.27540	-0.006	61.706	0.000
Average	3	9	1.85566		101	44	49.27560		61.706	
Minimum	3	9	1.85550		101	44	49.27538		61.700	
Maximum	3	9	1.85593		101	44	49.27584		61.713	
RMS (m)	0.000				0.000				0.000	
Diff between obs coordinate (average) with true value (mm)	-2.370				0.990				-15.600	

ANALYSIS OF SIMULATION TEST IN CONFINED AREA										
Station no	Point D				Epoch				2	
	Latitude (U)				Longitude (T)				Ellipsoid height(m)	
No of observation	°	‘	″	v (m)	°	‘	″	v (m)	Observation	v (m)
1	3	9	1.85584	0.001	101	44	49.27549	0.004	61.729	0.004
2	3	9	1.85582	0.001	101	44	49.27552	0.005	61.729	0.004
3	3	9	1.85586	0.002	101	44	49.27542	0.002	61.726	0.001
4	3	9	1.85588	0.002	101	44	49.27542	0.002	61.721	-0.004
5	3	9	1.85576	-0.001	101	44	49.27530	-0.001	61.724	-0.001
6	3	9	1.85582	0.001	101	44	49.27524	-0.003	61.728	0.003
7	3	9	1.85578	-0.001	101	44	49.27535	0.000	61.723	-0.002
8	3	9	1.85579	0.000	101	44	49.27531	-0.001	61.725	0.000
9	3	9	1.85577	-0.001	101	44	49.27514	-0.006	61.724	-0.001
10	3	9	1.85567	-0.004	101	44	49.27530	-0.001	61.721	-0.004
Average	3	9	1.85580		101	44	49.27535		61.725	
Minimum	3	9	1.85567		101	44	49.27514		61.721	
Maximum	3	9	1.85588		101	44	49.27552		61.729	
RMS (m)	0.000				0.000				0.000	
Diff between obs coordinate (average) with true value (mm)	1.770				-6.633				3.000	

ANALYSIS OF SIMULATION TEST IN CONFINED AREA										
Station no	Point D				Epoch				3	
	Latitude (U)				Longitude (T)				Ellipsoid height(m)	
No of observation	°	‘	″	v (m)	°	‘	″	v (m)	Observation	v (m)
1	3	9	1.85560	-0.004	101	44	49.27545	-0.003	61.723	0.010
2	3	9	1.85565	-0.002	101	44	49.27539	-0.005	61.719	0.006
3	3	9	1.85563	-0.003	101	44	49.27541	-0.004	61.717	0.004
4	3	9	1.85563	-0.003	101	44	49.27548	-0.002	61.715	0.002
5	3	9	1.85570	-0.001	101	44	49.27549	-0.002	61.709	-0.004
6	3	9	1.85582	0.003	101	44	49.27558	0.001	61.711	-0.002
7	3	9	1.85578	0.001	101	44	49.27569	0.004	61.713	0.000
8	3	9	1.85587	0.004	101	44	49.27578	0.007	61.705	-0.008
9	3	9	1.85585	0.004	101	44	49.27567	0.003	61.712	-0.001
10	3	9	1.85579	0.002	101	44	49.27564	0.002	61.711	-0.002
Average	3	9	1.85573		101	44	49.27556		61.714	
Minimum	3	9	1.85560		101	44	49.27539		61.705	
Maximum	3	9	1.85587		101	44	49.27578		61.723	
RMS (m)	0.000				0.000				0.000	
Diff between obs coordinate (average) with true value (mm)	-0.240				-0.360				-8.500	

APPENDIX E

GPS-BASED BUILDING MONITORING

ANALYSIS OF BUILDING P23										
Station no	Point B001				Epoch				1	
No of observation	Latitude (U)				Longitude (T)				Ellipsoid height(m)	
	°	‘	″	v (m)	°	‘	″	v (m)	Observation	v (m)
1	1	33	45.78138	-0.005	103	38	34.89420	-0.007	45.762	0.015
2	1	33	45.78137	-0.005	103	38	34.89423	-0.006	45.756	0.009
3	1	33	45.78161	0.002	103	38	34.89462	0.006	45.719	-0.028
4	1	33	45.78170	0.005	103	38	34.89464	0.006	45.714	-0.033
5	1	33	45.78157	0.001	103	38	34.89433	-0.003	45.761	0.014
6	1	33	45.78157	0.001	103	38	34.89445	0.001	45.758	0.011
7	1	33	45.78147	-0.002	103	38	34.89434	-0.003	45.755	0.008
8	1	33	45.78151	-0.001	103	38	34.89445	0.001	45.753	0.006
9	1	33	45.78156	0.001	103	38	34.89434	-0.003	45.752	0.005
10	1	33	45.78169	0.004	103	38	34.89464	0.006	45.745	-0.002
Average	1	33	45.78154		103	38	34.89442		45.748	
Minimum	1	33	45.78137		103	38	34.89420		45.714	
Maximum	1	33	45.78170		103	38	34.89464		45.762	
RMS (m)	0.000				0.000				0.001	
Diff between obs coordinate (average) with true value (mm)	2.190				-24.480				-1.500	

ANALYSIS OF BUILDING P23										
Station no	Point B002				Epoch				1	
	Latitude (U)				Longitude (T)				Ellipsoid height(m)	
No of observation	°	‘	″	v (m)	°	‘	″	v (m)	Observation	v (m)
1	1	33	49.62363	0.002	103	38	34.67254	0.000	50.162	-0.001
2	1	33	49.62359	0.001	103	38	34.67247	-0.002	50.159	-0.004
3	1	33	49.62363	0.002	103	38	34.67255	0.000	50.167	0.004
4	1	33	49.62352	-0.001	103	38	34.67255	0.000	50.169	0.006
5	1	33	49.62345	-0.003	103	38	34.67250	-0.001	50.167	0.004
6	1	33	49.62350	-0.001	103	38	34.67248	-0.002	50.165	0.002
7	1	33	49.62356	0.000	103	38	34.67262	0.002	50.163	0.000
8	1	33	49.62349	-0.002	103	38	34.67259	0.001	50.166	0.003
9	1	33	49.62356	0.000	103	38	34.67259	0.001	50.157	-0.006
10	1	33	49.62356	0.000	103	38	34.67260	0.002	50.159	-0.004
Average	1	33	49.62355		103	38	34.67255		50.163	
Minimum	1	33	49.62345		103	38	34.67247		50.157	
Maximum	1	33	49.62363		103	38	34.67262		50.169	
RMS (m)	0.000				0.000				0.000	
Diff between obs coordinate (average) with true value (mm)	2.370				-9.630				-5.600	

ANALYSIS OF BUILDING P23										
Station no	Point B003				Epoch				1	
No of observation	Latitude (U)				Longitude (T)				Ellipsoid height(m)	
	°	‘	″	v (m)	°	‘	″	v (m)	Observation	v (m)
1	1	33	47.35894	0.002	103	38	31.77270	0.000	41.169	-0.001
2	1	33	47.35900	0.003	103	38	31.77268	-0.001	41.172	0.002
3	1	33	47.35900	0.003	103	38	31.77261	-0.003	41.170	0.000
4	1	33	47.35890	0.000	103	38	31.77265	-0.001	41.174	0.004
5	1	33	47.35892	0.001	103	38	31.77265	-0.001	41.173	0.003
6	1	33	47.35873	-0.005	103	38	31.77262	-0.002	41.169	-0.001
7	1	33	47.35895	0.002	103	38	31.77271	0.000	41.171	0.001
8	1	33	47.35888	0.000	103	38	31.77281	0.003	41.168	-0.002
9	1	33	47.35882	-0.002	103	38	31.77276	0.002	41.170	0.000
10	1	33	47.35874	-0.004	103	38	31.77278	0.002	41.168	-0.002
Average	1	33	47.35889		103	38	31.77270		41.170	
Minimum	1	33	47.35873		103	38	31.77261		41.168	
Maximum	1	33	47.35900		103	38	31.77281		41.174	
RMS (m)	0.000				0.000				0.000	
Diff between obs coordinate (average) with true value (mm)	13.740				0.510				2.400	

ANALYSIS OF BUILDING P23										
Station no	Point B001				Epoch				2	
No of observation	Latitude (U)				Longitude (T)				Ellipsoid height(m)	
	°	‘	″	v (m)	°	‘	″	v (m)	Observation	v (m)
1	1	33	45.78229	0.000	103	38	34.89649	-0.003	45.715	-0.007
2	1	33	45.78219	-0.003	103	38	34.89655	-0.001	45.718	-0.004
3	1	33	45.78227	0.000	103	38	34.89670	0.003	45.724	0.002
4	1	33	45.78238	0.003	103	38	34.89672	0.004	45.724	0.002
5	1	33	45.78231	0.001	103	38	34.89663	0.001	45.726	0.004
6	1	33	45.78230	0.001	103	38	34.89668	0.003	45.727	0.005
7	1	33	45.78223	-0.002	103	38	34.89651	-0.003	45.714	-0.008
8	1	33	45.78228	0.000	103	38	34.89652	-0.002	45.727	0.005
9	1	33	45.78225	-0.001	103	38	34.89655	-0.001	45.726	0.004
10	1	33	45.78233	0.001	103	38	34.89659	0.000	45.724	0.002
Average	1	33	45.78228		103	38	34.89659		45.723	
Minimum	1	33	45.78219		103	38	34.89649		45.714	
Maximum	1	33	45.78238		103	38	34.89672		45.727	
RMS (m)	0.000				0.000				0.000	
Diff between obs coordinate (average) with true value (mm)	7.590				35.520				-7.500	

ANALYSIS OF BUILDING P23										
Station no	Point B002				Epoch				2	
No of observation	Latitude (U)				Longitude (T)				Ellipsoid height(m)	
	°	‘	″	v (m)	°	‘	″	v (m)	Observation	v (m)
1	1	33	49.62371	-0.003	103	38	34.67361	-0.002	50.094	-0.009
2	1	33	49.62385	0.001	103	38	34.67369	0.001	50.100	-0.003
3	1	33	49.62382	0.000	103	38	34.67364	-0.001	50.094	-0.009
4	1	33	49.62387	0.001	103	38	34.67370	0.001	50.099	-0.004
5	1	33	49.62385	0.001	103	38	34.67366	0.000	50.105	0.002
6	1	33	49.62386	0.001	103	38	34.67365	0.000	50.106	0.003
7	1	33	49.62385	0.001	103	38	34.67364	-0.001	50.109	0.006
8	1	33	49.62381	0.000	103	38	34.67369	0.001	50.106	0.003
9	1	33	49.62385	0.001	103	38	34.67368	0.001	50.104	0.001
10	1	33	49.62379	-0.001	103	38	34.67365	0.000	50.110	0.007
Average	1	33	49.62383		103	38	34.67366		50.103	
Minimum	1	33	49.62371		103	38	34.67361		50.094	
Maximum	1	33	49.62387		103	38	34.67370		50.110	
RMS (m)	0.000				0.000				0.000	
Diff between obs coordinate (average) with true value (mm)	5.280				10.530				-2.300	

ANALYSIS OF BUILDING P23										
Station no	Point B003				Epoch				2	
No of observation	Latitude (U)				Longitude (T)				Ellipsoid height(m)	
	°	‘	″	v (m)	°	‘	″	v (m)	Observation	v (m)
1	1	33	47.35834	0.002	103	38	31.77290	-0.002	41.195	-0.003
2	1	33	47.35837	0.003	103	38	31.77287	-0.003	41.195	-0.003
3	1	33	47.35831	0.001	103	38	31.77298	0.000	41.195	-0.003
4	1	33	47.35824	-0.001	103	38	31.77304	0.002	41.198	0.000
5	1	33	47.35828	0.000	103	38	31.77299	0.000	41.201	0.003
6	1	33	47.35823	-0.002	103	38	31.77295	-0.001	41.201	0.003
7	1	33	47.35832	0.001	103	38	31.77292	-0.002	41.200	0.002
8	1	33	47.35832	0.001	103	38	31.77294	-0.001	41.198	0.000
9	1	33	47.35823	-0.002	103	38	31.77309	0.003	41.201	0.003
10	1	33	47.35820	-0.003	103	38	31.77313	0.004	41.199	0.001
Average	1	33	47.35828		103	38	31.77298		41.198	
Minimum	1	33	47.35820		103	38	31.77287		41.195	
Maximum	1	33	47.35837		103	38	31.77313		41.201	
RMS (m)	0.000				0.000				0.000	
Diff between obs coordinate (average) with true value (mm)	1.020				3.030				16.300	

LIST OF PUBLICATIONS

Z. Nordin, W. A. W. M. Akib, and Z. M. Amin, "Assessing the potential of VRS-RTK technique for Structural Health Monitoring" presented at Postgraduate Research Seminar 2009, Faculty of Engineering and Science Geoinformation, Universiti Teknologi Malaysia, Ibnu Sina Institute, Universiti Teknologi Malaysia, Johor, 2009.

Z. Nordin, M. H. Yahya, W. A. W. Akib, and Z. M. Amin, "The Development of GPS Real-Time Instrumentation Control for Structural Health Monitoring" presented at National Postgraduate Conference in Science and Technology 2009 (NPC 2009), Universiti Teknologi Petronas, Tronoh, Perak, Malaysia, 2009.

M. H. Yahya, **Z. Nordin,** and M. N. Kamarudin, "The Influent of Malaysian Troposphere on the Performance of Satellite-Based Positioning System" presented at National Postgraduate Conference in Science and Technology 2009 (NPC 2009), Universiti Teknologi Petronas, Tronoh, Perak, Malaysia, 2009.

W. A. W. M. Akib, **Z. Nordin**, Z. M. Amin, M. H. Yahya, and S. K. Kok, "The Current and Future Trends on Structural Monitoring Scheme in Malaysia," presented at 2nd Engineering Conference on Sustainable Engineering Infrastructures Development & Management (ENCON 2008), Crowne Plaza Riverside, Kuching, Sarawak, Malaysia, 2008.

M. H. Yahya, **Z. Nordin,** and M. N. Kamarudin, "The Potential of Continuous Operating Network of Space-based Radio Navigation Satellites for Weather Information Retrieval," presented at International Conference and Expo on Environmental Management and Technologies (ICEEMAT 2008), Kuala Lumpur, Malaysia, 2008.

Z. Nordin, W. A. W. M. Akib, and Z. M. Amin, "Breakwater Structural Monitoring Using VRS-RTK Technique" presented at International Symposium on Geoinformation (ISG 2008), Kuala Lumpur, Malaysia, 2008.

Z. Nordin, W. A. W. M. Akib, and Z. M. Amin, "The Roles of Terrestrial and Satellite Methods in Investigating the Risk of Landslide Phenomenon in Malaysia" presented at Regional Conference on Science and Nature Environmental Resources (RSNER 2008), Kuala Lumpur, Malaysia, 2008.

Z. Nordin, M. H. Yahya, W. A. W. Akib, and Z. M. Amin, "The Utilization of RTK-GPS for Real-Time Structural Health Detection," presented at International Conference on Civil Engineering (ICCE08), Pahang, Malaysia, 2008.

Z. M. Amin, W. A. W. M. Akib, H. Setan and **Z. Nordin**, "Virtual Instrument Platform and the Global Positioning System for Real-time Monitoring of Structures", presented at Joint International Symposium & Exhibition on Geoinformation and Global Navigation Satellite System (ISG / GNSS 2007), Pesada, Johor Bahru, Johor, Malaysia, 2007.

Z. M. Amin, W. A. W. M. Akib, and **Z. Nordin**, "A Study on the Instrumentation Control between Global Positioning System and LabVIEW Software for Real-Time Monitoring Application", presented at Persidangan Kejuruteraan Awam: 50 Tahun Selepas Merdeka (AWAM' 07), Helang Hotel Langkawi, Kedah, Malaysia, 2007.

Z. M. Amin, W. A. W. M. Akib, and **Z. Nordin**, "The Impact of Radome on the GPS Observation", presented at International Symposium and Exhibition Geoinformation 2005 (ISG 05), Grand Plaza Park Royal, Batu Feringghi, Penang, Malaysia, 2005.